

INFORMATION TO USERS

This manuscript has been reproduced from the microfilm master. UMI films the text directly from the original or copy submitted. Thus, some thesis and dissertation copies are in typewriter face, while others may be from any type of computer printer.

The quality of this reproduction is dependent upon the quality of the copy submitted. Broken or indistinct print, colored or poor quality illustrations and photographs, print bleedthrough, substandard margins, and improper alignment can adversely affect reproduction.

In the unlikely event that the author did not send UMI a complete manuscript and there are missing pages, these will be noted. Also, if unauthorized copyright material had to be removed, a note will indicate the deletion.

Oversize materials (e.g., maps, drawings, charts) are reproduced by sectioning the original, beginning at the upper left-hand corner and continuing from left to right in equal sections with small overlaps.

Photographs included in the original manuscript have been reproduced xerographically in this copy. Higher quality 6" x 9" black and white photographic prints are available for any photographs or illustrations appearing in this copy for an additional charge. Contact UMI directly to order.

Bell & Howell Information and Learning
300 North Zeeb Road, Ann Arbor, MI 48106-1346 USA
800-521-0600

UMI[®]

UNIVERSITY OF ALBERTA

**UPPER ORDOVICIAN TRILOBITES FROM THE SOUTHERN
MACKENZIE MOUNTAINS, NORTHWEST TERRITORIES, CANADA**

BY

BRENDA HUNDA ©

A thesis submitted to the Faculty of Graduate Studies and Research in partial fulfillment of
the requirements for the degree of Master of Science

DEPARTMENT OF EARTH AND ATMOSPHERIC SCIENCES

Edmonton, Alberta

FALL, 1999



National Library
of Canada

Acquisitions and
Bibliographic Services

395 Wellington Street
Ottawa ON K1A 0N4
Canada

Bibliothèque nationale
du Canada

Acquisitions et
services bibliographiques

395, rue Wellington
Ottawa ON K1A 0N4
Canada

Your file Votre référence

Our file Notre référence

The author has granted a non-exclusive licence allowing the National Library of Canada to reproduce, loan, distribute or sell copies of this thesis in microform, paper or electronic formats.

The author retains ownership of the copyright in this thesis. Neither the thesis nor substantial extracts from it may be printed or otherwise reproduced without the author's permission.

L'auteur a accordé une licence non exclusive permettant à la Bibliothèque nationale du Canada de reproduire, prêter, distribuer ou vendre des copies de cette thèse sous la forme de microfiche/film, de reproduction sur papier ou sur format électronique.

L'auteur conserve la propriété du droit d'auteur qui protège cette thèse. Ni la thèse ni des extraits substantiels de celle-ci ne doivent être imprimés ou autrement reproduits sans son autorisation.

0-612-47043-1

Canada

UNIVERSITY OF ALBERTA

LIBRARY RELEASE FORM

Name of Author: Brenda Rosina Hunda

Title of Thesis: Upper Ordovician Trilobites from the Mackenzie Mountains,
Northwest Territories, Canada.

Degree: Master of Science

Year this Degree Granted: 1999

Permission is hereby granted to the University of Alberta Library to reproduce single copies of this thesis and to lend or sell such copies for private, scholarly, or scientific research purposes only.

The author reserves all other publication and other rights in association with the copyright in the thesis, and except hereinbefore provided, neither the thesis nor any substantial portion thereof may be printed or otherwise reproduced in any material form whatever without the author's prior written permission.

Brenda R. Hunda

Brenda R. Hunda
496 Dunluce Road
Edmonton, Alberta
T5X 5C8

27/Sept/99
Date

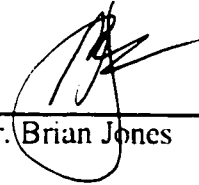
UNIVERSITY OF ALBERTA

FACULTY OF GRADUATE STUDIES AND RESEARCH

The undersigned certify that they have read, and recommend to the Faculty of Graduate Studies and Research for acceptance, a thesis entitled **Upper Ordovician Trilobites from the southern Mackenzie Mountains, Northwest Territories, Canada** submitted by Brenda Hunda in partial fulfillment of the requirements for the degree of Master of Science.



Dr. Brian D.E. Chatterton



Dr. Brian Jones



Dr. Mark V.H. Wilson

27/Sept/99
Date

I would like to dedicate this thesis to the memory of my mother, Solange Hunda, who always believed in me and taught me to reach for my dreams. Even though we are parted, her strength and love still finds me. I love you Mom.

ABSTRACT

Collections from the Whittaker Formation at Avalanche Lake 1 and Avalanche Lake 4B, near Avalanche Lake, N.W.T., demonstrate faunal changes through the Upper Ordovician, extending into the Silurian. 33 species, representing 15 families, were identified at AV4B and AV1. Thirteen new species were identified, described, and classified. Q-mode (sample by sample) and R-mode (taxon by taxon) biofacies analysis was conducted using the Jaccard Coefficient and UPGMA clustering. Three biofacies were recognized: the *Bathyurus* Biofacies, representing a nearshore environment; the *Tricopelta-Ceraurinella* Biofacies, representing a deeper water shelf environment; and the *Anataphrus-Cryptolithus* Biofacies, representing a slope environment. Changes in trilobite faunal composition, diversity, and sedimentology reveal the occurrence of the Rawtheyan extinction event at the Avalanche Lake sections. Evidence suggests that cooling ocean temperatures following the onset of the Gondwana glaciation during the Upper Ordovician may have been one of the factors that contributed to the Rawtheyan extinction event.

ACKNOWLEDGEMENTS

Greatest thanks go to Dr. B.D.E. Chatterton for both financial and academic support during field work and the preparation of this thesis. Few professors are able to be both a supervisor and friend at the same time and more rare are those who strive to build student's confidence. Thank you Brian.

I also would like to thank Dr B. Jones and Dr. M.V.H. Wilson for their constructive criticism of the thesis. Their comments greatly improved the final draft of the thesis. Thanks also to Dr. Wilson for assistance in the field during the summer of 1998.

The field work during the summer of 1998 was supported by funds from both Dr. B.D.E. Chatterton and from an NSTP grant from the Canadian Circumpolar Institute. The University of Alberta is thanked for all teaching assistantships for the academic years between 1997 to 1999.

Thanks also to the Dene and Metis people of the Northwest Territories First Nations for permission to use their traditional lands during the field season of 1998. The field work (1998) was carried out under a research license issued to Dr. M.V.H. Wilson and colleagues. The license was issued by the Aurora Institute, Inuvik.

I would like to recognize the hard and amazing work of George Braybrook, who supplied the expertise and jokes while on the SEM. I would also like to recognize Al Lindoe, who not only shared with me one of my best experiences, the trip to the Mackenzie Mountains, but also helped to develop my interest in photography along the way.

Thanks to my family and friends for moral support during my graduate program, especially to Ljubi M. Hunda and Fred T. Hanke for their affection, unerring ability to amuse during trying times and their assistance in filing papers.

Special recognition goes to those that had to put up with frustration, stress, and long hours. Gavin, I realize that living with me may have been trying at times, thanks for sticking with me and believing in me, and sharing my dreams. Mom, you did not have the chance to see me finish, I can tell you it does feel as good as we thought it would. My brothers, Brian and Ted, thank you for being proud of your big sister, and for holding me up when times got tough, I love you guys. And of course, to my best friend Sonya Castro. Who would of thought ten years ago we would be where we are today. We have done well!

TABLE OF CONTENTS

ABSTRACT

ACKNOWLEDGEMENTS

TABLE OF CONTENTS

LIST OF TABLES

LIST OF FIGURES

LIST OF PLATES

LIST OF APPENDICES

CHAPTER 1: INTRODUCTION

Introduction	1
Purpose and Scope of the Study	1
Previous Work	2
Methods and Materials	3
Regional Geology	4
Geology and Paleontology of AV4B and AV1	4
The Age of the Trilobites	10
The Hirnantia Fauna	15
The Ordovician Mass Extinctions	18
Literature Cited	20

CHAPTER II: SYSTEMATIC PALEONTOLOGY

Order Corynexochida Kobayashi, 1935	24
Family Illaenidae Hawle and Corda, 1847	24
<i>Bumastoides solangeae</i> n. sp.	24
<i>Failleana</i> sp.	27
Order Proetidae Fortey and Owens, 1975	28
Family Bathyruridae Walcott, 1886	28
<i>Bathyurus teresoma</i> n. sp.	28
Family Dimeropygidae Hupe, 1953	32
<i>Dimeropyge</i> sp.	32
Family Proetidae Hawle and Corda, 1847	33
<i>Decoroproetus hankei</i> n. sp.	33
Family Aulacopleuridae Angelin, 1854	36
<i>Harpidella kurrii</i> Adrain and Chatterton, 1995	37
Order Asaphidae Fortey and Chatterton, 1988	37

Family Asaphidae Burmeister, 1843	35
<i>Isotelus dorycephalus</i> n. sp.	38
<i>Anataphrus elevatus</i> n. sp.	41
Family Remopleurididae Hawle and Corda, 1847	45
<i>Robergia yukonensis</i> Lenz and Churkin, 1966	45
<i>Robergia</i> sp.	46
<i>Robergiella insolitus</i> n. sp.	46
<i>Hypodicranotus</i> sp.	50
Family Raphiophoridae Angelin, 1854	50
<i>Ampyxina pilatus</i> n. sp.	50
Family Trinucleidae Hawle and Corda, 1847	53
<i>Cryptolithus tessellatus</i> Green, 1832	53
Order Phacopida Salter, 1864	54
Family Cheiruridae Hawle and Corda, 1847	54
<i>Acanthoparypha palmapyga</i> n. sp.	54
<i>Acanthoparypha latipyga</i> n. sp.	57
<i>Acanthoparypha</i> sp.	61
Phylogenetic Analysis of <i>Acanthoparypha</i>	62
<i>Holia</i> sp.	66
<i>Ceraurinella lamiapyga</i> n. sp.	67
<i>Ceraurinella brevispina</i> Ludvigsen, 1979	69
<i>Ceraurus serratus</i> Ludvigsen, 1979	71
<i>Ceraurus mackenziensis</i> Ludvigsen, 1979	72
<i>Borealaspis whittakerensis</i> Ludvigsen, 1979	73
<i>Sphaerocoryphe</i> sp.	73
<i>Sphaerexochus</i> (<i>Korolevium</i>) sp.	74
Family Encrinuridae Angelin, 1854	74
<i>Curriella clancyi</i> Edgecombe and Chatterton, 1990	75
Encrinurid	75
<i>Cybeloides</i> sp.	76
Family Pterygometopidae Reed, 1905	76
<i>Sceptaspis avalanchensis</i> n. sp.	77
<i>Calyptaulax</i> n. sp. A	80
<i>Tricopelta mackenziensis</i> Ludvigsen and Chatterton, 1982	82
Family Calymenidae Milne Edwards, 1840	83
Calymenid	83

Order Lichida Moore, 1959	84
Family Lichidae Hawle and Corda, 1847	84
<i>Hemiarges</i> n. sp. A	84
<i>Amphilichas</i> sp.	85
Family Odontopleuridae Burmeister, 1843	85
Odontopleurid	85
Literature Cited	87
PLATES	92
CHAPTER III. UPPER ORDOVICIAN BIOFACIES	
Introduction	128
Previous Work	133
Methods of Analysis	134
Biofacies of Avalanche Lake	135
Environmental Controls of the Biofacies	139
Diversity within the Avalanche Lake Biofacies	142
Interaction within Biofacies	147
Comparison with other Biofacies Work	147
Lower Ordovician Biofacies	147
Middle Ordovician Biofacies	153
Upper Ordovician Biofacies	156
Biofacies Trends of the Ordovician of the Mackenzie Mountains	157
Discussion - The Late Ordovician extinctions at AV4B and AV1	159
Conclusions	164
Literature Cited	166
CHAPTER IV: CONCLUSIONS	
Systematics	169
Biofacies Analysis	169
The Rawtheyan Extinction Event at AV4B and AV1	171
Future Work	172
Literature Cited	173
APPENDICES	174

LIST OF TABLES

CHAPTER 2

- | | |
|---|----|
| 2.1 - Character matrix for cladistic analysis of 7 species of
<i>Acanthoparypha</i> and the outgroup <i>Holia secristi</i> . | 62 |
| 2.2 - Characters used in the phylogenetic analysis of
<i>Acanthoparypha</i> (character states unordered).
Characters 1-15 are taken from Adrain, (1998),
characters 16-23 have been added. | 63 |

LIST OF FIGURES

CHAPTER 1

1.1 - Study area and locality map of measured Avalanche Lake section in the southern Mackenzie Mountains. Inset shows relationship of measured Avalanche Lake sections to each other (after Over and Chatterton, 1987).	5
1.2 - Lithologic description and correlation of AV4B section based on the 1978 description by B.D.E. Chatterton and D.G. Perry and the 1998 description.	7
1.3 - Range chart of 28 species present at the Avalanche Lake 4B section.	8
1.4 - Range chart of 27 species present at the 98 Avalanche Lake 4B section.	9
1.5 - Lithologic description of AV1 described by B.D.E. Chatterton and D.G. Perry in 1978 and 1979.	11
1.6 - Range chart of 14 taxa present at the Avalanche Lake 1 section.	12
1.7 - Correlation chart of Ashgillian stratigraphic sequences in the Mackenzie Mountains, Yukon, and Nevada; age determination also based on previous work on conodonts, brachiopods, and ostracods within the Avalanche Lake 4B section.	14
1.8 - Global distribution patterns of Hirnantian faunas during the Late Ordovician (Ashgill); based on data from various sources, summarized in Rong, 1984; Rong and Harper, 1988.	16

CHAPTER 2

2.1 - Distribution of apomorphic characters on the consensus tree generated by PAUP 3.1.1. Strict, semistrict, majority rule, and adams consensus trees were all identical. <i>Holia secristi</i> was designated as outgroup.	64
2.2 - Distribution of apomorphic characters on the two shortest trees generated by PAUP 3.1.1 from data set (Table 2.1), characters unordered, outgroup designated as <i>Holia secristi</i> .	65
2.3 - Scatter diagram of 92 holaspid pygidia of <i>Ceraurinella brevispina</i> from Avalanche Lake 4B; relating width of pygidium across anterior margin (W) to length of first pygidial spines (L).	70

CHAPTER 3

3.1 - Relative abundance of genera in trilobite collections from the lower Whittaker Formation at the Avalanche Lake 4B section.	129
--	-----

3.2 - Relative abundance of genera in trilobite collections from the lower Whittaker Formation at the 98 Avalanche Lake 4B section.	130
3.3 - Relative abundance of genera in trilobite collections from the lower Whittaker Formation at the Avalanche Lake 1 section.	131
3.4 - Q-mode dendrogram of 24 horizons from the AV4B collection, 23 horizons from the 98AV4B collection, and 24 horizons from the AV1 collection, Whittaker Formation, Avalanche Lake, Mackenzie Mountains, Northwest Territories, Canada.	136
3.5 - R-mode dendrograms of 28 trilobite species occurring in AV4B collections, 27 species occurring in 98AV4B, and 13 species occurring in AV1 collections, Whittaker Formation, Avalanche Lake, Mackenzie Mountains, Northwest Territories, Canada.	137
3.6 - Biofacies maps of AV4B, 98AV4B, and AV1 sections. Collections from Q-mode dendrograms and genera from R-mode dendrograms from Figs. 3.4 and 3.5. Q-mode dendrogram order is in stratigraphic sequence.	138
3.7 - Q-mode dendrogram (top figure) of 70 combined Avalanche Lake collections from the Whittaker Formation. R-mode dendrogram (bottom figure) of 34 combined trilobite genera from all Avalanche Lake sections, Whittaker Formation, Mackenzie Mountains, Northwest Territories, Canada.	140
3.8 - Biofacies map of all 3 combined sections and genera within these sections. Collections from Q-mode dendrogram and genera from R-mode dendrogram order from Fig. 3.7.	141
3.9 - Diversity indices of AV4B trilobite collections from the Whittaker Formation. The vertical axis represents the measured section. A. Diversity indices tabulated using species counts at each horizon. B. Diversity indices tabulated using the Diversity Index of Ludvigsen (1978). Dotted lines represent intervals without data.	143
3.10 - Diversity indices of 98AV4B trilobite collections from the Whittaker Formation. The vertical axis represents the measured section. A. Diversity indices tabulated using species counts at each horizon. B. Diversity indices tabulated using the Diversity Index of Ludvigsen (1978). Dotted lines represent intervals without data.	144
3.11 - Diversity indices of AV1 trilobite collections from the Whittaker Formation. The vertical axis represents the measured section. A. Diversity indices tabulated using species counts at each horizon. B. Diversity indices tabulated using the Diversity Index of Ludvigsen (1978). Dotted lines represent intervals without data.	146

3.12 - Correlation of AV4B, 98AV4B, and AV1 sections based upon the three biofacies determined by the intersection of Q and R-mode clusters.	148
3.13 - Relative abundance of families in trilobite collections from the lower Whittaker Formation at the Avalanche Lake 4B section.	149
3.14 - Relative abundance of families in trilobite collections from the lower Whittaker Formation at the 98 Avalanche Lake 4B section.	150
3.15 - Relative abundance of families in trilobite collections from the lower Whittaker Formation at the Avalanche Lake 1 section.	151
3.16 - Biofacies trends through the Middle Ordovician to Upper Ordovician in the Mackenzie Mountains, Northwest Territories, Canada. A. Biofacies along a shelf profile for the Upper Whiterockian (Chazyan) and Blackriveran of the lower Esbataottine Formation (Chatterton and Ludvigsen, 1976). B. Biofacies along a shelf profile for the Upper Whiterockian (Chazyan) and Blackriveran of the Sunblood, Esbataottine, and lower Whittaker Formations (Ludvigsen, 1978). C. Biofacies along a shelf profile from the Upper Whiterockian (Chazyan) and Blackriveran of the Sunblood and Esbataottine Formations (Hayes, 1980). D. Trentonian biofacies shift of Ludvigsen (1978). E. Biofacies along a shelf profile from the lower Whittaker Formation, Avalanche Lake. The shelf profile was adapted from Ludvigsen (1978).	158
3.17 - Sequence of events at AV4B and AV1 based upon sedimentological and faunal changes that occur throughout the sections.	160

LIST OF PLATES

PLATE

1. <i>Bumastoides solangeae</i> n. sp. from the Ashgill of the Whittaker Formation, Avalanche Lake 4B, Mackenzie Mountains, Northwest Territories, Canada.	92
2. <i>Bathyurus teresoma</i> n. sp. from the Ashgill of the Whittaker Formation, Avalanche Lake 1 and 4B, Mackenzie Mountains, Northwest Territories, Canada.	94
3. <i>Decoroproetus hankei</i> n. sp. from the Ashgill of the Whittaker Formation, Avalanche Lake 4B, Mackenzie Mountains, Northwest Territories, Canada.	96
4. <i>Isotelus dorycephalus</i> n. sp. from the Ashgill of the Whittaker Formation, Avalanche Lake 4B, Mackenzie Mountains, Northwest Territories, Canada.	98
5. <i>Anataphrus elevatus</i> n. sp. from the Ashgill of the Whittaker Formation, Avalanche Lake 4B, Mackenzie Mountains, Northwest Territories, Canada.	100
6. <i>Robergia yukonensis</i> Lenz and Churkin, 1966 and <i>Robergia</i> sp. from the Ashgill of the Whittaker Formation, Avalanche Lake 4B, Mackenzie Mountains, Northwest Territories, Canada.	102
7. <i>Robergiella insolitus</i> n. sp. from the Ashgill of the Whittaker Formation, Avalanche Lake 4B, Mackenzie Mountains, Northwest Territories, Canada.	104
8. <i>Ampyxina pilatus</i> n. sp. from the Ashgill of the Whittaker Formation, Avalanche Lake 4B, Mackenzie Mountains, Northwest Territories, Canada.	106
9. <i>Cryptolithus tessellatus</i> Green, 1832 from the Ashgill of the Whittaker Formation, Avalanche Lake 4B, Mackenzie Mountains, Northwest Territories, Canada.	108
10. <i>Acanthoparypha palmapyga</i> n. sp. from the Ashgill of the Whittaker Formation, Avalanche Lake 4B, Mackenzie Mountains, Northwest Territories, Canada.	110
11. <i>Acanthoparypha latipyga</i> n. sp. from the Ashgill of the Whittaker Formation, Avalanche Lake 4B, Mackenzie Mountains, Northwest Territories, Canada.	112
12. <i>Acanthoparypha</i> sp. and <i>Ceraurinella lamiapyga</i> n. sp. from the Ashgill of the Whittaker Formation, Avalanche Lake 4B, Mackenzie Mountains, Northwest Territories, Canada.	114

13. <i>Ceraurina brevispina</i> Ludvigsen, 1979, <i>Ceraurinus serratus</i> Ludvigsen, 1979, and <i>Ceraurus mackenziensis</i> Ludvigsen, 1979 from the Ashgill of the Whittaker Formation, Avalanche Lake 4B, Mackenzie Mountains, Northwest Territories, Canada.	116
14. <i>Sceptaspis avalanchensis</i> n. sp. and <i>Calyptaulax</i> n. sp. A from the Ashgill of the Whittaker Formation, Avalanche Lake 4B, Mackenzie Mountains, Northwest Territories, Canada.	118
15. <i>Tricopelta mackenziensis</i> Ludvigsen and Chatterton, 1982, from the Ashgill of the Whittaker Formation, Avalanche Lake 4B, Mackenzie Mountains, Northwest Territories, Canada.	120
16. <i>Hemiarges</i> n. sp. A from the Ashgill of the Whittaker Formation, Avalanche Lake 4B, Mackenzie Mountains, Northwest Territories, Canada.	122
17. <i>Failleana</i> sp., <i>Dimeropyge</i> sp., <i>Harpidella kurrii</i> Adrain and Chatterton, 1995, <i>Hypodicranotus</i> sp., <i>Holia</i> sp., <i>Borealaspis whittakerensis</i> Ludvigsen, 1976, <i>Sphaerocoryphe</i> sp., and <i>Sphaerexochus</i> sp. from the Ashgill of the Whittaker Formation, Avalanche Lake 4B, Mackenzie Mountains, Northwest Territories, Canada.	124
18. <i>Curriella clancyi</i> Edgecombe and Chatterton, 1990, Encrinurid, <i>Cybeloides</i> sp., Calymenid, <i>Amphilichas</i> sp., and Odontopleurid from the Ashgill of the Whittaker Formation, Avalanche Lake 4B, Mackenzie Mountains, Northwest Territories, Canada.	126

LIST OF APPENDICES

Appendix I. 1998 geological description of Avalanche Lake 4B.	174
Appendix II. List of trilobite taxa present within the horizons of the 1978 collection from the Avalanche Lake 4B section.	178
Appendix III. List of trilobite taxa present within the horizons of the 1998 collection from the Avalanche Lake 4B section.	182
Appendix IV. List of trilobite taxa present within the horizons of the 1978 and 1979 collections from the Avalanche Lake 1 section.	186
Appendix V. 92 width and length measurements of holaspid pygidia of <i>Ceraurinella brevipina</i> . Width (W) is measured across the anterior margin, length (L) is of first pygidial spines.	189
Appendix VI. Diversity indices calculated for the AV4B, 98AV4B, and AV1 sections.	190

Chapter 1: Introduction

Introduction

Several previous publications describe Middle Ordovician and Silurian trilobite faunas of the southern Mackenzie Mountains (Chatterton and Ludvigsen, 1976; Ludvigsen, 1979; Perry and Chatterton, 1979; Chatterton, 1980; Chatterton and Perry, 1983, 1984; Edgecombe and Chatterton, 1990, 1992; Adrain and Chatterton, 1994, 1995a, 1995b; Siveter and Chatterton, 1996). Collections from exposed sections near Avalanche Lake, N.W.T. provide exceptionally well preserved Ordovician trilobite assemblages. The faunal composition, diversity patterns, and biostratigraphy of Late Ordovician trilobites from this region are poorly known. To date studies are limited to description and phylogenetic analysis of new taxa from the Middle Ordovician and Silurian, and studies of the Late Ordovician and Silurian extinction events in the Selwyn Basin (Chatterton et al., 1990; Wang et al., 1993).

Collections from Avalanche Lake 4B and Avalanche Lake 1 demonstrate faunal changes through the Upper Ordovician, extending into the Silurian. The Upper Ordovician is a period of particular interest to historical geologists because it includes a major episode of global glaciation, and at least two distinct episodes of ensuing mass extinction. The first episode of extinction, the Rawtheyan extinction event, is associated with a major reduction in species diversity and the appearance of new taxa. The second event near the end of the Ordovician (at the base of the *G. persculptus* zone) is associated with the extinction of many of the families that survived the Rawtheyan extinction event, and is followed by radiation of taxa into the Silurian.

Purpose and Scope of the Study

The objectives of this study were to collect and prepare fossils from a sequence of previously unstudied Late Ordovician trilobite assemblages in the lower Whittaker Formation, Mackenzie Mountains. The goal of the sampling strategy was to establish the taxonomic composition of several trilobite faunas spaced along a particular outcrop where it was suspected that faunal changes occurred in response to environmental changes during the Late Ordovician. New and existing species were identified, described and classified. The effects of the end-Ordovician glaciation, including rapid changes in sea level and temperature, on faunal composition, changes in abundance, and diversity were explored. Collections in the summer of 1998 have refined original descriptions of the geology of the Upper Ordovician parts of the section in this region, and have demonstrated facies changes in the interval that includes the extinction horizons. The finely resolved faunal and

stratigraphic data produced from Avalanche Lake will provide information on the Rawtheyan extinction event.

Previous Work

Papers discussing the fauna preserved in the Mackenzie Mountain sediments have focused primarily on the Middle Ordovician and Silurian. Within the Trilobita, Ludvigsen (1975) discussed the shelly faunas of Canadian to Maysvillian age in several formations within the southern Mackenzie Mountains. He identified seven discrete assemblages and described many previously unknown silicified trilobites. Chatterton and Ludvigsen (1976) described silicified trilobites of upper Whiterockian (late Chazyan) age from the lower half of the Esbataottine Formation from the South Nahanni River area, and discussed their biofacies and paleogeographic significance. Additional work by Chatterton (1980) described the ontogeny and functional morphology of many of the same species discussed in Chatterton and Ludvigsen (1976). Ludvigsen (1978) defined three platform trilobite biofacies according to generic composition and species diversity from the upper Whiterockian (Chazyan) to Edenian of the Sunblood, Esbataottine, and lower Whittaker Formations. Ludvigsen (1979) established the first macrofaunal zonation of the Middle Ordovician in western North America, in addition to describing twenty new species from the region.

Trilobite faunas of early Silurian age have been described by a number of workers. Perry and Chatterton (1979) discussed fifteen Wenlock trilobite genera and an associated brachiopod fauna from the beds of the Whittaker Formation and Delorme Formation. Chatterton and Perry (1983, 1984) continued work from the Avalanche Lake sections, describing silicified odontopleurid and cheirurid trilobites from early Llandovery to early Ludlow age. Edgecombe and Chatterton (1990, 1992) discussed the systematics of Silurian encrinurine trilobites from Llandovery strata of the Whittaker Formation. Adrain and Chatterton (1994, 1995a, 1995b) discussed new species of aulacopleurid trilobites from the Wenlock of the Whittaker Formation. Siveter and Chatterton (1996) discussed Llandovery and Wenlock calymenid trilobites from the Avalanche Lake sections.

Other faunal components discussed from Mackenzie Mountain sediments include conodonts (Over and Chatterton, 1987; Mitchell and Sweet, 1988; Nowlan et al., 1988), ostracods (Copeland, 1974; Copeland, 1978; Copeland, 1982; Copeland, 1989), brachiopods (Jin and Chatterton, 1997), rostroconchs (Johnson and Chatterton, 1983; Caldwell and Chatterton, 1995), and sponges (Rigby and Chatterton, 1994, 1999).

Chatterton et al. (1990) and Wang et al. (1993) discussed mass extinctions and faunal turnovers occurring in the Upper Ordovician and Silurian portions of the Avalanche

Lake sections. Chatterton et al. (1990) discussed trilobite and conodont lineage turnovers in Silurian shelf marginal sections of the Mackenzie Mountains and the relationship of these changes to fluctuations in sea level and migration of these organisms. Wang et al. (1993) presented a detailed study of the geochemistry, sedimentology, and fossil distribution in two Avalanche Lake sections at the Ordovician-Silurian boundary intervals in the Selwyn Basin. They found that trilobites and conodonts suffered a profound extinction at the end of the Ordovician that coincides with a maximum shallowing followed by a transgression, probably caused by a eustatic regression induced by Late Ordovician glaciation.

Materials and Methods

Two sections about 10 km east of Avalanche Lake were examined and described and bulk samples from each interval containing well preserved, distinct trilobite fossils were collected. Fossiliferous horizons were detected visually by the presence of silicified material such as corals. The trilobites in this study were extracted from samples from several collecting trips. In 1978 and 1979 material was collected from Avalanche Lake 4B and Avalanche Lake 1 and the sections were described by B.D.E. Chatterton and D.G. Perry. Additional specimens were recovered from AV4B and AV1 during the summer of 1998 by Dr. Brian D.E. Chatterton and others (including the writer). The Avalanche Lake 4B section was measured in detail and changes in lithology were described based on the Dunham carbonate classification, the allochems present, and sedimentary structures in order to determine depositional environment.

Bulk samples of fossiliferous limestone were collected from numerous horizons from Avalanche Lake 4B. The section was measured using a 1.5 metre stick, and samples were labeled according to their stratigraphic position above a datum. Approximately 3 metres of sediments were exposed during the 1998 trip that were not exposed in the previous trip to the locality. Measurement of the 1998 section started 3 m below the original datum established in 1978. Material collected from the 1998 field trip is labeled 98AV4B. Material collected previously by Brian Chatterton is labeled AV4B. Bulk samples collected from talus were indicated by a "T" on the field label.

Bulk samples of limestone were dissolved in 10% hydrochloric acid to extract silicified material. Dissolution of each sample required several days. The residue was then sieved into four size fractions, allowed to dry, and specimens were then picked from this residue.

Specimens were photographed with a Field-Emission Scanning Electron Microscope (FE-SEM) of the Earth and Atmospheric Sciences Department at the University of Alberta. SEM stubs were covered with exposed film to provide a smooth surface and

specimens were glued to the stubs with gum tragacanth, that dissolves in water to allow for easy removal of specimens at a later date.

Both new and known species were identified, described and classified based on morphology. Identification of most species was restricted to holaspid material, but later stage meraspid material was incorporated where material was abundant.

All specimens illustrated in this thesis are housed in the University of Alberta Paleontological Type collections and are identified by University of Alberta (UA) numbers.

Regional Geology

The Avalanche Lake sections are situated on the margin of the shelf or slope into the Selwyn Basin from the Redstone Arch region (Gabrielse et al., 1973). The sections are located approximately 10 km east of Avalanche Lake on the northeast flank of the Avalanche Syncline (Fig. 1.1). The Avalanche Lake sections include seven distinct exposures; AV1, AV2, AV3, AV4 and AV4B, AV5, AV6, and AV7. Over and Chatterton (1987) considered the lithology and faunas of these sections to be diagnostic of deeper water, deposited in a deep-shelf or slope setting. AV1 and AV2 are considered to represent environments more proximal to shore, AV3, AV4 and AV4B, AV5, AV6, and AV7 represent sections progressively more distal and deeper water environments (Over and Chatterton, 1987). Three Ordovician and Silurian formations are defined in the region. The Whittaker Formation contains Ordovician to Silurian strata, and interfingers with the Road River Formation in the Avalanche Lake area (Over and Chatterton, 1987). At AV1 and AV4B the Whittaker Formation crosses the boundary between the Upper Ordovician and Lower Silurian, ranging into the Wenlock (Copeland, 1989). The Whittaker Formation consists predominately of dark, fine-grained limestones, commonly argillaceous, with interbeds of carbonaceous shales. The Whittaker Formation is conformably overlain by the Delorme Formation, or the Road River Formation, where they occur together (Chatterton and Perry, 1984). The Delorme Formation consists of limestones, shales and dolomites and is Wenlock in age (Chatterton and Perry, 1984). The Road River Formation is a sequence of graptolite-bearing shales interbedded with calcareous strata (Chatterton and Perry, 1984). Chatterton and Perry (1983, 1984) recognized only the Whittaker and Delorme Formations in the Avalanche Lake sections.

Geology and Paleontology of Avalanche Lake 4B and Avalanche Lake 1

Sections AV1 and AV4B are located near the bases of adjacent valleys cut into the northeast slope of an unnamed mountain range, about 10 km east of Avalanche Lake, central Mackenzie Mountains, Northwest Territories (Wang et al., 1993). The strata in

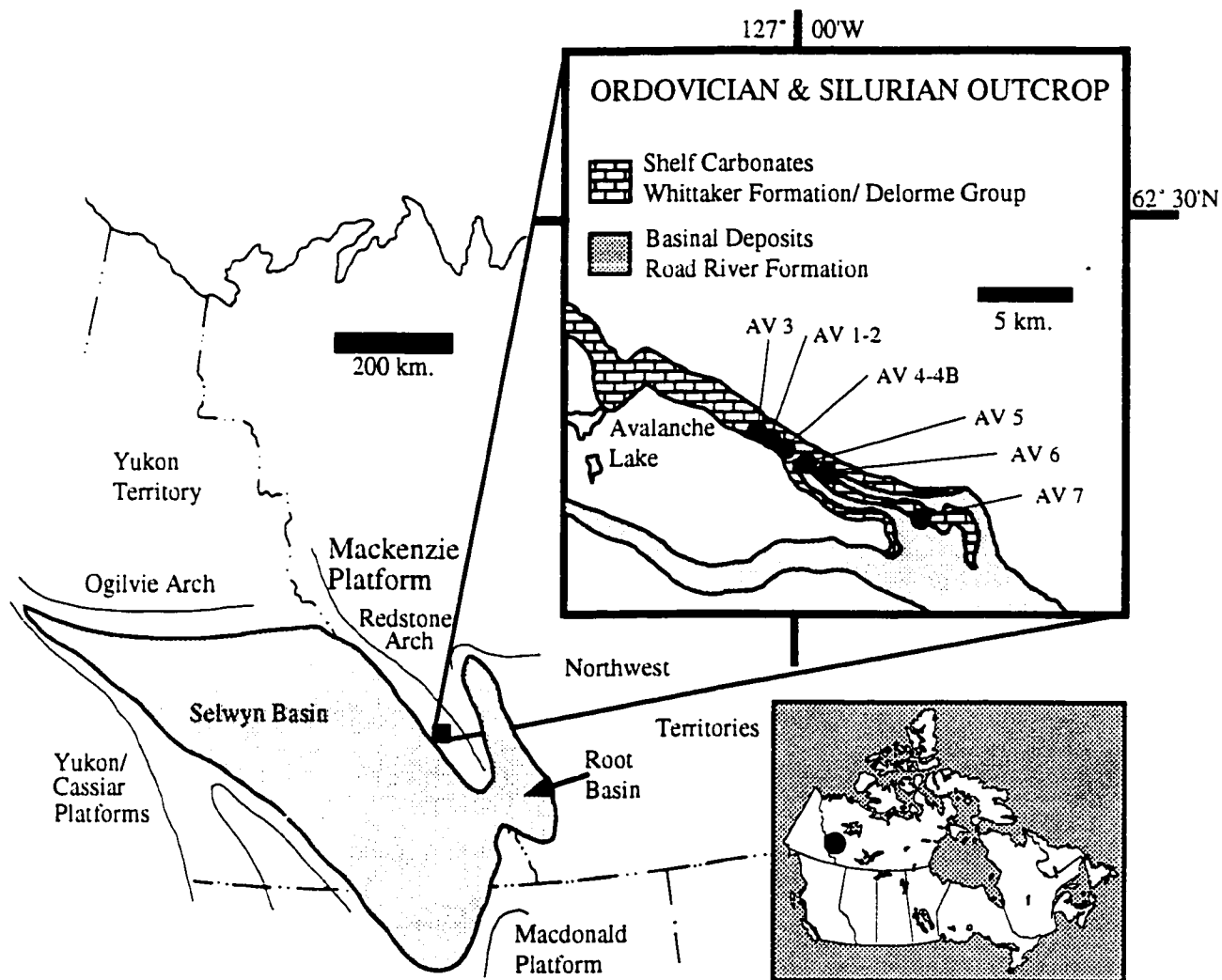


Figure 1.1. Study area and locality map of measured Avalanche Lake sections in the southern Mackenzie Mountains. Inset shows relationship of measured Avalanche Lake sections to each other (after Over and Chatterton, 1987).

AV4B are exposed through the uppermost Ordovician and lowermost Silurian; the AV1 section contains several covered intervals and therefore is less complete.

Minor differences in the sedimentological descriptions between the 1978 description and 1998 description account for variation between the two lithologs of the same section (Fig. 1.2). The 1978 measurement of AV4B revealed approximately 130 metres of section, of which 90.75 metres were sampled for silicified trilobites. The 1998 collection of AV4B spanned 110.9 metres, and was sampled more completely.

The section at AV4B consists of a series of dark, micritic mudstones and wackestones low in the section and interbedded argillaceous limestones and calcareous shales higher in the section. Interference ripples present at 2.75 m indicate shallow water deposition low within the section. Evidence of biogenic activity is indicated by burrows that occur low in the section. At approximately 21 m in the section a restricted interval of limestones with sparry calcite and mudstone intraclasts are found. These reworked mudstone intraclasts cemented by calcite spar indicate the occurrence of mass movement, possibly a slump or a slide. Wavy to planar laminations occur throughout the section, indicating variation in the nature or size of the carbonate material deposited through time, possibly resulting from current deposition (Boggs, 1987). At approximately 75.25 m, a distinct sedimentological change occurs, with dark micritic mudstones changing to calcareous shales that are interbedded with light gray, argillaceous limestones. The contact between the two is sharp. Chert nodules compose 10-20% of the limestone interbeds. The end-Ordovician mass extinction event was identified as occurring between two prominent beds sandwiched in a shaly-looking sequence of argillaceous limestones and shales (Wang et al., 1993). This level originally was placed by Nowlan et al. (1988) at 111.3 m. The 1998 measurements of the AV4B section place the same horizon at 110.6 m. The Ordovician-Silurian boundary was located 1 metre above this horizon based upon graptolite data (Wang et al., 1993)

Surface fossils visible at AV4B consist of rare tabulate and rugose corals, crinoid ossicles, brachiopod shell fragments, and rare trilobite fragments. Visual inspection of the outcrop indicated that surface fossils were prevalent within the wackestone interval. Above the 75.25 m horizon, exoskeletal fragments of *Cryptolithus* were visible on the surface and as crack-out specimens. Above 101.5 m, graptolites appear in the section.

Preparation of rock samples shows the distribution of in situ trilobite material at AV4B (Fig. 1.3, 1.4). Trilobites that occur 35 m below the Ordovician-Silurian boundary in the AV sections are dominated by the Ordovician genera *Cryptolithus*, *Anataphrus*, and *Robertiella*. Below this level, the fauna consists of typical Ordovician genera such as *Borealaspis*, *Ceraurinella*, *Tricopelta*, *Isotelus*, *Bumastoides*, *Ceraurus*, *Cybeloides*, *Holia*,

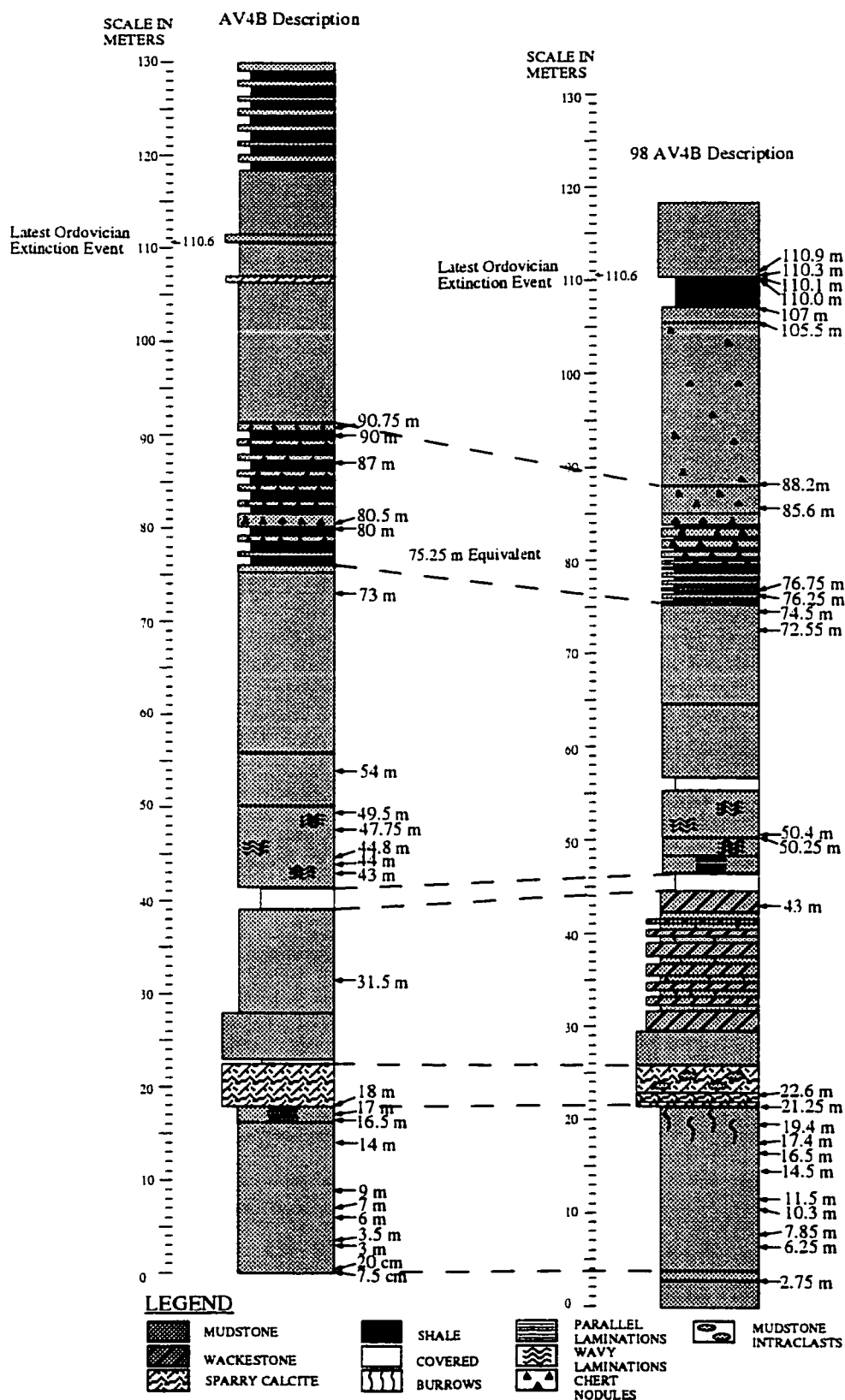


Figure 1.2. Lithologic description and correlation of AV4B sections based on the 1978 description by B.D.E. Chatterton and D.G. Perry and the 1998 description.

Harpidella, and *Sceptaspis*. Low in AV4B there is a restricted interval of approximately 2.75 m dominated by *Bathyurus*.

The Avalanche Lake 1 section originally was described in 1978 and 1979 by Dr. B.D.E. Chatterton and D.G. Perry. The section has a total thickness of 620 m, most of which occurs in the Llandovery. Only the lower 95.5 m of this section was studied in this thesis (Fig. 1.5). AV1 consists of a series of medium to dark grey micritic and argillaceous limestones. Minor chert lenses occur in argillaceous limestone beds along with evidence of convolute bedding. The interval between (-)60 m and 0 m was not formally described, but observation along this interval indicated that the sedimentology is dominated by micritic limestones. Evidence of shallow water deposition, such as mudcracks and syneresis cracks are found within this interval.

Section AV1 has a fossil distribution similar to that of AV4B (Fig. 1.6). Fossils such as bryozoans, corals, and trilobites are abundant in the section. In relation to AV4B, the AV1 section has a greater exposure of the lower interval where *Bathyurus* dominates the fauna. Above this interval *Ceraurinella* and *Isotelus* occur. At approximately 30 m, the faunal composition shifts to an assemblage dominated by deeper water trilobites such as *Cryptolithus* and *Anataphrus*.

The level of the faunal turnover at AV1 is between 76.5 m and 77.5 m based on changes in the trilobite and conodont assemblages above and below this interval (Wang et al., 1993).

Age of the Trilobites

Faunal correlation of the Upper Ordovician must be based on species similarity. Close generic similarity is no assurance of contemporaneity and is only an indication of a similar biofacies derivation (Chatterton and Ludvigsen, 1976). Since several of the trilobite taxa are new species, or have not been given a species designation, few key taxa within the collection from AV4B are available to establish an age correlation.

The age of the trilobite collections from the upper portions of the Avalanche Lake sections described in this thesis are determined to be Late Ashgillian in age (Rawtheyan and Hirnantian in the British series, Gamachian in the North American series). This age determination is based on previous work using brachiopod, ostracod, conodont, and graptolite correlations, as well as trilobite species correlations with other regions (Fig. 1.7).

The Upper Ordovician fauna of the Avalanche Lake region is distinct from other contemporary faunas from North America and other distant regions. The formation of a widespread Hirnantian fauna occurred during this time interval, and this fauna does not appear in the Mackenzie Mountains. Age correlation with other faunas was limited by the

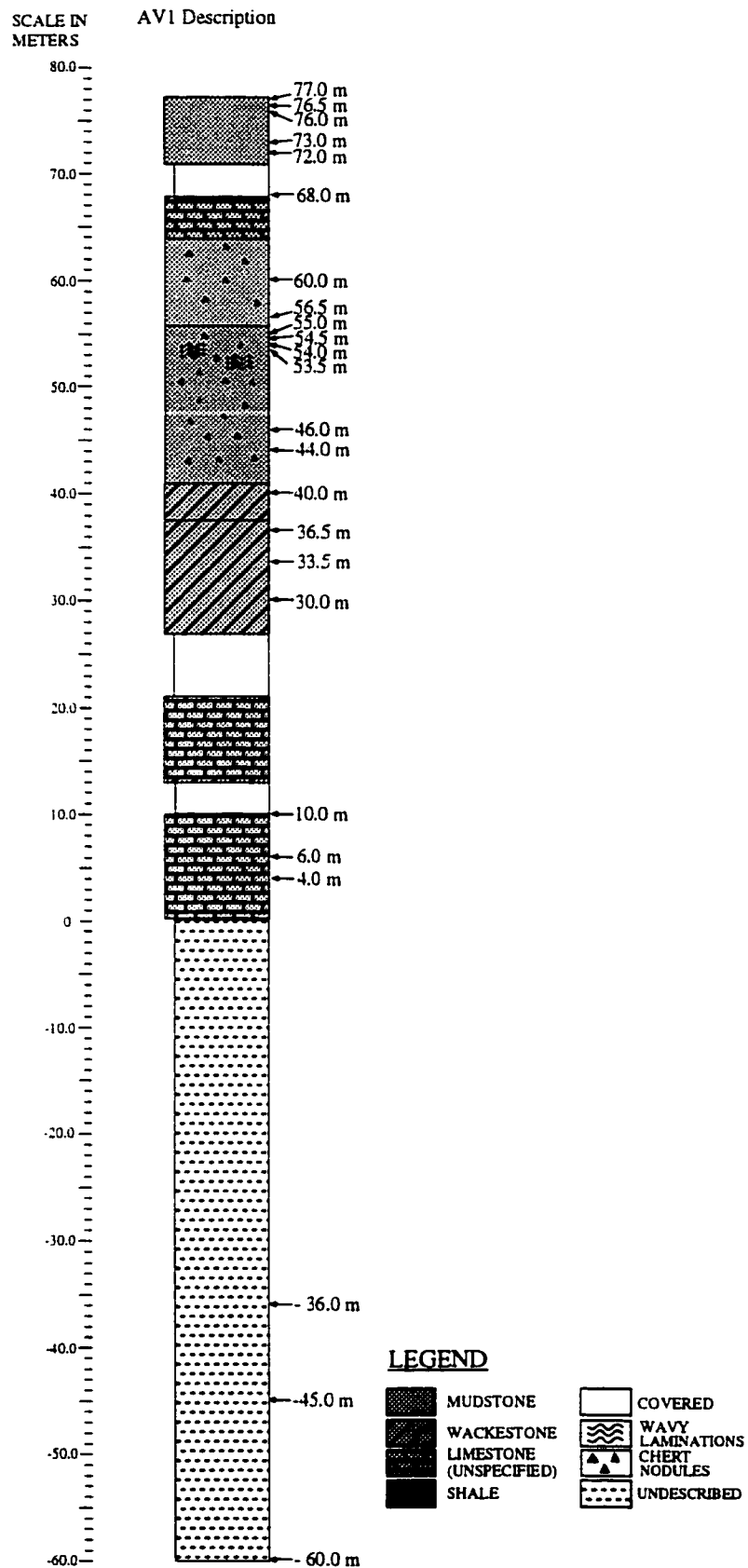


Figure 1.5. Lithologic description of the AV1 section described by B.D.E. Chatterton and D.G. Perry in 1978 and 1979.

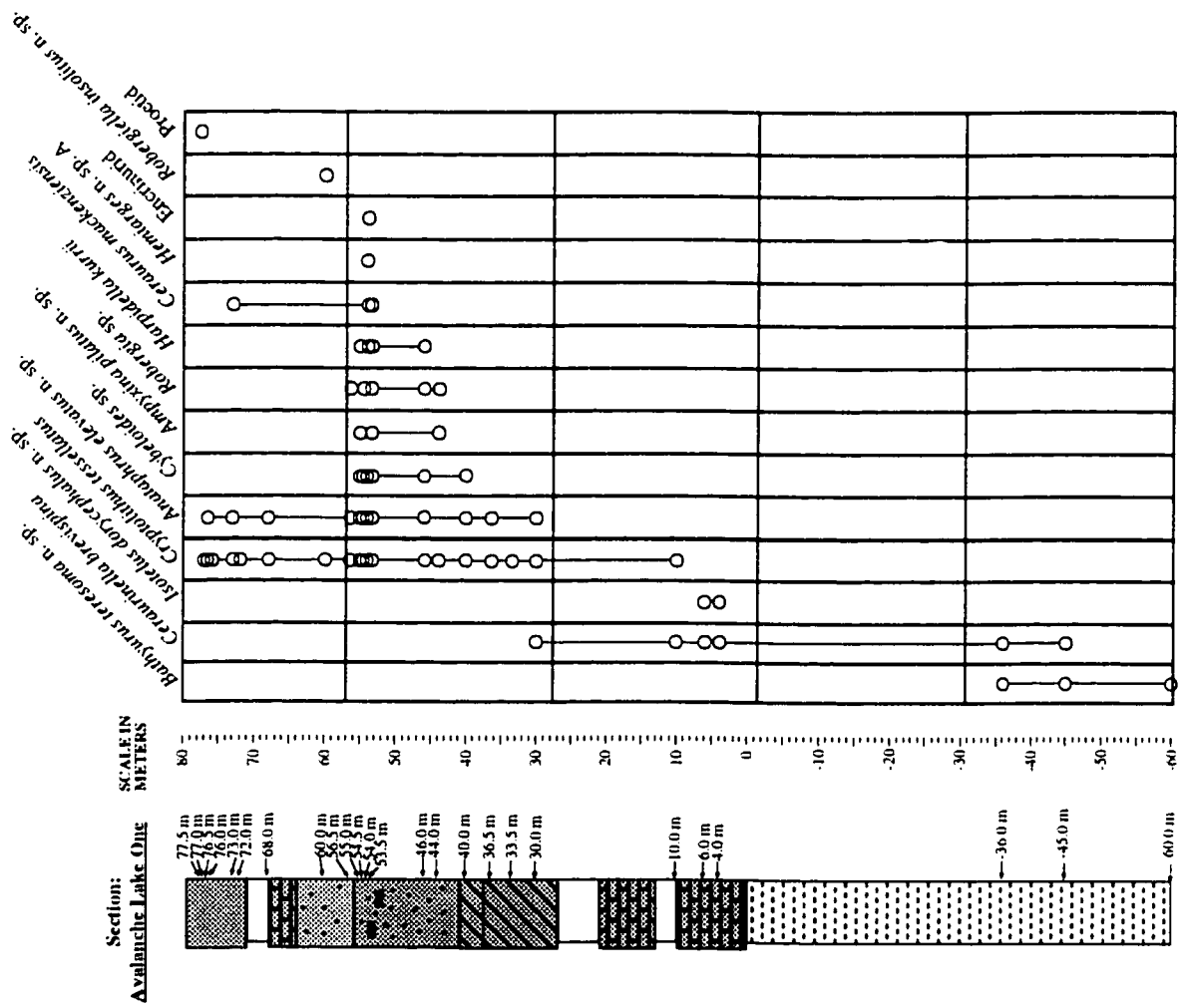


Figure 1.6. Range chart of 14 species present at the Avalanche Lake 1 section.

absence of this distinct association. Regions within close geographic proximity to the AV sections show some similarities to the trilobite composition of AV4B and AV1. A correlation with the Road River Formation, Yukon Territory is indicated by the presence of *Robergia yukonensis* Lenz and Churkin, and the presence of *Ampyxina salmoni* Churkin, which differs marginally from *Ampyxina pilatus* n. sp. from Avalanche Lake 4B.

Trilobites from the Hanson Creek Formation of Central Nevada show some similarity with trilobite genera from AV4B. *Anataphrus* sp., illustrated in Ross et al. (1979) and the unpublished masters thesis of Yu (1996) as a new species of *Anataphrus*, is thought to be conspecific with *Anataphrus elevatus* n. sp. of Avalanche Lake 4B. *Ceraurus mackenziensis* Ludvigsen differs only slightly from the material of *Ceraurus* (*Ceraurus*) *tuberosus* Troedsson, 1928.

Several previous studies of the Avalanche Lake sections allow for age correlation. Wang et al. (1993) described a distinct assemblage of *Cryptolithus*, *Anataphrus*, and *Robergiella* occurring below the latest Ordovician extinction within AV4B. This fauna occurs in association with latest Ordovician conodonts from AV4B described by Nowlan et al. (1988) and Over and Chatterton (1987). Chatterton and Ludvigsen (1983) assigned strata from Avalanche Lake 1 to the Upper Ordovician based on the occurrence of species of *Bathyrurus*, *Isotelus*, *Ceraurinella*, and rare specimens of *Dimeropyge* and *Ceraurus*, all of which appear in the Avalanche Lake 4B section. In addition, they recognized a deep water trilobite association dominated by species of *Cryptolithus* and *Anataphrus*, with rare specimens of *Ampyxina*, *Cybeloides*, *Harpidella*, and *Robergiella* that are identical to the shale fauna within the upper beds of AV4B.

Analysis of other faunal components that occur in association with the trilobites within the AV4B and AV1 sections also indicate an Ashgill age. Conodont biostratigraphy (Nowlan et al., 1988) of AV1 and AV4B shows the presence of *Decoriconus costulatus* (Rexroad) in the upper part of the sequence that is known from latest Ordovician to Silurian strata elsewhere. Jin and Chatterton (1997) note that the brachiopod faunal succession corresponds closely to the trilobite and conodont faunal turnovers in the Avalanche Lake area. Brachiopods such as *Epitomyonia sekwiensis*, *Dalmanella edgewoodensis*, and *Brevilamnulella laevis* are associated with the Ordovician-Silurian boundary, and indicate the presumed position of the boundary at AV4B and AV1. *Brevilamnulella* is considered primarily a genus of late Ashgill age, and occurrences are summarized by Jin and Chatterton (1997). Ostracod faunas (Copeland, 1989) from AV4B consisting of *Platylolbina* (*Reticulobolbina*) *lenzi*, *Steusloffina* sp. cf. *S. cuneata*, and *Lambeodella uniloculata*, components of the *P(R.) lenzi* assemblage, indicate an Upper Ordovician (Richmondian-Gamachian?) age.

Trilobite material from lower in the Avalanche Lake sections may not be Ashgill in age. The section consists of over 100 m of strata from the lowest level of exposure to the Ordovician-Silurian boundary. *Bathyurus teresoma* n. sp. within the low intervals of AV4B and AV1 is most similar to *Bathyurus esbataottinensis*, described and illustrated by Ludvigsen (1979) from the Blackriveran of the Mackenzie Mountains. The new species of *Bathyurus* indicates that the Avalanche Lake material is at least younger than the Blackriveran. Other species described from the Blackriveran of the Mackenzie Mountains by Ludvigsen (1979) also appear in the Avalanche Lake material, including *Ceraurina brevispina*, *Ceraurus mackenziensis*, *Borealaspis whittakerensis*, *Ceraurus serratus*, and species of *Sphaerocoryphe*, *Acanthoparypha*, *Holia*, *Sphaerexochus*, and *Cybeloides*. The overlap of species composition with the Blackriveran material suggests a similar age, and possibly slightly younger, for the lower portions of the Avalanche Lake sections.

The Hirnantia Fauna

Throughout the world, the uppermost Ordovician trilobite and brachiopod faunas are distinctive and differ markedly from those of the underlying middle Ashgill in composition and diversity.

The Hirnantian fauna is a geographically widespread and distinctive brachiopod fauna that occurs near the boundary between the Ordovician and Silurian. It appeared suddenly at the beginning of the Hirnantian (Late Ashgill), spread rapidly, and became extinct as a complete fauna beneath the *G. persculptus* Zone. In recent years, several workers have recognized the extraordinarily widespread brachiopod fauna that occurs in the Hirnantian. Rong (1984) summarized previous studies on this fauna from different regions of the world. Despite the widespread geographical distribution of the fauna and variation in generic composition, the majority of the typical Hirnantian faunas are comprised of *Hirnantia sagittifera* (M'Coy), *Dalmanella testudinaria* (Dalman), *Kinnella kielanae* (Temple), *Paromalomena polonica* (Temple), *Eostropheodonta hirnantensis* (M'Coy) and *Plectothyrella crassica* (Dalman). This brachiopod fauna usually is associated with the trilobite genera *Dalmanitina*, *Brongniartella*, *Platycoryphe*, and *Eoleonaspis* (Rong, 1984). In addition, most Hirnantian trilobite faunas are low diversity (Owen et al., 1991).

Sheehan (1975) postulated that the development of glaciers during the end-Ordovician was accompanied by the expansion of a cold water fauna that originated in the high latitudinal Mediterranean Province. The hypothesized configuration of continents in the Late Ordovician (Fig. 1.8) shows that the Hirnantian fauna existed in eastern North America, northern Europe, and Asia; these paleocontinents were widely separated, and situated close to the paleoequator during the Late Ordovician. Contraction of temperate

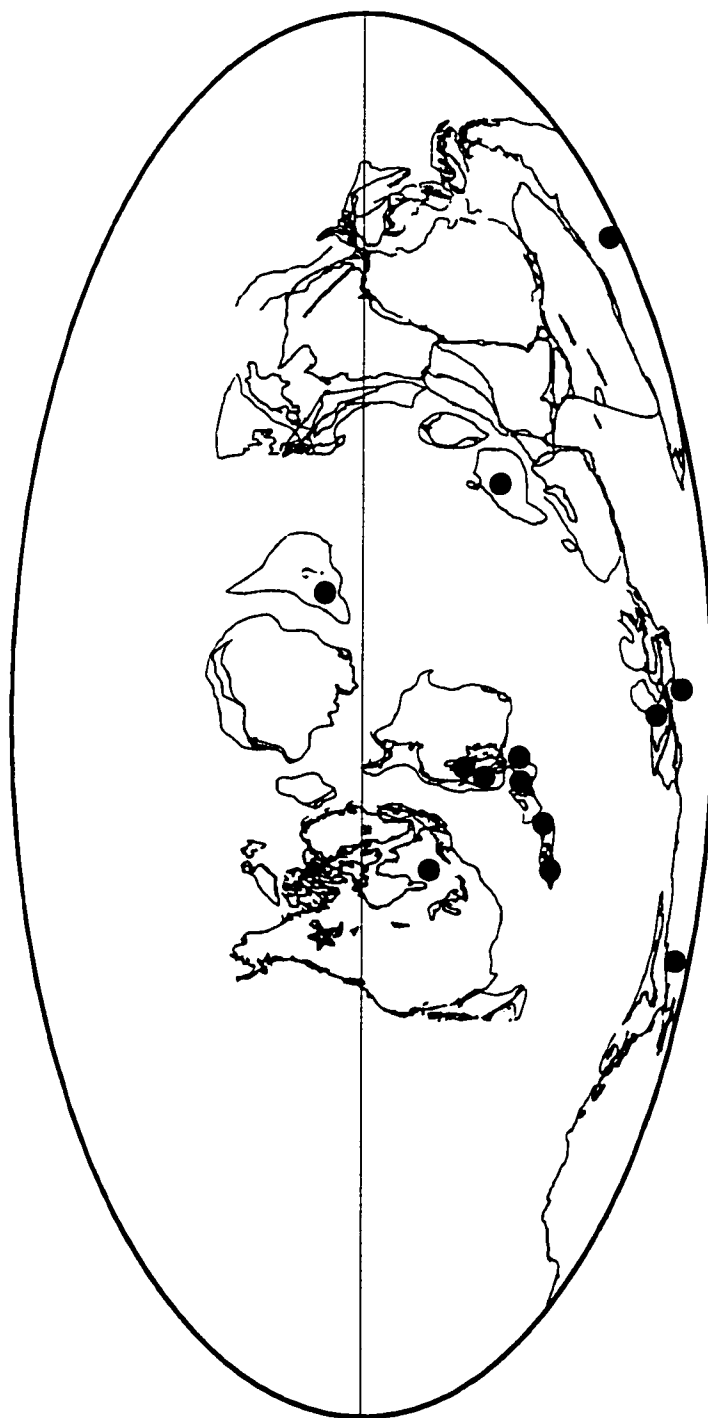


Figure 1.8. Global distribution pattern of Hirnantian faunas during the late Ordovician (Ashgill); based on data from various sources, summarized in Rong, 1984; Rong and Harper, 1988. Selwyn Basin indicated by the star. Ordovician globe after Scotese and McKerrow, 1991.

climatic belts during the Late Ordovician glaciation, as suggested by Brenchley and Cullen (1984), and extension of cooler surface waters during the glaciation would allow the range of the fauna to extend into temperate and subtropical climatic belts (Rong, 1984).

Lenz and Churkin (1966) described a late Upper Ordovician (Ashgill) trilobite fauna from the Road River Formation of the Yukon that is consistent with material from AV4B and does not contain any index species of the Hirnantian fauna. This assemblage occurs within the same region as Avalanche Lake 4B, in the Selwyn Basin. The fact that these two assemblages do not contain any representatives of the Hirnantian fauna suggests that a regional distinction, either physical or environmental, did not allow for migration or occurrence of the Hirnantian fauna into this region.

There are several possible explanations for the absence of the Hirnantian fauna at Avalanche Lake. Reconstruction of the continental configurations and Hirnantian faunal distributions for the Late Ashgill indicate a strong relationship between the location of known Hirnantian faunas and the position of the Gondwanan ice sheets (Fig. 1.8). Most apparent is the observation that most occurrences of the Hirnantian fauna are situated in the Southern Hemisphere, in a polar or subtemperate climatic belt. The position of North America during the Ordovician places the Avalanche Lake region in an equatorial climatic belt, slightly above the equator. These latitudinal differences would account for variation in climate and oceanic temperatures that may have been a barrier to the dispersal of the Hirnantian fauna into the Avalanche Lake region. The Hirnantian fauna is considered to be a cool, shallow water fauna that evolved in the cool surface waters of the end-Ordovician glaciation event (Brenchley and Cullen, 1984). Equatorial waters, such as at Avalanche Lake, may have been too warm for the Hirnantian fauna to develop, and therefore a barrier to dispersal. In contradiction, Kazakhstan occurred within a similar latitudinal belt as the Selwyn Basin, yet the Hirnantian fauna is present. There is debate as to the position and configuration of Kazakhstan during the Late Ordovician that makes the data from this region questionable. Previous reconstructions have treated Kazakhstan as a separate and independently moving paleocontinent. Scotese and McKerrow (1991) now propose that Kazakhstan was an amalgamation of volcanic arcs and independent terranes. In light of this new view, the position and configuration of the part of Kazakhstan containing these faunas in the Upper Ordovician is uncertain, and paleogeographical data derived from this region currently have limited value.

Several researchers have suggested that the Selwyn Basin was restricted during the Late Ordovician and Early Silurian. Goodfellow and Jonasson (1984) proposed restriction of the Selwyn Basin based upon increased values in isotopes of pyrite. Their data suggests that during the Late Ordovician and Early Silurian the Selwyn Basin was at least partially

restricted from open ocean waters. Deposition of dark, well-laminated micritic limestones and shales at AV4B resulted from these reducing environments (Wang et al., 1993). Lenz and McCracken (1982) suggested that the lowering of the sea level during the end-Ordovician glaciation may have caused a sufficient restriction of basinal areas to hamper migration into the region. They concluded that restriction of the Sewlyn Basin may have been the result of fluctuating sea levels near the Ordovician-Silurian boundary. Nowlan et al. (1988) noted that conodonts of North Atlantic Province affinity are sparse to absent in the Upper Ordovician of the Avalanche Lake sections and that trilobites of deeper, quieter water aspect occur in the Avalanche Lake samples which may suggest that the basin was cut off from open ocean circulation. Conodonts of North Atlantic affinity are present during the Middle Ordovician of the southern Mackenzie Mountains (Tipnis et al., 1978). Restricted circulation of the Selwyn Basin during the Upper Ordovician and Lower Silurian may account for the absence of the distinctive, biostratigraphically important North Atlantic Province conodonts and the cosmopolitan Hirnantian fauna from the region, which prevented index species of the latest Ordovician conodont zone from entering the basin.

The Late Ordovician Mass Extinctions

The end of the Ordovician is known as one of the several Phanerozoic mass extinctions (Sepkoski, 1982). Although there have been several glaciations during the history of the earth, the glaciation at the end of the Ordovician is of particular interest because of the short duration of the pronounced glaciation and resultant facies changes can often be identified precisely in the stratigraphic record (Brenchley and Newall, 1984). Paleontological studies in northern Canada have shown that this extinction affected many faunal groups, including trilobites, conodonts, graptolites, and ostracodes of northwestern Laurentia (Wang et al., 1993).

During the Upper Ordovician a series of sea level changes occurred that coincided with a well established glacial episode in the Southern Hemisphere. Evidence for glaciation on Gondwana, such as the presence of glaciomarine diamictites, center around Saharan Africa and South Africa, with evidence for the presence of ice in present day Portugal, Czechoslovakia, Morocco, South America, and Europe (Brenchley et al., 1991). The late Ordovician Gondwana glaciation was of continental dimensions and appears to have extended from the south pole through at least 40 degrees of latitude (Brenchley, 1988).

The Late Ordovician extinction occurred in two main phases, separated by approximately 0.5-1 m.y.a. (Brenchley and Marshall, 1999). The first phase, thought to occur across the Rawtheyan-Hirnantian boundary is indicated by a dramatic decrease in animal diversity, and a lithofacies change on marine clastic shelves from mudstones to a

variety of shallow marine lithofacies (Brenchley, 1988). This change coincided approximately with the start of a substantial glacio-eustatic drop in sea level. Generic diversity shows a decrease at the end of the Rawtheyan, with only a 25% survival rate into the Hirnantian (Brenchley, 1984). Evidence suggests that this initial wave of extinction was the result of global cooling rather than a reduction in habitable area resulting from lowering sea level. Cooling temperatures, contraction of climatic belts, and related climatic changes would certainly have had an influence on the distribution of fauna in the short term (Brenchley and Newall, 1984). The second phase of extinction, occurring near the Ordovician-Silurian boundary, correlates with the melting of the ice cap and a resultant rapid global transgression, marked by a major lithofacies change from shallow to deep water facies.

Avalanche Lake 4B and Avalanche Lake 1 are important sections because they span the Ordovician-Silurian boundary. The finely resolved faunal and stratigraphic data from these sections provide vital information regarding faunal and sedimentological changes during this time of environmental instability.

Literature Cited:

- Adrain, J.M., and Chatterton, B.D.E. 1994. The aulacopleurid trilobite *Otarion*, with new species from the Silurian of northwestern Canada. *Journal of Paleontology*, 68(2): 305-323.
- Adrain, J.M., and Chatterton, B.D.E. 1995a. Aulacopleurine trilobites from the Llandovery of northwestern Canada. *Journal of Paleontology*, 69(2): 326-340.
- Adrain, J.M., and Chatterton, B.D.E. 1995b. The otarionine trilobites *Harpidella* and *Maurotarion*, with species from northwestern Canada, the United States, and Australia. *Journal of Paleontology*, 69(2): 307-326.
- Boggs, S., jr. 1987. *Principles of Sedimentology and Stratigraphy*. Merrill Publishing Company. Columbus, Ohio, 784 p.
- Brenchley, P.J. 1984. Late Ordovician extinctions and their relationship to the Gondwana glaciation. In: P.J. Brenchley (ed.), *Fossil and Climate*, John Wiley and Sons Ltd., pgs. 291-315.
- Brenchley, P.J. 1988. Environmental changes close to the Ordovician-Silurian boundary. *Bulletin of the British Museum of Natural History*, 43: 377-385.
- Brenchley, P.J., and Cullen, B. 1984. The environmental distribution of associations belonging to the Hirnantia fauna - evidence from North Wales and Norway. In: Bruton, D.L. (ed.), *Aspects of the Ordovician System*. Palaeontological Contributions from the University of Oslo, 295: 113-125.
- Brenchley, P.J., and Marshall, J.D. 1999. Relative timing of critical events during the late Ordovician mass extinction - new data from Oslo. *Acta Universitatis Carolinae - Geologica*, 43(1-2): 187-190.
- Brenchley, P.J., and Newall, G. 1984. Late Ordovician environmental changes and their effect on faunas. In: D.L. Bruton (ed.), *Aspects of the Ordovician System*. Palaeontological Contributions from the University of Oslo, 295: 65-79.
- Brenchley, P.J., Romano, M., Young, T.P., and Storch, P. 1991. Hirnantian glaciomarine diamictites - evidence for the spread of glaciation and its effect on Upper Ordovician faunas. In: *Advances in Ordovician Geology*, C.R. Barnes and S.H. Williams (eds.), Geological Survey of Canada, Paper 90-9: 325-336.
- Caldwell, M.W., and Chatterton, B.D.E. 1995. Phylogenetic analysis of some Silurian rostroconchs (Mollusca) from northwestern Canada. *Canadian Journal of Earth Sciences*, 32(6): 806-827.
- Chatterton, B.D.E. 1980. Ontogenetic studies of Middle Ordovician trilobites from the Esbataottine Formation, Mackenzie Mountains, Canada. *Palaeontographica Abt. A*, 171: 1-74.
- Chatterton, B.D.E., and Ludvigsen, R. 1976. Silicified Middle Ordovician trilobites from the South Nahanni River area, District of Mackenzie, Canada. *Palaeontographica Abt. A*, 154: 1-106.

- Chatterton, B.D.E., and Ludvigsen, R. 1983. Trilobites from the Ordovician-Silurian boundary of the Mackenzie Mountains, northwestern Canada. Papers for the Symposium on the Cambrian-Ordovician and Ordovician-Silurian Boundaries. Nanjing Institute of Geology and Palaeontology, Academia Sinica, p. 146-147.
- Chatterton, B.D.E., and Perry, D.G. 1983. Silicified Silurian odontopleurid trilobites from the Mackenzie Mountains. *Palaeontographica Canadiana*, 1: 1-127.
- Chatterton, B.D.E., and Perry, D.G. 1984. Silurian cheirurid trilobites from the Mackenzie Mountains, northwestern Canada. *Palaeontographica*, Abt. A, 184: 1-78.
- Chatterton, B.D.E., Edgecombe, G.D., and Tuffnell, P.A. 1990. Extinction and migration in Silurian trilobites and conodonts of northwestern Canada. *Journal of the Geological Society, London*, 147: 703-715.
- Copeland, M.J. 1974. Middle Ordovician Ostracoda from southwestern District of Mackenzie. *Geological Survey of Canada, Bulletin* 244: 1-55.
- Copeland, M.J. 1978. Some Wenlockian (Silurian) Ostracoda from southwestern District of Mackenzie. *Geological Survey of Canada, Paper* 78-1B: 65-72.
- Copeland, M.J. 1982. Bathymetry of early Middle Ordovician (Chazy) ostracodes, lower Esbataottine Formation, District of Mackenzie. *Geological Survey of Canada, Bulletin* 347: 1-39.
- Copeland, M.J. 1989. Silicified Upper Ordovician-Lower Silurian ostracodes from the Avalanche Lake area, southwestern District of Mackenzie. *Geological Survey of Canada, Bulletin* 341: 1-100.
- Edgecombe, G.D., and Chatterton, B.D.E. 1990. Systematics of *Encrinuroides* and *Curriella* (Trilobita), with a new Early Silurian encrinurine from the Mackenzie Mountains. *Canadian Journal of Earth Sciences*, 27: 820-833.
- Edgecombe, G.D., and Chatterton, B.D.E. 1992. Early Silurian (Llandovery) encrinurine trilobites from the Mackenzie Mountains, Canada. *Journal of Paleontology*, 66(1): 52-74.
- Gabrielse, H., Blusson, S.L., and Roddick, J.A. 1973. Geology of Flat River, Glacier Lake, and Wrigley Lake Map-Areas, District of Mackenzie and Yukon Territory, Pt I: General geology, structural geology, and economic geology; Pt. 2: Measured sections. *Geological Survey of Canada, Memoir* 366: Pt. 1: 1-153; Pt. 2: 1-267.
- Goodfellow, W.D., and Jonasson, I.R. 1984. Ocean stagnation and ventilation defined by $\delta^{34}\text{S}$ secular trends in pyrite and barite, Selwyn Basin, Yukon. *Geology*, 12: 583-586.
- Jin, J., and Chatterton, B.D.E. 1997. Latest Ordovician-Silurian articulate brachiopods and biostratigraphy of the Avalanche Lake area, southwestern District of Mackenzie, Canada. *Palaeontographica Canadiana*, 13: 1-167.

- Johnson, D.I., and Chatterton, B.D.E. 1983. Some silicified Middle Silurian rostroconchs (Mollusca) from the Mackenzie Mountains, N.W.T., Canada. *Canadian Journal of Earth Sciences*, 20: 844-858.
- Lenz, A.C., and Churkin, M. 1966. Upper Ordovician trilobites from Northern Yukon. *Palaeontology*, 9(1): 39-47.
- Lenz, A.C., and McCracken, A.D. 1982. The Ordovician-Silurian boundary, northern Canadian Cordillera: graptolite and conodont correlation. *Canadian Journal of Earth Sciences*, 19: 1308-1322.
- Ludvigsen, R. 1975. Ordovician formations and faunas, southern Mackenzie Mountains. *Canadian Journal of Earth Sciences*, 12: 663-697.
- Ludvigsen, R. 1978. Middle Ordovician trilobite biofacies, southern Mackenzie Mountains. In, *Western and Arctic Canadian Biostratigraphy*, C.R. Stelck and B.D.E. Chatterton (eds.), Geological Association of Canada Special Paper 18: 1-37.
- Ludvigsen, R. 1979. A trilobite zonation of Middle Ordovician rocks, southwestern District of Mackenzie. *Geological Survey of Canada, Bulletin* 312: 1-99.
- Mitchell, C.E., and Sweet, W.C. 1989. Upper Ordovician conodonts, brachiopods, and chronostratigraphy of the Whittaker Formation, southwestern District of Mackenzie, N.W.T., Canada. *Canadian Journal of Earth Sciences*, 26: 74-87.
- Nowlan, G.S., McCracken, A.D., and Chatterton, B.D.E. 1988. Conodonts from Ordovician-Silurian boundary strata, Whittaker Formation, Mackenzie Mountains, Northwest Territories. *Geological Survey of Canada, Bulletin* 373: 1-99.
- Over, D.J., and Chatterton, B.D.E. 1987. Silurian conodonts from the southern Mackenzie Mountains, Northwest Territories, Canada. *Geologica et Palaeontologica*, 21: 1-49.
- Owen, A.W., Harper, D.A.T., and Rong, J. 1991. Hirnantian trilobites and brachiopods in space and time. In, C.R. Barnes and S.H. Williams (eds.), *Ordovician Geology*. Geological Survey of Canada, Paper 90-9: 179-190.
- Perry, D.G., and Chatterton, B.D.E. 1979. Wenlock trilobites and brachiopods from the Mackenzie Mountains, northwestern Canada. *Palaeontology*, 22(3): 569-607.
- Rigby, J.K., and Chatterton, B.D.E. 1994. New Middle Silurian hexactinellid sponge from the Mackenzie Mountains, Northwest Territories, Canada. *Journal of Paleontology*, 68(2): 218-223.
- Rigby, J.K., and Chatterton, B.D.E. 1999. Silurian (Wenlock) demosponges from the Avalanche Lake area of the Mackenzie Mountains, southwestern District of Mackenzie, Northwest Territories, Canada. *Palaeontographica Canadiana*, 16: 1-43.
- Rong, J. 1984. Distribution of the Hirnantia fauna and its meaning. In, Bruton, D.L. (ed.), *Aspects of the Ordovician System*. *Palaeontological Contributions from the University of Oslo*, 295: 113-125.

- Rong, J., and Harper, D.A.T. 1988. A global synthesis of the latest Ordovician Hirnantian brachiopod faunas. *Transactions of the Royal Society of Edinburgh: Earth Sciences*, 79: 383-402.
- Ross, R.J., Nolan, T.B., and Harris, A.G. 1979. The Upper Ordovician and Silurian Hanson Creek Formation of Central Nevada. *Shorter Contributions to Stratigraphy and Structural Geology*. United States Geological Survey, Professional Paper 1126-C: C1-C22.
- Scotese, C.R., and McKerrow, W.S. 1991. Ordovician plate tectonic reconstructions: In *Advances in Ordovician Geology*, C.R. Barnes and S.H. Williams (eds.), Geological Survey of Canada, Paper 90-9: 271-282.
- Sepkoski, J.J., Jr. 1982. Mass extinctions in the Phanerozoic oceans: A review. *Geological Society of America, Special Paper* 190: 283-289.
- Siveter, D.J., and Chatterton, B.D.E. 1996. Silicified calymenid trilobites from the Mackenzie Mountains, northwest Canada. *Palaeontographica Abt. A*, 239: 43-60.
- Sheehan, P.M. 1975. Brachiopod synecology in a time of crisis (Late Ordovician-Early Silurian). *Paleobiology* 1: 205-212.
- Tipnis, R.S., Chatterton, B.D.E., and Ludvigsen, R. 1978. Ordovician conodont biostratigraphy of the southern District of Mackenzie, Canada. In, C.R. Stelck and B.D.E. Chatterton (eds.), *Western and Arctic Canadian Biostratigraphy*, Geological Association of Canada Special Paper 18: 39-91.
- Troedsson, G.T. 1928. On the Middle and Upper Ordovician faunas of northern Greenland, part 2. *Jubilae Umsekspeiditionen Nord om Gronland. Meddelelser om Gronland*, 72: 1-197.
- Wang, K., and Chatterton, B.D.E., Attrep, M., and Orth, C.J. 1993. Late Ordovician mass extinction in the Selwyn Basin, northwestern Canada: geochemical, sedimentological, and paleontological evidence. *Canadian Journal of Earth Sciences*, 30: 1870-1880.
- Yu, F. 1996. Ontogeny, taxonomy, and taphonomy of some Upper Ordovician silicified trilobites from eastern Nevada, U.S.A. Unpublished M.Sc. thesis, University of Alberta at Edmonton, Alberta, 154 p.

Chapter 2: Systematic Paleontology

Order Corynexochida Kobayashi, 1935

Suborder Illaenina Jaausson, 1959

Family Illaenidae Hawle & Corda, 1847

Subfamily Illaeninae Hawle & Corda, 1847

Genus *Bumastoides* Whittington, 1954

Type Species: *Illaeus milleri* Billings, 1859, from the Trentonian of Ontario and Quebec.

Diagnosis: This diagnosis follows Whittington, 1954. Axial furrows of cephalon faint or absent. Raised crescentic area visible on inner surface of exoskeleton. Eye lobe small, less prominent, farther from midline; 8 to 10 thoracic segments; maximum width (tr.) of pygidium opposite point about half length (sag.).

Bumastoides solangeae n. sp.

Pl. 1, figs. 1-26

Etymology: This species is named for my mother, Solange.

Material: 74 cranidia, 150 librigenae, 21 hypostomes, 60 thoracic segments, and 139 pygidia.

Stratigraphic Occurrence: AV4B 3m - 47.75m; 98AV4B 6.25m - 50.4m.

Holotype: Holotype pygidium UA 15535; paratypes UA 11517 - UA 11534, UA 11536 - UA 11539.

Diagnosis: A species of *Bumastoides* with a subcircular cranidial outline; dorsal axial furrows on cephalon imperceptible; free cheek with subtriangular outline and subangular genal angles; margin of free cheek distinctly deflected outward in a curve a short distance behind most anterior part of dorsal surface; anterior margin of pygidium strongly convex; posterior margin of pygidium weakly convex backwards medially; pygidial length to width ratio approximately 3:4; no ventral protuberant ridge along sagittal line of doublure.

Description:

Cranidium: Cranidium is subcircular in outline, inflated, globose. Axial furrows are imperceptible to absent on dorsal and ventral surfaces. Anterior margin distinctly convex forward. Anterior slope of cranidium is moderately steep. Cranidium most inflated near midlength of glabella. Outer surface lacks any sculpture. Facial suture is laterally convex at palpebral lobes. Anterior branch of facial suture runs anteromedially from eyes, at about 10 to 20 degrees to exsagittal line. Posterior branch of facial suture runs back and downward a short distance, diverging slightly from exsagittal line. Palpebral lobes are situated posteriorly. Weak expression of medially convex lunettes occurs ventrally,

opposite palpebral lobe, approximately one-quarter width of cephalon from lateral margin. Occipital doublure is weakly convex forward, broadest (sag.) medially, tapers out laterally.

Free Cheek: Free cheek subtriangular in outline, lacks genal spines in mature stages. Eyes are small, laterally convex, and placed posteriorly. Dorsal surface lacks sculpture. Weak terrace lines are visible on anterolateral margin, on ventral surface anteriorly, particularly along inner margin of doublure. Surface of free cheek is upturned along base of visual surface. Doublure is turned sharply inward around margin. Inner margin of anterior portion of doublure extends medially under front of cranidium. Doublure is broadest (tr.) at genal angle, and thins anteriorly. Inner margin of doublure is approximately transverse. Margin of cheek distinctly deflected outward a short distance behind anterior extension of dorsal surface.

Hypostome: Hypostome is subtrapezoidal in outline. Anterior margin is slightly concave forward medially, convex forward laterally. Anterior border furrow imperceptible. Anterior lobe is subtriangular, bordered by moderately impressed, broad lateral border furrows and shallow middle furrows. Posterior lobe is small, crescentic, slightly inflated. Maculae are indistinct. Posterior border furrow and posterior parts of lateral border furrows are broad and shallow. Shoulders are rounded convex laterally opposite end of middle furrows. Short anterior wings project outward and upward. Doublure is of sub-even width medially and laterally. Posterior border is slightly convex backward to transverse. No sculpture visible.

Thorax: Number of thoracic segments not known. Thoracic segments are moderately arched. Axis is broad, approximately two-thirds width of segments. Axial furrows are weak to imperceptible. Axial doublure is longest (sag.) medially, tapers laterally to axial furrow. Axial doublure covers approximately two-thirds of distance to anterior margin of thoracic segment. Anterior portions of pleurae are faceted. Pleural doublure broad, extending almost to axial furrow along posterior margin. Medially and anteriorly doublure extends about one-half distance from distal end of segment to axial furrow before terminating in a fairly straight inner margin (sag.). Inner margin of doublure is slightly raised in front of weak panderian notch. Articulating devices consist of a socket on anterior margin and a process on posterior margin, both located in region of axial furrow of pleurae. Pleural tips are pointed posteriorly.

Pygidium: Pygidium is rounded and flared backward in outline, moderately inflated. Anterior margin is strongly convex forward. Articulating devices along anterior margin are present as notches. Anterior margin has thickening of exoskeleton in band, visible on ventral surface. No ornamentation on dorsal surface. Axial furrows absent on dorsal surface. Interpleural furrows (2 to 3) visible anteriorly on dorsal and ventral surfaces

of transitory pygidia. Doublure is broad; longest (exsag.) on either side of a median concave region of internal margin giving internal scalloped appearance; length of doublure fairly even lateral of medially scalloped region. Posterior margin slightly convex backwards.

Discussion:

Bumastoides solangeae n. sp. is placed with other members of the genus *Bumastoides* based on the absence of dorsal axial furrows, lunettes visible on the inner surface of the cranidium, and small eye lobes situated far from the midline (Raymond, 1916). The material of *B. solangeae* n.sp. from the Whittaker Formation, Avalanche Lake closely resembles middle Ordovician material of *Bumastoides lenzi* described from the Esbataottine Formation, District of Mackenzie by Chatterton and Ludvigsen (1976). Based on ventral cephalic characters outlined in Lane and Thomas (in Thomas, 1978). *Bumastoides* was elevated to generic level in Chatterton (1980).

Other similar species from the middle Ordovician of eastern North America include *Bumastoides milleri* (Billings, 1859; Whittington, 1954), *B. billingsi* (Raymond and Narraway, 1908), *B. porrectus* (Raymond, 1925) and *B. aplatus*. *Bumastoides aplatus* was originally described by Raymond (1925) as a species of *Bumastus* and later placed in *Bumastoides* by Shaw (1968).

Bumastoides solangeae n. sp. is distinguished from previously described species by the shape of the cranidium and pygidium. The cranidium is more circular in outline, with an approximately equivalent length to width ratio relative to all other described species. The anterior margin of the pygidium is more convex forward and the posterior margin is more transverse than in any other described species.

In addition, the Whittaker material differs from the types of *Bumastoides lenzi* in a less strongly down-curved anterior lateral profile, the absence of dorsal axial furrows, a more triangular outline of the free cheek, a more transverse inner margin of the doublure of the free cheek, and the absence of a median sagittal ridge on the doublure of the pygidium. The free cheek of *Bumastoides solangeae* retains the triangular outline found in juveniles of *B. lenzi*, but has lost the genal spine, unlike the juveniles of *B. lenzi*. The Whittaker material differs from the types of *B. milleri* in the lack of a median pustule on the cranidium, lack of visible lunettes on the dorsal surface of the cranidium, and in the absence of a low sagittal ridge on the inner surface of the pygidium.

Features of the cranidium of the Whittaker material differs from *Bumastoides billingsi* and *B. porrectus* in the absence of axial furrows and lunettes on the dorsal surface and a less strongly down-curved anterior lateral profile.

Bumastoides solangeae differs from *B. aplatus* in the absence of dorsal axial furrows, absence of a median tubercle on the posterior part of the glabella, the more angular shape of the genal angle of the free cheek, the convex anterior margin of the pygidium (angulate margin absent) and the absence of a low median ridge on the doublure of the pygidium.

Specimens from the Whittaker Formation, Avalanche Lake include transitory pygidia. These differ from the other pygidia by the presence of 2 to 3 anterior furrows that delineate the protothoracic segments and are visible on the dorsal and ventral surfaces, and a shallower scalloping of the doublure of the pygidia. These transitory pygidia are smaller in size, adult pygidia are approximately 2.5 times larger.

Genus *Failleana* Chatterton & Ludvigsen, 1976

Type Species: *Failleana calva* Chatterton and Ludvigsen, 1976, from the lower Esbataottine Formation, Sunblood Range, southern District of Mackenzie.

Diagnosis: This diagnosis follows Chatterton and Ludvigsen, 1976. Illaenids that are slightly or moderately inflated; have a broad thoracic axis; large eyes placed far back on the head; and shallow axial furrows in mature individuals. The axial furrows converge forward sharply opposite the occipital ring, converge moderately from the occipital furrow to a point opposite or in front of the eyes, and then diverge forward as far as a pair of faint pits (in the dorsal surface - or medially socketed projections of the ventral surface). In front of the pits, the axial furrows either disappear or diverge laterally. The pygidial doublure is broad and similar in width from front to back. The pygidial axis, when visible, is comparatively short. The length/width ratio of the pygidium apparently increases with maturity; and the pygidium is semicircular to semi-elliptical.

Failleana sp.

Pl. 17, figs. 1-2

Material: 2 cranidia; UA 11784, UA 11785.

Stratigraphic Occurrence: AV4B 9m; 98AV4B 10.3m - 14.5m.

Discussion:

The material of *Failleana* sp. is restricted to two partial cranidia. The material appears characteristic of the genus based on the path of the axial glabellar furrows. Species designation is not permissible with the limited material.

Order Proetida Fortey & Owens, 1975

Family **Bathyuridae** Walcott, 1886

Genus *Bathyurus* Billings, 1859

Type Species: *Asaphus? extans* Hall, 1847, from the Lowville Formation, Mohawk Valley, New York State.

Diagnosis: This diagnosis follows Tremblay and Westrop, 1991. Bathyurine genus with inflated, parallel-sided or forwardly expanded glabella. Axial furrows bowed outwards between palpebral areas in some species. Two or three pairs of shallow, oblique lateral glabellar furrows present. Genal spines long and tapering. Hypostome quadrate in outline with narrow convex borders, deep border furrows and maculae, high anterior wings. Thin, crescentic rostral plate strongly flexed (sag.) and waisted by connective sutures. Pygidium semi-circular to sub-triangular, with deep axial furrows, four pleural furrows, flattened borders.

Bathyurus teresoma n. sp.

Pl. 2, figs. 1-27

Etymology: teres = smooth; soma = body; for the smooth outer surface of the exoskeleton.

Material: 61 cranidia, 184 librigenae, 23 hypostomes, 5 rostral plates, 100 thoracic segments, and 76 pygidia.

Stratigraphic Occurrence: AV4B 14m - 18m; 98AV4B 2.75m - 22.6m; AV1 (-)60m - (-)36m.

Holotype: Holotype cranidium UA 11540; paratypes UA 11541 - UA 11563.

Diagnosis: A species of *Bathyurus* with an effaced dorsal surface; broad anterior cephalic border; lateral glabellar furrows very shallow to imperceptible; palpebral furrow very shallow; palpebral lobe situated posteriorly, posterior edge of lobe opposite S0; shoulders of hypostome project farther laterally than anterior wings; pleural tips of thoracic segments long, pointed posteriorly; pygidial doublure broad.

Description:

Cranidium: Cranidium moderately convex (sag. and tr.). In lateral view, glabella slopes down anteriorly to shallow anterior border furrow; posterior two-thirds of glabella slopes faintly backwards. Glabella subparallel-sided; length (sag.) to width ratio of 3:2; maximum width across frontal lobe. Axial furrow shallow; from occipital ring, axial furrows are subparallel; converging slightly anterior to palpebral lobe to form a slight constriction of glabella; axial furrows curve slightly out and then inward around anterior lobe of glabella to merge with preglabellar furrow. Preglabellar furrow broad, shallow; lateral glabellar furrows very shallow to imperceptible. Width across palpebral area approximately equal to

sagittal length of cranium. Palpebral area semicircular in outline; length (exsag.) approximately one-half length of glabella; posterior edge of lobe situated opposite S0. Palpebral furrow very shallow to imperceptible. In lateral view, palpebral lobe stands below crest of glabella. S0 shallow, transverse. L0 lenticular in outline, distinctly arched (pl. 2, fig. 8); four times as wide as long; longest medially, tapering laterally; stands below crest of glabella. Anterior branch of facial suture strongly divergent; extends from gamma (acute angle) forward in an even curve along path slightly more divergent than glabellar margin. Posterior branch of facial suture proceeds a very short distance backwards and immediately outward from epsilon and proceeds transversely intersecting posterior margin. On interior, occipital doublure extends about one-half distance across occipital ring (sag.). Cranium smooth, fine ridges run around anterior margin (pl. 2, fig. 5).

Free Cheek: Free cheek curved, subtriangular in outline. Genal field slopes steeply to flat lateral border which is broadest anteriorly. Lateral border furrow shallow, represented by a change in slope. Posterior border furrow shallow, almost imperceptible. Inner margin of doublure curved, with suggestion of panderian notch; doublure narrowest anteriorly, widening posteriorly toward genal spine. Genal spine long, gradually tapering, weakly curved backward. Ornamentation consists of parallel running terrace lines along doublure, extending to tip of genal spine.

Rostral plate: Short (tr.) subtriangular anterior portion is bounded by transverse to slightly convex (tr.) rostral suture and strongly anteriorly divergent branches of connective sutures, and wide (tr.), strongly curved (tr.) thin crescentic posterior portion is bounded by posteriorly divergent hypostomal suture. Anterior portion is approximately one-third width (tr.) of posterior section. Surface covered by numerous, transverse, parallel terrace lines.

Hypostome: Hypostome rounded orthogonal in outline; length slightly greater than maximum width across shoulders. Anterior body subcircular in outline, little inflated; posterior body crescentic; also little inflated. Middle furrows faint, directed posteromedially, shallow medially, length at least one-fourth width of middle body. Lateral border furrows shallow, relatively broad; convex laterally opposite shoulders. Posterior border furrow shallow and broad; shallower medially. From anterior wings, lateral border diverges outwards and backwards, opposite middle furrows, lateral border converges posteromedially towards posterior border. Posterior border slightly concave forward and slightly wider (sag.) than lateral border (tr.) at shoulder. Anterior border convex forward; anterior border furrow imperceptible. On interior, posterior doublure narrow (sag.) medially; widens laterally.

Thorax: Number of thoracic segments unknown. Width of axis almost one-third total width of segment. Articulating furrow distinct, nearly straight, bending slightly forward

near axial furrow (pl. 2, fig. 21). Articulating half-ring lenticular in outline, longest medially. Axial furrow weakly incised. Pleural furrow shallow, deepest at midlength, extends approximately one-half length (tr.) of pleura. On interior, axial doublure extends nearly to articulating furrow medially; tapers strongly towards axial furrow (pl. 2, fig. 20). Pleural doublure restricted to pleural spine on, extends one-half distance of pleurae along posterior edge. Inner margin of doublure slightly raised in front of panderian notch. Pleurae terminate in a long, pointed tip. Ornamentation consists of parallel terrace lines that run along inner margin of doublure.

Pygidium: Pygidium subtriangular in outline; maximum width (tr.) slightly greater than length. Anterolateral corner oblique. Axis high and vaulted; one-quarter width of pygidium. Anterior margin of inner regions of pleurae transverse. First axial ring furrow shallow, additional ring furrows imperceptible. Axial furrows shallow, even shallower behind midlength of pygidium (pl. 2, fig. 26). In lateral profile, crest of axis curves downward and backward so that it declines steeply to posterior border. Pleural field declines to flat, moderately broad, concave lateral border. Pleural field crossed by three equally spaced, almost straight interpleural furrows. First pleural furrow very faint on pleural field (pl. 2, fig. 24); additional pleural furrows even shallower to imperceptible. Interpleural furrows shallow near axis, deepening toward lateral border. Doublure broad; widest (exsag.) on either side of a median concave region under axis on internal margin (pl. 2, fig. 27). Posterior margin strongly convex and subangular. Ornamentation consists of terrace lines which run parallel to inner margin of doublure.

Discussion:

Bathyurus teresoma n. sp. is the stratigraphically youngest species of *Bathyurus* in North America. Whittington (1953) initially restricted *Bathyurus* to rocks of Blackriveran age. Ludvigsen (1979) extended the range to include the Upper Whiterock (Chazyan) to near the top of the Blackriveran from his stratigraphic sequences in the Mackenzie Mountains. Tremblay and Westrop (1991) also extended the middle Ordovician range into the Whiterockian with the recognition of three new species from the South Nahanni River District of the Mackenzie Mountains. The presence of *B. teresoma* in the Ashgill of the Mackenzie Mountains further extends the temporal range of the genus.

Other similar *Bathyurus* species from the Middle Ordovician of North America include *Bathyurus ulu*, *Bathyurus esbataottinensis*, *Bathyurus granulosis*, and *Bathyurus platyparius* from the Upper Whiterock (Chazyan) and Blackriveran of the middle and upper Esbataottine Formation, southern Mackenzie Mountains, described and illustrated by Ludvigsen (1979); *Bathyurus nevadensis* Ross 1967 from the Upper Whiterock (Chazyan)

of the southern Mackenzie Mountains (Ludvigsen, 1979); *Bathyurus angustus* from the Upper Whiterock (Chazy) of Nevada, illustrated and described by Ross, 1967; *Bathyurus mackenziensis*, *Bathyurus sunbloodensis*, and *Bathyurus margareti* from the Whiterockian of the South Nahanni River District, Mackenzie Mountains, described and illustrated by Tremblay and Westrop (1991); *Bathyurus superbus* Raymond 1910, from the Middle Ordovician of Oklahoma (Ludvigsen, 1978); and *Bathyurus extans* Hall, 1847 from the Blackriveran, upper Bromide Formation, Oklahoma (Ludvigsen, 1978).

Bathyurus teresoma has several unique characteristics that distinguish the Avalanche Lake material from other Laurentian material. Most striking is the effaced dorsal surface, resulting in a shallow appearance to the furrows of the entire exoskeleton. In addition, the cranidium possesses a broad anterior cephalic margin, surpassed in width (sag.) only by *B. platyparius* (compare Pl. 2, fig. 20 of Ludvigsen, 1979 with Pl. 2, fig. 1 herein); strongly divergent anterior facial sutures; a gently sloping glabella; palpebral lobes which are situated farther posteriorly resulting in the position of the posterior edge of the lobe opposite the occipital furrow; shoulders of the hypostome which project farther laterally than the anterior wings; pleural tips of the thoracic segments that are long and pointed posteriorly; and a broad pygidial doublure.

In addition to the characteristics mentioned above, several features distinguish *B. teresoma* from *B. ulu*. The posterior margin of the hypostome lacks posterolateral spines, and the surface is not covered with a microsculpture of small, asymmetric, chevron-shaped scales.

The Whittaker species differs from *B. esbataottinensis* in having a more rounded outline to the posterior border of the hypostome, and the lack of chevron-shaped scales on the glabella. From *B. granulosus* and *B. platyparius*, *B. teresoma* can be further distinguished by the rounded posterior margin of the pygidium. *B. platyparius* has a unique ornamentation consisting of fine, irregular ridges not found on *B. teresoma*. *B. nevadensis* possesses posterolateral spines on the hypostome, and *B. angustus* possesses a terminal pygidial spine not found in the Whittaker material.

The material of Tremblay and Westrop (1991) differs from the Whittaker material by having a rectangular shaped hypostome with an inflated middle body and the presence of posterolateral spines. In addition to this, *B. mackenziensis* has high, slender, vertically directed anterior wings and *B. sunbloodensis* has a prosopon of coarse granules and irregular wrinkles on the palpebral areas not seen in *B. teresoma*.

Bathyurus superbus Raymond, 1910 differs from *B. teresoma* predominately in the forward position and smaller size of the palpebral lobes.

Family Dimeropygidae Hupe, 1953
Genus *Dimeropyge* Opik, 1937

Type Species: *Sphaerexochus minuta* Nieszkowski, 1857, from the Middle Ordovician Kukruse beds of Estonia.

Diagnosis: This diagnosis follows Chatterton, 1994. Glabellar furrows represented by oval, thinner areas of unornamented shell close to axial furrows, with S2 and S3 distinctly larger than S1, which is located slightly more adaxially; prosopon of tubercles separated by finer granules; free cheek has sharply pointed and hooked tip to conical genal spine, with distinct pit in doublure at genal angle, and anteromedian extension of doublure that curves downward medially; librigenal field usually narrower than lateral border at midlength of free cheek (without genal spine). Hypostome short, subquadrate, and has incomplete anterior margin, which may or may not have anterior median projection; seven or eight thoracic segments, with distinct tuberculose swellings or prominent spinose tubercles on pleurae adjacent to axial furrows, and serially homologous continuations of this pair of rows extend onto front of pygidium and back of cranidium. Pygidial axis has sagittal depression, and composed of three rings and terminal piece; three distinct segments on pygidial pleurae, composed of anterior and posterior pleural bands, and fourth segment represented by pair of subsemicircular areas on either side of terminal piece; marginal spines present on pygidium occur above a steep to subvertical and granulose marginal band.

Dimeropyge sp.

Pl. 17, fig. 3

Material: 1 pygidium; UA 11786.
Stratigraphic Interval: AV4B 44.8m.

Discussion:

The material of *Dimeropyge* sp. consists of one poorly preserved pygidium. Chatterton (1994) illustrated the presence of *Dimeropyge speyeri* from the Upper Whiterockian (Chazy) of the Esbataottine Formation, Mackenzie Mountains. Although very similar, the Whittaker pygidium does not appear to possess the numerous tubercles present on the pygidium of *D. speyeri*. This may be a result of the poor preservation which, in addition to the limited material, does not allow a species diagnosis.

Family Proetidae Hawle & Corda, 1847
Subfamily Tropidocoryphinae Pribyl, 1946
Genus *Decoroproetus* Pribyl, 1946

Type Species: *Proetus decorus* Barrande, 1846.

Diagnosis: This diagnosis follows Owens, 1973. Lateral glabellar furrows commonly weak or absent; prelabellar field typically sigmoidal, but may be concave or straight; tropidium absent; lateral occipital lobes commonly absent, but weakly developed ones occur in some species. Eye socle commonly distinct, with lower margin in some cases defined by incised furrow; thorax of 10 segments; pygidial axis with 5-10 rings, pleural areas with 4-6 pairs of ribs whose pleural furrows deepen and curve more strongly backwards abaxially; postaxial ridge commonly present; sculpture of continuous or discontinuous striations, covering entire dorsal exoskeleton, or localized.

Decoroproetus hankei n. sp.

Pl. 3, figs. 1-26

Etymology: This species is named for paleontologist Gavin F. Hanke.

Material: 79 cranidia, 163 librigenae, 6 hypostomes, and 34 pygidia.

Stratigraphic Interval: AV4B 3m - 16.5m; 98AV4B 6.25m - 17.4m; AV1 77.5m - 95.5m.

Holotype: Holotype cranidium UA 11566; paratypes UA 11564, UA 11565, UA 11567 - UA 11580.

Diagnosis: A species of *Decoroproetus* with wide (sag.) prelabellar field; strongly divergent anterior facial sutures; a slightly upturned anterior border; hypostome with small projections on shoulders and posterior margin; V-shaped terrace lines along anterior margin and anterior lobe of hypostome; imperceptible posterior border furrow of pygidium.

Description:

Cranidium: Cranidium subelliptical in outline. Glabella weakly convex (sag), moderately convex (tr.); as long as wide, moderately inflated, maximum width across L1. Anterior cephalic margin convex forward. Moderately deep axial furrows converge forward slightly across S1 before curving strongly inward to form prelabellar furrow. Glabella weakly pinched across S2. Occipital lobes weak to imperceptible. Occipital furrow moderately deep, weakly convex forward medially and concave forward laterally. Anterior border broad and flat; slightly dorsally upturned, sharply downturned anteriorly; convex (tr.) in anterior view. Anterior border furrow shallow. Palpebral lobes convex laterally slightly, displaced laterally from axial furrow; occur opposite L1; do not stand as high as glabella. Facial suture strongly divergent from palpebral lobe to anterior border furrow; strongly convergent forward opposite anterior border; subparallel a short distance behind palpebral

lobes before diverging strongly backward to posterior margin. S1 moderately impressed, S2 and S3 weakly impressed to almost imperceptible in some specimens. S1 originating opposite anterior half of palpebral lobe; directed strongly inwards and backwards, not reaching occipital furrow; S1 branches medially to form small, elongate transeverse furrow (pl. 3, fig. 4). S2 straight, directed slightly inwards and backwards; S3 small, subparallel with S2, isolated from axial furrow. Adaxial terminations of glabellar furrows reaching equal distance, approximately one-third to one-quarter of maximum distance across glabella. L1 subcircular in outline, slightly inflated; L2 and L3 subrectangular in outline, decreasing in size anteriorly. Preglabellar field wide (sag.), flat, slightly downturned anteriorly prior to reaching anterior border furrow; sigmoidal in lateral view. Occipital ring lenticular in outline; tapers slightly laterally; not as high as glabella; posterior margin of occipital ring weakly convex backwards; in smaller specimens, posterior margin becomes strongly convex backwards (pl. 3, fig. 5). Occipital doublure convex forward; longest medially, tapering laterally. Sculpture on glabella and palpebral lobes consists of fine closely spaced granules; anterior cephalic margin with subparallel ridges and grooves.

Free Cheek: Free cheek subtriangular in outline; have well developed genal spines. Cheek below eye surface descends to flat, shelf-like lateral border. Posterior border furrow deep, shallows posteriorly towards genal spine to join shallower and more angular lateral border furrow at genal angle; both furrows run onto and terminate on genal spine. Doublure of even width from front to back, inner margin slightly curved anteromedially. Ornamentation consists of fine granules on field and lateral border of librigenae; ridges and grooves run parallel along edge of lateral border, along doublure and genal spine.

Hypostome: Hypostome subtrapezoidal in outline, widest anteriorly, outline indented by antennal notch behind a pair of dorsolaterally directed, flat and trapezoidal anterior wings. Anterior border slightly convex forward. Lateral border directed almost backwards behind anterior wings, diverges slightly at shoulders, and behind shoulders border converges slightly to merge with posterior border. Shoulders with small, posterolaterally directed spines. Anterior lobe of middle body long and moderately inflated; posterior lobe short, crescentic, and weakly inflated. Middle body subdivided by shallow to medially imperceptible posteromedially directed middle furrows. Anterior portion of anterior lobe pinched laterally slightly in front of shoulders. Lateral and posterior borders narrow. Lateral border furrow weakly impressed opposite anterior wings, deepening posteriorly towards shoulders; merges posteromedially with a slightly shallower and broader posterior border furrow. Lateral edges of posterior border contain small, posteriorly directed spines. Ornamentation of hypostome consists of inverted V-shaped terrace lines along anterior

margin and on anterior lobe of hypostome and terrace lines that run parallel with lateral and posterior margins.

Thorax: Thoracic segments unknown.

Pygidium: Pygidium semicircular in outline, with at least 3 distinct axial rings and terminal piece in the axis; 5 pairs of ribs visible on each pleurae. Axis of moderate width (tr.), approximately one-third width (tr.) of pygidium; outlined by moderately deep, slightly posteriorly convergent axial furrows. More posterior axial ring furrows shallow medially, deepen laterally. Very short (sag.) interannular lobes behind first two axial rings. Pleurae divided into convex ribs by moderately deep pleural furrows and shallow interpleural furrows. Pleural furrows moderately deep near axis, shallowing and broadening distally to lateral border. Interpleural furrows shallow near axis, deepen near lateral margin. Posterior border furrow very shallow to imperceptible; posterior border poorly defined. Doublure of moderate width, slight concavity present medially. Ornamentation consists of fine closely-spaced granules on dorsal surface and terrace lines that run parallel with margins on doublure surface.

Discussion:

The Whittaker material was assigned to *Decoroproetus* based on the weak to absent lateral glabellar furrows, the sigmoidal preglabellar field (in lateral view), the absence of occipital lobes, and the pleural areas with 4 to 6 pair of ribs. *Decoroproetus* appears to be a conservative genus, and its morphology changes little between species. Material from the Arctic of North America appears similar to the material of Scandinavia, Norway, and the British Isles.

Decoroproetus hankei n. sp. is the first Upper Ordovician proetid described from the Mackenzie Mountains. The literature on Ordovician proetids of North America is limited. Whittington (1963, 1965) described a species of *Phaseolops* from the early Middle Ordovician of the Table Head Formation, western Newfoundland. This taxon shares a broad (sag.) preglabellar field and forwardly divergent anterior facial sutures with *D. hankei*.

Owens (1973) wrote an extensive monograph on the Ordovician and Silurian Proetidae of the British Isles. Nine species of *Decoroproetus* were discussed from Llandeilo to Wenlock strata. Of particular interest, due to similar temporal ranges, are *Decoroproetus piriceps* from the Ashgill (Cautleyan Stage) of Yorkshire; *Decoroproetus* cf. *subornatus* from the Ashgill (?Cautleyan Stage) of Yorkshire; *Decoroproetus asellus* from the Ashgill (Rawtheyan Stage) of the Girvan District, Ayrshire; and *Decoroproetus papyraceus* from the Ashgill (Rawtheyan Stage) of Yorkshire. There are several distinctions between the

Mackenzie Mountains and British species. *D. piriceps* has weakly developed lateral lobes on the occipital ring and a sculpture of fine, continuous striations not found in *D. hankei*. The Whittaker material differs from *D. cf. subornatus* in having a subcircular glabella, the lack of a median occipital tubercle, slightly more divergent anterior facial sutures, and the presence of evenly distributed granules on the cranidium instead of fine raised striations. Differences from *D. asellus* include a sigmoidal preglabellar field in longitudinal section, and the lack of fine continuous striations on the cranidium. Finally, *D. hankei* differs from *D. papyraceus* in having 4 distinct pygidial axial rings, and a granular ornamentation.

Ordovician Scandinavian proetids were described by Owens (1973) and included 9 species of *Decoroproetus*. The Whittaker material appears similar to *Decoroproetus furubergensis* Owens, 1970 with the exception of the lack of a median occipital tubercle and the presence of a granular ornamentation.

Owen (1981) discussed three species of *Decoroproetus* from the Ashgill of the Oslo Region, Norway. These species are similar to those discussed by Owens (1973). *Decoroproetus* aff. *asellus* Esmark, 1833 has a slightly concave preglabellar field, a parallel-sided glabella, and an ornamentation of fine ridges which distinguishes it from the Whittaker material. *Decoroproetus solenotus* Owens, 1970 is different from *D. hankei* in having a narrower anterior cephalic border, and distinct axial and pleural furrows in the pygidium.

Ludvigsen (1978) noted the presence of a proetid from the Trentonian of the Whittaker Formation, southern Mackenzie Mountains. The material is poor and incomplete but represents the closest proetid geographically to *D. hankei*. This proetid appears to have a broad (sag.) preglabellar field, similar to the Avalanche Lake material, but further comparison is difficult.

Other work on the Proetidae of North America include Chatterton and Perry (1977), and Adrain (1997). These studies concentrate on Silurian taxa which are quite distinct from the Whittaker material and will not be discussed.

Family Aulacopleuridae Angelin, 1854
Subfamily Otariioninae Richter & Richter, 1926
Genus Harpidella M'Coy, 1849

Type Species: *Harpes? megalops* M'Coy, 1846, from the middle Llandovery, Silurian, of Boocaun, Cong, Co. Galway, Ireland.

Diagnosis: This diagnosis follows Adrain and Chatterton, 1995. Otariionines with L1 large and with prominent lateral displacement from remainder of glabella; cranidium with strong, even dorsal convexity; preglabellar field typically short, glabella and occipital ring occupying about 70 percent of sagittal length of cranidium in dorsal view; anterior border

short (sag., exsag.), with strong and even dorsal convexity, and similar in length medially and laterally; palpebral lobe of moderate size; lateral and posterior librigenal borders usually of nearly equal width; genal spine long; eye socle prominent and usually bilobate; thoracic axial spine present; pygidium small, even for subfamily, with as few as two, most commonly three, and as many as five axial rings.

Harpidella kurrii Adrain & Chatterton, 1995

Pl. 17, figs. 4-10

Harpidella kurrii Adrain and Chatterton, 1995, p. 310, Pl. 3, figs. 1-15; Pl. 4, figs. 1-32

Material: 68 cranidia, 22 librigenae, and 9 pygidia; UA 11787 - UA 11793.

Stratigraphic Occurrence: AV4B 44m - 90.75m; 98AV4B 6.25m; AV1 46m - 55m.

Holotype: Complete cranidium, UA 9045 from the Whittaker Formation, section Avalanche Lake One, 53.5 - 54.0 m above base (Ashgill), central Mackenzie Mountains, Northwest Territories, Canada, described by Adrain and Chatterton (1995).

Discussion:

The Avalanche Lake material is easily assignable to *Harpidella kurrii* by comparison with the material of Adrain and Chatterton (1995) from the Ashgill of the Whittaker Formation, central Mackenzie Mountains. In addition to the similar temporal and geographic location of the collections, the AV4B specimens have the diagnostic characteristics of this species. These include strongly divergent anterior facial sutures, narrow L1, long occipital ring, and 3 or 4 axial rings on the pygidium.

Order Asaphida Fortey & Chatterton, 1988

Family Asaphidae Burmeister, 1843

Subfamily Isotelinae Angelin, 1854

Genus *Isotelus* DeKay, 1824

Type Species: *Isotelus gigas* DeKay, 1824.

Diagnosis: The diagnosis of the genus follows Moore, 1959. Cephalon and pygidium mostly with poorly defined flattened border. Frontal area moderately long, cephalic axis ill defined, almost obsolete in several species, slightly expanding in front of medium-sized eyes situated somewhat behind transverse mid-line of cranidium; no posterior border furrow; genal angles rounded, pointed, or with short genal spines. Hypostoma almost parallel-sided, posterior margin with broad (tr.), deep notch; anterior lobe short. Thoracic axis considerably broader than pleurae. Pygidial axis broad, poorly defined, almost obsolete in several species; pleural fields smooth or very faintly ribbed.

Isotelus dorycephalus n. sp.

Pl. 4, figs. 1-27

Etymology: dory = spear, cephalus = head; named for the spear shape of the cranidium.
Material: 29 cranidia, 49 librigenae, 62 hypostomes, 78 thoracic segments, and 26 pygidia.
Stratigraphic Occurrence: AV4B 6m - 73m; 98AV4B 6.25m - 48.55m; AV1 46m - 76.5m.
Holotype: Holotype cranidium UA 11582; paratypes UA 11581, UA 11583 - UA 11598.

Diagnosis: A species of *Isotelus* with a broad (sag.) anterior border; strongly angular anterior margin; dorsally upturned anterior border; inner margin of posterior projections of hypostome slightly divergent backward; subangular genal angle; and posterior margin of larger pygidium broad (sag.) forming a posterior projection.

Description:

Cranidium: Glabella moderately convex (sag. and tr.); maximum width across glabella approximately midlength of frontal lobe. Glabella is slightly inflated and surrounded by shallow axial and preglabellar furrows. Axial furrows diverge forward in front of eyes before curving inward to become broad (sag.), shallow preglabellar furrow. Glabella slopes moderately steeply to convex (sag.) preglabellar furrow and flat anterior border. Anterior border sharply angular medially; slightly upturned in lateral view. Occipital and lateral glabellar furrows absent on large cranidia; imperceptible on immature cranidia (pl. 4, fig. 9,12). Palpebral lobes small; subcircular in outline; situated posteriorly; elevated high above glabella. Anterior branch of facial suture diverges forward in front of eye before curving inward joining anterior margin at sagittal line; posterior branch diverges strongly backward to a point beyond palpebral lobe, curving backward to join posterior margin. Posterior border furrow subtransverse; shallow close to axial furrows, slightly deeper distally. Occipital doublure narrow (sag.); slightly wider medially than distally. Glabella smooth in large cranidia; sculpture indistinct in immature cranidia. Immature cranidia possess relatively larger palpebral lobes; wider (tr.) anterior part of fixigena in front of palpebral lobes; and a shorter (sag.) anterior border.

Free Cheek: Main portion of free cheek subtrapezoidal in outline; lack genal spines in largest individuals. Outer surfaces of free cheeks slope down steeply from subvertical eyes. Eyes are stalked, prominent, and raised above rest of genae. Lateral and posterior border furrows shallow to imperceptible. Doublure is broad, sharply inturned posteriorly. A small panderian opening is present anteromedially of genal angle. Anterior edge of opening slightly raised to form panderian notch. An elongate vincular socket is present close to lateral margin of doublure, anterior to genal angle. Genal angle subangular; protruding

slightly beyond posterior border. Ornamentation consists of fine terrace lines that run parallel with margin of doublure.

Hypostome: Hypostome subquadrate in outline; posterior margin deeply notched. Anterior margin subtransverse, curves backward laterally. Anterior margin slopes slightly dorsally in lateral view. Middle body not obviously separated from borders by border furrows. Rounded lateral shoulders present a short distance behind anterior margin. Small, low maculae are present just in front of lateral shoulders. Posterior projections prominent; slightly less than half entire length (exsag.) of hypostome; tapering to a pointed tip; inner margins slightly divergent backward. Doublure is short posteromedially; broad over two posterior projections of posterior border, forms a pair of medially concave and dorsally subangular ridges. Ornamentation consists of fine terrace lines that run subparallel with margins along marginal portions of hypostome and weakly along doublure.

Thorax: Number of thoracic segments unknown. Axis moderately convex (tr.); slightly less than one-third width (tr.) of entire segment. Inner portion of pleurae subhorizontal; outer portion steeply downturned. Moderately impressed pleural furrow runs posterolaterally from near anterior edge of segment, close to axial furrow; shallows and terminates distally on outer portion of pleurae. Outer portion of pleurae curved posteriorly then anteriorly; terminates in rounded to subquadrate tip. Axial doublure short (sag.); anterior margin weakly convex forward; widest medially, tapers laterally toward axial furrow. Pleural doublure widest (tr.) along posterior edge of segment; inner margin transverse, runs exsagittally. A small panderian opening present in doublure lateral of inner margin; anterior edge of opening slightly raised forming panderian protuberance.

Pygidium: Pygidium subtriangular in outline; strongly convex (tr.). In lateral view, pygidium slopes gradually posteriorly for 85% of length (sag.); slopes steeply toward lateral border for remaining length (pl. 4, fig. 25). Axial furrows shallow; deepest anteriorly, shallowing slightly posteriorly. Pleural furrow firmly impressed in first segment. Articulating, axial ring, interpleural and other pleural furrows very shallow to imperceptible. Posterior border furrow shallow. All furrows on dorsal surface of transitory pygidia deeper (pl. 4, fig. 20); posterior margins of transitory pygidia notched posteromedially. Posterior and lateral margins of even width in smaller specimens; in larger forms, posterior margin broad (sag.) medially forming posterior projection; evenly curved (pl. 4, fig. 4). Doublure is moderately wide; even width (tr.) along lateral margin; widest posteromedially. Inner margin more strongly intumed than outer portions. Ornamentation consists of fine terrace lines that run parallel with inner margins of doublure.

Discussion:

Isotelus dorycephalus n. sp. most closely resembles *Isotelus parvirugosus* from the Upper Whiterock (Chazy) of the Esbataottine Formation from the District of Mackenzie (Chatterton and Ludvigsen, 1976). These species both possess a shallow posterior border furrow, the lack of genal spines in mature individuals, posteriorly situated palpebral lobes which are highly elevated above the cranidium, and a strongly convex (tr.) pygidium. There are several features which distinguish *I. dorycephalus* from the Esbataottine material, including a strongly angular and dorsally upturned anterior border, subangular genal angles, slightly divergent inner margins of the posterior projections of the hypostome, the lack of an articulating furrow and fine ridges on the dorsal surface of the thoracic segments, and a broader (sag.) posterior margin of larger holaspide pygidia.

The Whittaker material shows distinctive features that separate it from *Isotelus gigas* (Dekay, 1824) and *Isotelus walcotti*, both described and illustrated by Rudkin and Tripp (1989) from the early Shermanian of the Denley Formation, Trenton Falls Gorge, New York State. *I. dorycephalus* does not possess the fine micro-ornament of fine punctae found on the dorsal surface of *I. gigas*. In addition, the eyes are placed farther posteriorly on the cranidium, the anterior border is strongly angular medially and dorsally upturned, the genal angle is subangular, the pygidium is strongly convex (tr.) without distinct pleural furrows on the dorsal surface, the lateral borders are well defined, and the posterior margin is broad (sag.) in large holaspide pygidia. These differences between *I. dorycephalus* and *I. walcotti* are similar with the addition of narrower (tr.) lateral borders on the cranidium in the latter form.

Ross and Shaw (1972) described and illustrated *Isotelus copenhagenensis* from the Middle Ordovician of the Copenhagen Formation, Nevada. In addition to the distinctive anterior border, *I. dorycephalus* lacks the micro-ornament of fine pits on the dorsal surface, has an angular genal angle, has slightly more divergent forward anterior facial sutures, and slightly divergent inner margins of the posterior projections of the hypostome.

Finally, several new species of *Isotelus* were described by Tripp and Evitt (1986) from the Middle Ordovician of the lower Edinburg, lower and upper Lincolnshire, Oranda, and Martinsburg Formations of Virginia. *Isotelus giselae* has slightly posteriorly divergent inner margins of the posterior projections of the hypostome in a similar manner to the Whittaker material. In all other respects, the two species are quite different. In addition to the unique anterior border, *I. dorycephalus* does not have well defined axial furrows, the palpebral lobes are larger and situated farther posteriorly on the cranidium, and there is a shallow posterior border furrow present. *Isotelus* spp. A-E of Tripp and Evitt (1986) are identified on incomplete material. *Isotelus* sp. A has small palpebral lobes which are

situated further anteriorly and not elevated above the cranidium, a weakly convex (tr.) pygidium, and a poorly defined lateral pygidial border. *Isotelus* sp. B has a finely pitted surface, anteriorly positioned palpebral lobes, and narrower (tr.) posterior projections of the hypostomes with a less convex lateral outline. *Isotelus* spp. C-E are defined solely on the hypostomes which appear in Tripp and Evitt (1986) as reconstructions. Each hypostome is slightly different from each other and *I. dorycephalus* with the main distinctions including a less convex lateral outline, smaller anterior wings and smaller posterior projections. Beyond this, the material and illustrations are insufficient for further comparison.

Ontogeny of *Isotelus* has been discussed in detail by Raymond (1914), Chatterton and Ludvigsen (1976), and Chatterton (1980).

Genus *Anataphrus* Whittington, 1954

Type Species: *Anataphrus borraeus* Whittington, 1954.

Diagnosis: This diagnosis follows Whittington, 1954. Asaphid trilobites in which axial furrows are absent, and axial and pleural parts of exoskeleton form smooth convex curve in transverse profile. Articulating processes and sockets indicate position of axis and show it is broad, almost two-thirds total width. Anteriorly, glabella and adjacent parts of cheeks slope steeply, more steeply than do lateral cheek areas. Eye lobes large, situated far apart and at about half cephalic length; facial sutures asaphid, anterior branches meet at obtuse angle at anterior margin, and continued by median suture across doublure. Narrow flattened border along anterolateral cephalic margin. Hypostome forked. Thorax of eight segments. Axis not defined on outer surface of exoskeleton of pygidium, and pleural parts without border.

Anataphrus elevatus n. sp.

Pl. 5, figs. 1-26

Anataphrus sp. Ross et al., 1979, Pl. 4, figs. al-au; Pl. 5, figs. v-ad.

Etymology: *elevatus* = raised, elevated; named for the highly raised palpebral lobes above the cranidium.

Material: 365 cranidia, 435 librigenae, 252 hypostomes, 145 thoracic segments, and 446 pygidia.

Stratigraphic Occurrence: AV4B 7.5cm - 3.5m, 80m - 90.75m; 98AV4B 76.75m - 110.1m; AV1 46.0m - 76.5m.

Holotype: Holotype cranidium UA 11599; paratypes UA 11600 - UA 11617.

Diagnosis: A species of *Anataphrus* with minute palpebral lobes situated far apart and highly elevated above cranidium; absence of axial furrows on dorsal surface of cranidium; cephalic border absent or poorly defined; pygidium without axial furrow and border; dorsal surface of exoskeleton smooth.

Description:

Cranidium: Cranidium slightly convex (tr.), moderately convex (sag.); width (tr.) at palpebral lobes slightly less than two-thirds length (sag.) of cranidium. Sagittal cephalic profile increases in convexity anterior to palpebral lobe; horizontal behind palpebral lobes. Cephalic border absent or poorly defined. Axial, glabellar and occipital furrows absent in larger specimens; in smaller specimens axial and occipital furrows are moderately impressed. Palpebral lobe minute; situated behind cranidial midlength (sag.); stands well above glabella in lateral profile. In smaller specimens, palpebral lobes are large, stand as high as glabella in lateral view. Anterior facial sutures diverge in front of palpebral lobes, curve distally to distance apart equal to width between palpebral lobes, recurve sharply to join cephalic margin at sagittal line; posteriorly sutures run posterolaterally, distal portion curving slightly more backward to intersect posterior cephalic border. Dorsal surface of cranidium smooth.

Free Cheek: Free cheeks lack genal spines in mature individuals. Free cheek subtrapezoidal in outline; lateral margin evenly curved inward. Outer surface of field slopes down from eye. Lateral and posterior border furrows absent. Genal angles of mature individuals rounded. Doublure broad; a small panderian opening is present in doublure anteromedially of genal angle; a prominent elongate vincular socket occurs close to margin of doublure, in front of genal angle. Doublure is ornamented with fine terrace lines that run subparallel with margins.

Hypostome: Hypostome subquadrate in outline; deeply notched posterior margin. Anterior margin concave forward medially, curves backward slightly laterally. Shoulders prominent; rounded in larger specimens, sharply angular in smaller specimens. Posterior projections narrowing steadily backward; inner margins slightly divergent backward; length (exsag.) greater than length (sag.) of middle body. Median portion of hypostome not ornamented, marginal portions are ornamented with fine terrace lines that run subparallel with margins. Doublure narrow anterolaterally and posteromedially; broad over two posterior projections of posterior border.

Thorax: Number of thoracic segments unknown. Articulated material shows at least 8 segments (pl. 5, figs. 16, 17). Axis two-thirds of total width (tr.) of segment. Inner portion of pleura subhorizontal, outer portion of pleura slightly downturned. Axial and

pleural furrow shallow to imperceptible. In dorsal view, distal portions of pleurae are faceted to accommodate next more posterior segment. Pleural doublure widest (tr.) along posterior edge of segment, almost extending to axial furrow. A small panderian opening is present in doublure, anterior edge is raised forming a panderian protuberance. Articulating devices consist of an articulating socket present on anterior edge of pleurae and an articulating process present on posterior edge of pleurae. In smaller forms, pleural tips terminate in posteriorly pointed tips (pl. 5, fig. 17); in larger forms, pleural tips are rounded.

Pygidium: Pygidium sub-semicircular in outline; smoothly convex in lateral view. Anterior margin slightly convex forward, anterolaterally truncated by a pair of facets. Axial, axial ring, interpleural and other pleural furrows absent. All furrows on dorsal surface are more impressed in transitory pygidia (pl. 5, fig. 26). Posterior margins of transitory pygidia are notched posteromedially. In smaller holaspid pygidia, the axis is slightly differentiated by change in slope and shallow axial furrows (pl. 5, figs. 21, 22). Posterior margin of holaspid pygidia evenly rounded. Doublure broad (sag., tr.); of even width from front to back; outline of proximal margin V-shaped with small median notch. Dorsal surface of pygidium smooth; doublure ornamented with fine terrace lines that run subparallel with margins.

Discussion:

Anataphrus elevatus n. sp. most closely resembles *Anataphrus martinensis*, described and illustrated by Ross and Shaw (1972) from the Middle Ordovician of the Copenhagen Formation, Nevada. The subtle differences between the two species include a more posterior position of the palpebral lobe which is situated behind the midlength (sag.) of the cranidium as opposed to opposite the midlength of the cranidium as in *A. martinensis*, and the absence of axial furrows on the glabella which appear on *A. martinensis* as shallow troughs circling the base of the palpebral lobes.

Other Ordovician species from North America include *Anataphrus spurius* from the Middle Ordovician of the Barrel Spring Formation, California (Phleger, 1933; Ross and Shaw, 1972), *Anataphrus gigas* from the Maquoketa Formation, Iowa (Raymond, 1920; Whittington, 1954), *Anataphrus borraeus* from the Upper Ordovician of Silliman's Fossil Mount, Baffin Island (Whittington, 1954), *Anataphrus glomeratus* from the Middle Ordovician of the Lourdes Limestone of the Long Point Group, Port au Port Peninsula, Newfoundland (Dean, 1979), *Anataphrus bromidensis* from the Bromide Formation, Oklahoma (Esler, 1964; Whittington, 1954), *Anataphrus raymondi* from the Richmondian of the Cape Calhoun beds of Northern Greenland (Troedsson, 1928; Whittington, 1954),

Anataphrus cf. *borraeus* Whittington, 1954, from the Blackriveran to Trentonian of the Esbataottine Formation, southern Mackenzie Mountains (Ludvigsen, 1979a), and *Anataphrus* cf. *martinensis* Ross and Shaw, 1972 from the Trentonian to ?Maysvillian of the lower Road River Formation, southern Mackenzie Mountains (Ludvigsen, 1975).

The Whittaker material is distinguished from *Anataphrus borraeus* by having a strongly convex (sag.) cranidium, smaller palpebral lobes which are elevated highly above the glabella, wider (tr.) posterior halves of the fixigenae, a wider (tr.) anterior glabellar lobe, and the absence of a pygidial axis outline. *A. glomeratus* has larger palpebral lobes which are only slightly elevated above the glabella, and axial furrows which appear as shallow, longitudinal depressions at the adaxial sides of the palpebral lobes.

Anataphrus bromidensis, originally described as *Homotelus bromidensis* by Esker, 1964 based on the presence of two pairs of glabellar furrows, was reassigned to *Anataphrus* by Ross and Shaw, 1972 because of the difficulty in seeing the furrows in the specimens. The poor illustrations make comparison of the two species difficult.

Anataphrus raymondi, originally described and illustrated as *Vogdesia raymondi* by Troeddsen, 1928, was included in the new genus of Whittington, 1954. The Whittaker material is distinct from *A. raymondi* by having small, highly elevated palpebral lobes which are situated behind the midlength (sag.) of the cranidium, and slightly more divergent anterior facial sutures.

Anataphrus elevatus has smaller palpebral lobes, longer posterior halves of the fixigenae, and the lack of a faint trace of a pygidial axis that makes this species distinct from *Anataphrus* cf. *borraeus*.

Yu (1996) considered material of *Anataphrus* from the Upper Ordovician of the Hanson Creek Formation, Nevada identical to *Anataphrus* cf. *martinensis*. Yu (1996) described and named this new species but never published this material. The synonymy with *A.* cf. *martinensis* is based on poorly preserved specimens that lack the palpebral lobes and obscure a view of the anterior lobe of the glabella along with the distal ends of the posterior portions of the fixigenae. This makes the association questionable. The material from the Hanson Creek Formation appears identical to the Avalanche Lake material, with the exception of the absence of a shallow pygidial axial furrow. Smaller pygidia from Avalanche Lake show the differentiation of an axis with a very shallow axial furrow (pl. 5, figs. 21, 22). The indication of an axis disappears in larger pygidia (pl. 5, figs. 20, 24). The Avalanche Lake material has been assigned to *Anataphrus elevatus* n. sp. since Yu's description has not been published.

Ross et al. (1979) illustrated a species of *Anataphrus* from the Hanson Creek Formation, Nevada. This material appears identical to the species mentioned in Yu (1996) and is therefore considered conspecific with the Avalanche Lake material.

Family Remopleurididae Hawle & Corda, 1847
Subfamily Remopleuridinae Hawle & Corda, 1847
Genus *Robergia* Wiman, 1905

Type Species: *Remopleurides microphthalmus* Linnarsson, 1875.

Diagnosis: This diagnosis follows Moore, 1959. Length of eye lobes less than 0.5 of cephalon (sag.); glabella narrow posteriorly, expanding between eye lobes, glabellar tongue long (sag.) and broad (tr.); three pairs of deep lateral furrows present; with narrow cephalic border and doublure anteriorly and laterally; genal spines originating opposite mid-point of eye lobes; posterior sections of facial sutures running out to posterolateral corners of fixigenae. Thorax of 11 segments; pleurae transversely directed, terminating in small posteriorly directed spines, with deep diagonal pleural furrows. Pygidium with length about equal to width; axis extending close to posterior margin; pleural fields flat, with three pairs of pleural furrows and posterior spines.

Robergia yukonensis (Lenz and Churkin, 1966)

Pl. 6, figs. 1-8

Material: 18 cranidia, 3 librigenae, 2 hypostomes, 23 thoracic segments, and 21 pygidia: UA 11618 - UA 11625.

Stratigraphic Occurrence: 98AV4B 76.75m - 88.2m; AV1 44.0m - 56.5m.

Holotype: G. S. C. no. 19864, Geological Survey of Canada, Ottawa.

Description: New material from the Whittaker Formation allows for the description of the hypostome to be added to the original description of Lenz and Churkin (1966).

Hypostome: Hypostome subcircular in outline. Anterior border forwardly convex; medially forms subangular projection. Lateral border furrow moderately impressed, originates slightly less than one-third length (sag.) of middle body, travels posteromedially a short distance, curves posteriorly to join shallow posterior border furrow. Lateral border moderately wide (tr.), originates approximately half length (sag.) of hypostome, converges backwards to become posterior border.

Discussion:

The Whittaker material agrees in morphological detail with *Robergia yukonensis* originally described from above the Ashgill of the Road River Formation, Northern Yukon

(Lenz and Churkin, 1966). The Avalanche Lake material shares the presence of a faint axial furrow, and the distinctive configuration of the two pleural furrows on the thoracic segments with *Robergia yukonensis*. The axial furrow is absent in other species of *Robergia* and Lenz and Churkin (1966) have considered *Robergia yukonensis* to possibly represent a new genus.

Lenz and Churkin (1966) note that *Robergia* has mostly been recorded from Middle Ordovician rocks. *Robergia yukonensis* from the northern Yukon and Avalanche Lake extend the range of this genus to include the Upper Ordovician.

Robergia sp.

Pl. 6, figs. 9-17

Material: 17 cranidia, 8 librigenae, 9 thoracic segments, and 4 pygidia; UA 11626 - UA 11634.

Stratigraphic Occurrence: AV4B 80m - 90.75m.

Discussion:

The dorsal features of *Robergia* sp. are poorly preserved and indiscernible in the Avalanche Lake material. Due to the poorly preserved material, a species name was not assigned.

Genus *Robergiella* Whittington, 1959

Type Species: *Robergiella sagittalis* Whittington, 1959.

Diagnosis: This diagnosis follows Whittington, 1959. Eye lobe relatively long and palpebral rim broad; the glabellar tongue expands forward, but not as strong as in *Robergia*.; basal glabellar lobe slightly inflated. Free cheek is relatively broad with a narrow border and doublure, base of genal spine being opposite the occipital ring. Thoracic segments lack large axial articulating processes and sockets, inner part of pleurae crossed by a broad shallow pleural furrow. Axis of pygidium includes only two pleural rings, the second divided by a median longitudinal furrow, post-axial ridge present. Pleural regions flattened, bordered by two pairs of long, tapering spines directed backwards, a strong interpleural ridge separating the proximal parts of the pleurae.

Robergiella insolitus n. sp.

Pl. 7, figs. 1-22

Etymology: *insolitus* = rare, uncommon; named for the rare occurrence of *Robergiella* in the Avalanche Lake section.

Material: 66 cranidia, 79 librigenae, 7 hypostomes, 7 thoracic segments, and 3 pygidia.

Stratigraphic Occurrence: AV4B 20cm - 3.5m; 98AV4B 85.6m - 110.1m; AV1 60m.
Holotype: Holotype cranidium UA 11641; paratypes UA 11635 - UA 11640, UA 11642 - 11651.

Diagnosis: A species of *Robergiella* with a laterally broadened (tr.) preglabellar area; glabellar tongue slightly less than one-half length (sag.) of glabella; weakly defined pleural and postaxial ridges on pygidium; tips of second pleural spines on pygidium extend behind first pleural spines, and second pleural spines separated by short rounded third pygidial spines and a median notch.

Description:

Cranidium: Cranidium moderately convex (sag.), more convex anteriorly than behind gamma; relatively flat (tr.) across palpebral lobes but strongly convex (tr.) anterior to palpebral lobes. In front of narrow (sag.) S0, width of glabella about same as at base of glabellar tongue; short distance in front of S0 glabella expands between palpebral rims; at front of palpebral rims, glabella constricted at base of tongue. Glabellar tongue long, slightly less than half length (sag.) of glabella in front of S0. Preglabellar area short (sag.) medially, longer laterally (pl. 7, fig. 4). S1 moderately impressed; initiated within glabella opposite delta, proceeds a short distance inwards and then curves posteromedially, terminating in front of occipital furrow. S2 shallower than S1, slightly curved in same sense as S1; initiated close to axial furrow behind anterior edge of palpebral lobe, proceeds inwards and backwards, extending one-third distance across glabella. S3 weakly impressed, straight; initiated at axial furrow close to anterior edge of palpebral lobe, and extending one-quarter way across glabella. Palpebral lobe sub-semicircular; approximately half length (exsag.) of glabella in front of S0; palpebral rim continuous with narrow anterior area of fixed cheek and preglabellar area, palpebral furrow moderately deep, cannot be discriminated from axial furrow. S0 deep, subtransverse. Occipital ring longest sagittally, with posterior margin convex backwards, tapers laterally to pointed side behind eye. In ventral view, occipital doublure longest (sag.) medially, tapers laterally. Sculpture of low tubercles seen on glabella of some specimens.

Free Cheek: Free cheek subtriangular in outline. Below visual surface occurs a raised rim (socle). Genal field slopes to lateral border. Lateral border furrow moderately impressed, becomes shallower a short distance in front of genal angle. Lateral border of even width. Posterior border furrow moderately impressed, converges with lateral border furrow at genal angle. Conjoined furrows travel some distance posteriorly along genal spine. Posterior border narrowest (exsag.) medially (constrained by facial suture), gradually broadening towards subangular projection in margin medial of base of genal

spine (pl. 7, figs. 3, 5). Genal spine long, gently tapering. On ventral surface, doublure of even width (tr.) along lateral margin, narrower along posterior margin, terminating at subangular projection of posterior border. Sculpture consisting of low tubercles on genal field and terrace lines on doublure running parallel with inner margin and along outer surface of genal spine.

Hypostome: Hypostome subrectangular to shield shaped in outline. Anterior border convex forward. Middle body slightly inflated. Lateral border furrow deep opposite shoulders, gradually shallowing posteriorly, merging in curve with shallow, posteriorly convex posterior border furrow. Lateral and posterior borders narrow; posterolateral corners of margin shaped into two small, posterolaterally directed spines. Subangular projections present towards sides of posterior margin. Middle furrows very shallow to inconspicuous.

Thorax: Number of thoracic segments unknown (at least 5). Axial ring about one-third width (tr.) of segment. Inner portion of pleura horizontal, transversely directed, crossed by moderately deep diagonal pleural furrow. Axial furrow moderately deep. Articulating ring furrow concave forward (may be convex forward medially in some segments); isolating lenticular articulating ring. Outer portion of pleura curved posteriorly, terminating in a short pointed spinose tip. Pleural furrow extends into outer portion of pleura becoming shallower distally. Sculpture of weak tubercles on dorsal surface.

Pygidium: Pygidium subquadrate in outline. Axis convex (tr.), with two axial rings and terminal piece, becoming progressively shorter (sag.) and narrower (tr.) posteriorly. Axial ring furrows transverse: shallowest medially, becoming deeper towards shallow axial furrow. Pleural regions horizontal; weakly crossed by pleural furrow which curves slightly outward and much more backward on anterior pleural segment. First interpleural furrow distinct and curves back to margin, second pleural and interpleural furrows shallower and more posteriorly to posteromedially directed. Pleural and postaxial ridges weakly developed. First two pleurae terminating in backwardly directed gently tapering spines. Second pleural spines extend farther back than first pleural spines; separated by short, rounded third pleural spines and median notch (pl. 7, fig. 19). Doublure broad (sag.), extending inward to tip of axis. Sculpture of low tubercles may be visible on axial rings, sculpture of doublure consists of terrace lines running subparallel with inner margin of doublure.

Discussion:

Ludvigsen (1975, 1978) illustrated a species of *Robergiella* from the Road River Formation, southern Mackenzie Mountains, which he attributed to be a component of a

deep water *Cryptolithus-Anataphrus* fauna. This fauna is normally found in shales and black limestones which he considered equivalent to the faunas of the lower Whittaker Formation. The Whittaker material is very similar to this species and occurs in the same faunal association. The pygidium appears slightly different in having more weakly developed pleural and postaxial ridges, and second pleural spines which extend farther back than first pleural spines, and are separated by a median notch. The Road River Formation material is limited in the number of specimens, making comparison difficult at present. Therefore, it is not ruled out that these are the same species.

Middle Ordovician species of *Robergiella* described include *Robergiella* sp. from the Middle Ordovician of the Copenhagen Formation, Nevada (Ross and Shaw, 1972); *Robergiella* cf. *sagittalis* from the lowest Caradoc of Mount Burgess, northern Yukon Territory (Ludvigsen, 1980); and *Robergiella sagittalis* from the Early Caradoc of the Liberty Hall facies of the Lower Edinburg Formation, Virginia (Whittington, 1959).

Material of *R.* sp. is difficult to compare with *R. insolitus* due to the limited number of specimens illustrated in Ross and Shaw, 1972. In the description, the preglabellar area and anterior area of the fixed cheek are described as very narrow and uniform in length. *Robergiella insolitus* has a broadened (tr.) lateral preglabellar area that distinguishes it from *R.* sp.

Robergiella cf. *sagittalis* has a narrower (tr.) and longer (sag.) glabellar tongue, a narrow anterior genal field, and a curving junction between the lateral and posterior border furrows of the librigena that distinguish this species from *Robergiella insolitus*.

Robergiella insolitus can be easily distinguished from *Robergiella sagittalis* by having smaller palpebral lobes, a broadened (tr.) lateral preglabellar area, a wider anterior genal field of the librigena, weakly defined pygidial pleural and postaxial ridges, the second axial ring lacking separation into two subcircular lobes by a median furrow, shorter first pleural spines relative to the second pleural spines; and the second pleural spines separated by short third pygidial spines and a median notch.

Genus *Hypodicranotus* Whittington, 1952

Type Species: *Remopleurides striatulus* Walcott, 1875, from the Denley Formation (Franklinian) at Trenton Falls, New York.

Diagnosis: This diagnosis follows Ludvigsen and Chatterton, 1991. A remopleuridine genus with a cephalon like that of *Remopleurides*, but with a long falcate genal spine located in front of an acutely angled genal corner. Hypostome has the shape of a tuning fork and is nearly three times as long as wide; oval areas are small; long slender

posterolateral projections taper to sharp points. Minute oval pygidium consists of a single segment; it lacks a defined axis; a pair of triangular marginal spines is closely aligned; its ventral side is completely covered by flat doublure.

Hypodicranotus sp.

Pl. 17, fig. 11

Material: 1 hypostome; UA 11794.

Stratigraphic Occurrence: AV4B 7m.

Discussion:

The material of *Hypodicranotus* sp. is restricted to 1 hypostome. This hypostome has been assigned to this genus based on the diagnostic “tuning fork” shape with long, slender posterolateral projections. Ludvigsen and Chatterton (1991) described and illustrated *Hypodicranotus striatulus* Walcott 1875 from the Edenian of the Lower Whittaker Formation in the South Nahanni River area. The lack of material and poor preservation of the Avalanche Lake hypostome does not permit an accurate comparison with *H. striatulus* or a species designation.

Family Raphiophoridae Angelin, 1854

Genus *Ampyxina* Ulrich, 1922

Type Species: *Endymionia bellatula* Savage, 1917, from the Thebes Sandstone (Middle Ordovician) of Illinois.

Diagnosis: This diagnosis follows Moore, 1959. No glabellar spine; alae large; rolled cephalic border narrow. Thorax with five segments, first longer (sag., exsag.) than others; pleural furrows curving forward, convex toward front. Pygidium with six pairs of pleural furrows curving outward and backward.

Ampyxina pilatus n. sp.

Pl. 8, figs. 1-17

Etymology: *pilatus* = armed with a javelin; named for the anterior glabellar spine.

Material: 10 complete holaspids, 50 cranidia, 1 librigena, 3 thoracic segments, and 19 pygidia.

Stratigraphic Occurrence: AV4B 80m - 90.75m; 98AV4B 75.36m - 79m; AV1 44m - 55m.

Holotype: Holotype cranidium UA 11652; paratypes UA 11655 - UA 11663.

Diagnosis: A species of *Ampyxina* with moderately convex (sag.) glabella; convex forward anterior cephalic border (in ventral view); strongly tapering glabella between alae; large alae

approximately one-half length (sag.) of glabella; posterior edge of fixigenae rounded; S0 of moderate depth; posterior border furrow curved anteriorly at distal corner of fixigenae; and posteriorly flexed interpleural furrows of pygidium.

Description:

Cranidium: Cranidium rounded to subtriangular in outline. Occipital ring short and narrow (sag. and tr.), strongly convex (tr.); in dorsal view, curved convex backwards; S0 of moderate depth. In front of occipital ring, glabella expands forward to maximum width (tr.) anterior to ala (pl. 8, fig. 1). Glabella strongly convex (tr.), moderately convex (sag.), sloping distinctly to occipital furrow. In most specimens, glabella bears a short anterior glabellar spine approximately one-quarter length of glabella. Lateral glabellar furrows imperceptible or absent. Frontal lobe gently rounded in dorsal view, overhangs convex forward anterior cephalic border (pl. 8, figs. 3, 7); separated from anterior border by shallow preglabellar furrow. Fixigenae moderately convex (exsag.); horizontal proximal to glabella, outer portion flexed steeply downward. Ala lenticular in outline; approximately third length of glabella; separated from glabella and fixigena by moderately impressed axial and alar furrows. Posterior border furrow moderately impressed, curves forward distally, and appears to be shallower behind ala in some specimens. Posterior border lengthens (exsag.) towards genal angle. External surface of cranidium smooth (coarsely silicified in most of available specimens).

Free Cheek: Free cheek unknown.

Hypostome: Hypostome unknown.

Thorax: Thorax of five segments. Axis approximately one-quarter of width of segment. Axial rings convex (tr.). Distinct pleural furrows present near midlength of pleurae, die out near distal ends of segments. Further description of thoracic segments obscured by poor preservation of dorsal and ventral surface.

Pygidium: Pygidium rounded to subtriangular in outline; with three axial rings outlined by transverse ring furrows shallowing posteriorly. Four pairs of pleural furrows cross pleural field, only first interpleural furrow distinguishable (narrow, shallow, deepest distally); shallow distally towards lateral border; pleural ribs and furrows progressively curved posteriorly distally on more posterior segments. Posterior border furrow distinct, isolates narrow border and steeply inclined margin. A shallow median notch occurs in ventral side of margin in posterior view (pl. 8, fig. 16).

Discussion:

The material of *Ampyxina pilatus* n. sp. from the Whittaker Formation closely resembles *Ampyxina lanceola* from the Middle Ordovician of the Lower Edinburg Limestone, Virginia (Whittington, 1959). Other similar species of *Ampyxina* from the Ordovician of North America include *A. powelli* Raymond, 1920 and *A. elegans*, illustrated and described by Cooper, 1953 from the Middle Ordovician of the Lower Champlainian Formations, Appalachian Valley, *A. bellatula* Savage, 1917 from the Richmondian (Upper Ordovician) of the Thebes Sandstone, Illinois (Savage, 1917) and further illustrated by Whittington (1950), *A. salmoni* Churkin, 1963 from the Upper Ordovician of the Saturday Mountain Formation, Idaho (Churkin, 1963), and *A. sp.* from the Trentonian of the Road River Formation, southern Mackenzie Mountains (Ludvigsen, 1978).

Several unique features serve to distinguish the Whittaker material from previously described species of *Ampyxina*. *Ampyxina pilatus* possesses a moderately convex (sag.) glabella, a strongly backward tapering glabella between the alae, large alae approximately one-half the length (sag.) of the glabella, a shallow occipital ring furrow, a convex forward anterior cephalic border (in ventral view), a rounded posterior fixigenal edge, a posterior border furrow which curves anteriorly at the distal corners of the fixigenae, and posteriorly flexed interpleural furrows.

Although *Ampyxina pilatus* and *Ampyxina lanceola* are very similar, *A. lanceola* has more deeply incised axial and alar furrows and a more strongly convex (sag.) glabella.

In addition to the above features, *A. pilatus* differs from *A. powelli* by the absence of muscle scars on the glabella, which would indicate the presence of glabellar furrows, more inflated alae, and a gradual tapering of the crest of the glabella to the occipital ring.

The most striking difference between *A. pilatus* and *A. bellatula*, the type species, is the presence of a frontal glabellar spine in *A. pilatus*. In addition, the glabella is less inflated giving a narrower appearance, and the pleural and axial ring furrows of the pygidium are shallower and less distinguishable posteriorly.

A. pilatus is easily separated from *A. elegans* by the inflated alae, the less inflated glabella, the lack of ornamental ridges on the fixigenae, the posteriorly flexed pleural furrows and the prominent lateral border of the pygidium.

Lenz and Churkin (1966) described *A. salmoni* from above the Ashgillian of the Road River Formation, Northern Yukon. Although the Whittaker material is very similar in appearance, the presence of a frontal glabellar spine, a less inflated glabella, longer alae, and posteriorly flexed interpleural furrows distinguish *A. pilatus* from *A. salmoni*.

The species of *Ampyxina* illustrated by Ludvigsen, 1975 is the closest species geographically to *A. pilatus*. Although the illustration consists of one cranidium and one

pygidium, it appears that the two species are similar. In addition to the characteristics mentioned above, the only other distinction would be a less inflated glabella and larger alae in *A. pilatus*.

Family Trinucleidae Hawle & Corda, 1847
Subfamily Cryptolithinae Angelin, 1854
Genus *Cryptolithus* Green, 1832

Type Species: *Cryptolithus tessellatus* Green, 1832, from the Middle Ordovician of New York.

Diagnosis: This diagnosis follows Moore, 1959. Fringe with concentric rows of pits that show radial arrangement also anteriorly, characteristically with raised radial ridges between outer row or rows and concentric ridges between inner rows, one row of pits external to girder.

Cryptolithus tessellatus Green, 1832

Pl. 9, figs. 1-13

Cryptolithus tessellatus Green, 1832, p. 560, Pl. 14, fig. 4.

Trinucleus bellulus Ulrich, 1878, p. 99, Pl. 4, fig. 15.

Cryptolithus lorettensis Foerste, 1924, p. 236, Pl. 43, figs. 15, 16.

Material: 1995 cranidia, 345 thoracic segments, and 795 pygidia; UA 11664 - UA 11673.
Stratigraphic Interval: AV4B 7.5cm - 3.5m, 73m - 90.75m; 98AV4B 72.55m - 110.1m;
AV1 10m - 77m.

Holotype: The location of the holotype is unknown. Neotype designated by Shaw and Lesperance (1994) is MCZ 8160/18, collected by Whittington (1968), from the Shoreham Limestone, Rathbun Brook, New York.

Discussion:

The Avalanche Lake material shows characteristics that ally it with *Cryptolithus tessellatus* Morph F, discussed and illustrated by Shaw and Lesperance (1994). Shaw and Lesperance (1994) studied all known geographic and stratigraphic occurrences of *Cryptolithus* in eastern North America. Following earlier suggestions by Lesperance and Bertrand (1976), Owen (1980), and Shaw (1991), they designated a neotype for *Cryptolithus tessellatus* Green, 1832 and all other eastern cryptolithines were assigned to morph status within that species. The material was considered to be separate morphotypes based on the fact that the forms studied failed to show clear stratigraphic, geographic, or morphological boundaries, and therefore could not be considered separate species. Morphotypes were defined entirely on the number of I arcs. *Cryptolithus tessellatus* morphotype F, formerly known as *Cryptolithus bellulus*, is considered to be present in the Avalanche Lake section based on the well developed I3 row on the fringe of the cranidium.

Order Phacopida Salter, 1864
Suborder Cheirurina Harrington & Leanza, 1957
Family Cheiruridae Hawle & Corda, 1847
Subfamily Acanthoparyphinae Whittington & Evitt, 1954
Genus *Acanthoparypha* Whittington & Evitt, 1954

Type Species: *Acanthoparypha perforata* Whittington and Evitt, 1954, from the Edinburgh Formation, Virginia.

Diagnosis: This diagnosis follows Whittington and Evitt, 1954. Cephalon is moderately convex longitudinally and transversely, in height about half the width. Glabella widest across basal lobes, narrowing forward. The eye is opposite the anterior part of the basal glabellar lobe and close to the axial furrow, and the posterior branch of the facial suture runs forward and outward, absence of glabellar spine. The pleurae of the thorax are horizontal inside the fulcrum, and each has a median row of pits. The axis of the pygidium is divided into two rings. The pleural lobes consist of two pairs of spines subequal in length.

Acanthoparypha palmapyga n. sp.

Pl. 10, figs. 1-20

Etymology: This species is named for the palmate shape of the pygidium.

Material: 6 cranidia, 6 librigenae, 3 hypostomes, 3 thoracic segments, and 8 pygidia.

Stratigraphic Occurrence: AV4B 6m - 7m; 98AV4B 10.3m - 11.5m.

Holotype: Holotype cranidium UA 11674; paratypes UA 11675 - UA 11688.

Diagnosis: A species of *Acanthoparypha* with a large, inflated glabella; axial furrow broadens opposite and in front of S3; S3 shallows adjacent to axial furrow; occipital ring long (sag.), pygidium with indistinct axial furrows, first axial ring furrow shallows medially so as to be inconspicuous medially in large pygidia; first axial ring and terminal piece weakly separated from each other and pleural regions by slight change in relief; shallow rounded furrow on dorsal surface of pleural spines of larger pygidia.

Description:

Cranidium: Cranidium subcircular in outline, moderately convex (sag.) and strongly convex (tr.) toward front of glabella. Glabella narrowing slightly forward; maximum width occurs across L1. Axial and preglabellar furrows moderately deep (sag.), continuous; isolate short, convex (sag.) anterior border. Anterior border shortest (sag.) medially, lengthens gradually laterally. Axial furrow broadens opposite and in front of S3 (pl. 10, fig. 8). S1 longest and deepest of glabellar furrows; runs diagonally inwards and backwards; curves slightly backwards medially in sigmoid; terminates well in front of

occipital furrow. S2 and S3 not as deep as S1, gently curving. S1 one-third, S2 one-quarter, and S3 one-fifth width of glabella. L1 longest (exsag.), subtrapezoidal, slightly swollen over axial furrow and occipital furrow laterally; L2 and L3 progressively narrower (tr.), more trapezoidal, and slightly inflated; anterior lobe shortest, triangular, not inflated. Occipital ring arched, almost as wide (tr.) as maximum width of glabella, slightly longer (sag.) medially than laterally, does not stand as high as glabella. Palpebral lobe narrow (tr.); lenticular in outline; close to axial furrow; delta located slightly anterior to S1, opposite L2; slightly arched upward in lateral view. Anterior border and anterior part of fixigena continuous in lateral view, width of anterior part of fixigena maintained from opposite L3 to opposite L1. Facial suture proceeds forward and slightly inward from palpebral lobe subparallel with axial furrow; posterior facial suture and genal spine unknown since all cranidia found lack posterior area of fixigena. Cranium covered by densely distributed granules. Additional sculpture consists of widely spaced, small circular tubercles on occipital ring; tubercles possess minute central perforations.

Free Cheek: Cheek subtriangular in outline, steeply inclined distally. Genal field below eye surface descends steeply to roll-like lateral border. Lateral border furrow broad and shallow, steeper distally than proximally; lateral border of even width, margin curves evenly and is indented anteriorly by a shallow antennal notch. Surface covered in small granules and widely spaced pits; lateral border covered in fine tubercles.

Hypostome: Hypostome subtrapezoidal to hexagonal in outline; ratio of length to maximum width across anterior wings 3:4. Anterior margin convex forward, subangular medially; lateral margin, behind shoulders, straight and convergent posteriorly; posterior margin convex and subangular medially. Middle body slightly inflated; outlined by moderately deep lateral border furrows which merge with shallower, gently curving posterior border furrow. Anterior border furrow convex forward, shallowest medially and deepening laterally; narrow and firmly impressed; medially almost reaching anterior margin. Lateral and posterior borders broad; modified anteriorly into small shoulders which project laterally almost as far as anterior wings. Middle body partly separated into subtriangular anterior lobe and crescentic posterior lobe by medially narrow, inconspicuous to absent, and distally moderately deep middle furrow. Middle furrow initiated inside lateral border furrow in front of shoulders; from shoulders furrow runs posteromedially. Maculae imperceptible.

Thorax: Number of thoracic segments unknown. Axial furrows shallow dorsally, obvious ventrally. Pleural furrow imperceptible. Pleurae gradually curve posteriorly, terminating in a blunt point. Pleural doublure extends from tip to approximately or almost half distance towards axial furrow under blunt spine; terminates in a raised inner lip (pl. 10,

fig. 16). Single row of widely spaced pits bisects inner portion of pleurae (pl. 10, fig. 16). Dorsal surface covered by small granules.

Pygidium: Pygidium, including spines, subrectangular to slightly splayed backward in outline; axial furrows and proximal parts of axial rings and axial ring furrows indistinct. Distal parts of first ring furrow convergent, anteromedially shallowing pits (pl. 10, fig. 19). First ring furrow more distinct medially in small pygidia. Four marginal spines broad, closely aligned and subparallel to slightly flaring posteriorly. In larger specimens, pleurae have shallow median groove (pl. 10, fig. 19). On inner surface, spine bases end posterior to slightly raised inner portion of doublure (pl. 10, fig. 20). Margin of doublure curves evenly concave forward. Doublure forms small shoulders laterally. Dorsal sculpture of pygidium consists of fine granulation. Granules also present towards anterior margin of doublure.

Discussion:

The material of *Acanthoparypha palmapyga* n. sp. from the Whittaker Formation, Avalanche Lake most closely resembles middle Ordovician *Acanthoparypha goniopyga* Ludvigsen, 1979 described from the Lower Whittaker Formation (Ludvigsen, 1979). Pygidial synapomorphies of these species include axial rings that are not distinct (at least medially), shallow to indistinct axial furrows, and the presence of a pair of anteriorly convergent, anteromedially shallowing pits (distal parts of first ring furrow) on the anterior portion of the pygidium. Pygidial features that distinguish *A. palmapyga* from *A. goniopyga* include the almost parallel pleurae, and the presence of a shallow central groove on the dorsal surface of the marginal spines of larger specimens. Characteristics of the cranidium that distinguish *A. palmapyga* include a longer (sag.) occipital ring, a more convex anterior margin, and comparatively straight S1 furrows.

Other similar *Acanthoparypha* species from the middle Ordovician of North America include *A. evitti* and *A. echinodermata* from the Upper Whiterockian (Chazy), Lower Esbatoattine Formation, District of Mackenzie (Chatterton and Ludvigsen, 1976), *A. perforata* from the lower Middle Ordovician, Edinburg Limestone, Virginia (Whittington and Evitt, 1953), *A. chiropyga* from the lower Middle Ordovician, Lincolnshire Limestone, Virginia (Whittington and Evitt, 1953), and *A. sp.* from the Upper Whiterock (Chazy) Group of New York (Shaw, 1968). Characteristics of the cranidium that distinguish *A. palmapyga* from these other Ordovician species include a longer occipital ring (sag.), a distinctly distally lengthened anterolateral border (exsag.), and the lack of increased convexity of the glabella inside the adaxial termination of the glabellar furrows. Pygidial autapomorphies of *A. palmapyga* include indistinct axial furrows, axial rings, and medial

parts of axial ring furrows, the anteromedially shallowing distal parts of the first ring furrow, the presence of a median groove in the marginal spines of larger specimens.

In addition to the characteristics mentioned above, several features of the pygidium further distinguish *A. palmapyga* from *A. echinodermata* (compare Chatterton and Ludvigsen 1976, pl. 12, fig. 14 with pl. 10, fig. 19 of this chapter). They are the pleurae terminating in a pointed tip, and the absence of tubercles.

The Whittaker species differs from *A. perforata* in having a circular outline of the glabella, a less anteriorly tapering glabella, a subangular median projection of the posterior border of the hypostome, wider lateral and posterior borders of the hypostome, subparallel pygidial marginal spines that terminate a greater distance behind the raised inner lip of the doublure, and a lack of tubercles on the pygidium.

In addition, features distinguishing *A. palmapyga* from *A. chiropyga* include a more convex anterior margin (tr.), wider lateral and posterior borders of the hypostome, a shallower posterior border furrow of the hypostome, pygidial marginal spines that terminate a greater distance behind the raised inner lip of the doublure, and the absence of tubercles on the pygidium.

A. sp. from the Chazy Group of New York described by Shaw (1968) is not known well enough to allow detailed comparisons to be made.

Acanthoparypha latipyga n. sp.

Pl. 11, figs. 1-29

Etymology: The name is given for the broad pygidium in holaspid specimens.

Material: 21 cranidia, 35 librigenae, 8 hypostomes, 10 thoracic segments, and 14 pygidia.

Stratigraphic Occurrence: AV4B 16.5m - 18m; 98AV4B 22.6m - 48.55m.

Holotype: Holotype cranidium UA 11689; paratypes UA 11690 - UA 11709.

Diagnosis: A species of *Acanthoparypha* with broad axial furrow opposite and in front of S3; broad posterior cranidial border furrow at genal angle; fixigenal lateral border furrow shallow and broad, almost imperceptible; pygidium with indistinct axial furrows; first axial ring furrow shallows medially so as to be inconspicuous in large pygidia; first axial ring and terminal piece weakly separated from each other and pleural regions by slight change in relief; pleural spines broadened on larger specimens; shallow rounded furrow on dorsal surface of pleural spines of larger pygidia.

Description:

Cranidium: Cranidium semicircular in outline, moderately convex (sag.). Glabella oval in outline; narrowing forward anterior to S2, maximum width across L1. In smaller specimens, glabella subrectangular in outline. Axial furrows moderately deep, shallowing

and broadening opposite and in front of S3. Preglabellar furrow shallow laterally, isolating moderately wide anterior border. S1 longest and deepest; runs diagonally inwards and backward, curves slightly backwards medially and terminates well in front of occipital furrow; S2 and S3 parallel to each other, gently curving, not as deep as S1; S3 shortest, approximately two-thirds length of S1; does not reach axial furrow. L1 longest (exsag.), subrectangular, slightly inflated near occipital furrow; L2 and L3 progressively shorter, subrectangular in dorsal view, less inflated than L1. Occipital ring arched forwards, slightly wider (sag.) medially than laterally. In smaller specimens, occipital ring stands approximately the same height as glabella (pl. 11, fig. 12). Palpebral lobe narrow (tr.), lenticular in outline, triangular in outline in smaller specimens; palpebral lobe positioned close to axial furrows, opposite L2; inclined from glabella at approximately 45 degrees from the horizontal; does not stand as high as glabella. Anterior facial suture proceeds in a curve subparallel with axial furrow; posterior facial suture directed outwards and forwards. Lateral border possesses blunt, posterior fixigenal spine behind facial suture. In smaller specimens, two prominent anterior and mid-fixigenal spines occur, one positioned directly behind facial suture, the second occurring more posteriorly along lateral border. Posterior border broadens and shallows gradually (exsag.) at midlength of fixigena; fixigenal lateral border furrow shallow and broad, almost imperceptible. Posterior fixigenal spine short; in smaller specimens, genal spine lengthens. Exoskeletal surface covered by granules and widely spaced circular tubercles, larger tubercles possess a central perforation; tubercles concentrated on glabella, sparse on fixigenal area and palpebral lobe. In smaller specimens, tubercles and granules more prominent and dense, covering entire cephalon. On the ventral surface, occipital doublure does not reach occipital furrow; widest medially. Posterior doublure convex, extending along posterior border, widening laterally to incorporate inner portion of genal spine. Axial, glabellar and occipital furrows expressed as ridges on interior surface of cranium.

Free Cheek: Cheek subtriangular in outline, steeply inclined distally. Visual surface occupies highest position on cheek. Lateral border furrow shallow, broad. Eye surface convex, oval in outline. Genal field below eye surface descends steeply to roll-like lateral border. Width of lateral border maintained from antennal notch to base of genal spine. Doublure of even thickness across body of librigenae, tapers quickly anteriorly, widens gradually posteriorly. Dorsal surface of free cheek covered entirely by small granules and widely spaced pits; perforated tubercles limited to lateral border.

Hypostome: Hypostome subtriangular in outline. Ratio of length to maximum width across anterior wings approximately 1:1. Anterior margin gently curved forward; lateral margins slightly convergent medially; posterior margin curved, terminating in a posterior

projection. Middle body slightly inflated, outlined by moderately deep lateral border furrows which merge with broader, shallower and curved posterior border furrow. Anterior border furrow curved, narrow and moderately deep, shallowing medially; closest to anterior border medially. Lateral border moderately broad, extending posteriorly to a very broad, "shelf-like" posterior border; modified anteriorly into small shoulders which do not project laterally as far as anterior wings. Anterior lobe subtriangular; posterior lobe crescentic. Anterior lobe outlined by deep, narrow middle furrows; middle furrow initiated inside lateral border furrow opposite shoulders, curves medially and posteriorly. Maculae imperceptible. Lateral portions of doublure broad, slightly concave. Narrowest portion of doublure on either side of midpoint of posterior margin. Junction of doublure at shoulders angular; anterior of lateral notch doublure flares into anterior wings.

Thorax: Number of thoracic segments unknown. Anterior thoracic segments with narrow spine, oriented parallel with axial ring about one-third the distance from axial furrow, curving posteriorly (pl. 11, fig. 21 and 22). On anterior inner surface near axial furrow small articulating knob occurs; opposite knob along posterior margin near axial furrow a complementary socket occurs. From axial furrow knob, a thin articulating flange follows gentle curve along anterior side of inner portion of pleura, terminating at forwardly projecting spine approximately half length of pleura (pl. 11, fig. 22). Posterior segment with broad axis and pleura (pl. 11, fig. 19). Axial furrow moderately deep. Posterior pleura curves and terminates as short, tapering, posteriorly directed spine. Pleural furrows imperceptible to absent. Doublure extend two-thirds distance across axis. Pleural doublure extends from pleural tip to approximately one-third length of pleura in anterior segments and half length of pleura in posterior segments. Inner margin of pleural doublure slightly raised. Articulating half-ring prominent, broadest medially, tapering towards axial furrow. Dorsal surface of anterior and posterior segments covered with fine granules; posterior segments covered in small tubercles, concentrated on posterior edge of pleurae and axial ring. Single row of widely-spaced pits bisects inner portion of pleura.

Pygidium: Pygidium, including spines, square in outline; axial furrows and proximal parts of axial rings and axial ring furrows indistinct; distal parts of first axial ring furrow expressed as convergent, anteromedially shallowing pits (pl. 11, fig. 28). Pleural spines broad, pointed and slightly divergent from each other, gradually tapering to blunt point; pleural spines subcircular in cross-section in smaller specimens (pl. 11, fig. 27). In larger specimens, pleurae have shallow median groove (pl. 11, fig. 28). In lateral view, axis of pygidium steeply sloping; pleural spines horizontal. On inner surface, spine bases end posterior to slightly raised inner portion of doublure (pl. 11, fig. 26). Doublure curves

evenly, forming small shoulders laterally. Ornamentation consists of fine granulation. Tubercles present on smaller pygidia, concentrated on pleural spines (pl. 11, fig. 25).

Discussion:

Acanthoparypha palmapyga and *Acanthoparypha latipyga* both occur in the Upper Ordovician Whittaker Formation, Mackenzie Mountains. Associations of pygidia and cranidia of the two species from the AV4B collection are based on a stratigraphic separation of 9m and co-occurrences of materials in separate horizons. These two species exhibit features discernible from middle Ordovician *Acanthoparypha* species. These include a widening of the anterolateral border (exsag.) across the anterior lobe of the glabella; broadening of the axial furrow anterior to the S2; S3 not in contact with axial furrow; lack of increased convexity of the glabella inside the adaxial terminations of the glabellar furrows; and the presence of shallow median grooves on the dorsal surface of the pygidial spines of the larger specimens. *A. latipyga* is distinguished from all other species by having broadening and shallowing of the lateral border furrow of the fixigenae, the presence of a strong median projection of the posterior border of the hypostome, and broadened pygidial spines in larger pygidia. In addition, *A. latipyga* can be distinguished from *A. palmapyga* by a smaller L1, an anterior border that is continuous (in dorsal view) along the glabella (compare pl. 2, fig. 1 and pl. 11, fig. 1 of this chapter), and smoother ornamentation.

Acanthoparypha palmapyga and *A. latipyga* most closely resemble middle Ordovician *A. goniopyga* described from lower in the Whittaker Formation, in the same region by Ludvigsen (1979). The diagnostic feature uniting these taxa is the morphology of the pygidium, previously known in *A. goniopyga* (compare Ludvigsen 1979, pl. 19, fig. 7 and 8 with pl. 10, fig. 19 and pl. 11, fig. 28 of this chapter). The pygidium is unique in having indistinct axial furrows, axial ring furrows, and axial rings. In addition, a pair of dorsally convergent, anteromedially shallowing pits (axial furrows) mark the anterior portion of the pygidium. Ludvigsen (1979) attributed these pits to be structurally equivalent to the second axial ring furrow. The pits found in the pygidia of the Avalanche Lake material are attributed to the first axial ring furrow. Pygidial features that distinguish *A. latipyga* from *A. goniopyga* include a broadening of the pygidial spines in larger specimens, and a shallow medial convergence of the pits (pl. 11, fig. 28). Characteristics of the cephalon that distinguish *A. palmapyga* and *A. latipyga* from *A. goniopyga* include a more convex anterior margin, a less tapered glabella, straight S1 and shorter fixigenal spines.

In addition to the forementioned characteristics, features that distinguish *A. latipyga* n. sp. from *A. evitti* and *A. echinodermata* include a more semicircular outline of the glabella,

palpebral lobes situated more proximal to the axial furrow, and an evenly curved forward anterior border of the hypostome.

Exoskeletal features that differentiate *A. latipyga* n. sp. from *A. perforata* and *A. chiropyga* include a less tapering glabella, a subrectangular L1, a laterally tapering occipital ring, a palpebral lobe situated farther forward opposite L2, and shorter genal spines. Pygidial features include subparallel pleurae, termination of pleurae posterior to the slightly raised inner lip of the doublure, and the lack of tubercles.

Meraspid material was assigned to this taxon based on features characteristic of the ontogenetic sequence, previously outlined by Whittington and Evitt (1954) and Chatterton (1980).

Acanthoparypha sp.

Pl. 12, figs. i-6

Material: 1 cranidium: UA 11710.

Stratigraphic Occurrence: 98AV4B 10.3m

Discussion:

Acanthoparypha sp. is distinguished from *Acanthoparypha palmapyga* and *Acanthoparypha latipyga* based upon the distinct ornamentation consisting of large, closely spaced tubercles, deeply incised lateral glabellar furrows, a weakly convex (tr.) glabella, the presence of an increased convexity inside the adaxial terminations of the lateral glabellar furrows, and the absence of the anterior cephalic border in dorsal view. In addition, the palpebral lobes are different in both shape and position. They are subcircular in outline, situated farther away from the axial furrow and farther anteriorly, opposite L2 as opposed to S1.

Acanthoparypha sp. is similar to the smaller cranidia of *A. latipyga*. The subquadrate shape of the cranidium and the position of the palpebral lobes situated opposite of L2 is slightly posterior relative to the position of the palpebral lobes in the smaller cranidia of *A. latipyga* which are situated opposite S2 separate these two taxa.

These distinctions also apply to the Middle Ordovician species of *Acanthoparypha*. *A. sp.* is different from *A. evitti* and *A. echinodermata* in having straighter lateral glabellar furrows. *A. perforata* has stronger ornamentation with larger and more numerous tubercles, and a strongly forwardly tapering glabella.

Phylogenetic Analysis of *Acanthoparypha*.

Adrain (1998) performed a cladistic analysis of the trilobite subfamily Acanthoparyphinae Whittington and Evitt, 1954, with species from the Silurian of Arctic Canada. The addition of the two new species of *Acanthoparypha* from the Upper Ordovician of the Avalanche Lake section may help to clarify the relationships within the genus. This analysis concentrated on species of *Acanthoparypha* and required several new characters that were not relevant in the expanded analysis of Adrain (1998). Many of the characters in Adrain (1998) are relevant to other genera and were not needed in this analysis. The data matrix and characters used here are found on Table 2.1 and 2.2.

Table 2.1. Character matrix for cladistic analysis of 7 species of *Acanthoparypha* and the outgroup *Holia secristi*.

Taxon	Character																						
	1	2	3	4	5	6	7	8	9	1	1	1	1	1	1	1	1	1	1	2	2	2	2
										0	1	2	3	4	5	6	7	8	9	0	1	2	3
<i>Holia secristi</i>	0	0	0	0	0	0	0	0	0	0	0	0	0	0	0	0	0	0	0	0	?	0	0
<i>A. chiropyga</i>	0	1	1	0	1	0	0	0	0	1	1	1	0	1	0	1	0	0	0	0	1	1	0
<i>A. echinoderma</i>	0	1	1	0	1	1	0	0	0	1	1	1	0	2	0	1	0	0	0	0	0	0	0
<i>A. evitti</i>	1	1	1	0	1	1	0	1	0	1	1	1	0	2	1	1	1	0	0	0	1	1	0
<i>A. goniopyga</i>	0	1	0	0	0	0	0	1	0	?	1	1	0	1	0	0	0	0	0	0	1	0	0
<i>A. perforata</i>	0	1	1	2	0	0	1	0	0	1	0	1	0	1	0	1	1	0	0	0	2	1	0
<i>A. palmapyga</i>	?	1	0	1	1	?	1	1	1	0	?	0	1	1	1	2	1	1	1	1	0	0	1
<i>A. latipyga</i>	1	1	0	1	1	0	1	1	1	0	0	0	1	1	1	0	?	1	1	1	0	0	1

Table 2.2. Characters used in the phylogenetic analysis of *Acanthoparypha* (character states unordered). Characters 1-15 are taken from Adrain (1988), characters 16-23 have been added.

1. Size of genal spine: (0) large, elongate; (1) small, not elongate, thorn-like.
2. Size of occipital spine in large holaspids: (0) robust and elongate; (1) not developed.
3. Size of anterior border: (0) visible in dorsal view; (1) obscured by frontal part of glabella in dorsal view.
4. Style of glabellar sculpture: (0) moderately, evenly tuberculate; (1) dominated by fine tubercles.
5. Glabellar outline: (0) subrectangular; (1) subcircular.
6. Size of posterior fixigena: (0) broad, large area; (1) significantly reduced but still protruding laterally in dorsal view.
7. Librigenal lateral border tuberculation: (0) small granules only; (1) coarse tubercles.
8. Length of anterior projection of librigena: (0) as long or longer than maximum exsagittal length of field; (1) shorter than field.
9. Thoracic pleural structure: (0) pleural furrow defined as a row of pits; (1) pleural furrow absent.
10. Presence of preannular area behind axial ring: (0) absent; (1) developed as broad, smooth area.
11. Outline of pygidial spines in transverse section: (0) subelliptical or subcircular; (1) flattened.
12. Presence of small, dorsally upturned, node-like pits on spines: (0) absent; (1) present.
13. Development of first pygidial ring furrow: (0) incised, transverse slot; (2) reduced to lateral pits.
14. Development of second pygidial ring furrow: (0) reduced to pair of lateral pits (1) reduced to single median pit or effaced; (2) incised, transverse slot.
15. Shape of last spine pair: (0) simple; (1) spatulate.
16. Position of palpebral lobes: (0) opposite L2; (1) opposite S1; (3) slightly anterior to S1.
17. Occipital ring length: (0) 3x as wide (tr.) as long (sag.); (1) 4x as wide (tr.) as long (sag.).
18. Median convexity inside adaxial terminations of lateral glabellar furrows: (0) present; (1) absent.
19. Convexity of S2: (0) slightly convex forward; (1) transverse.
20. Broadening of axial furrow opposite S2: (0) absent; (1) present.
21. Spacing of spines in holaspid pygidia: (0) closely spaced; (1) slightly divergent; (2) widely divergent.
22. Tubercles on first axial ring of pygidium: (0) absent; (1) present.
23. Shallow rounded furrow on dorsal surface of spines of holaspid pygidia: (0) absent; (1) present.

Parsimony analysis was performed using PAUP version 3.1.1 (Swofford, 1993). *Holia secristi* was designated the outgroup. All characters were unordered. An exhaustive search yielded 2 equally parsimonious trees, each with a branch length of 38, consistency index of 0.711, and a retention index of 0.694. Strict, semistrict, majority rule, and Adams consensus trees were identical, shown in Figure 2.1. Although *Pandaspinyga salsa* occupies a basal position within the *Acanthoparypha* polytomy, it was not used as the outgroup because at present no potential synapomorphies for the genus have been outlined and the lack of autapomorphies questions the validity of the genus (Adrain, 1998).

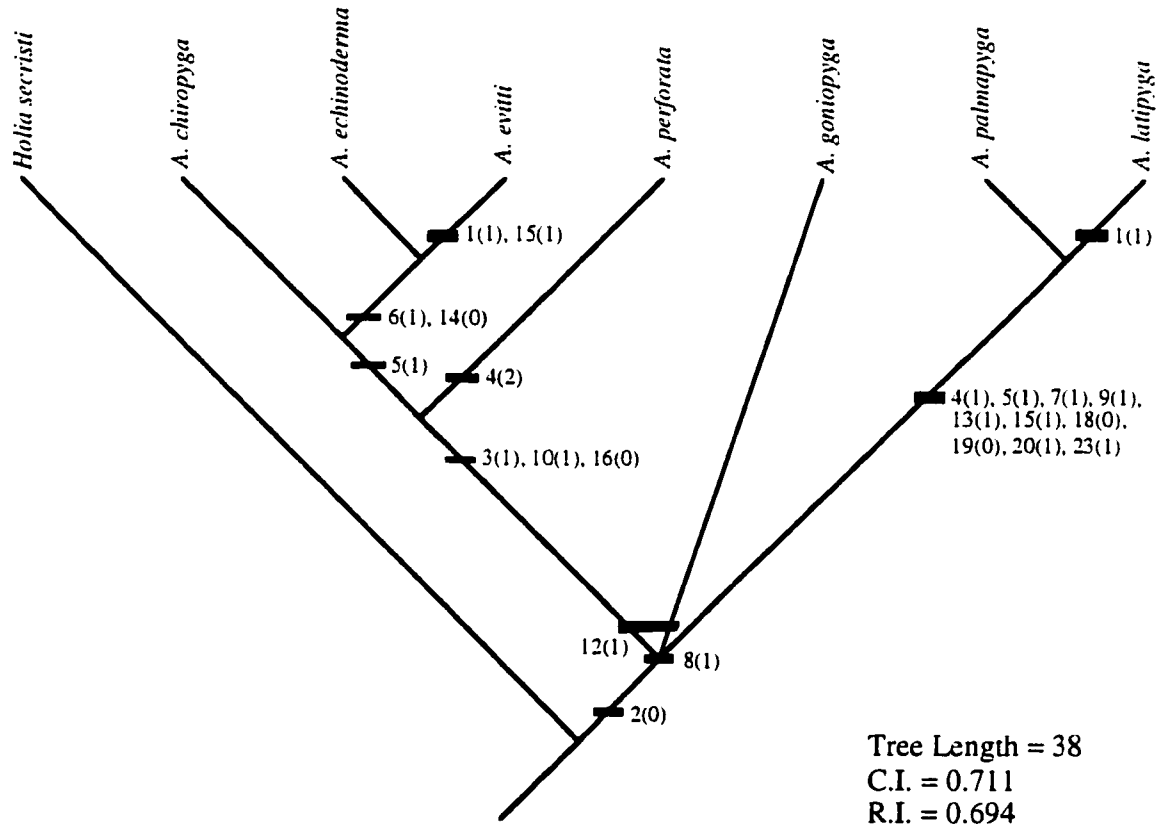


Figure 2.1. Distribution of apomorphic characters on the consensus tree generated by PAUP 3.1.1. Strict, semistrict, majority rule and Adams consensus trees were all identical. *Holia secristi* was designated as outgroup.

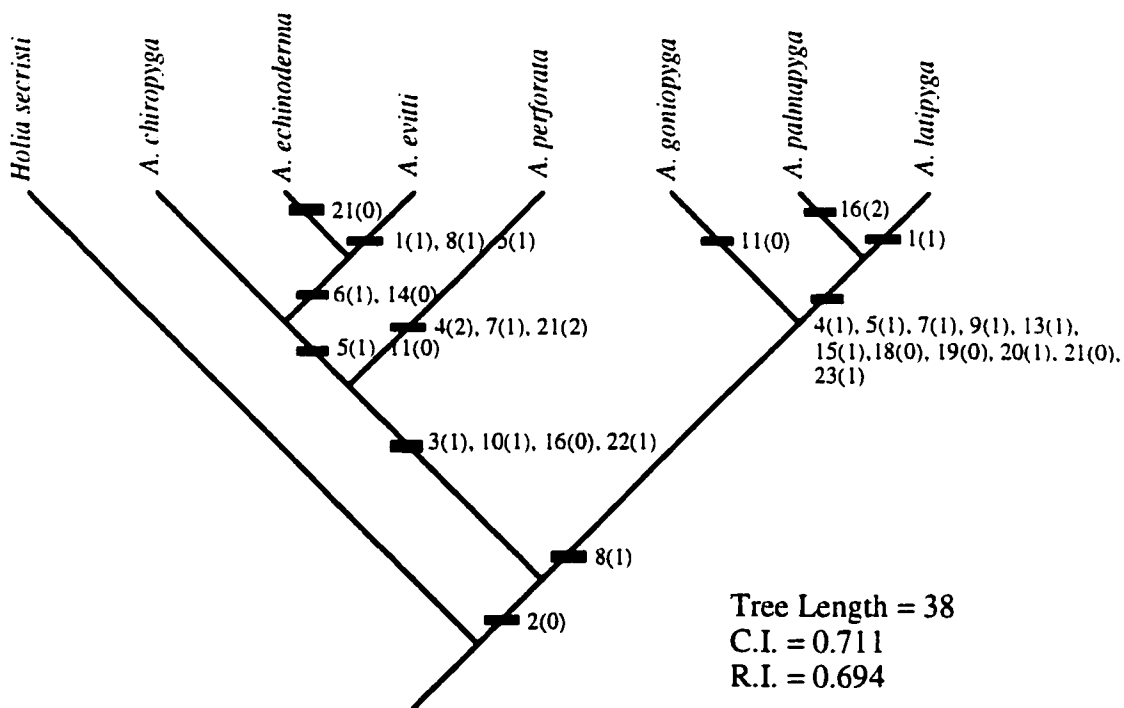
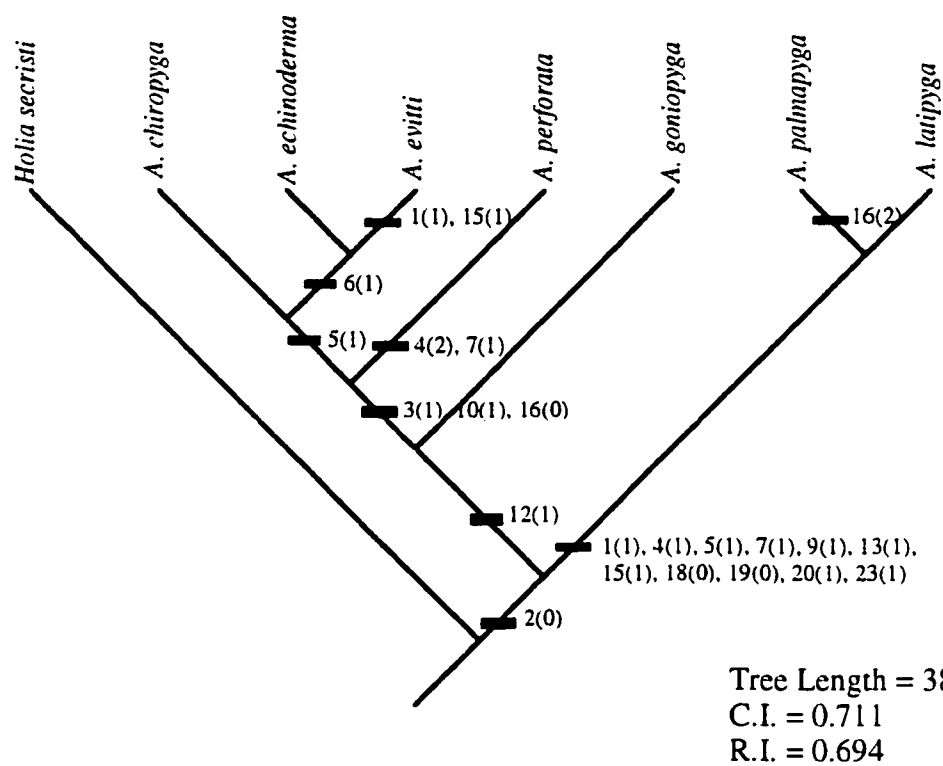


Figure 2.2. Distribution of apomorphic characters on the two shortest trees generated by PAUP 3.1.1 from data set (Table 2.1), characters unordered, outgroup designated as *Holia secrisi*.

There is only one area of disagreement between the two cladograms (Fig. 2.2). The position of *A. goniopyga* relative to the clade containing *A. chiropyga*, *A. echinoderma*, *A. evitti*, and *A. perforata* and the clade containing *A. palmapyga* and *A. latipyga* is unresolved. This is illustrated in the polytomy of the consensus tree (Fig. 2.1). The relationships of the other species appear to be consistent between the two shortest trees. These relationships appear to support stratigraphic information, with the Upper Ordovician taxa distinct from the Middle Ordovician species.

The genus *Acanthoparypha* is supported by character 2. The grouping of the Upper Ordovician species, *A. palmapyga* and *A. latipyga* is strongly supported with numerous synapomorphies. In addition, a consistent grouping exists between *A. chiropyga*, *A. echinoderma*, *A. evitti*, and *A. perforata*. This clade is supported by at least 3 synapomorphies.

The analysis of *Acanthoparypha* in Adrain (1998) presented the relationships between the species as a polytomy. There appears to be no support for the existence of the genus due to the polytomy between *A. goniopyga*, *A. echinoderma*, *A. evitti*, and *A. chiropyga*, the lack of resolution between *Pandaspinypha salsa* and the *Acanthoparypha* species, and the basal position of *A. perforata* to the clade containing *Youngia*, *Parayoungia*, and *Hyrokybe*. The addition of 8 new characters and two new taxa has shown that relationships exist within *Acanthoparypha*. The relationships of *Acanthoparypha* to *Youngia*, *Parayoungia*, and *Hyrokybe* need to be determined.

Genus *Holia* Bradley, 1930

Type Species: *Holia magnaspina* Bradley, 1930, from the Kimmswick Limestone of Missouri and Illinois.

Diagnosis: This diagnosis follows Adrain, 1998. Robust occipital spine developed in derived species; hypostomal shoulder set on posterior half (sag.) of hypostome; first pygidial spines with strong dorsal elevation; second pygidial ring furrow reduced to prominent pair of lateral pits.

Holia sp.

Pl. 17, figs. 12-14

Material: 2 crania, 1 hypostome; UA 11795 - UA 11797.

Stratigraphic Occurrence: AV4B 6m - 31.5m.

Discussion:

The material from AV4B consists of 2 partial crania, and 1 partial hypostome. Previous species described from the Mackenzie Mountains include *Holia secristi* from the

Upper Whiterock (Chazyan) of the Esbataottine Formation (Chatterton and Ludvigsen, 1976), and *Holia anacantha* from the Trentonian of the Lower Whittaker Formation (Ludvigsen, 1979). The Avalanche Lake material is distinguished from *Holia anacantha* by the presence of an occipital spine. Although the material is incomplete, there appears to be a few characteristics that allow differentiation between the cranidium and hypostome of *Holia secristi* and *Holia* sp. The anterior border of the glabella appears to be more square in outline, the S1 appears straighter without the strong backwards curve towards the occipital furrow, and the furrows of the hypostome are much shallower, without strong definition of the maculae. The material is too limited and fragmentary to provide a conclusive species designation, although the slight differences in morphology between previously described Middle Ordovician and Avalanche Lake material suggests that this may be a new species.

Subfamily Cheirurinae Salter, 1864
Genus *Ceraurinella* Cooper, 1953

Type Species: *Ceraurinella typa* Cooper, 1953, from the Edinburg Formation, Strasburg Junction, Virginia.

Diagnosis: This diagnosis follows Cooper, 1953. Cheirurid trilobites with the characteristic glabellar lobation, anterior part of the fixed cheeks narrow, short genal spines, and deeply impressed diagonal rib furrows of *Ceraurinus* (Barton, 1913), but with pygidium like that of *Ceraurus*. The ornamentation of the glabella and fixed cheeks consists of a mixture of fine granules and coarser tubercles, the latter not always developed on the glabella. Surface granulation not so coarse, nor the granules so regularly and evenly spaced as those of typical ceraurids.

Ceraurinella lamiapyga n. sp.

Pl. 12, figs. 7-17

Etymology: lamia = vampire; pyga = tail. This species is named for the fang-like appearance of the pygidium.

Material: 21 librigenae, 17 pygidia.

Stratigraphic Occurrence: AV4B 43m; 98AV4B 48.55m.

Holotype: Holotype pygidium UA 11713; paratypes UA 11711, UA 11712, UA 11714 - UA 11717.

Diagnosis: A species of *Ceraurinella* with posteriorly broadened (tr.) librigenal doublure; quadrate pygidial outline; absence of pygidial axial furrows; broad anterior portion of first pygidial spines; slightly incurved first pygidial spines; broad pygidial doublure encasing approximately half length (sag.) of pygidium; and flattened inner margin of doublure.

Description:

Cranidium: Cranidium unknown.

Free Cheek: Cheek triangular in outline; palpebral lobe occupies highest position. Field slopes steeply to wide (tr.) lateral border. Lateral border furrow shallow. Lateral border widens posteriorly, tapers strongly at anterior end. Inner margin of doublure curved upwards slightly; doublure widest posteriorly, gradually tapering anteriorly to narrow tip. Ornamentation consisting of granules and faint pitting on cheek field (expressed on ventral surface).

Hypostome: Hypostome unknown.

Thorax: Thoracic segments unknown.

Pygidium: Pygidium subtriangular in outline (without spines), width (tr.) slightly greater than length (sag.). Axis short, triangular in outline, composed of an articulating half ring, three axial rings, and a short terminal piece. Articulating ring furrow moderately deep; first axial ring furrow moderately deep, transverse, distal ends terminate in deep, posterolaterally directed appendiferal pits; second axial ring furrow shallow, transverse medially, distal ends terminate in straight, posteriorly directed appendiferal pits; third axial ring furrow shallower. Axial furrow imperceptible to absent. Axis initially high and convex, sloping steeply in lateral view, becoming faintly convex near terminal piece. First axial ring convex (sag.), four times as wide (tr.) as long (sag.). Second and third segments slightly shorter (sag.) than first and progressively narrower (tr.). First segment bears thick, long, and gradually tapering marginal spine which has a slight inward curvature in dorsal view. Second segment bears short, blunt, straight to slightly curved spines. Third set of spines of approximate equal length, closely spaced, nearly conjoined. Doublure (pl. 12, fig. 16,17) encasing half of ventral surface of pygidium; anterior margin deflected into U-shaped notch behind axis. Sparse to dense granulation on dorsal surface of pygidium.

Discussion:

Ceraurinella lamiapyga n.sp. occurs in a restricted stratigraphic interval within the Avalanche Lake sections. Although it occurs in association with *Ceraurinella brevispina*, the unique features of the pygidia and librigenae permit differentiation between the two taxa. Cranidia of *Ceraurinella* are morphologically conservative between species, and with the presence of *C. brevispina* in the same horizons, distinction between the morphology of cranidia of *C. brevispina* and *C. lamiapyga* was difficult. Therefore, no cranidia have been attributed to *C. lamiapyga* with certainty.

Ludvigsen (1979) described 8 species of *Ceraurinella* from the Upper Whiterock (Chazyan) to Edenian of the Lower and Upper Esbataottine and Lower Whittaker

Formations of the Southern Mackenzie Mountains. The material of *C. lamiapyga* is distinct from the Middle Ordovician material in several characteristics. The first striking feature that distinguishes the Avalanche Lake material is the broadened anterior portion of the first pygidial spines. The lateral margins of the first pygidial spines extend farther laterally than the articulating flange of the anterior border. This gives the pygidium a wide (tr.) and quadrate appearance. This feature is not found in any other species of *Ceraurinella*. Also unique to the Upper Ordovician material is the broadening (tr.) of the posterior portion of the librigenal doublure, the absence of axial furrows, the broad pygidial doublure encasing half the length (sag.) of the pygidial axis, and the flattened inner margin of the doublure. The third pygidial spines have a median notch which further distinguish *C. lamiapyga* from *Ceraurinella media*, *Ceraurinella longspina*, *Ceraurinella arctica*, *Ceraurinella necra*, and *Ceraurinella brevispina* described and illustrated by Ludvigsen (1979). These differences also apply to *Ceraurinella typa* and *Ceraurinella chondra* from the lower Middle Ordovician of the Lincolnshire and Edinburg Limestone from Virginia (Whittington and Evitt, 1953).

Ceraurinella brevispina Ludvigsen, 1979

Pl. 13, figs. 1-13

Ceraurinella n. sp. 9 Ludvigsen, 1975, Pl. 15, figs. 14, 15.

Ceraurinella brevispina Ludvigsen, 1979, Pl. 10, figs. 31-57.

Material: 235 cranidia, 830 librigenae, 373 hypostomes, 1556 thoracic segments, and 396 pygidia; UA 11718 - UA 11730.

Stratigraphic Occurrence: AV4B 3m - 73m; 98AV4B 6.25m - 50.4m; AV1 (-)45m - 30m.

Holotype: A pygidium (GSC 44059) from the lower Whittaker Formation, Mackenzie Mountains, illustrated and described in Ludvigsen (1979) (Pl. 10, figs. 31-57).

Discussion:

The Avalanche Lake material is extremely similar to the type material from the lower Whittaker Formation (Ludvigsen, 1979) and does not seem to indicate a new species designation.

Measurement of width (across anterior border) and length (of first pygidial spines) of 92 holaspide pygidia of *Ceraurinella brevispina* from Avalanche Lake 4B were plotted to show allometric changes during the holaspide period (Fig. 2.3).

The material of *Ceraurinella brevispina* from AV4B is unique in that it shows three distinct pygidial morphologies. The first morphology (represented by circles in Fig. 2.3) has a length to width ratio of 1:1.15. These pygidia bear long, outwardly directed first pygidial spines, which are directed upwards 45 degrees from the horizontal. The second morphology (represented by squares in Fig. 2.3) has a length to width ratio of 1:1.5 with shorter and wider (tr.) first pygidial spines that are more closely aligned with the second

and third pygidial spines. The third morphology (represented by triangles in Fig. 2.3) has the shortest and widest (tr.) pygidial spines with a length to width ratio of 1:1.85.

These distinct morphologies are considered to represent growth allometry within a single species instead of separate species. There appears to be an overall trend towards shortening and fattening of the first pygidial spines representing a linear ontogenetic sequence of morphological changes during the holapsid period. This transition was also noted by Ludvigsen (1979) in the four successive species, *C. longspina*, *C. arctica*, *C. necra*, and *C. brevispina* from the Blackriveran to Edenian of the southern Mackenzie Mountains. These four species possess pygidia that show a gradual decrease in the length of the first pygidial spine and a gradual alignment of the first spines with the posterior three spines (Ludvigsen, 1979). The ontogenetic changes occurring in the pygidia of *Ceraurinella brevispina* mimic the *Ceraurinella* lineage outlined by Ludvigsen (1979).

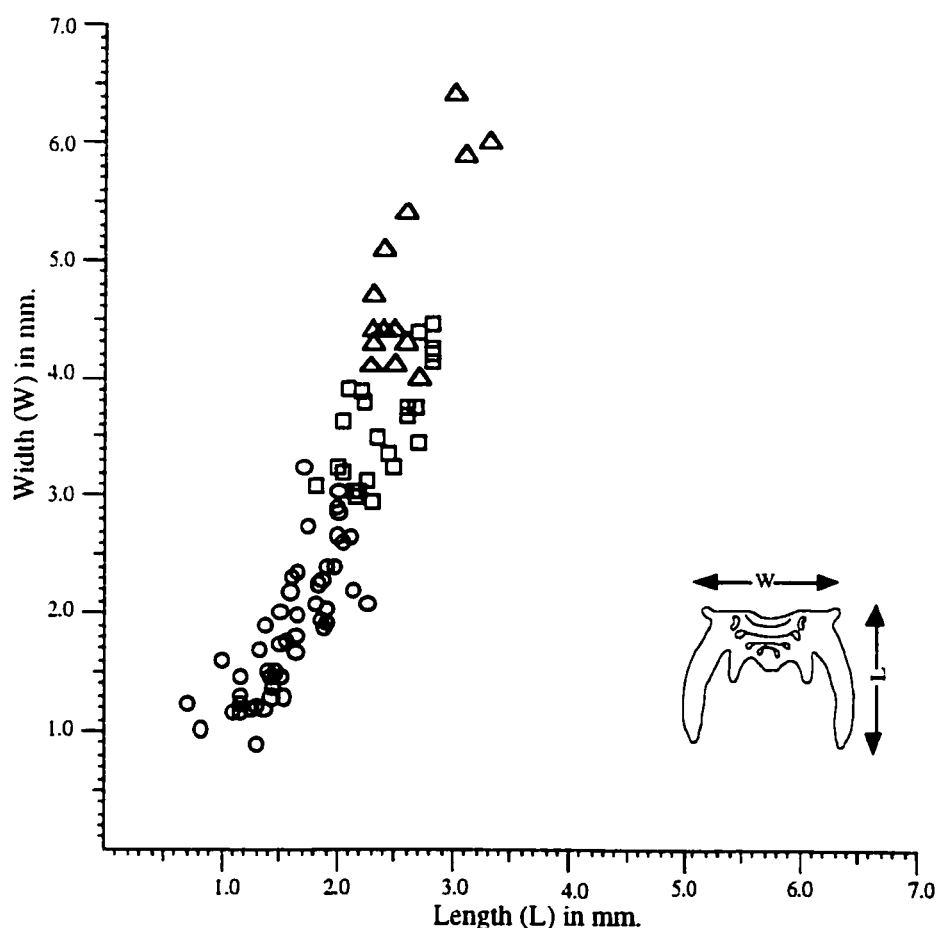


Figure 2.3. Scatter diagram for 92 holapsid pygidia of *Ceraurinella brevispina* from Avalanche Lake 4B, relating width of pygidium across anterior margin (W) to length of first pygidial spines (L).

Genus *Ceraurinus* Barton, 1913

Type Species: *Ceraurinus marginatus* Barton, 1913.

Diagnosis: This diagnosis follows Ludvigsen, 1977. A genus of Cheirurinae with a quadrate, smooth, slightly inflated glabella; three transversely directed lateral glabellar furrows of equal depth that are straight or faintly backwardly curving; a palpebral lobe located opposite S2; flat cephalic borders; a moderately short and faintly carinate genal spine; a pygidium with three pairs of marginal spines, the anterior pair curves backwardly and outwardly and is carinate and slightly to markedly expanded laterally, the posterior pairs are shorter and may be carinate.

Ceraurinus serratus Ludvigsen, 1979

Pl. 13, figs. 14-17

?*Ceraurinus icarus* (Billings) Troedsson, 1928, Pl. 19, fig. 1.
Remipyga cf. *daedulus* (Cox) Ludvigsen, 1975, Pl. 5, figs. 6, 7.
Ceraurinus n. sp. Ludvigsen, 1977a, Text-fig. 3.
Ceraurinus serratus Ludvigsen, 1979, Pl. 18, figs. 1-32.

Material: 3 cranidia, 107 thoracic segments, and 12 pygidia; UA 11731 - UA 11734.
Stratigraphic Occurrence: AV4B 3m - 73m; 98AV4B 7.85m - 11.5m.
Holotype: A pygidium (GSC 40446) from the lower Whittaker Formation, Mackenzie Mountains, illustrated by Ludvigsen (1979) (Pl. 18, figs. 1-32).

Discussion:

The Avalanche Lake material is assigned to *Ceraurinus serratus* described and illustrated by Ludvigsen, 1979. The diagnostic features of *C. serratus* center mainly on the morphology of the pygidium. These include flat, carinate, and curved first pygidial spines and pointed, non-carinate second and third pygidial spines. The Avalanche Lake material shows little variation from the Middle Ordovician material and is easily attributed to this species.

Genus *Ceraurus* Green, 1832

Type Species: *Ceraurus pleurexanthemus* Green, 1832 from the Trenton Group of New York State.

Diagnosis: This diagnosis follows Ludvigsen, 1979. A genus of Cheirurinae with forwardly expanding glabella, three pairs of generally narrow (tr.) glabellar furrows, and long genal spines. Glabellar ornament of coarse granules or tubercles, commonly paired. Hypostome triangular in outline with inflated central body, posteriorly placed maculae, and narrow

convex borders. Pygidium with long curving first spines; second and third spines are either very short or completely missing.

Ceraurus mackenziensis Ludvigsen, 1979

Pl. 13, figs. 18-24

Ceraurus cf. *pleurexanthemus* (Green) Troedsson, 1928, p. 68, Pl. 16, fig. 22.

Ceraurus sp. Ludvigsen, 1975, Pl. 5, figs. 8, 9.

Ceraurus mackenziensis Ludvigsen, 1979, Pl. 15, figs. 1-44.

Material: 23 cranidia, 16 librigenae, 22 hypostomes, and 32 pygidia; UA 11735 - UA 11741.

Stratigraphic Occurrence: AV4B 16.5m; 98AV4B 6.25m - 22.6m; AV1 53.5m - 73m.

Holotype: An incomplete cranidium (GSC 44156) from the lower Whittaker Formation, Mackenzie Mountains, illustrated and described by Ludvigsen (1979) (Pl. 15, figs. 1-44).

Discussion:

The abundance of specimens from the AV4B section allows the assignment of this material to *Ceraurus mackenziensis* with confidence. The material shares several diagnostic charactersitics including broad lateral cephalic borders, short (tr.) lateral glabellar furrows perpendicular to axial furrows, small glabellar lobes, posterior position of the eye opposite L2, strongly narrowed anterior border of the free cheek, and a small pygidium with very long and diverging first pygidial spines. Although the material is very similar, a few subtle differences are noted. The glabellar axial furrows are not as strongly divergent compared with the Middle Ordovician material (compare pl. 15, fig. 5 from Ludvigsen, 1979 with pl. 13, figs. 18,19 herein). In addition, ornamentation of the Avalanche Lake material is quite different, appearing to have a stronger ornamentation on the cranidium and the lateral border of the librigenae consisting of larger and more densely distributed tubercles. The ornamentation conceals the triangular arrangement of three pits seen on the middle part of the anterior glabellar lobe, considered by Ludvigsen, 1979 to be a uniting feature of several species of *Ceraurus*.

Ludvigsen (1979) did not describe the thoracic segments of *C. mackenziensis*. Material of *C. brevispina* is always found in association with *C. mackenziensis* in the Avalanche Lake Sections, making an assignment of thoracic segments to *C. mackenziensis* difficult. Therefore, no thoracic segments have been attributed to *C. mackenziensis* with certainty.

Genus *Borealaspis* Ludvigsen, 1976

Type Species: *Borealaspis whittakerensis* Ludvigesen, 1976, from the Lower Whittaker Formation, Funeral Range, District of Mackenzie.

Diagnosis: This diagnosis follows Ludvigsen, 1976. A genus of Cheirurinae possessing an evenly inflated bulb-shaped glabella. Maximum width of glabella across L3. It may possess a pair of swellings or spines on the anterior lobe and a single median occipital or preoccipital spine. Presence/absence of median cephalic spine may reflect sexual dimorphism. Occipital ring stand lower than glabella in front of occipital furrow. Palpebral lobes are small and located opposite L3 or S3. In front of eye, facial suture descends vertically.

Borealaspis whittakerensis Ludvigsen, 1976

Pl. 17, fig. 15

"*Ceraurus*" cf. *numitor* (Billings) Ludvigsen, 1975, Pl. 5, fig. 11.
Borealaspis whittakerensis Ludvigsen, 1976, p. 953, Pl. 2, figs. 1-7.

Material: 9 cranidia; UA 11798.

Stratigraphic Interval: AV4B 3m: 98AV4B 6.25m.

Holotype: A cranidium (GSC 40450) from the lower Whittaker Formation, Mackenzie Mountains, illustrated by Ludvigsen, 1979 (Pl. 17, figs. 1-12).

Discussion:

The material from Avalanche Lake consisted of 2 incomplete cranidia and several incomplete meraspid pygidia. Although the material is fragmentary, several diagnostic characteristics of the cranidium permit the assignment of this material to *Borealaspis whittakerensis*, primarily the short glabellar furrows and the presence of a long, stout spine which occupies a median position between the 1p lobes. The position of the median spine eliminates the possibility of *Borealaspis biformis* (Ludvigsen, 1976) which is occipital in this species rather than preoccipital as in *Borealaspis whittakerensis*.

Subfamily Deiphoninae Raymond, 1913
Genus *Sphaerocoryphe* Angelin, 1854

Type Species: *Sphaerocoryphe dentata* Angelin, 1854, from the Late Ordovician of Sweden.

Diagnosis: This diagnosis follows Moore, 1959. Well-developed fixigenae with genal spine; like *Hemisphaerocoryphe* but with bulbous part of glabella more dominating.

Sphaerocoryphe sp.

Pl. 17, fig. 16

Material: 2 cranidia; UA 11799.

Stratigraphic Occurrence: 98AV4B 6.25m.

Discussion:

The material of *Sphaerocoryphe* sp. from Avalanche Lake is restricted to two partial cranidia and therefore does not permit a species designation. However, several diagnostic features can be seen in this material which permit assignment to this genus, namely the circularly inflated glabella anterior of the S1 furrow, and the large, strongly curved genal spines. Comparison of this material can be made with Lane (1971), Chatterton and Ludvigsen (1976), Ludvigsen (1979), and Chatterton (1980).

Subfamily Sphaerexochinae Opik, 1937
Genus *Sphaerexochus* (*Korolevium*) Pribyl & Vanek, 1984

Type Species: *Sphaerexochus arenosus* Chatterton and Ludvigsen, 1976, from the Esbataottine Formation (Caradocian), South Nahanni River area, District of Mackenzie.

Diagnosis: This diagnosis follows Pribyl, Vanek, and Pek, 1985. Fixigenae with short genal spines. Hypostome with a deep notch at the posterior border. On the pygidium 3 (+1) rings, the third of them fuses incompletely with the terminal piece.

Sphaerexochus (*Korolevium*) sp.

Pl. 17, fig. 17

Material: 1 pygidium; UA 11800.

Stratigraphic Occurrence: 98AV4B 7.85m.

Discussion:

The material of *Sphaerexochus* (*Korolevium*) sp. from Avalanche Lake is limited to one pygidium. Pribyl and Vanek (1984) placed material of Chatterton and Ludvigsen (1976) from the Esbataottine Formation of the Mackenzie Mountains into this subgenus. The pygidium is considered to belong to this subgenus based upon comparison with material from Chatterton and Ludvigsen (1976) and the geographical proximity of the material.

Family Encrinuridae Angelin, 1854
Genus *Curriella* Lamont, 1978

Type Species: *Curriella newlandensis* Lamont, 1978, from the Newlands Formation (Aeronian), Newlands Farm, near Girvan, Strathclyde, Scotland.

Diagnosis: This diagnosis follows Edgecombe and Chatterton, 1990. Encrinurinae of *Encrinurus* group (librigenal field thickly covered with tubercles; hypostomal rhynchos weakly tapering forward). Eye forward, in front of S2; fine, dense genal tuberculation

interrupted by broad, non-tuberculate ring around eye; 7-10 tubercles aligned on adaxial part of fixigenal field; anterior cranial border bears 14 or more tubercles, often paired.

Curriella clancyi Edgecombe & Chatterton, 1990

Pl. 18, figs. 1-4

Material: 4 cranidia, 11 librigenae, 5 hypostomes, and 5 pygidia; UA 11801 - UA 11804.

Stratigraphic Occurrence: 98AV4B 110.9m

Holotype: Cranidium (UA 7872) from the earliest Llandovery of the Whittaker Formation, Mackenzie Mountains, Northwest Territories, illustrated by Edgecombe and Chatterton, 1990 (Pl. 2-4).

Discussion:

Curriella clancyi was originally discovered at the AV1 section, above the latest Ordovician mass extinction level at 95.5m above base (Edgecombe and Chatterton, 1990). Wang et al. (1993) placed *Curriella clancyi* at 111.3 - 111.8 m, slightly above the faunal turnover, at the AV4B section. They suggest that *Curriella* is diagnostic of Llandovery strata because all other species of *Curriella* found in Scotland and Illinois are of Llandovery age (Wang et al., 1993). Collections at AV4B have shown that this material agrees with the findings of Wang et al. (1993), occurring slightly above the latest Ordovician extinction boundary, within the upper Ashgill. This material was assigned to *Curriella clancyi* based on the close proximity geographically and temporally to the holotype, and morphological similarities.

Encrinurid

Pl. 18, figs. 5-6

Material: 1 librigena, and 1 hypostome; UA 11805, UA 11806.

Stratigraphic Occurrence: 98AV4B 85.6m; AV1 54m.

Discussion:

The material of a partial hypostome and librigena does not provide enough information to permit a generic assignment. The morphology of the hypostome and librigena suggests it belongs to the Family Encrinuridae.

Subfamily Cybelinae Holliday, 1942

Genus *Cybeloides* Slocum, 1913

Type Species: *Cybeloides iowensis* Slocum, 1913, from the Maquoketa Group, Iowa.

Diagnosis: This diagnosis follows Cooper, 1953. Encrinurid trilobites with strongly pustulose and spiny cranidia. Glabella marked by longitudinal furrows and bordered by

broad dorsal furrows containing deep pits. Pygidium highly arched along anterior margin, with vertical margins, converges to acutely rounded posterior tip; segments strongly ankylosed with anterior pleura bent posteriorly so as to enclose the narrower segments of the middle and posterior portions.

Cybeloides sp.

Pl. 18, figs. 7-13

Material: 23 cranidia, 26 librigenae, 12 hypostomes, and 5 pygidia; UA 11807 - UA 11813.

Stratigraphic Interval: AV4B 87m - 90.75m; 98AV4B 10.3m; AV1 40m - 55m.

Discussion:

The material of *Cybeloides* sp. from AV4B is fragmentary and poorly preserved. The material looks superficially similar to *C. cimelia* described and illustrated by Chatterton and Ludvigsen (1976) from the Esbataottine Formation, Mackenzie Mountains. Poor preservation of the Avalanche Lake material obscures surface details such as the position of tubercles on the cranidium and pygidium and does not provide sufficient morphological details to allow comparison. Material of *Cybeloides* sp. from the AV1 section shows the six pairs of glabellar tubercles restricted on the median lobe of the cranidium, a diagnostic feature of *C. cimelia*, as outlined by Chatterton and Ludvigsen (1976). However, the AV1 material appears to have tubercles on the tricomposite lobes, a feature contrasting with the Esbataottine material.

Suborder Phacopina Struve, 1959
Family Pterygometopidae Reed, 1905
Subfamily Eomonorachinae Pillet, 1954
Genus *Sceptaspis* Ludvigsen and Chatterton, 1982

Type Species: *Pterygometopus lincolnensis* Branson, 1909, from the Plattin Formation (Rocklandian) of Missouri.

Diagnosis: This diagnosis follows Ludvigsen and Chatterton, 1982. A genus of Eomonorachinae with laterally confluent and swollen L2 and L3; shallow longitudinal furrows connect adaxial tips of glabellar furrows; S3 concave forward; palpebral lobe stands as high as glabella and does not project in front of S3; palpebral area wide (tr.); narrow horizontal cephalic doublure lacks vincular furrow; genal spines long and horizontal; and glabellar prosopon consists of small tubercles. Triangular pygidium is long, highly arched, and acutely pointed; slender axis is equally divided into apodemal sector or seven rings and post-apodemal sector of 10-14 rings; pleural field is crossed by 10 well incised pleural furrows; intrepleural furrows are faint; and border is lacking.

Sceptaspis avalanchensis n. sp.

Pl. 14, figs. 1-16

Etymology: Named after the Avalanche Lake locality.

Material: 72 cranidia, 1 hypostome, and 18 pygidia.

Stratigraphic Occurrence: AV4B 6m - 18 m; 98AV4B 11.5m - 14.5m.

Holotype: Holotype cranidium UA 11742; paratypes UA 11743 - UA 11752.

Diagnosis: A species of *Sceptaspis* with a weak S1 posterior fork; occipital ring twice as wide (tr.) as long (sag.); palpebral lobe stands below glabella; transverse anterior border of hypostome; short pygidium with slightly rounded to subangular posterior margin; 3 to 4 distinct axial rings; and pleural field crossed by 3 distinct pleural and interpleural furrows.

Description:

Cranidium: Cranidium semicircular in outline; moderately convex (tr.) and slightly convex (sag.). Glabella expands forward to maximum width across midlength of anterior lobe from minimum between occipital furrow and L1. Axial furrow shallow; subparallel opposite L1, then curves outward to anterior part of L3 and recurves slightly inward for a short distance to terminate at distal ends of S3. Convexity of glabella greatest across occipital ring, decreases gradually forward. In lateral view, glabellar height greatest in front of palpebral lobes; gradually slopes posteriorly toward occipital furrow, gradually slopes anteriorly toward anterior margin. Occipital furrow straight, short (sag.) medially; descends distally into deep slot-like apodemal pits. Occipital ring lenticular in outline; twice as wide (tr.) as long (sag.); slightly wider than glabella cross L1; posterior margin convex backward. S1 initially deep; proceeds a short distance inwards and slightly backwards from axial furrow; splits at apodemal pit, anterior fork curves inward and forward, terminates one-quarter way across glabella; posterior fork very shallow to imperceptible, weakly isolates L1 (pl. 14, fig. 1, 2); smaller specimens show splitting of S1 at apodemal pit: posterior fork shallow, curves back to occipital furrow to isolate subrectangular L1 (pl. 14, fig. 6). S2 shallower than S1, curves forward and inward one-quarter way across glabella; shallows close to axial furrow. L2 subtrapezoidal in outline; approximately same size as L1. S3 moderately deep; proceeds inwards and backwards from anterior edge of palpebral lobe in a gentle concave-forward curve; extends one-third way across glabella. L3 subtriangular in outline. Anterior lobe rhomboid to semicircular in outline; length (sag.) one-half maximum width (tr.); laterally and anteriorly delimited by faint preglabellar furrow. Palpebral lobe outlined by shallow palpebral furrow; stands below glabella (pl. 14, fig. 3); posterior edge of palpebral lobe initiated above posterior border furrow, anterior

edge opposite distal ends of S3. In smaller crania, palpebral lobes become progressively smaller and positioned farther forward, posterior edge opposite S1 furrow and anterior edge opposite distal ends of S3. Posterior border furrow transverse, moderately impressed. Posterior border approximately one-half length (exsag.) of occipital ring. Ornamentation consists of fine granules and closely spaced tubercles on glabella. Tubercles sparse on palpebral lobes. In smaller specimens, proportionately larger tubercles are present on the cranium, concentrated on fixigenae and anterior lobe. Tubercles along anterior cephalic margin form spinose projections in small crania.

Hypostome: Hypostome shield-shaped in outline. Anterior margin transverse medially; curves backwards distally extending into a pair of posterolaterally and dorsally diverted anterior wings. Anterior border furrow convex forward; shallow medially, becoming imperceptible distally towards anterior wings. Middle body of hypostome ovoid in outline, defined laterally by shallow border furrows. Lateral border furrow converges with shallower, almost imperceptible posterior border furrow. Lateral margin extends backwards from anterior wing to small pointed shoulder, then curves inwards towards long (sag.), tongue-shaped posterior border with slight posteromedial projection. Ventral surface of hypostome finely granulose. On interior, doublure very narrow at base of anterior wings, expands slightly posteriorly; inner margin of doublure evenly curved posteriorly.

Thorax: Thorax unknown.

Pygidium: Pygidium subtriangular in outline; twice as wide (tr.) across anterior margin than long (sag.); posterolateral margin straight, converges at 45 degrees to sagittal line to form subangular apex. Axis high and convex (tr.), narrowing slightly backwards to rounded termination; bounded by moderately deep, straight axial furrows. Axis consists of 3 to 4 well defined axial rings which become shorter (sag.) and narrower (tr.) posteriorly. More posterior axial rings and terminal piece poorly defined. Axial ring furrows slightly convex forward; median portion of first axial ring modified by faint forwardly curved furrow which isolates narrow, spindle-shaped preannulus. Pleural field initially flat, curves steeply to lateral margin; crossed by three distinct and nearly straight pleural furrows which begin at axial furrow and terminate well inside lateral margin; and by three distinct interpleural furrows which initiate close to axial furrow and curve outward and backward to terminate nearly at lateral margin. Posterior margin rounded to subangular; slightly deflected upward at apex. On ventral surface, moderately broad and flat doublure extends to distal ends of pleural furrows and tip of axis.

Discussion:

Ludvigsen and Chatterton (1982) described *Sceptaspis*, a new genus of pterygometopid, to recognize separate species of *Calyptaulax* with a long and acutely pointed pygidium. Silicified material from the Whittaker Formation, District of Mackenzie provided knowledge of the distinctive hypostome. This hypostome was used to associate the Avalanche Lake material with the genus *Sceptaspis*.

In addition to the hypostome, *Sceptaspis avalanchensis* n. sp. appears to have laterally confluent L2 and L3, although in the Avalanche Lake material the S2 appears longer and may shallow and broaden towards the axial furrow instead of terminating prior to reaching it. The pygidium of *S. avalanchensis* provide an interesting conflict with the original diagnosis of *Sceptaspis*. Considered to be a diagnostic feature for the genus, the long and acutely pointed pygidium does not appear associated with the Avalanche Lake material. Instead, the pygidium is short with a slightly rounded to subangular posterior border. The pleural and axial furrows are shallow, less numerous and indistinctive posteriorly. These pygidia are associated with *Sceptaspis* n. sp. based on co-occurrences of material within several horizons of the section. Above and below these sections, *Tricopelta mackenziensis*, another pterygometopid from the Whittaker Formation, is found. The pygidia appear to conform to the morphology of *T. mackenziensis* with some ease, with the exception of the shallow pleural and axial furrows which may be attributed to poor preservation of the material. If the pygidia do not belong to *T. mackenziensis*, revision of the diagnostic features of the genus *Sceptaspis* would be appropriate, excluding the morphology of the pygidium.

Until further material is studied and associations clearer, the pygidia found to co-occur with the cranidia of *Sceptaspis* in the Avalanche Lake section will remain associated with that genus.

Sceptaspis avalanchensis can be distinguished from *Sceptaspis lincolnensis*, described and illustrated from the Rocklandian to Kirkfieldian of the lower Whittaker Formation, District of Mackenzie (Ludvigsen and Chatterton, 1982) by the longer S2 which does not unite the L2 and L3 as strongly, the transverse anterior border and shallower middle furrow of the hypostome, and the morphology of the pygidium which was previously discussed. In addition, the position of the palpebral lobes are forward slightly in *Sceptaspis avalanchensis*, with the posterior edge opposite the occipital furrow to opposite of the L1 (pl 14, figs. 1, 2). This feature is also variable in *S. lincolnensis* with the posterior edge opposite the midpoint (sag.) of the occipital ring and equal in position with the posterior border furrow (see pl. 5, fig. 1, Ludvigsen and Chatterton, 1982) to slightly forward of the

posterior border of the occipital ring and below the posterior border furrow (see pl. 5, fig. 3, Ludvigsen and Chatterton, 1982).

Genus *Calyptaulax* Cooper, 1930

Type Species: *Calyptaulax glabella* Cooper, 1930, from the Whitehead Formation (Ashgill), Gaspé, Quebec.

Diagnosis: This diagnosis follows Ludvigsen and Chatterton, 1982. A genus of Eomonorachinae with backwardly deflected and frequently effaced S2; straight or forwardly convex S3; palpebral lobe large, back opposite L1 or S0 and stands as high as or lower than glabella; palpebral area wide; broad cephalic doublure is upturned anteriorly, carries deep vincular furrow laterally; genal angle rounded or with short, pointed genal spine; glabellar prosopon of low tubercles and granules or absent. Pygidium is slightly arched, with posterior apex pointed; axis unequally subdivided into shorter apodemal sector of three rings and longer post-apodemal sector of seven to eight rings; pleural field is crossed by six to eight sharply incised pleural furrows and shallower interpleural furrows that extend to margin.

Calyptaulax n. sp. A

Pl. 14, figs. 17-23

Material: 6 cranidia; UA 11753.

Stratigraphic Occurrence: AV4B 73m.

Discussion:

The material of *Calyptaulax* n. sp. A consists of several cranidia that are restricted to one horizon within the Avalanche Lake section. It is distinct from other species of *Calyptaulax* by having an anterior lobe with a width (tr.) to length (sag.) ratio of 2:1, shallowing axial furrows opposite L3, a large quadrate L1, a S2 that shallows and broadens close to the axial furrow, an occipital ring that is three times as wide (tr.) as long (sag.), palpebral lobes that are below the crest of the glabella, and are positioned relatively forward.

The position of the palpebral lobes seems to be variable both within species and between species. The palpebral lobes of *Calyptaulax callirachis* (see in Chatterton and Ludvigsen, 1976) vary in position from having the posterior edge of the lobe opposite the midlength (sag.) of the occipital ring, below the posterior border furrow to having the posterior edge of the palpebral lobe equal to or slightly above the posterior border furrow (see plate 16, fig. 1 and figs. 5, 9 from Chatterton and Ludvigsen, 1976). The posterior edge of the palpebral lobes of *Calyptaulax* n. sp. A are positioned opposite the midlength (sag.) of the occipital ring, however, the posterior border furrow has travelled posteriorly distally to

allow the palpebral lobe to be positioned above the furrow. In other species of *Calyptaulax*, the posterior border furrow is transverse.

Other similar Ordovician species include *Calyptaulax callirachis* from the Upper Whiterock (Chazy) of the Esbataottine Formation, Mackenzie Mountains (Chatterton and Ludvigsen, 1976); *Calyptaulax* sp. 2 from the Upper Whiterock (Chazy) of the Esbataottine Formation, Mackenzie Mountains (Ludvigsen, 1975); *Calyptaulax glabella* from the Ashgill of the Whitehead Formation, Quebec (Cooper, 1930), illustrated by Ludvigsen and Chatterton (1982); and *Calyptaulax annulata* Raymond 1905 from the early Middle Ordovician of New York (Shaw, 1968, 1974).

Chatterton and Ludvigsen (1976) considered *C. callirachis* and *C. annulata* closely related and their differences distinctive but few. With the lack of material of *C. n. sp. A*, except for the cranidia, differences between these taxa are similar. In addition to the features outlined above, the preglabellar furrow of *C. n. sp. A* is very faint, the lateral glabellar and palpebral furrows appear shallower, the anterior edge of the palpebral lobe is opposite S3 not anterior to it, and the cranidium is not as strongly ornamented with low tubercles restricted mainly to the anterior lobe.

Although *C. n. sp. A* and *Calyptaulax* sp. 2 have several similarities, including shallower lateral glabellar and palpebral furrows and palpebral lobes that have a slightly forward position with the posterior edge anterior of the posterior border furrow, there are several features that allow a distinction. In addition to the previously outlined features, the cranidium of *C. n. sp. A* is not as strongly ornamented with low tubercles restricted mainly to the anterior lobe.

The Whittaker material differs from *Calyptaulax glabella* in having a longer and firmly impressed S2 that is not completely isolated from the axial furrow, a less convex forward anterior margin, a S3 that travels medially at a shallower angle, and low tubercles that are restricted to the anterior lobe. Although the material illustrated by Ludvigsen and Chatterton (1982) has a smooth glabella, they acknowledge that this is a variable characteristic and that the glabella may have fine granules and very low granulose tubercles.

Due to the variability of the genus, as pointed out by previous work (Shaw, 1968, 1974; Chatterton and Ludvigsen, 1976) further comparisons with the numerous species of *Calyptaulax* will await a comprehensive study of the Laurentian genus to establish intrageneric relationships.

Genus *Tricopelta* Ludvigsen & Chatterton, 1982

Type Species: *Tricopelta mackenziensis* Ludvigsen and Chatterton, 1982, from the lower Whittaker Formation (Edenian) of the southern Mackenzie Mountains, District of Mackenzie.

Diagnosis: This diagnosis follows Ludvigsen and Chatterton, 1982. A genus of Eomonorachinae with laterally confluent and swollen L2 and L3; L1 and L2 extremely short (exsag.); S3 convex forward; palpebral lobe inclined inward and stands well above glabella; narrow cephalic doublure has median downward deflection, lacks vincular furrow; genal spines long and horizontal; and glabellar prosopon consists of coarse tubercles. Triangular pygidium is short, highly arched, and rounded posteriorly; short axis unequally divided into longer apodemal sector of five rings and post-apodemal sector of five to six rings; pleural field is crossed by seven to eight sharply incised pleural furrows; interpleural furrows extremely faint.

Tricopelta mackenziensis Ludvigsen & Chatterton, 1982

Pl. 15, figs. 1-19

Chasmops n. sp. Ludvigsen, 1979a, Pl. 1, fig. 12.

Tricopelta mackenziensis Ludvigsen & Chatterton, 1982, Pl. 6, fig. 14; Pl. 7, figs. 1-15; Fig. 9.

Material: 437 cranidia, 1256 librigenae, 349 hypostomes, 176 thoracic segments, and 555 pygidia; UA 11754 - UA 11770.

Stratigraphic Occurrence: AV4B 3m - 73m; 98AV4B 6.25m - 23.8m.

Holotype: An incomplete cephalon from the lower Whittaker Formation, District of Mackenzie, illustrated and described by Ludvigsen and Chatterton (1982).

Description: The following is to be added to the description of *Tricopelta mackenziensis* from Ludvigsen and Chatterton (1982):

Thorax: Number of thoracic segments unknown. Axis high, convex (tr.); one-quarter as wide (tr.) as complete segment; composed of convex (sag.), lenticular articulating half ring and axial ring, separated by moderately deep articulating furrow which travels distally into deep anteriorly diverging apodemal pits. Posterior edge of axial rings curves slightly posteriorly; in lateral view, anterior side curves steeply out of articulating furrow. Axial furrow shallow, more steeply incised posteriorly. Inner portion of pleura flat and horizontal. Pleura divided by moderately deep pleural furrow which originates at anterior end of axial furrow, cross one-half length (exsag.) of segment, after slope change furrow continues downwards curving slightly toward anterior edge, fades out near spatulate tip of thoracic segment. Outer portion of pleura slightly expanded distally and slightly curved anteriorly. Occipital doublure of axial ring extends approximately half length (sag.) of axial

ring medially. Distal tip of pleura encased by flat doublure whose posterior edge narrows and terminates at fulcrum; anterior edge without extension of doublure; inner margin of doublure evenly curved. Articulating devices not visible. Ornamentation smooth.

Discussion:

Tricopelta mackenziensis is one of the more numerous taxa within the Avalanche Lake material. At 581 specimens, material is plentiful to permit this designation. The occurrence of *Tricopelta mackenziensis* in the Avalanche Lake section extends the range of this taxon from the Edenian (Ludvigsen and Chatterton, 1982) to the Ashgill (Upper Ordovician).

In the description of *Tricopelta mackenziensis*, Ludvigsen and Chatterton (1982) noted the absence of thoracic segments. The Avalanche Lake material provides thoracic segments attributed to *Tricopelta mackenziensis* based on association of material within the collection. Although *Sceptaspis avalanchensis* n. sp. occurs in several of the same horizons, the thoracic segments also occur in several horizons where there is an absence of *Sceptaspis avalanchensis* n. sp. and they always occur in association with *Tricopelta mackenziensis*.

Although the general morphology of the thoracic segments of the Family Pterygometopidae appears to be conservative, there are a few notable differences between the thoracic segments of *Tricopelta mackenziensis* and *Calyptraulax callirachis* from the Upper Whiterock (Chazy) of the Esbataottine Formation, Mackenzie Mountains (Chatterton and Ludvigsen, 1976). The thoracic segments of *Tricopelta mackenziensis* can be distinguished from *C. callirachis* by a shallower axial furrow, a pleural doublure that does not extend along the anterior margin of the pleura and as far medially encasing a smaller portion of the pleural tip, and a lack of tubercles on the axial rings.

Suborder Calymenina Swinnerton, 1915
Family Calymenidae Milne Edwards, 1840

Calymenid

Pl. 18, figs. 14-15

Material: 1 hypostome and 1 rostral plate; UA 11814, UA 11815.
Stratigraphic Occurrence: AV4B 43m - 49.5m.

Discussion:

Several genera of silicified calymenid trilobites have been described from the Silurian of the Mackenzie Mountains by Perry and Chatterton (1979), Chatterton et al. (1990), and Siveter and Chatterton (1996). The Upper Ordovician material, consisting of a hypostome and a rostral plate, is too fragmentary for a detailed comparison with the Silurian material.

The material is placed within the Family Calymenidae based on the typical morphology of the rostral plate which consists of an outer, arched (tr.) border sector and reflexed doublure sector (Siveter and Chatterton, 1996).

Order Lichida Moore, 1959
Family Lichidae Hawle & Corda, 1847
Subfamily Trochurinae Phleger, 1936
Genus *Hemiarges* Gurich, 1901

Type Species: *Lichas wesenbergensis* Schmidt, 1885, from the Rakvere Limestone (Caradocian) of Estonia.

Diagnosis: This diagnosis follows Moore, 1959. Bicomposite and basal lateral glabellar lobes partially confluent (in typical species); genal angles produced in stout, broad-based spines.

Hemiarges n. sp. A

Pl. 16, figs. 1-17

Material: 27 cranidia, 33 librigenae, 27 hypostomes, and 47 pygidia; UA 11771 - UA 11783.

Stratigraphic Occurrence: AV4B 3m - 73m; 98AV4B 6.25m - 22.6m; AV1 54m.

Discussion:

The lichid material from Avalanche Lake 4B was previously described and identified as *Hemiarges avalanchensis* n. sp. by Campbell (1994) in her unpublished MSc. thesis. This work is currently in preparation for publication by Campbell and Chatterton (2000). The material from Avalanche Lake is in general agreement with the description by Campbell (1994). The hypostome is slightly variable in proportion with a more quadrate outline and a length to width ratio of 1:1.35, in contrast with the subrectangular outline of Campbell's material and a length to width ratio of 1:1.84. This subtle difference may be accounted for by compression of the material during preservation. Distortion can also be seen in the cranidia of the material so little consideration is given to this difference. The Avalanche Lake material will follow the designation given by Campbell (1994).

Subfamily Tetralichinae Phleger, 1936
Genus *Amphilichas* Raymond, 1905

Type Species: *Platymetopus lineatus* Angelin, 1854, from the Boda Limestone (Upper Ordovician) of Sweden.

Diagnosis: This diagnosis follows Moore, 1959. Longitudinal furrows short (in type species) but mostly reaching occipital furrow. Pygidium usually with pointed axis reaching posterior margin, and unfurrowed 3rd pleurae with single free points.

Amphilichas sp.

Pl. 18, figs. 16-17

Material: 1 hypostome; UA 11816.

Stratigraphic Occurrence: 98AV4B 22.6m.

Discussion:

The material from Avalanche Lake consists of only one hypostome. Comparison with *Amphilichas* material in Chatterton and Ludvigsen (1976) illustrates the generic association of this material. The hypostome of *Amphilichas* has several diagnostic features that distinguish it from another similar genus, *Hemiarges*, which is also present in the Avalanche section at the same horizon. The hypostome of *Hemiarges* possesses strong pitting on the ventral surface of the middle body not seen in *Amphilichas*. In addition, the lateral portions of the doublure of *Hemiarges* forms platform-like shoulders, whereas in *Amphilichas*, these are formed into pointed tips which project beyond the lateral border in ventral view. Finally, both genera have a strongly notched posteromedian portion of the posterior margin which forms an excavation in the dorsal surface of the doublure. In *Hemiarges*, the inner margin of this notch is evenly curved, whereas in *Amphilichas*, the notch appears quadrate.

A similar lichid, *Platylichas* (*Rontripia*) n. sp., described by Campbell (2000, in prep) from the AV1 section, Whittaker Formation has a similar hypostome morphology to the *Amphilichas* sp. hypostome from AV4B. The AV4B material was judged not to be associated with the AV1 taxon based on the morphology of the doublure and the Llandovery age assigned to the AV1 material.

The lack of material for this genus would not allow a species determination.

Family Odontopleuridae Burmeister, 1843 **Subfamily Odontopleurinae Burmeister, 1843**

Odontopleurid

Pl. 18, figs. 18-19

Material: 1 librigena and 2 pygidia; UA 11817, UA 11818.

Stratigraphic Occurrence: AV4B 20cm.

Discussion:

The Avalanche Lake material consists of one poorly preserved librigena and a partial pygidium. The material is placed within the Subfamily Odontopleurinae based on the slender base of the genal spine, a diagnostic feature of the subfamily according to Ramskold and Chatterton (1991). The position of two marginal spines on the anterolateral margin of the genal spine may be one of the features that can be used for diagnosis within the Subfamily Odontopleurinae. This feature can be observed in *Kettneraspis* and *Diacanthaspis*, but without more material, the generic designation is inconclusive.

Literature Cited:

- Adrain, J.M. 1998. Systematics of the Acanthoparyphina (Trilobita), with species from the Silurian of Arctic Canada. *Journal of Paleontology*, 72(4): 698 - 718.
- Adrain, J.M. 1997. Proetid trilobites from the Silurian (Wenlock-Ludlow) of the Cape Phillips Formation, Canadian Arctic Archipelago. *Palaeontographica Italica* 84: 21-111.
- Adrain, J.M., and Chatterton, B.D.E. 1995. The Otariionine trilobites *Harpidella* and *Maurotarion*, with species from northwestern Canada, the United States, and Australia. *Journal of Paleontology*, 69 (2), p. 307-326.
- Billings, E. 1859. Descriptions of some new species of trilobites from the Lower and Middle Silurian rocks of Canada. *Canadian Naturalist and Geologist*, 4: 367-383.
- Campbell, M. J. 1994. Systematics of Silurian lichid trilobites from the Mackenzie Mountains, Canada. Unpublished Msc. Thesis, University of Alberta at Edmonton, Alberta, 197 p.
- Campbell, M. J., and Chatterton, B.D.E. 2000. (in prep).
- Chatterton, B.D.E. 1980. Ontogenetic studies of Middle Ordovician trilobites from the Esbataottine Formation, Mackenzie Mountains, Canada. *Paleontographica, Abt. A.*, 1-73.
- Chatterton, B.D.E. 1994. Ordovician proetide trilobite *Dimeropyge*, with a new species from Northwestern Canada. *Journal of Paleontology*, 68 (3): 541-556.
- Chatterton, B.D.E., and Ludvigsen, R. 1976. Silicified Middle Ordovician trilobites from the South Nahanni River area, District of Mackenzie, Canada. *Palaeontographica, Abt. A.*, 1-106.
- Chatterton, B.D.E., and Perry, D.G. 1977. Lochkovian trilobites and conodonts from Northwestern Canada. *Journal of Paleontology* 51(4): 772-796.
- Chatterton, B.D.E., Siveter, D.J., Edgecombe, G.D. and Hunt, A.S. 1990. Larvae and the relationships of the Calymenina (Trilobita). *Journal of Paleontology*, 64: 255-277.
- Churkin, M. 1963. Ordovician trilobites from graptolitic shale in central Idaho. *Journal of Paleontology*, 37(2): 421-428.
- Cooper, B.N. 1930. In Schuchert, C. and Cooper, G.A. Upper Ordovician and Lower Devonian stratigraphy and paleontology of Perce, Quebec. Part II. New species from the Upper Ordovician of Perce. *American Journal of Science*, 20: 365-392.
- Cooper, B.N. 1953. Trilobites from the Lower Champlainian Formations of the Appalachian Valley. *The Geological Society of America, Memoir* 55, pp. 1-68.
- Dekay, J.E. 1824. Observations on the structure of trilobites and description of an apparently new genus. *Ann. Lyc. Nat. Hist. N.Y.*, 1: 174 - 189.

- Dean, W.T. 1979. Trilobites from the Long Point Group (Ordovician), Port au Port Peninsula, southwestern Newfoundland. Geological Survey of Canada, Bulletin 290: 1-53.
- Edgecombe, G.D., and Chatterton, B.D.E. 1990. Systematics of *Encrinuroides* and *Curriella* (Trilobita), with a new Early Silurian encrinurine from the Mackenzie Mountains. Canadian Journal of Earth Sciences, 27, p. 820-833.
- Esker, G.C. 1964. New species of trilobites from the Bromide Formation (Poolverille member) of Oklahoma. Oklahoma Geological Notes, 24: 195-209.
- Esmark, H.M.T. 1833. Om nogle nye Arter af Trilobiter. Mag. f. Naturvid, 11: 268-270.
- Green, J. 1832. Synopsis of the trilobites of North America. Monthly American Journal of Geology and Natural History, 1(12): 558-560.
- Hall, J. 1847. Palaeontology of New York, v. 1. Natural History of New York, Albany, p. 338.
- Lane, P.D. 1971. British Cheiruridae (Trilobita). Palaeontographical Society Monograph, 125 :1-95.
- Lenz, A.C., and Churkin, jr., M. 1966. Upper Ordovician trilobites from Northern Yukon. Palaeontology, 9 (1): 39-47.
- Lesperance, P.J. and Bertrand, R. 1976. Population systematics of the Middle and Upper Ordovician trilobite *Cryptolithus* from the St. Lawrence lowlands and adjacent areas of Quebec. Journal of Paleontology, 50: 598-613.
- Ludvigsen, R. 1975. Ordovician formations and faunas, southern Mackenzie Mountains. Canadian Journal of Earth Sciences, v. 12, p. 663-697.
- Ludvigsen, R. 1976. New cheirurid trilobites from the lower Whittaker Formation (Ordovician), southern Mackenzie Mountains. Canadian Journal of Earth Sciences, v. 13, p. 947-959.
- Ludvigsen, R. 1977. The Ordovician trilobite *Ceraurinus* Bolton in North America. Journal of Paleontology. v. 51, p. 959-972.
- Ludvigsen, R. 1978. The trilobites *Bathyurus* and *Eomonorachus* from the Middle Ordovician of Oklahoma and their biofacies significance. Life Sciences Contribution, Royal Ontario Museum, Number 114, p. 1 - 18.
- Ludvigsen, R. 1979. A trilobite zonation of Middle Ordovician rocks, southwestern District of Mackenzie. Geological Survey of Canada Bulletin 312, p. 1-99.
- Ludvigsen, R. 1979a. Middle Ordovician trilobite biofacies, southern Mackenzie Mountains. In C.R. Stelck and B.D.E. Chatterton (eds.): Western and Arctic Canadian Biostratigraphy. Geological Association of Canada, Special Paper 18, p. 1-37.
- Ludvigsen, R. 1980. An unusual trilobite faunule from Llandeilo or Lowest Caradoc strata (Middle Ordovician) of Northern Yukon Territory. In, Current Research, Part B, Geological Survey of Canada, Paper 80-1B: 97-106.

- Ludvigsen, R., and Chatterton, B. D. E. 1982. Ordovician Pterygometopidae (Trilobita) of North America. *Canadian Journal of Earth Sciences*, 19 (11): 2179-2206.
- Ludvigsen, R., and Chatterton, B.D.E. 1991. The peculiar Ordovician trilobite *Hypodicranotus* from the Whittaker Formation, District of Mackenzie. *Canadian Journal of Earth Sciences* 28, p. 616-622.
- Moore, R.C. (editor), 1959. *Treatise on Invertebrate Paleontology, Part O, Arthropoda 1*. Geological Society of America, University of Kansas Press, Lawrence.
- Owen, A.W. 1980. A new species of *Cryptolithus* (Trilobita) from the Late Ordovician of Norway. *Journal of Paleontology*, 54:144-149.
- Owen, A.W. 1981. The Ashgill trilobites of the Oslo Region, Norway. *Palaeontographica*. Abt. A, 1-88.
- Owens, R.M. 1973. British Ordovician and Silurian Proetidae (Trilobita). *Palaeontographical Society Monograph* 127: 1-98.
- Owens, R.M. 1973. Ordovician Proetidae (Trilobita) from Scandinavia. *Norsk Geologisk Tidsskrift*, 53: 117-181.
- Perry, D.G., and Chatterton, B.D.E. 1979. Wenlock trilobites and brachiopods from the Mackenzie Mountains, Northwestern Canada. *Palaeontology* 22(3): 569-607.
- Phleger, F.B. 1933. Notes on certain Ordovician faunas of the Ingo Mountains, California. *Bulletin of the Southern California Academy of Sciences*, 32: 1-21.
- Pribyl, A., Vanek, J., and Pek, I. 1984. Phylogeny and taxonomy of Family Cheiruridae (Trilobita). *Acta Universitatis Palackianae Olomucensis Facultas Rerum Naturalium Geographica-Geologica*, 83: 107-193.
- Ramskold, L., and Chatterton, B.D.E. 1991. Revision and subdivision of the polyphyletic "*Leonaspis*" (Trilobita). *Transactions of the Royal Society of Edinburgh: Earth Sciences*, 82:333-371.
- Raymond, P.E. 1905. The trilobites of the Chazy Limestone. *Annals of the Carnegie Museum*, 3: 328-386.
- Raymond, P.E. 1910. Notes on the Ordovician trilobites: IV. New and old species from the Chazy. *Annals of the Carnegie Museum*, 7: 60 - 79.
- Raymond, P.E. 1914. Notes on the ontogeny of *Isotelus gigas* Dekay. *Bulletin of the Museum of Comparative Zoology at Harvard College* 58: 247-263.
- Raymond, P.E. 1916. New and old Silurian trilobites from southeastern Wisconsin, with notes on the genera of the Illaenidae. *Bulletin of the Museum of Comparative Zoology Harvard*, 60: 1-41.
- Raymond, P.E. 1920. Some new Ordovician trilobites. *Bulletin of the Museum of Comparative Zoology, Harvard*, 64: 273-296.

- Raymond, P.E. 1925. Some trilobites of the lower Middle Ordovician of eastern North America. *Bulletin of the Museum of Comparative Zoology Harvard*, 67: 1-180.
- Raymond, P.E. and Narraway, J.E. 1908. Notes on Ordovician trilobites: Illaenidae from the Black River Limestone, near Ottawa, Canada. *Annals of the Carnegie Museum*, 4: 242-255.
- Ross, R.J., jr. 1967. Middle Ordovician brachiopods and trilobites from the Basin Ranges, western United States. Professional Paper, U.S. Geological Survey, 523-D: 1-43.
- Ross, R.J., jr., and Shaw, F.C. 1972. Distribution of the Middle Ordovician Copenhagen Formation and its trilobites in Nevada. Professional Paper, U.S. Geological Survey, 749: 1-33.
- Ross, R.J., jr., Nolan, T.B., and Harris, A.G. 1979. The Upper Ordovician and Silurian Hanson Creek Formation of Central Nevada. Shorter Contributions to Stratigraphy and Structural Geology, Geological Survey Professional Paper 1126-C: C1-C22.
- Rudkin, D.M., and Tripp, R.P. 1989. The type species of the Ordovician trilobite genus *Isotelus*: *I. gigas* Dekay, 1924. *Royal Ontario Museum, Life Sciences Contributions* 152, p. 1-19.
- Savage, T.E. 1917. The Thebes Sandstone and Orchard Creek Shale and their faunas in Illinois. *Acad. Sci. Illinois. Trans.*, 10: 261-275.
- Shaw, F.C. 1968. Early Middle Ordovician Chazy trilobites of New York. *Memoirs of the New York State Museum of Natural History*, 17: 1-163.
- Shaw, F.C. 1974. Simpson Group (Middle Ordovician) trilobites of Oklahoma. *The Paleontological Society, Memoir* 6: 1-54.
- Shaw, F.C. 1991. Viola Group (Ordovician, Oklahoma) cryptolithinid trilobites: biogeography and taxonomy. *Journal of Paleontology*, 65: 919-935.
- Shaw, F.C., and Lesperance, P.J. 1994. North American biogeography and taxonomy of *Cryptolithus* (Trilobita, Ordovician). *Journal of Paleontology*, 68 (4), p. 808-823.
- Siveter D.J. and Chatterton, B.D.E. 1996. Silicified calymenid trilobites from the Mackenzie Mountains, Northwest Canada. *Palaeontographica Abt. A.*, 43-60.
- Swofford, D.L. 1993. PAUP: Phylogenetic Analysis Using Parsimony, Version 3.3.1. Program distributed by the Illinois Natural History Survey, Champaign.
- Thomas, A.T. 1978. British Wenlock trilobites, Part 1. *Palaeontographical Society Monograph*: 1-56.
- Tremblay, J.V., and Westrop, S.R. 1991. Middle Ordovician (Whiterockian) trilobites from the Sunblood Formation, District of Mackenzie, Canada. *Journal of Paleontology*, 65 (5), p. 801-824.
- Tripp, R.P., and Evitt, W.R. 1986. Silicified trilobites of the family Asaphidae from the Middle Ordovician of Virginia. *Palaeontology*, 29(4): 705-724.

- Troedsson, G.T. 1928. On the Middle and Upper Ordovician faunas of northern Greenland, Part 2. Jubilaeumsekspeditionen Nord om Gronland. Meddelelser om Gronland, v. 72, p. 1-197.
- Walcott, C.D. 1875. Description of a new species of trilobite. Cincinnati Quarterly Journal of Science, 2: 273-274.
- Wang, K., Chatterton, B.D.E., Attrep, M., and Orth, C.J. 1993. Late Ordovician mass extinction in the Selwyn Basin, northwestern Canada: geochemical, sedimentological, and paleontological evidence. Canadian Journal of Earth Sciences, 30: 1870-1880.
- Whittington, H.B. 1950. Sixteen Ordovician genotype trilobites. Journal of Paleontology, 24: 531-565.
- Whittington, H.B. 1954. Ordovician trilobites from Silliman's Fossil Mount. Geological Society of America Memoir, 62: 119-225.
- Whittington, H.B. 1959. Silicified Middle Ordovician trilobites: Remopleurididae, Trinucleidae, Raphiophoridae, Endymioniidae. Bulletin of the Museum of Comparative Zoology, Harvard, 121(8): 369-496.
- Whittington, H.B. 1963. Middle Ordovician trilobites from Lower Head, western Newfoundland. Bulletin of the Museum of Comparative Zoology, Harvard, 129: 1-118.
- Whittington, H.B. 1965. Trilobites of the Ordovician Table Head Formation, western Newfoundland. Bulletin of the Museum of Comparative Zoology, Harvard, 132(4): 275-442.
- Whittington, H.B., and Evitt, W.R. 1953. Silicified Middle Ordovician trilobites. Memoir of the Geological Society of America, 59: 1-137.
- Yu, F. 1996. Ontogeny, taxonomy, and taphonomy of some Upper Ordovician silicified trilobites from eastern Nevada, U.S.A. Unpublished M.Sc. thesis, University of Alberta at Edmonton, Alberta, 154 p.

Plate 1

Figs. 1-26. *Bumastoides solangeae* n.sp.

1. Dorsal view of cranidium UA 11517, x 3.7.
2. Anterior view of cranidium UA 11518, x 10.4.
3. Ventral view of cranidium UA 11519, x 2.
4. Ventral view of rostral plate UA 11520, x 3.1.
5. Ventral view of librigena UA 11521, x 2.9
6. Ventral view of librigena UA 11522 x2.9
7. Dorsal view of librigena UA 11523, x 1.8.
- 8 & 12. Dorsal and lateral views of cranidium UA 11518, x 1.8 and x 2.24.
9. Dorsal view of free cheek UA 11524, x 1.9.
10. Ventral view of hypostome UA 11525, x 4.9.
11. Dorsal view of hypostome UA 11526, x 4.13.
13. Dorsal view of transitory pygidium UA 11527, x 4.8.
14. Ventral view of transitory pygidium UA 11528, x 4.7.
15. Anterior view of thoracic segment UA 11529, x 4.1.
16. Posterior view of thoracic segment UA 11530, x 2.8.
17. Ventral view of thoracic segment UA 11531, x 6.2.
18. Ventral view of thoracic segment UA 11532, x 4.9.
19. Ventral view of thoracic segment UA 11533, x 2.6.
20. Dorsal view of thoracic segment UA 15534, x 11.8.
21. Ventral view of pygidium UA 15535, x 2.
22. Dorsal view of pygidium UA 15536, x 3.4.
23. Ventral view of transitory pygidium UA 11537, x 3.8.
24. Dorsal view of pygidium UA 15538, x 12.
25. Lateral view of pygidium UA 15539, x 15.7.
26. Ventral view of pygidium UA 11540, x 4.1.

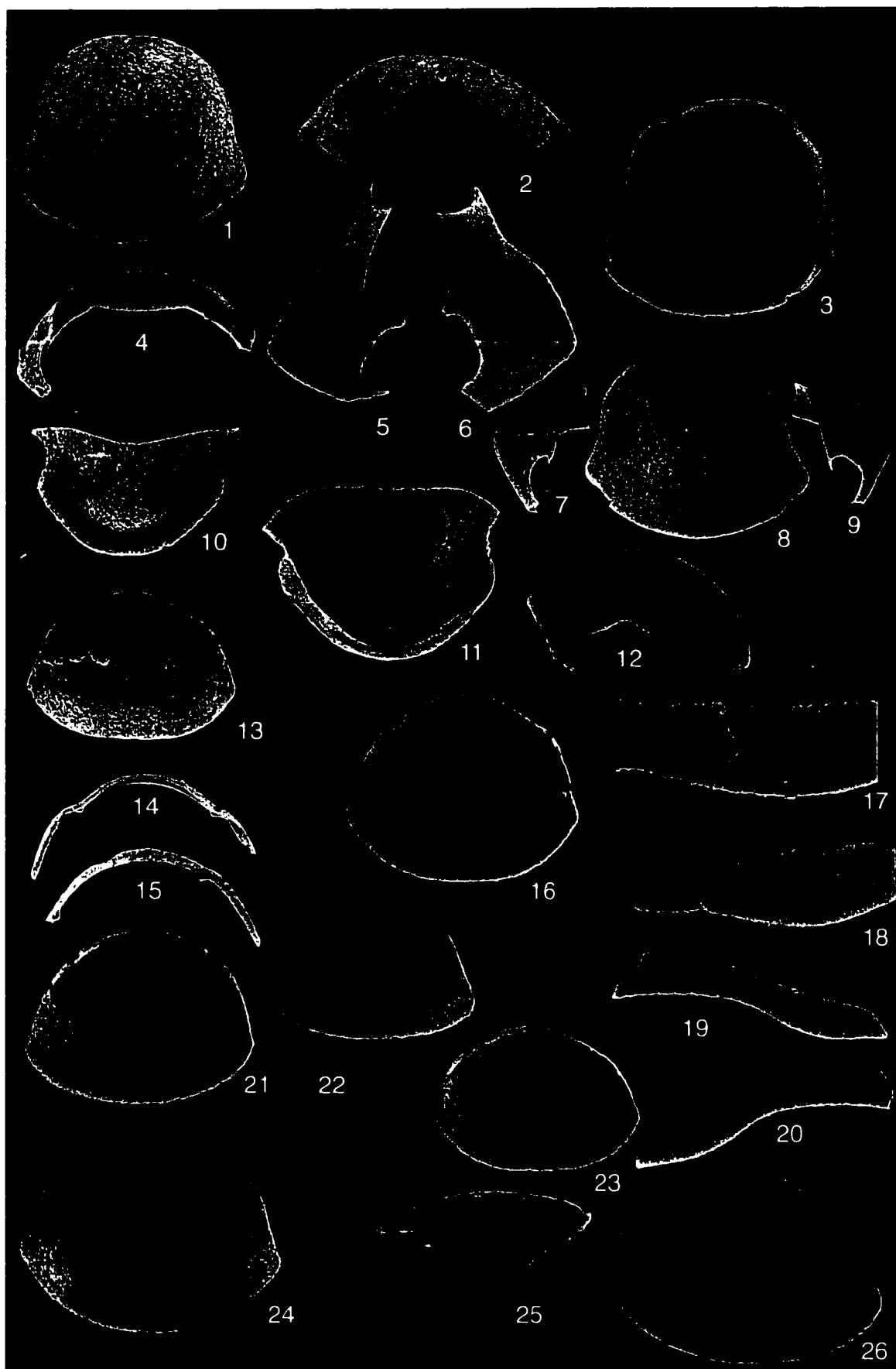


Plate 2

Figs. 1-27. *Bathyurus teresoma* n. sp.

1. Dorsal view of cranidium UA 11540, x 16.2.
2. Dorsal view of cranidium UA 11541, x 11.5.
3. Ventral view of cranidium UA 11542, x 17.2.
4. Dorsal view of cranidium UA 11543, x 17.8.
5. Anterior view of cranidium UA 11544, x 11.6.
6. Dorsal view of cranidium UA 11545, x 17.7.
7. Lateral view of cranidium UA 11546, x 12.4.
8. Posterior view of cranidium UA 11543, x 19.7.
9. Lateral view of cranidium UA 11543, x 21.3.
10. Ventral view of librigena UA 11547, x 4.5.
11. Ventral view of cranidium UA 11548, x 13.9.
12. Ventral view of librigena UA 11549, x 9.2.
13. Dorsal view of rostral plate UA 11550, x 12.8.
14. Ventral view of rostral plate UA 11551, x 8.9.
15. Ventral view of hypostome UA 11552, x 33.
16. Dorsal view of hypostome UA 11553, x 17.4.
17. Ventral view of hypostome UA 11554, x 12.7.
18. Dorsal view of librigena UA 11555, x 11.
19. Ventral view of librigena UA 11556, x 9.6.
20. Ventral view of thoracic segment UA 11557, x 3.9.
21. Dorsal view of thoracic segment UA 11558, x 6.6.
22. Ventral view of thoracic segment UA 11559, x 6.8.
23. Ventral view of thoracic segment UA 11560, x 10.4.
24. Dorsal view of pygidium UA 11561, x 12.3.
25. Dorsal view of pygidium UA 11562, x 12.3.
26. Lateral view of pygidium UA 11561, x 17.
27. Ventral view of pygidium UA 11563, x 11.6.

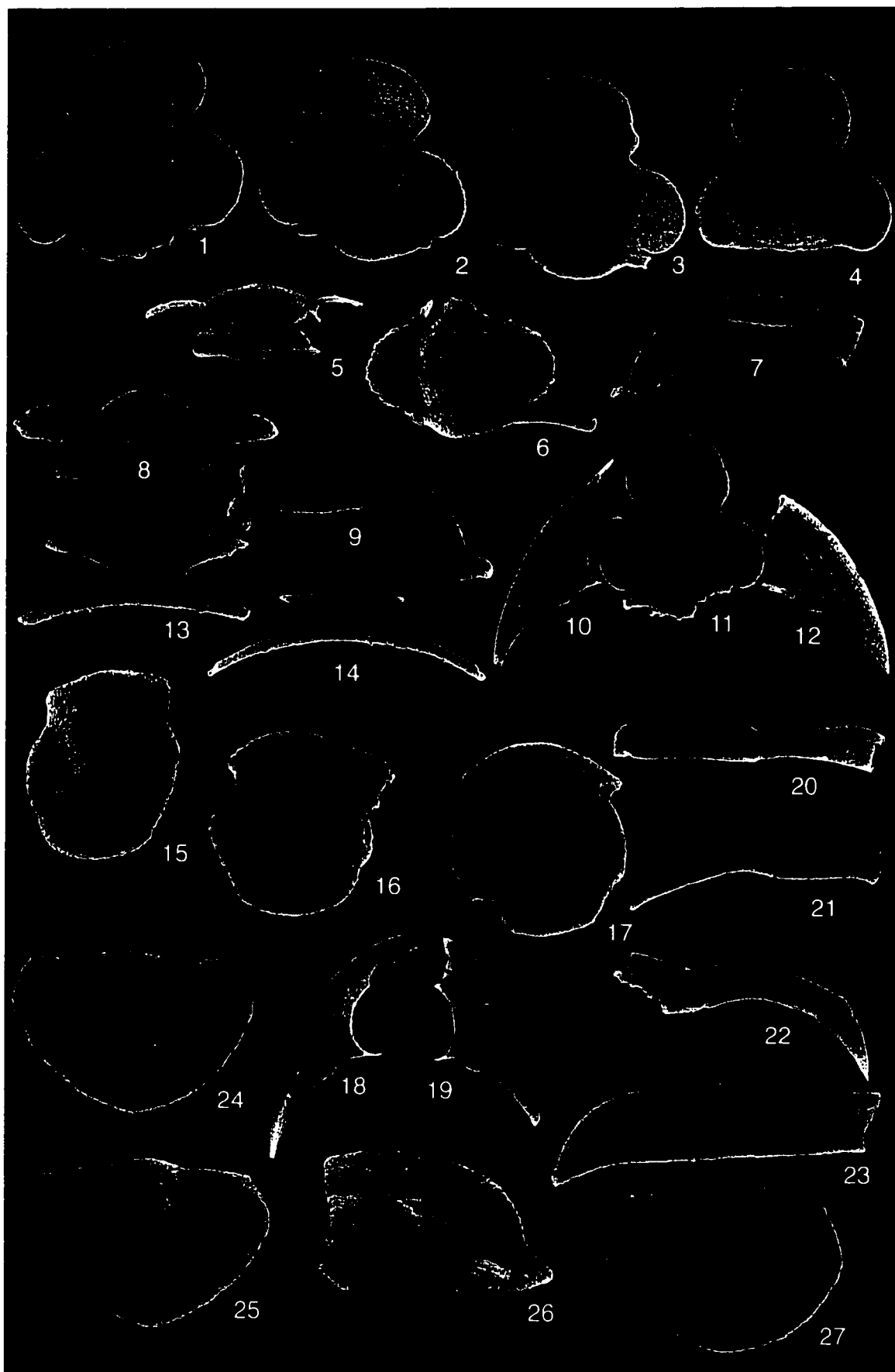


Plate 3

Figs. 1-23. *Decoroproetus hankei* n. sp.

1. Dorsal view of cranidium UA 11564, x 11.7.
2. Dorsal view of cranidium UA 11565, x 14.5.
3. Dorsal view of cranidium UA 11566, x 9.5.
4. Dorsal view of cranidium UA 11567, x 11.7.
5. Ventral view of cranidium UA 11568, x 18.5.
6. Ventral view of cranidium UA 11569, x 14.
7. Dorsal view of librigena UA 11570, x 11.
8. Dorsal view of cranidium UA 11571, x 17.1.
9. Dorsal view of librigena UA 11572, x 9.75.
10. Anterior view of cranidium UA 11566, x 14.4.
11. Lateral view of cranidium UA 11566, x 11.2.
12. Ventral view of hypostome UA 11573, x 17.6.
13. Dorsal view of hypostome UA 11574, x 22.
14. Dorsal view of hypostome UA 11573, x 25.
15. Lateral view of hypostome UA 11573, x 24.8.
16. Dorsal view of librigena UA 11575, x 11.
17. Ventral view of librigena UA 11576, x 10.6.
18. Lateral view of pygidium UA 11577, x 20.2.
19. Posterior view of pygidium UA 11577, x 13.5.
20. Ventral view of pygidium UA 11578, x 15.6.
21. Dorsal view of pygidium UA 11579, x 15.
22. Ventral view of pygidium UA 11580, x 16.6.
23. Dorsal view of pygidium UA 11577, x 14.6.

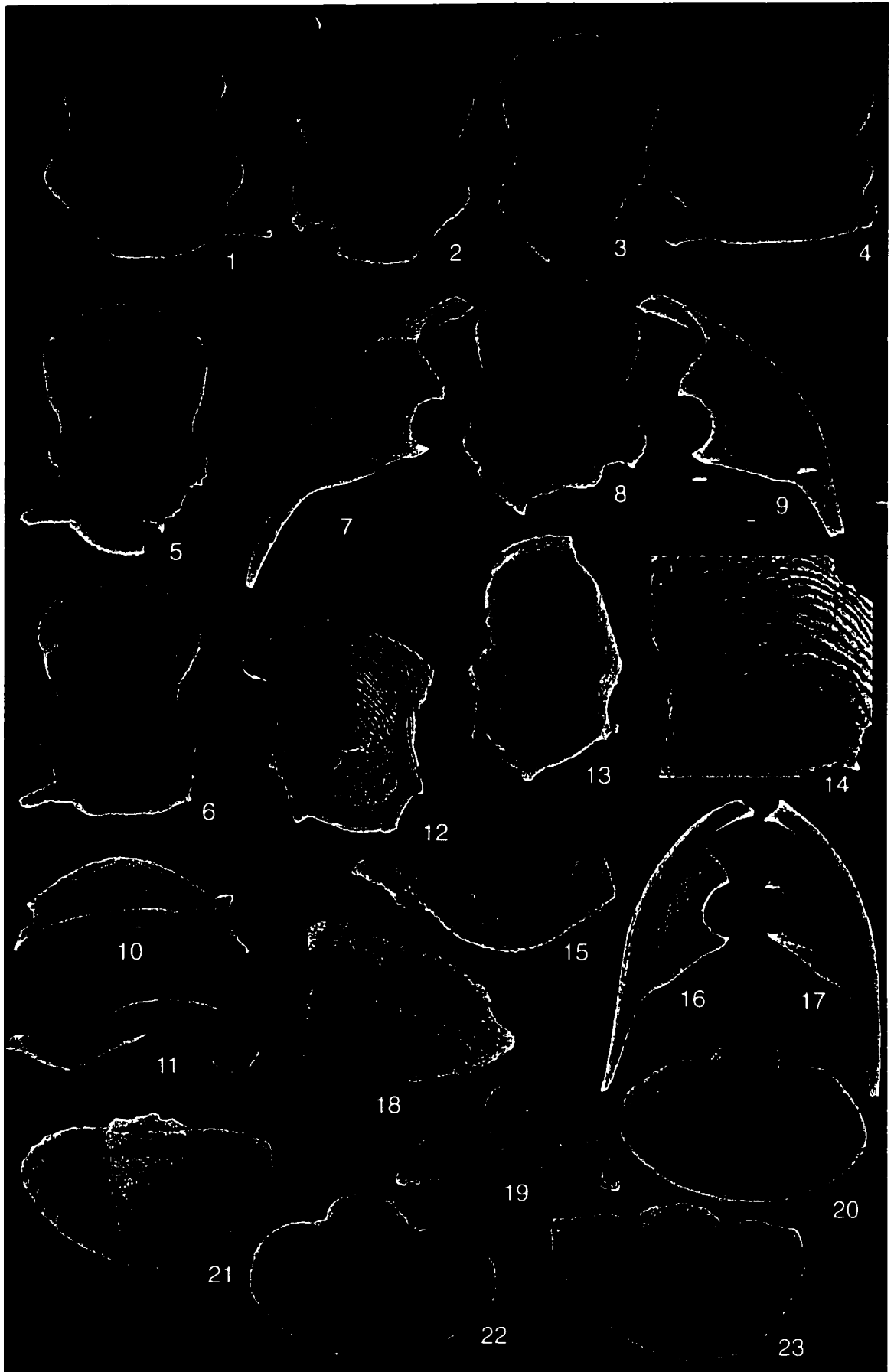


Plate 4

Figs. 1-27. *Isotelus dorycephalus* n. sp.

1. Dorsal view of librigena UA 11581, x 6.5.
2. Dorsal view of cranidium UA 11582, x 8.1.
3. Dorsal view of librigena UA 11583, x 7.0.
4. Dorsal view of pygidium UA 11584, x 1.7.
5. Anterior view of cranidium UA 11582, x 9.6.
6. Posterior view of cranidium UA 11582, x 9.6.
7. Oblique dorsal view of cranidium UA 11582, x 8.8.
8. Oblique dorsal view of cranidium UA 11582, x 8.7.
9. Dorsal view of meraspid cranidium UA 11585, x 9.3.
10. Lateral view of cranidium UA 11582, x 14.4.
11. Ventral view of meraspid cranidium UA 11585, x 12.4.
12. Dorsal view of meraspid cranidium UA 11586, x 18.8.
13. Ventral view of librigena UA 11587, x 6.5.
14. Ventral view of cranidium UA 11582, x 7.8.
15. Ventral view of librigena UA 11589, x 8.2.
16. Ventral view of pygidium UA 11584, x 3.9.
17. Ventral view of hypostome UA 11589, x 6.8.
18. Lateral view of hypostome UA 11590, x 10.4.
19. Dorsal view of hypostome UA 11590, x 8.3.
20. Dorsal view of transitory pygidium UA 11591, x 26.
21. Ventral view of thoracic segment UA 11592, x 16.5.
22. Ventral view of thoracic segment UA 11593, x 5.9.
23. Dorsal view of thoracic segment UA 11594, x 6.3.
24. Dorsal view of pygidium UA 11595, x 12.7.
25. Lateral view of pygidium UA 11596, x 17.4.
26. Anterior view of thoracic segment UA 11597, x 4.4.
27. Posterior view of pygidium UA 11598, x 11.8.

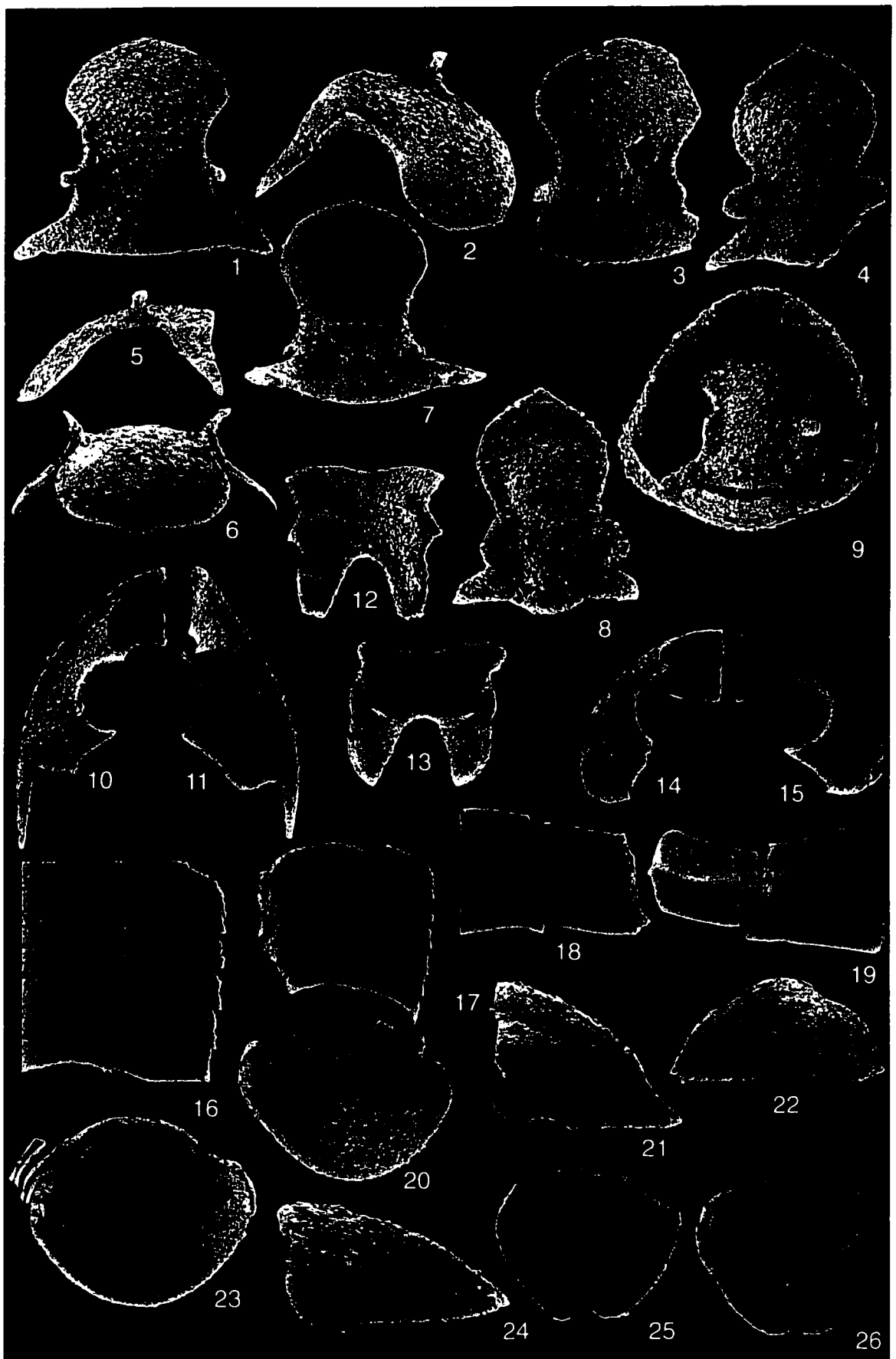


Plate 5

Figs. 1-26. *Anataphrus elevatus* n. sp.

1. Dorsal view of cranidium UA 11599, x 10.3.
2. Oblique view of cranidium UA 11599, x 10.2
3. Dorsal view of cranidium UA 11600, x 9.2.
4. Dorsal view of meraspid cranidium UA 11601, x 22.5.
5. Lateral view of cranidium UA 11599, x 9.8.
6. Anterior view of cranidium UA 11599, x 10.9.
7. Ventral view of cranidium UA 11599, x 8.2.
8. Dorsal view of meraspid cranidium UA 11602, x 29.
9. Dorsal view of cranidium of enrolled individual UA 11603, x 10.6.
10. Dorsal view of librigena UA 11604, x 13.5.
11. Ventral view of librigena UA 11605, x 10.6.
12. Ventral view of hypostome UA 11606, x 22.8.
13. Dorsal view of hypostome UA 11607, x 10.9.
14. Dorsal view of librigena UA 11608, x 8.7.
15. Dorsal view of librigena UA 11609, x 7.9.
16. Ventral view of articulated thoracic segment UA 11610, x 12.7.
17. Ventral view of thoracic segments UA 11610, x 8.4.
18. Ventral view of thoracic segments UA 11611, x 21.
19. Dorsal view of thoracic segments UA 11612, x 4.1.
20. Dorsal view of pygidium UA 11613, x 9.3.
21. Lateral view of pygidium UA 11614, x 22.4.
22. Posterior view of pygidium UA 11614, x 15.7.
23. Ventral view of pygidium UA 11615 x 9.2.
24. Lateral view of pygidium UA 11613, x 16.4.
25. Ventral view of meraspid pygidium UA 11616, x 18.9.
26. Dorsal view of meraspid pygidium UA 11617, x 19.1.

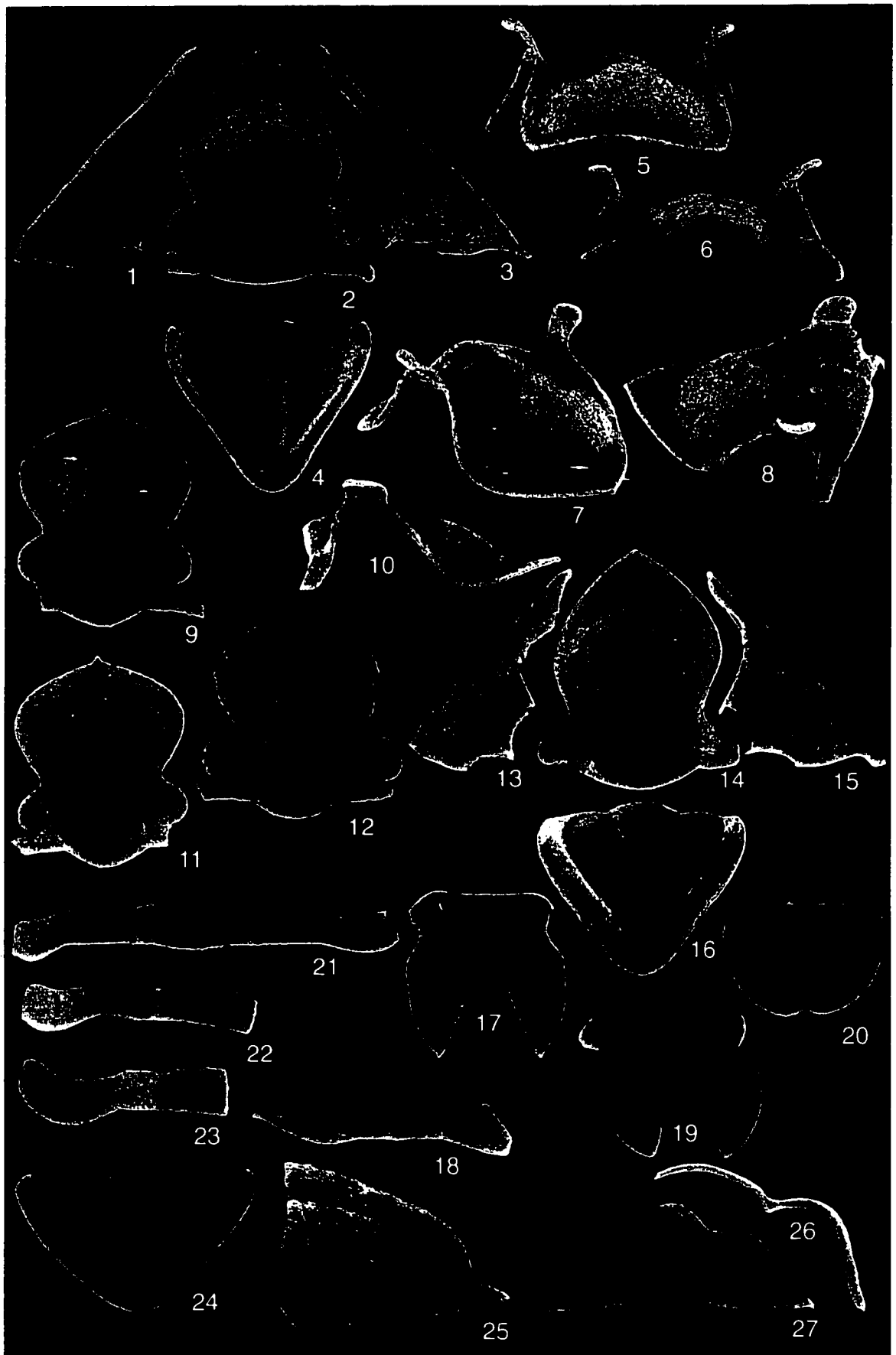


Plate 6

Figs. 1-8. *Robergia yukonensis*

1. Dorsal view of cranidium UA 11618, x 4.8.
2. Ventral view of cranidium UA 11619, x 5.9.
3. Ventral view of hypostome UA 11620, x 4.5.
4. Dorsal view of thoracic segment UA 11621, x 3.5.
5. Ventral view of thoracic segment UA 11622, x 8.1.
6. Dorsal view of pygidium UA 11623, x 5.2.
7. Dorsal view of pygidium UA 11624, x 8.7.
8. Ventral view of pygidium UA 11625, x 7.4.

Figs. 9-17. *Robergia* sp.

9. Dorsal view of cranidium UA 11626, x 34.8.
10. Dorsal view of librigena UA 11627, x 31.8.
11. Dorsal view of librigena UA 11628, x 19.2.
12. Dorsal view of articulated individual lacking pygidium UA 11629, x 29.
13. Dorsal view of librigena UA 11630, x 26.6.
14. Dorsal view of thoracic segment UA 11631, x 21.6.
15. Dorsal view of thoracic segment UA 11632, x 22.4.
16. Dorsal view of pygidium UA 11633, x 36.7.
17. Ventral view of librigena UA 11634, x 41.7.



Plate 7

Figs. 1-22. *Robergiella insolitus* n. sp.

1. Dorsal view of cranidium UA 11635, x 11.1.
2. Ventral view of cranidium UA 11636, x 28.6.
3. Dorsal view of librigena UA 11637, x 18.5.
4. Dorsal view of cranidium UA 11638, x 22.2.
5. Dorsal view of librigena UA 11639, x 10.8.
6. Posterior view of cranidium UA 11640, x 30.5.
7. Lateral view of cranidium UA 11635, x 14.8.
8. Anterior view of cranidium UA 11635, x 16.
9. Oblique dorsal view of cranidium UA 11640, x 28.3.
10. Dorsal view of cranidium UA 11641, x 12.7.
11. Ventral view of librigena UA 11642, x 31.
12. Ventral view of cranidium UA 11643, x 24.3.
13. Ventral view of librigena UA 11644, x 18.8.
14. Ventral view of hypostome UA 11645, x 28.
15. Dorsal view of hypostome UA 11646, x 21.9.
16. Dorsal view of thoracic segments UA 11647, x 30.
17. Dorsal view of thoracic segment UA 11648, x 29.
18. Dorsal view of thoracic segment UA 11649, x 13.3.
19. Dorsal view of pygidium UA 11650, x 21.6.
20. Ventral view of pygidium UA 11651, x 36.
21. Oblique dorsal view of pygidium UA 11650, x 27.3.
22. Lateral view of pygidium UA 11650, x 31.

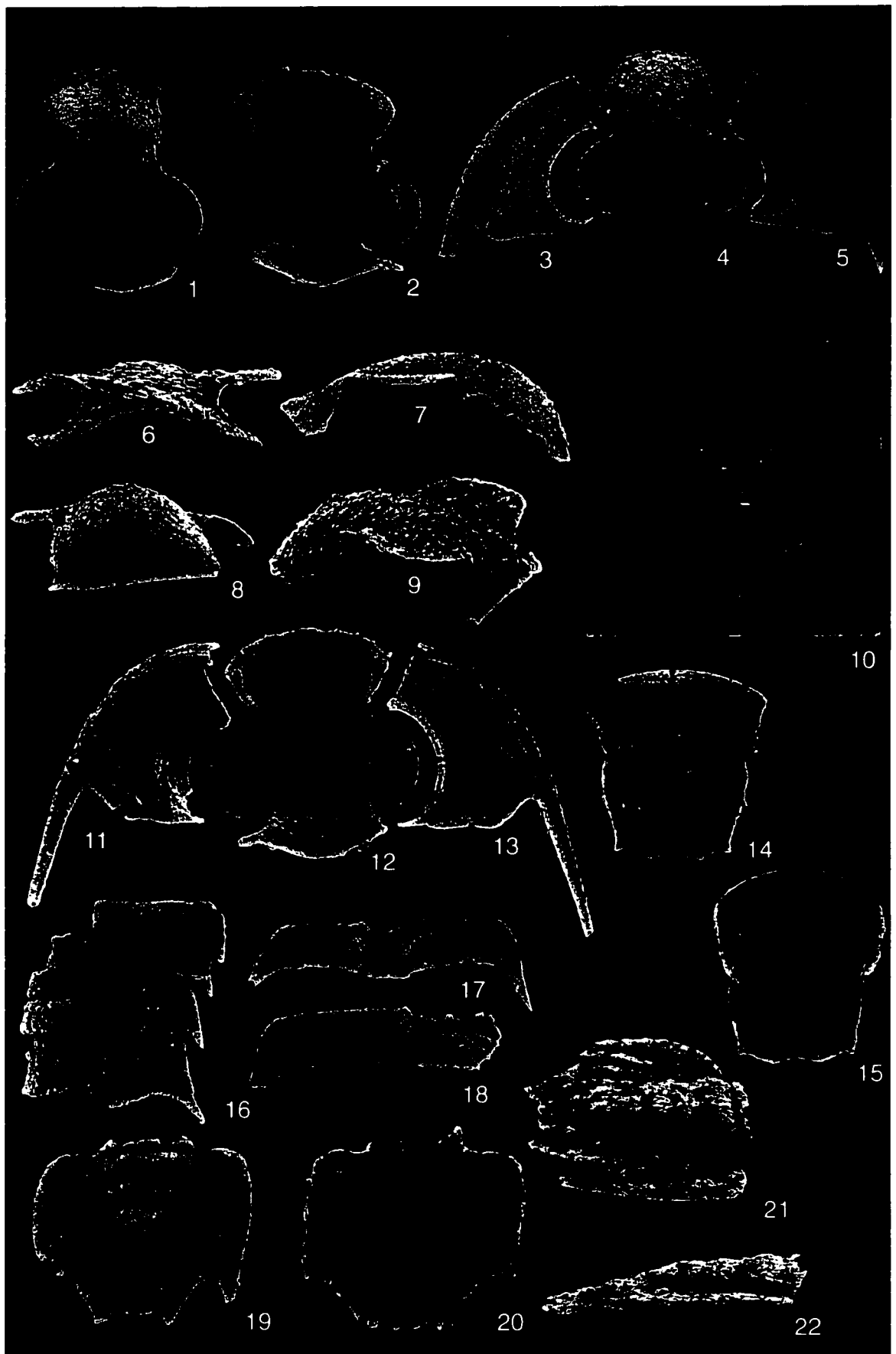


Plate 8

Figs. 1-17. *Ampyxina pilatus* n. sp.

1. Dorsal view of cranidium UA 11652, x 23.4.
2. Dorsal view of cranidium UA 11653, x 19.8.
3. Ventral view of cranidium UA 11654, x 21.
4. Lateral view of cranidium UA 11655, x 26.3.
5. Lateral view of cranidium UA 11653, x 20.6.
6. Dorsal view of holaspis individual UA 11656, x 20.
7. Ventral view of cranidium UA 11657, x 18.5.
8. Dorsal view of cranidium of enrolled individual UA 11658, x 22.
9. Anterior view of cranidium UA 11655, x 23.8.
10. Ventral view of holaspis individual UA 11659, x 20.8.
11. Dorsal view of pygidium UA 11660, x 23.5.
12. Dorsal view of pygidium UA 11661, x 29.
13. Ventral view of thoracic segments + pygidium UA 11662, x 20.
14. Dorsal view of pygidium UA 11663, x 20.
15. Lateral view of pygidium UA 11660, x 49.
16. Posterior view of pygidium UA 11663, x 47.
17. Lateral view of pygidium UA 11663, x 43.

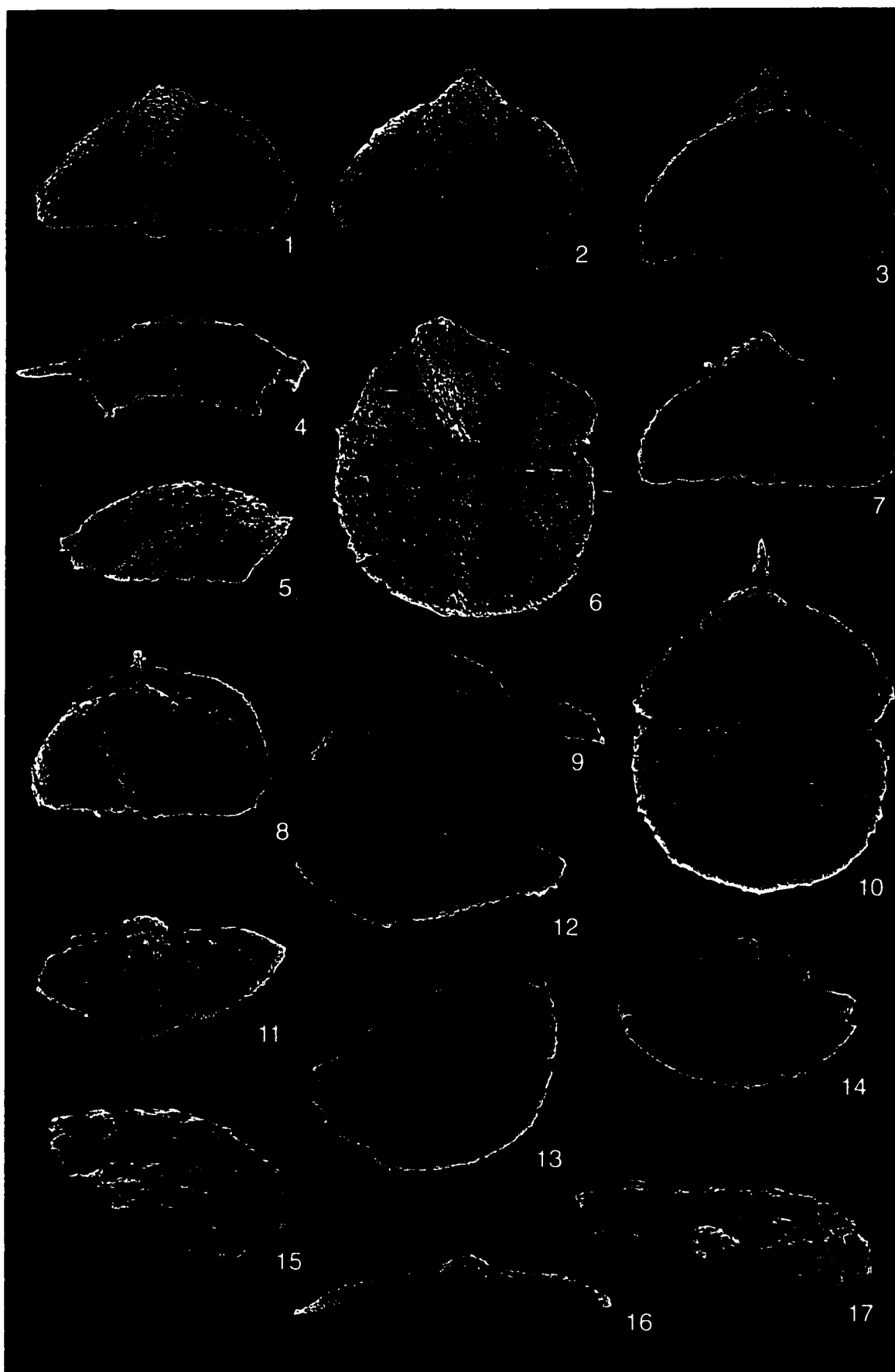


Plate 9

Figs. 1-13. *Cryptolithus tessellatus*

1. Dorsal view of cranidium UA 11664, x 5.2.
2. Lateral view of cranidium UA 11664, x 8.2.
3. Dorsal view of cranidium UA 11665, x 4.5.
4. Ventral view of cranidium UA 11666, x 6.
5. Anterior view of cranidium UA 11664, x 6.
6. Ventral view of cranidium UA 11667, x 4.1.
7. Dorsal view of holapsid individual UA 11668, x 6.2.
8. Oblique lateral view of cranidium UA 11664, x 8.6.
9. Ventral view of thoracic segment UA 11669, x 6.3.
10. Dorsal view of thoracic segment UA 11670, x 8.
11. Dorsal view of thoracic segments + pygidium UA 11671, x 5.7.
12. Dorsal view of thoracic segments + pygidium UA 11672, x 4.9.
13. Ventral view of pygidium UA 11673, x 9.3.

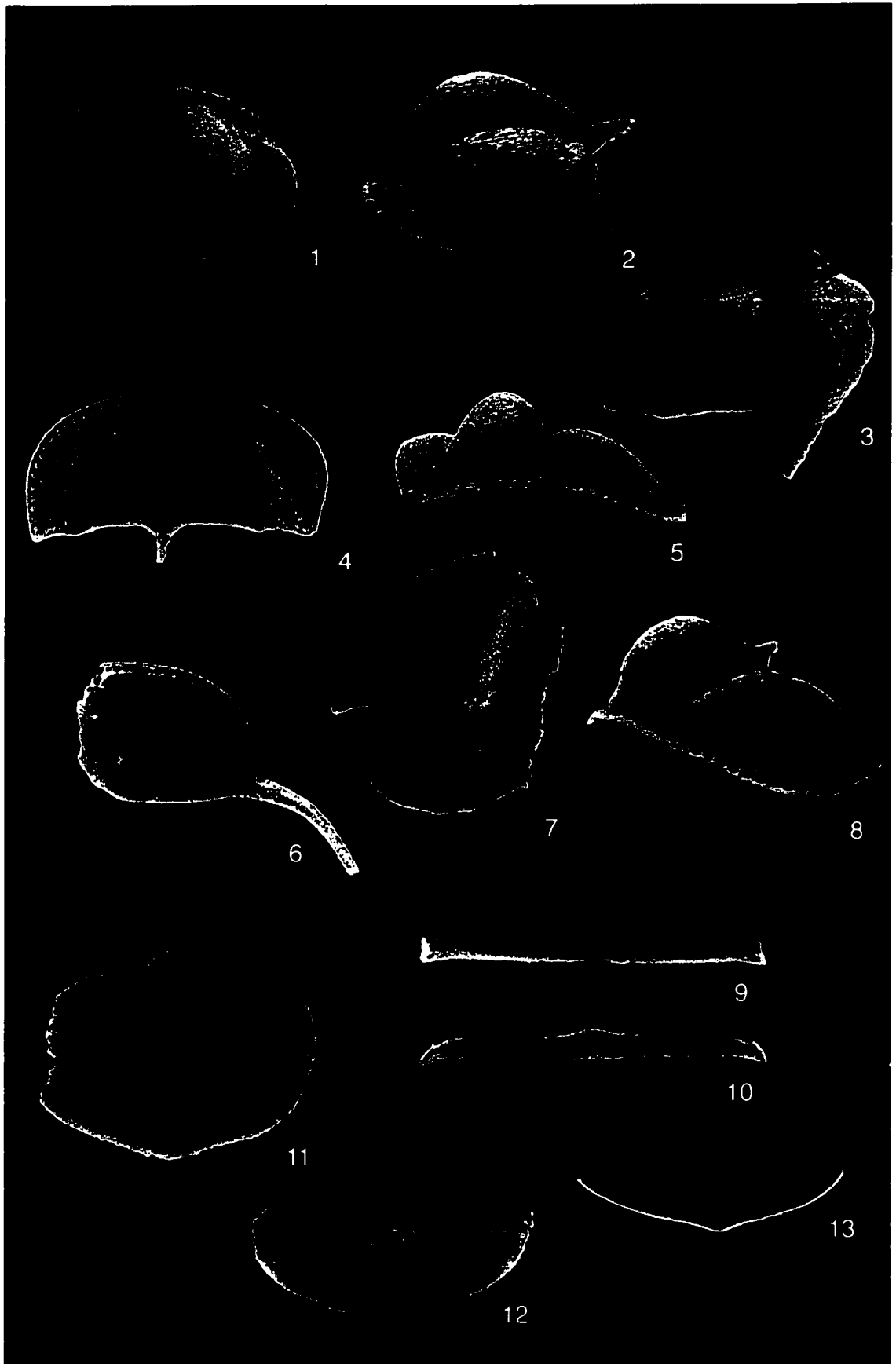


Plate 10

Figs. 1-20. *Acanthoparypha palmapyga* n. sp.

1. Dorsal view of cranidium UA 11674, x 15.6.
2. Oblique view of cranidium UA 11674, x 16.7.
3. Frontal view of cranidium UA 11674, x 17.3.
4. Ventral view of cranidium UA 11675, x 18.5.
5. Oblique lateral view of cranidium UA 11676, x 19.
6. Posterior view of cranidium UA 11674, x 15.9.
7. Dorsal view of cranidium UA 11677, x 38.
8. Lateral view of cranidium UA 11674, x 16.8.
9. Oblique posterior view of cranidium UA 11678, x 19.
10. Ventral view of hypostome UA 11679, x 25.
11. Dorsal view of hypostome UA 11680, x 24.3.
12. Ventral view of librigena UA 11681, x 20.8.
13. Dorsal view of librigena UA 11682, x 11.5.
14. Dorsal view of thoracic segment UA 11683, x 13.9.
15. Ventral view of thoracic segment UA 11684, x 18.
16. Ventral view of thoracic segment UA 11685, x 8.5.
17. Ventral view of thoracic segment UA 11685, x 16.7.
18. Dorsal view of pygidium UA 11686, x 22.5.
19. Dorsal view of pygidium UA 11687, x 40.
20. Ventral view of pygidium UA 11688, x 31.

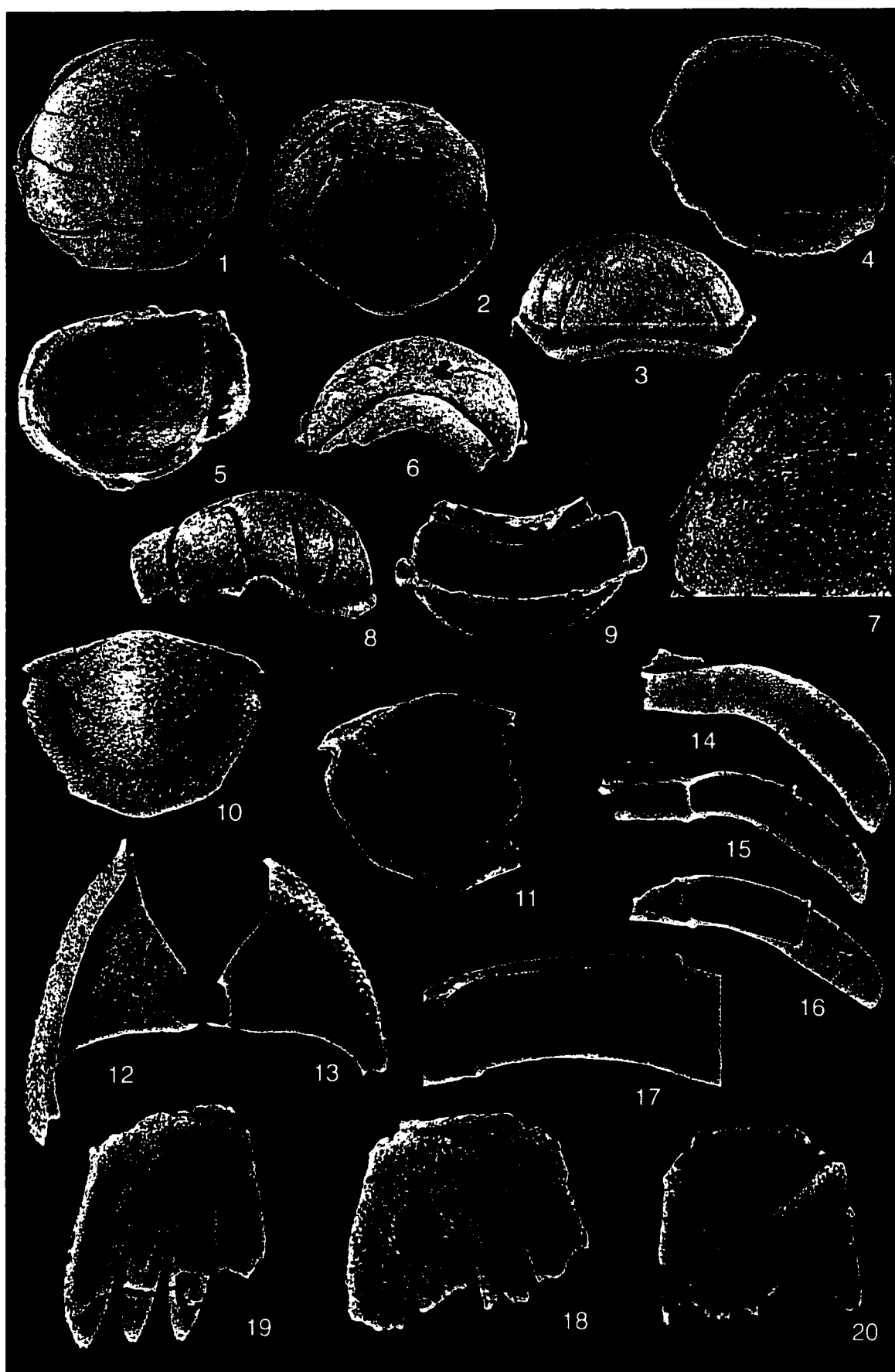


Plate 11

Figs. 1-29. *Acanthoparypha latipyga* n. sp.

1. Dorsal view of cranidium UA 11689, x 9.5.
2. Dorsal view of cranidium UA 11690, x 13.8.
3. Lateral view of cranidium UA 11689, x 11.7.
4. Dorsal view of cranidium (genal angle) UA 11689, x 26.7.
5. Dorsal view of cranidium UA 11689, x 28.4.
6. Anterior view of cranidium UA 11689, x 11.
7. Oblique lateral view of cranidium UA 11689, x 8.5.
8. Ventral view of meraspid cranidium UA 11691, x 26.7.
9. Ventral view of cranidium UA 11692, x 12.
10. Lateral oblique view of cranidium UA 11690, x 23.
11. Dorsal view of librigena UA 11693, x 15.5.
12. Lateral view of cranidium UA 11694, x 23.7.
13. Dorsal view of meraspid cranidium UA 11695, x 23.
14. Dorsal view of meraspid cranidium UA 11696, x 23.5.
15. Dorsal view of hypostome UA 11697, x 19.
16. Ventral view of hypostome UA 11798, x 16.4.
17. Ventral view of librigena UA 11799, x 11.4.
18. Dorsal view of librigena UA 11700, x 15.9.
19. Ventral view of anterior thoracic segment UA 11701, x 15.7.
20. Dorsal view of posterior thoracic segment UA 11702, x 34.
21. Ventral view of posterior thoracic segment UA 11703, x 14.3.
22. Dorsal view of posterior thoracic segment UA 11704, x 21.
23. Dorsal view of transitory pygidium UA 11705, x 51.4.
24. Dorsal view of transitory pygidium UA 11706, x 52.
25. Dorsal view of pygidium UA 11707, x 33.4.
26. Ventral view of pygidium UA 11708, x 32.7.
27. Anterior view of pygidium UA 11708, x 33.8.
28. Dorsal view of pygidium UA 11709, x 19.5.
29. Lateral view of pygidium UA 11709, x 22.8.



Plate 12

Figs. 1-6. *Acanthoparypha* sp.

1. Dorsal view of cranidium UA 11710, x 21.5.
2. Lateral view of cranidium UA 11710, x 30.4.
3. Dorsal view of cranidium UA 11710, x 56.6.
4. Anterior view of cranidium UA 11710, x 23.
5. Lateral view of cranidium UA 11710, x 30.4
6. Oblique dorsal view of cranidium UA 11710, x 23.3.

Figs. 7-17. *Ceraurinella lamiapyga* n. sp.

7. Ventral view of librigena UA 11711, x 21.2.
8. Dorsal view of librigena UA 11712, x 17.5.
9. Dorsal view of pygidium UA 11713, x 21.
10. Dorsal view of pygidium UA 11714, x 24.4.
11. Oblique dorsal view of pygidium UA 11713, x 17.8.
12. Oblique anterior view of pygidium UA 11713, x 18.8.
13. Lateral view of pygidium UA 11713, x 21.7.
14. Anterior view of pygidium UA 11713, x 21.7.
15. Dorsal view of pygidium UA 11715, x 22.7.
16. Ventral view of pygidium UA 11716, x 14.8.
17. Ventral view of pygidium UA 11717, x 21.

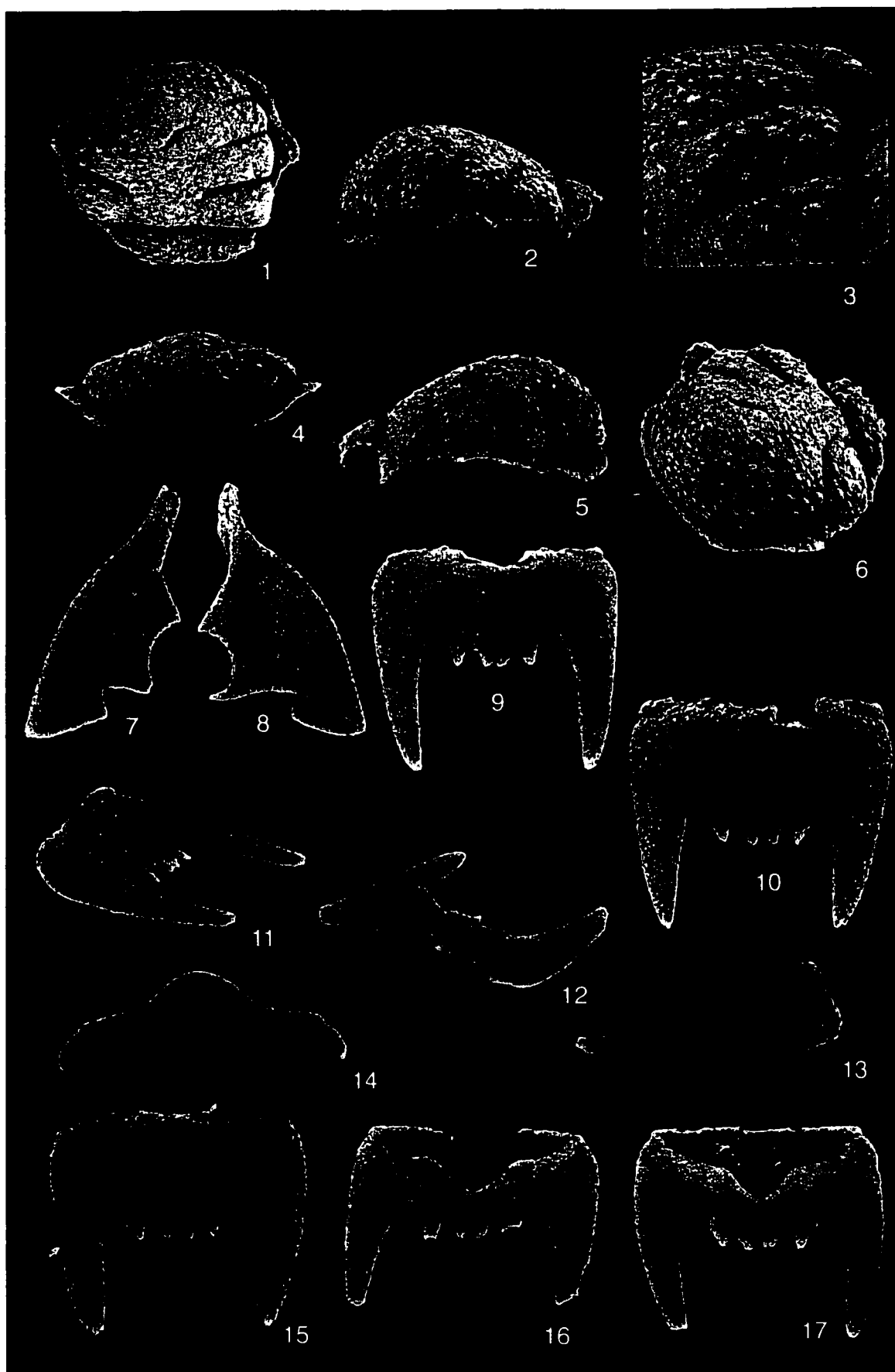


Plate 13

Figs. 1-13. *Ceraurinella brevispina*

1. Dorsal view of cranidium UA 11718, x 2.8.
2. Dorsal view of cranidium UA 11719, x 5.
3. Dorsal view of librigena UA 11720, x 8.9.
4. Dorsal view of librigena UA 11721, x 8.9.
5. Anterior view of thoracic segment UA 11722, x 7.4.
6. Ventral view of thoracic segment UA 11723, x 9.9.
7. Dorsal view of hypostome UA 11724, x 9.5.
8. Dorsal view of pygidium UA 11725, x 15.4.
9. Ventral view of pygidium UA 11726, x 9.8.
10. Dorsal view of pygidium UA 11727, x 25.3.
11. Dorsal view of pygidium UA 11728, x 13.4.
12. Dorsal view of pygidium UA 11729, x 10.8.
13. Ventral view of pygidium UA 11730, x 9.1.

Figs. 14-17. *Ceraurinus serratus*

14. Dorsal view of pygidium UA 11731, x 10.
15. Dorsal view of pygidium UA 11732, x 4.2.
16. Ventral view of thoracic segment UA 11733, x 11.3.
17. Ventral view of pygidium UA 11734, x 4.8.

Figs. 18-24. *Ceraurus mackenziensis*

18. Dorsal view of cranidium UA 11735, x 20.
19. Dorsal view of cranidium UA 11736, x 9.9.
20. Dorsal view of librigena UA 11737, x 9.3.
21. Ventral view of librigena UA 11738, x 15.1.
22. Dorsal view of pygidium UA 11739, x 10.3.
23. Dorsal view of hypostome UA 11740, x 8.3.
24. Ventral view of pygidium UA 11741, x 9.

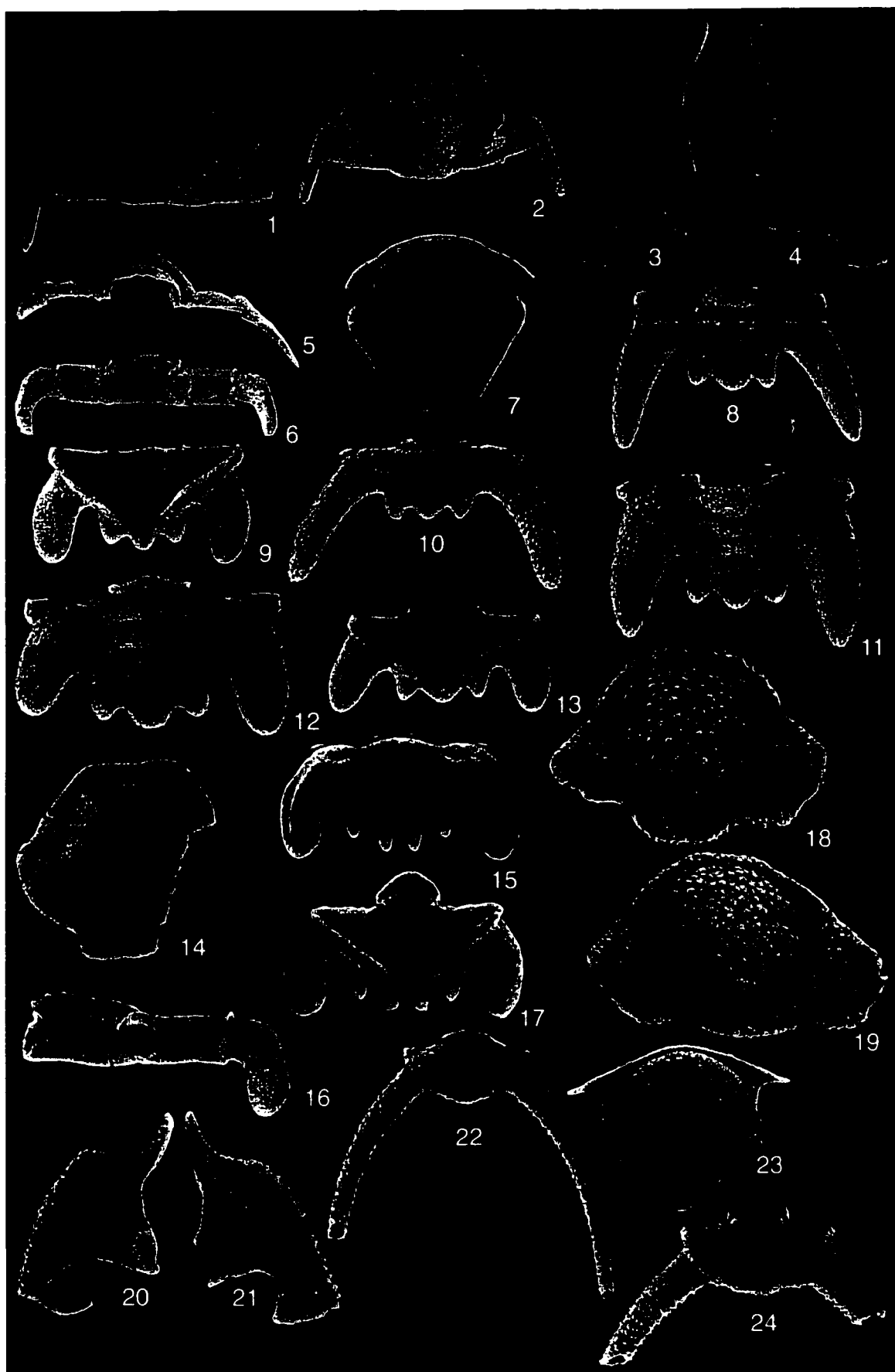


Plate 14

Figs. 1-16. *Sceptaspis avalanchensis* n. sp.

1. Dorsal view of cranidium UA 11742, x 14.8.
2. Dorsal view of cranidium UA 11743, x 13.6.
3. Lateral view of cranidium UA 11742, x 21.5.
4. Anterior view of cranidium UA 11742, x 16.2.
5. Oblique dorsal view of cranidium UA 11742, x 17.8.
6. Dorsal view of cranidium UA 11744, x 23.9.
7. Ventral view of cranidium UA 11745, x 13.9.
8. Dorsal view of meraspid cranidium UA 11746, x 30.4.
9. Dorsal view of hypostome UA 11747, x 14.8.
10. Dorsal view of cranidium UA 11748, x 45.
11. Ventral view of hypostome UA 11749, x 17.7.
12. Oblique dorsal view of cranidium UA 11742, x 18.3.
13. Oblique lateral view of pygidium UA 11750, x 27.6.
14. Ventral view of pygidium UA 11751, x 18.5.
15. Lateral view of pygidium UA 11750, x 31.
16. Dorsal view of pygidium UA 11752, x 21.4.

Figs. 17-23. *Calyptaulax* n. sp. A

17. Dorsal view of cranidium UA 11753, x 8.9.
18. Anterior view of cranidium UA 11753, x 9.6.
19. Lateral view of cranidium UA 11753, x 12.7.
20. Lateral view of cranidium UA 11753, x 13.6.
21. Oblique dorsal view of cranidium UA 11753, x 10.6.
22. Oblique dorsal view of cranidium UA 11753, x 11.6.
23. Dorsal view of cranidium UA 11753, x 70.2.

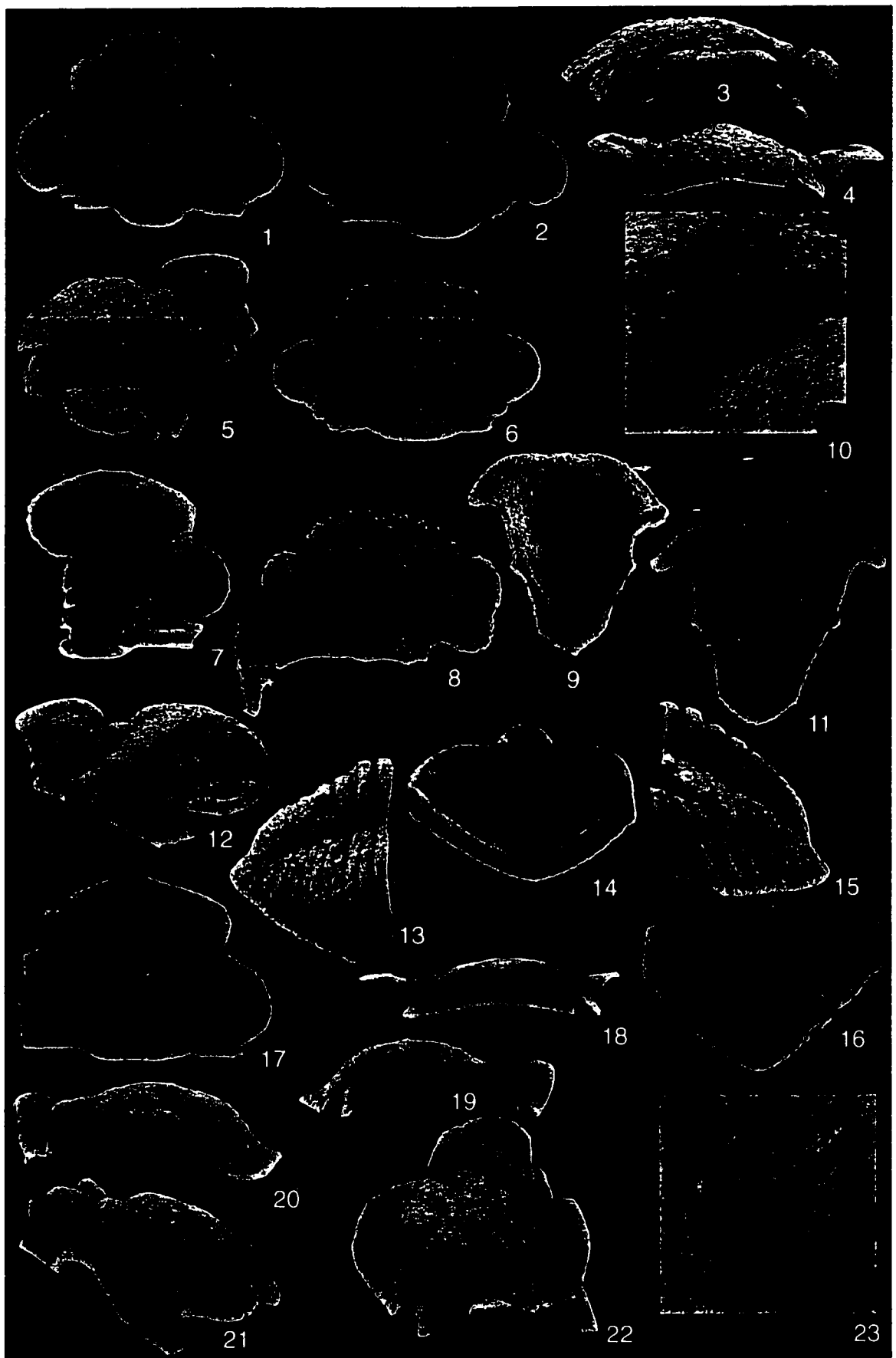


Plate 15

Figs. 1-19. *Tricopelta mackenziensis*

1. Dorsal view of cranidium UA 11754, x 8.4.
2. Dorsal view of cranidium UA 11755, x 8.2.
3. Dorsal view of cranidium UA 11756, x 10.4.
4. Ventral view of rostral plate UA 11757, x 6.8.
5. Dorsal view of librigena UA 11758, x 7.1.
6. Dorsal view of cranidium UA 11759, x 8.3.
7. Dorsal view of librigena UA 11760, x 6.8.
8. Dorsal view of hypostome UA 11761, x 15.6.
9. Dorsal view of hypostome UA 11762, x 16.9.
10. Anterior view of thoracic segment UA 11763, x 9.8.
11. Posterior view of thoracic segment UA 11764, x 8.9.
12. Dorsal view of thoracic segment UA 11765, x 11.4.
13. Ventral view of thoracic segment UA 11766, x 2.4.
14. Ventral view of thoracic segment UA 11767, x 9.5.
15. Lateral view of thoracic segment UA 11768, x 15.2.
16. Dorsal view of pygidium UA 11769, x 38.8.
17. Dorsal view of pygidium UA 11770, x 8.8.
18. Lateral view of thoracic segment UA 11768, x 16.9.
19. Lateral view of axial ring of thoracic segment UA 11768, x 23.3.



Plate 16

Figs. 1-17. *Hemiarges* n. sp. A.

1. Dorsal view of cranidium UA 11771, x 25.5.
2. Dorsal view of cranidium UA 11772, x 19.4.
3. Ventral view of cranidium UA 11773, x 28.2.
4. Oblique dorsal view of cranidium UA 11771, x 21.1.
5. Anterior view of cranidium UA 11771, x 19.1.
6. Ventral view of cranidium UA 11774, x 30.8.
7. Ventral view of hypostome UA 11775, x 28.
8. Dorsal view of hypostome UA 11776, x 17.3.
9. Lateral view of cranidium UA 11771, x 28.
10. Dorsal view of cranidium UA 11777, x 23.
11. Dorsal view of librigena UA 11778, x 9.4.
12. Ventral view of hypostome UA 11779, x 8.
13. Dorsal view of articulated thoracic segments + pygidium UA 11780, x 37.7.
14. Dorsal view of pygidium UA 11781, x 20.7.
15. Ventral view of pygidium UA 11782, x 14.2.
16. Dorsal view of pygidium UA 11783, x 18.5.
17. Lateral view of pygidium UA 11781, x 27.7.

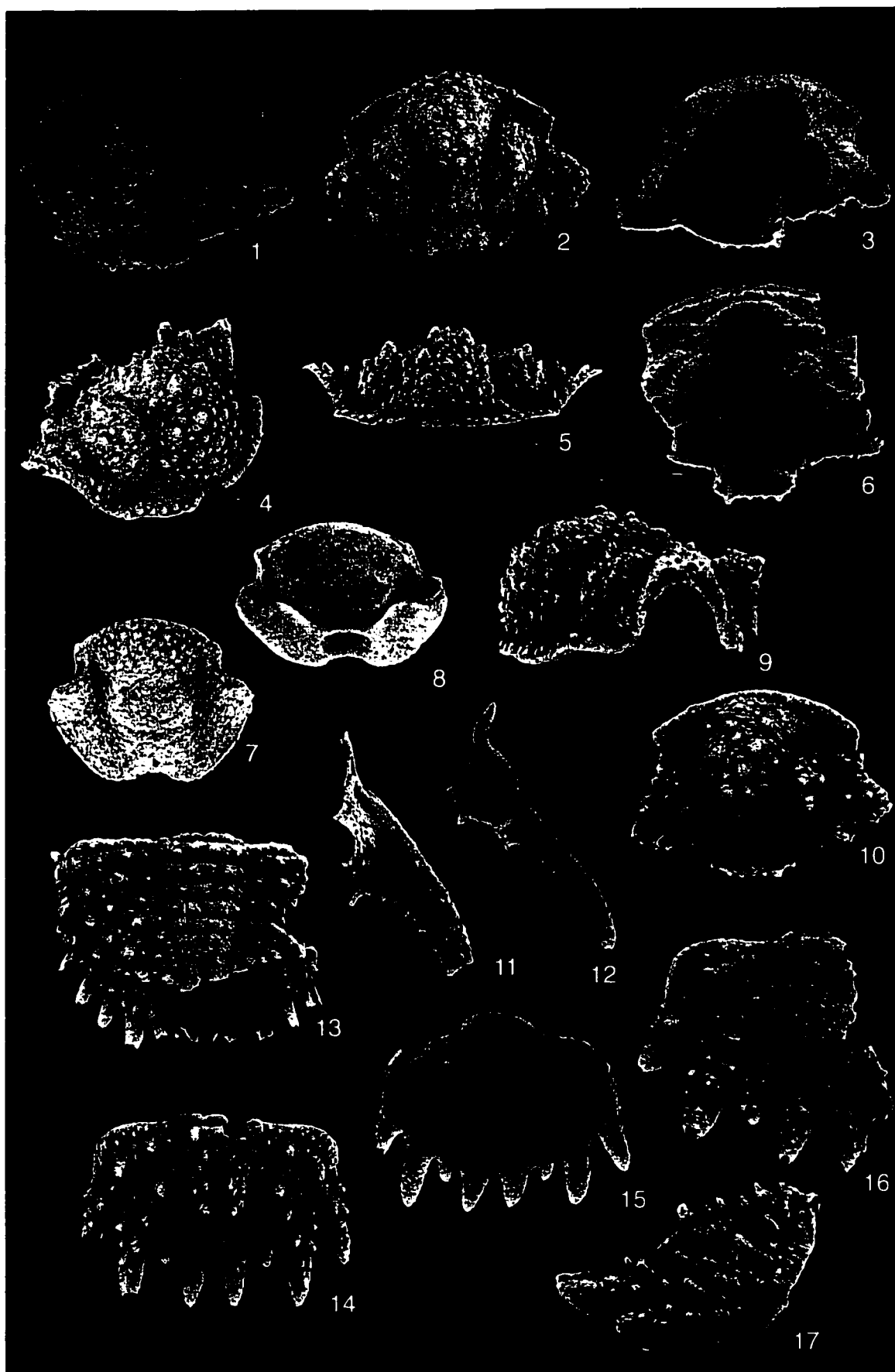


Plate 17

Figs. 1-2. *Faillleana* sp.

1. Dorsal view of cranidium UA 11784, x 9.2.
2. Dorsal view of cranidium UA 11785, x 10.

Fig. 3. *Dimeropyge* sp.

3. Dorsal view of pygidium UA 11786, x 23.1.

Figs. 4-10. *Harpidella kurrii*

4. Dorsal view of librigena UA 11787, x 17.4.
5. Dorsal view of cranidium UA 11788, x 18.
6. Dorsal view of librigena UA 11789, x 16.3.
7. Dorsal view of cranidium UA 11790, x 15.2.
8. Dorsal view of cranidium UA 11791, x 18.
9. Ventral view of cranidium UA 11792, x 21.1.
10. Dorsal view of pygidium UA 11793, x 30.4.

Fig. 11. *Hypodicranotus* sp.

11. Ventral view of hypostome UA 11794, x 20.8.

Figs. 12-14. *Holia* sp.

12. Dorsal view of cranidium UA 11795, x 23.1.
13. Dorsal view of meraspid cranidium UA 11796, x 33.
14. Ventral view of hypostome UA 11797, x 11.4.

Fig. 15. *Borealaspis whittakerensis*

15. Dorsal view of cranidium UA 11798, x 9.7.

Fig. 16. *Sphaerocoryphe* sp.

16. Dorsal view of cranidium UA 11799, x 11.

Fig. 17. *Sphaerexochus* (*Korolevium*) sp.

17. Dorsal view of pygidium UA 11800, x 29.2.

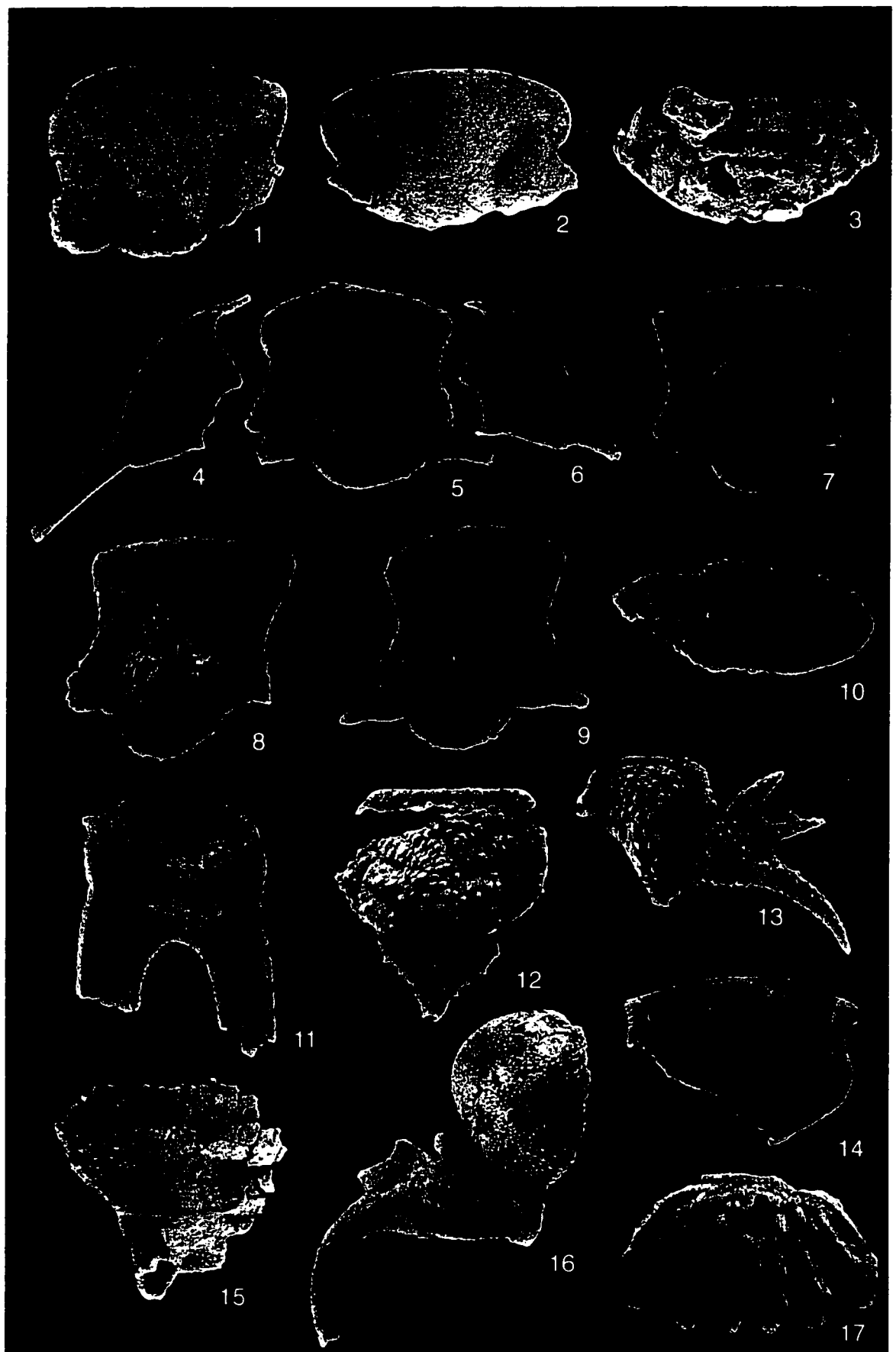


Plate 18

Figs. 1-4. *Curriella clancyi*

1. Dorsal view of cranidium UA 11801, x 9.1.
2. Dorsal view of librigena UA 11802, x 10.2.
3. Dorsal view of pygidium UA 11803, x 11.
4. Ventral view of hypostome UA 11804, x 10.6.

Figs. 5-6. Encrinurid

5. Dorsal view of librigena UA 11805, x 5.8.
6. Ventral view of hypostome UA 11806, x 7.8.

Figs. 7-13. *Cybeloides* sp.

7. Dorsal view of cranidium UA 11807, x 24.7.
8. Dorsal view of librigena UA 11808, x 28.
9. Ventral view of cranidium UA 11809, x 28.
10. Ventral view of hypostome UA 11810, x 55.2.
11. Dorsal view of pygidium UA 11811, x 24.
12. Dorsal view of cranidium UA 11812, x 19.8.
13. Dorsal view of cranidium UA 11813, x 27.3.

Figs. 14-15. Calymenid

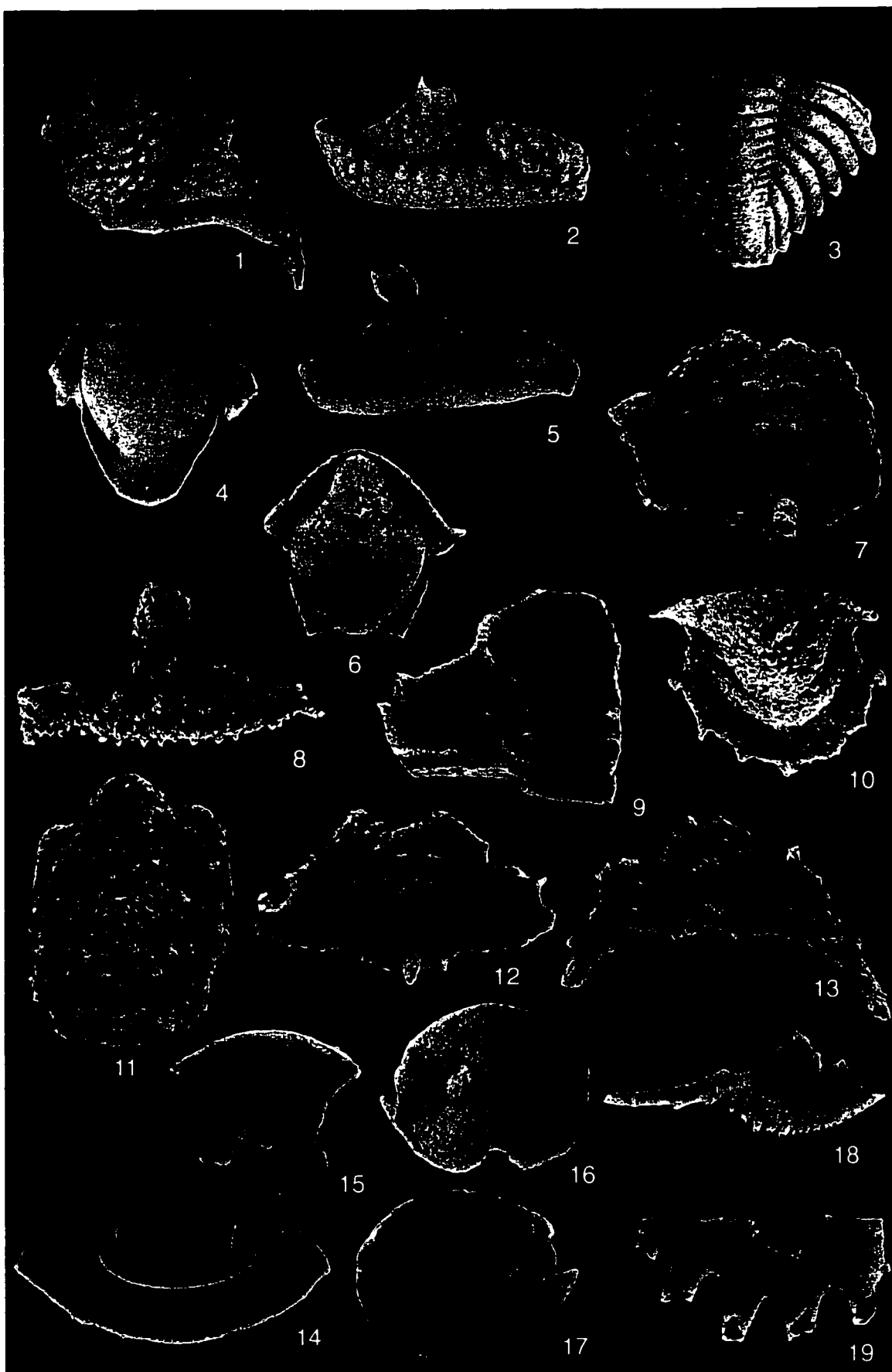
14. Ventral view of rostral plate UA 11814, x 9.
15. Ventral view of hypostome UA 11815 x 17.1.

Figs. 16-17. *Amphilichas* sp.

16. Ventral view of hypostome UA 11816, x 13.7.
17. Dorsal view of hypostome UA 11816, x 14.

Figs. 18-19. Odontopleurid

18. Dorsal view of librigena UA 11817, x 12.9.
19. Incomplete pygidium UA 11818, x 10.5.



Chapter 3: Upper Ordovician Biofacies from the Mackenzie Mountains, Northwest Territories, Canada.

Introduction

In extant and fossil communities, the distribution of organisms depends on a number of environmental controls. These include bathymetry, temperature, substrate, salinity, oxygen content, and nutrient supply. Study of the fossil biota from ancient marine sediments should reveal distinctive fossil communities, their distribution, and allow inferences to be made regarding the controlling environmental parameters responsible for these distributions (Hayes, 1980).

The study of the distribution of fossil communities centers around distinct associations of organisms, referred to as biofacies. Branchley (1990) stated that biofacies can be interpreted in two ways: in a stratigraphic sense that emphasizes a geographically or vertically restricted body of rock that is distinct based on its fossil content, and an ecological sense that expresses spatial and temporal variation in biota in relation to environmental variation. The focus of this chapter will be on the ecological aspects of biofacies, relating changes and patterns in the composition of trilobite communities to the lithology of the rock and interpretation of environmental differences.

The question always remains as to whether the fossil assemblage adequately represents the original population of trilobites in a specific environment. It is recognized that it is virtually impossible to obtain a completely unbiased sample which reflects the initial population of the fossils. This may never be sufficiently answered, but the large collection of trilobites at Avalanche Lake 4B provides a sufficient number of individuals and taxa to conduct a biofacies analysis.

According to Ludvigsen (1978), 3 assumptions must be made for a biofacies analysis to be valid:

1. Mappable biofacies must exist in the strata.
2. A fossil population of trilobites must be adequately represented by the exoskeletal elements recovered. Preservation must not be selective among the trilobites.
3. The trilobite remains have not been transported a significant distance from the area that the living animals inhabited.

It became apparent during preliminary assessment of the faunal composition at AV4B that the taxa were consistently distributed in discrete associations throughout the section. Histograms of relative abundance of taxa at each horizon (Figs. 3.1, 3.2, 3.3) show that distinctive groups exist within each of the sections. A diverse collection of 33

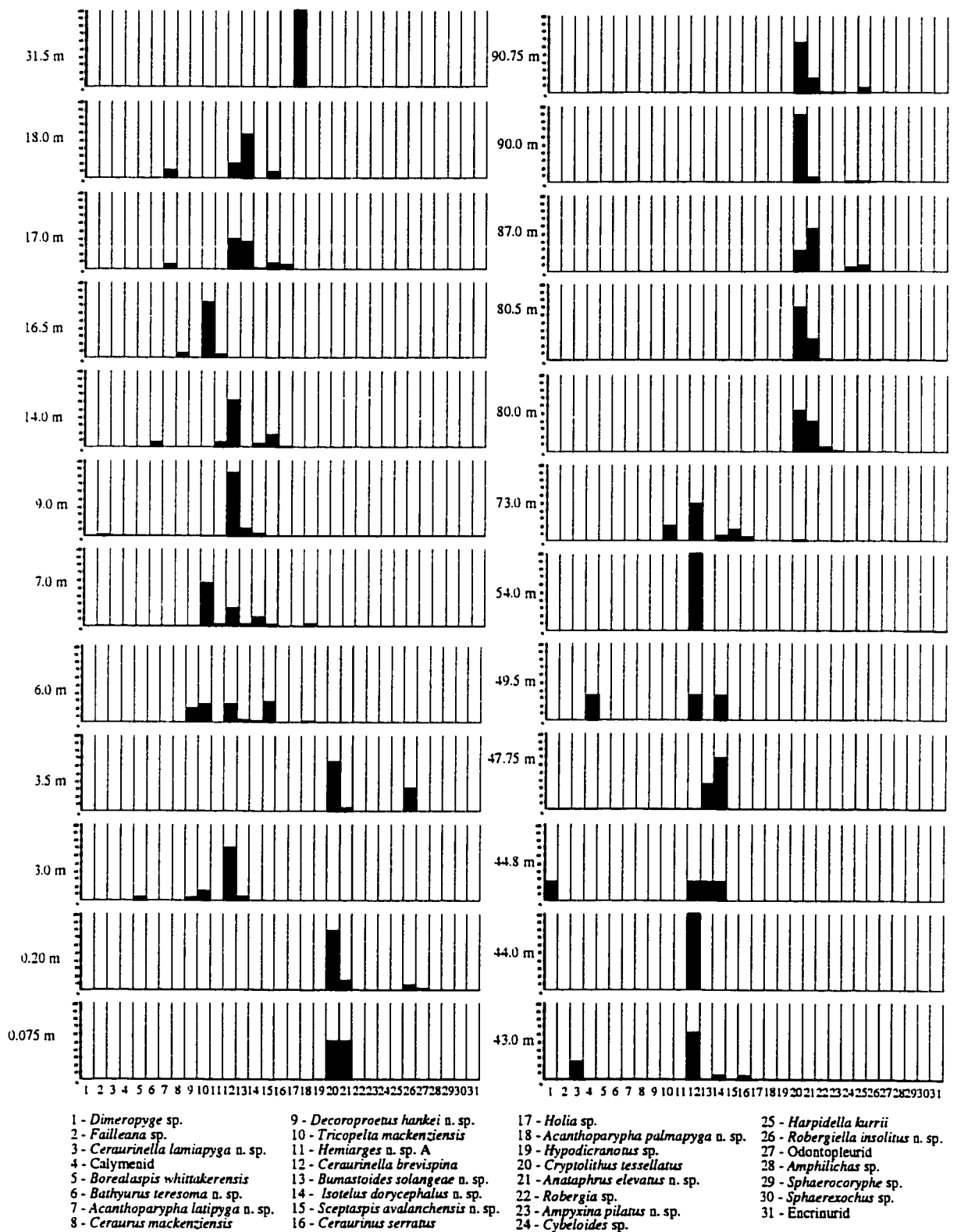


Figure 3.1. Relative abundance of trilobite genera in collections from the lower Whittaker Formation at the Avalanche Lake 4B section.

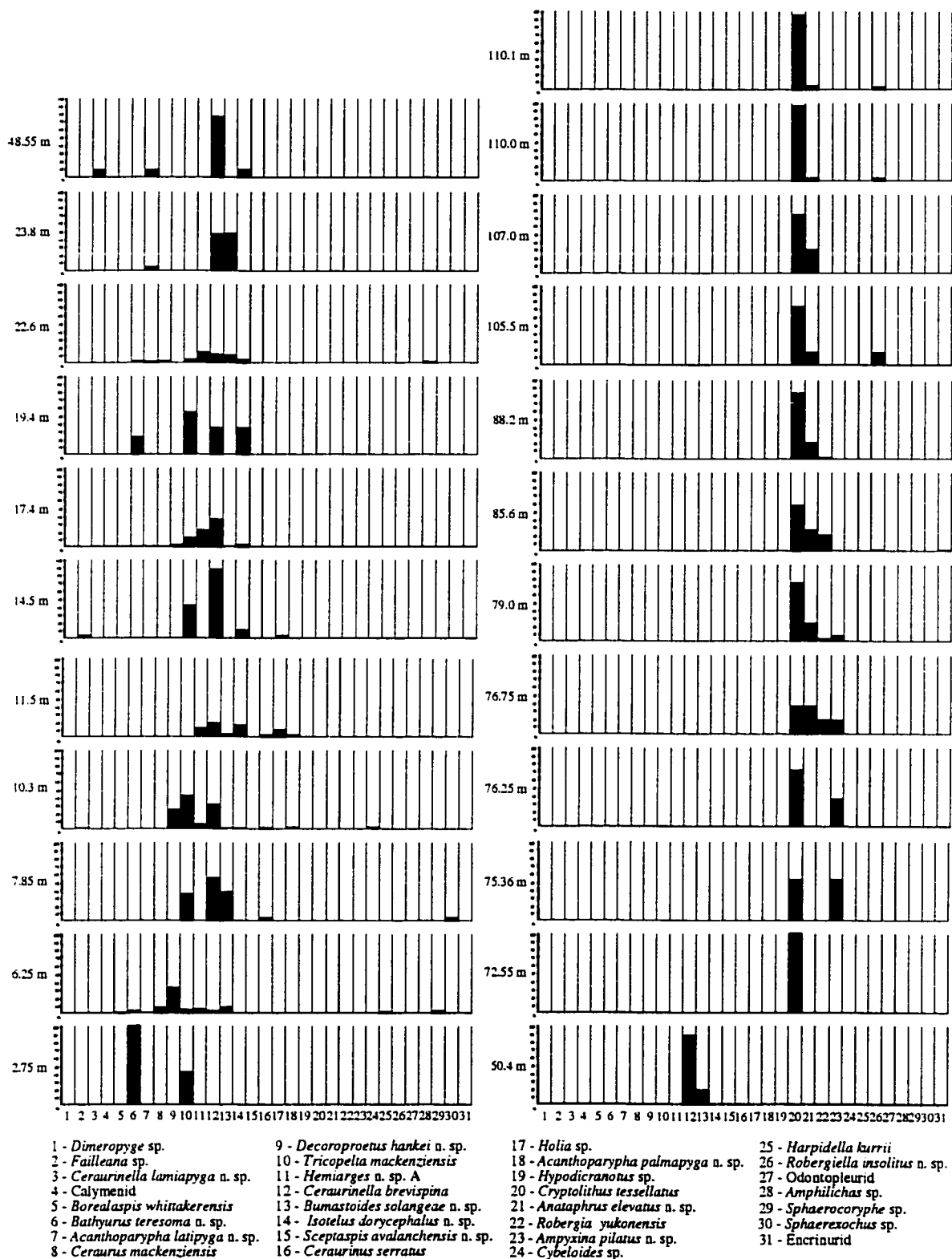


Figure 3.2. Relative abundance of trilobite genera in collections from the lower Whittaker Formation at the 98 Avalanche Lake 4B section.

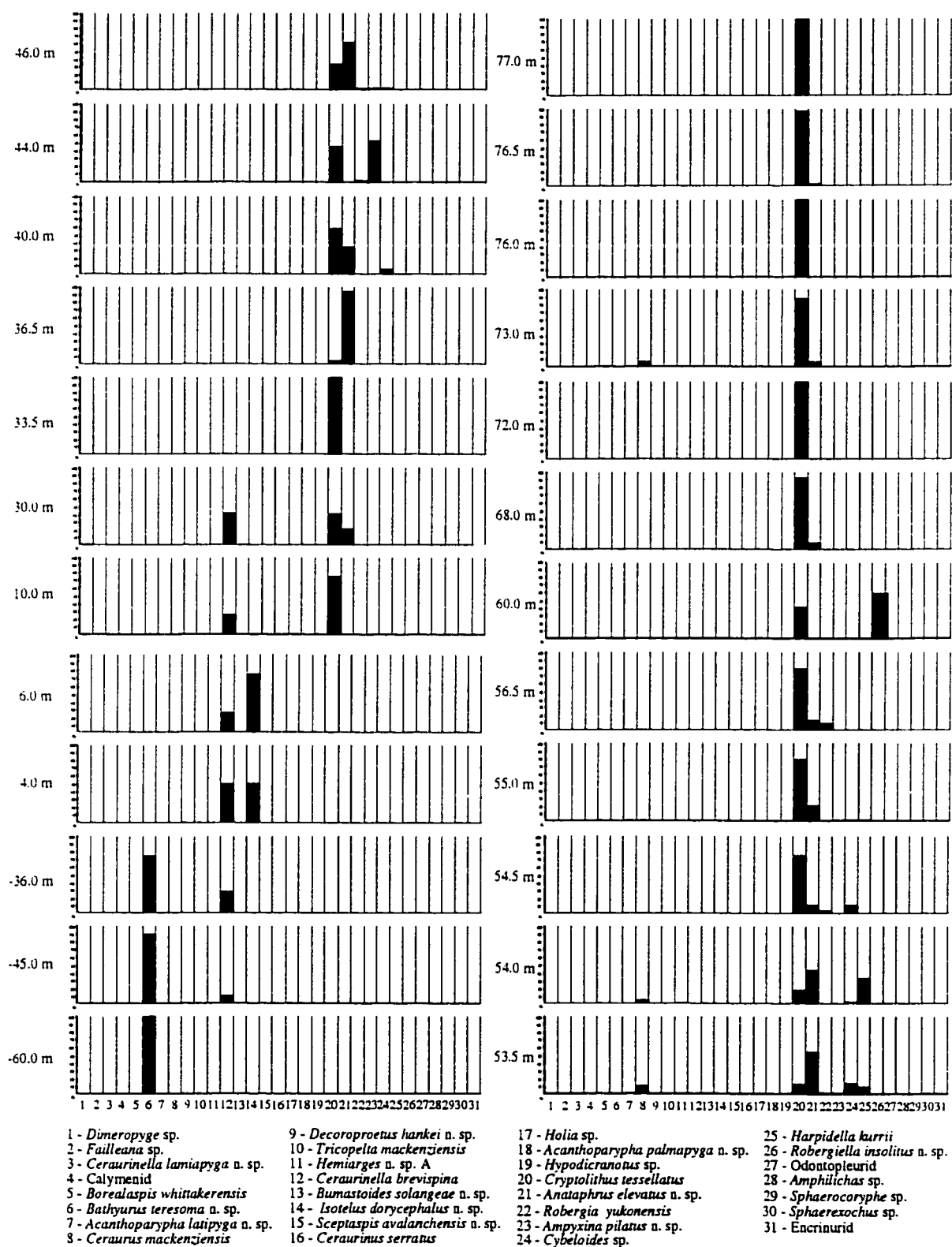


Figure 3.3. Relative abundance of trilobite genera in collections from the lower Whittaker Formation at the Avalanche Lake 1 section.

genera, including 13 new species identified from AV4B and AV1, provides an adequately diverse and non-selective fossil population for analysis. Although disarticulation and abrasion of the material consistently occurs in certain taxa within the collection, indicating possible transport from the original place of habitation, the fact that the taxa remain in discrete units persistently throughout the section indicates that transport of material may not have been a significant distance. Excellent preservation does occur in many horizons throughout the section; specimens consist of articulated remains with preservation of fine structures such as ornamentation and delicate exoskeletal remains. The retention of fine structures indicates that these remains are found close to their original area of habitation.

Fortey (1975) noted that one of the major problems with paleoecological work is whether the assemblages in the rock reflect the living population, in, on and above the sediment surface. He addressed the problem of recognizing autochthonous and allochthonous assemblages. Autochthonous beds reflect the initial population of a fossil community that has not been moved from the original place of deposition. Allochthonous beds show evidence of transport and may not reflect a living association of animals. The presence of autochthonous beds in a section can be recognized by the presence of articulated exoskeletons indicating the lack of disturbance of remains, the preservation of delicate structures, the lack of disturbance of fine-scale sedimentary structures such as laminae, and the lack of scour structures or conglomerates indicating sediment accumulation under quiet water conditions. A strong indication for autochthonous beds is the occurrence of growth stages in the same horizon where different stages differ greatly in size indicating the lack of size sorting and winnowing of material that is considered to occur in sediments that have undergone transport. In contrast, allochthonous beds have fossils concentrated in thin bands, fossil material is often disarticulated, abraded and poorly sorted, faunal content between adjacent beds differs greatly, and current activity is indicated by sedimentary structures such as conglomerates and turbidity flows.

The sedimentary structures and faunal composition of AV4B indicate that both autochthonous and allochthonous beds may occur. Within the first 2.75 metres and above the 73 metre horizon in the AV4B section material is generally articulated and shows excellent preservation of delicate structures and fine details, indicating an autochthonous assemblage. Between these horizons, material is generally disarticulated, abraded and broken. This may indicate transport, and the presence of allochthonous beds. This does not appear to be a significant problem, because the same genera are associated throughout several horizons indicating that the original faunal composition is maintained regardless of disturbance.

Study of taxonomic composition and associations of trilobites at AV4B will contribute to the limited data of community structure during the Upper Ordovician. The finely resolved faunal and stratigraphic data will be important in helping to understand changes in diversity and abundance of trilobite taxa in response to the global Late Ordovician mass extinction events.

Previous Work

Previous work on Ordovician biofacies has been concentrated on the Middle Ordovician with little emphasis on the Lower and Upper Ordovician. Fortey (1975) and Fortey and Barnes (1977) deciphered conodont and trilobite biofacies from the Valhallfonna Formation of the Arenig-Llandvirn of northern Spitsbergen. Whittington (1963) described an assemblage from a single boulder in the Cow Head Breccia at Lower Head, Newfoundland. The Table Head Formation, Newfoundland also contained an impoverished trilobite fauna described by Whittington (1965).

Ludvigsen (1975) synthesized 18 sections of Ibexian to Maysvillian age of the southern Mackenzie Mountains into seven broad biostratigraphic divisions. Chatterton and Ludvigsen (1976), Ludvigsen (1978), and Hayes (1980) analyzed material from the Upper Whiterockian (Chazyan), Blackriveran, and Trentonian of the southern Mackenzie Mountains. Chatterton and Ludvigsen (1976) discussed 4 distinct recurrent associations of trilobite genera from the Upper Whiterock (Chazyan) of the lower Esbataottine Formation, Mackenzie Mountains. Ludvigsen (1978) incorporated the trilobite distributional data previously used by Chatterton and Ludvigsen (1976) into a cluster analysis of silicified trilobite collections from the Upper Whiterockian (Chazyan) to Edenian of the upper Sunblood, Esbataottine, and lower Whittaker Formations of the Mackenzie Mountains, deciphering 4 distinct trilobite associations. Hayes (1980) analyzed an extension of Ludvigsen's work, incorporating ostracods, bryozoans, and conodonts to the analysis to more completely represent the faunal composition of the biofacies.

Ludvigsen (1978a) noted the presence of a distinct bathyurid assemblage from the Blackriveran of the Upper Bromide Formation, Oklahoma. More recently, Fortey and Droser (1996) noted the presence of a bathyurid association from the Whiterockian of the Wahwah and overlying Juab Limestone Formations from western Utah and eastern Nevada. Price (1980) studied faunas ranging from Cautleyan to Rawtheyan in age (Upper Ordovician) from the Sholeshook Limestone Formation of South Wales, describing two trilobite associations representing a shelf-edge and deep slope environment. Bretsky (1969) undertook a study of the faunal associations along a Late Ordovician shelf and shoreline in the Central Appalachians. Although the study concentrated on bryozoans, gastropods, and

bivalves, these fossils were grouped into communities in a similar fashion to trilobites. These three communities were composed of species that showed a high degree of affinity, and a tendency to occur together throughout the Upper Ordovician.

Shaw and Fortey (1977) attempted to trace the relationships of trilobite faunas for the Middle Ordovician over the whole North American plate, including northwest Canada, Utah, Nevada, southern Appalachians, eastern New York State, New England, and Newfoundland. They defined a platform profile consisting of the interior carbonates of the shelf, reefs or mounds of the shelf-edge, and shaly limestones and shales of the slope, allowing trilobite faunas to be related to their environmental positions.

Methods of Analysis

33 distinct species, including 13 new species, were identified at the Avalanche Lake sections. Silicified material ranged from one individual for a taxon to over 2000. Absolute numerical counts of complete, disarticulated, and broken specimens were tabulated. The number of individuals at each horizon was determined by the highest number of a skeletal element throughout the disarticulated remains. The number of the skeletal remain is divided by the number of that element within a particular species. For example, cranidia, pygidia, and hypostomes are divided by one, librigenae are divided by two, and thoracic segments are divided by the number of segments within the thorax of that species.

Individual taxa were plotted according to their percent composition at each horizon to show consistent associations of trilobites. Percentages of trilobite families were also plotted for each horizon within the sections to show changes in faunal composition between families. Plotting data in percent was used to overcome the problem of sample size, allowing each sample to become a standard size (Jones, 1987).

The technique of cluster analysis was described by Ludvigsen (1978) and Hazel (1970). Both Q-mode (sample by sample) and R-mode (taxon by taxon) analysis was completed. For this present work, Unweighted Pair Group Method Using Arithmetic Averages (UPGMA) clustering of Jaccard Coefficients have been used to analyze binary data of 33 taxa of Upper Ordovician trilobites from both collections of the AV4B and AV1 sections. Analysis of data with the Ochiai coefficient for comparison of results showed identical clusters, indicating that the data set is robust. Cluster analysis was run using SYN-TAX 5.0 (Podani, 1993). The Q and R-mode dendrograms for each section were then replotted in a biofacies map, with the Q-mode order plotted in stratigraphic sequence. All three sections were then plotted together to show a final biofacies consensus. Intersections of Q and R-mode clusters defined three biofacies.

The diversity of the three collections was analyzed. Diversity is defined as the number of species forming a community and living in a particular area (Pickerill and Brenchley, 1991). However, the total population is never completely sampled and the number of species in a sample is affected by the sample size. Sanders (1968) stated that “as sample size increases, individuals are added at a constant arithmetic rate but species accumulate at a decreasing logarithmic rate”. To correct for this relationship Ludvigsen’s diversity index was used, stated as: $D.I. = \text{no. of species} / \log_{10} \text{no. of individuals}$ (Ludvigsen, 1978).

Biofacies of Avalanche Lake

Results of the cluster analysis (Figs. 3.4, 3.5, 3.7) and intersection of the Q and R-mode dendrograms (Figs. 3.6, 3.8) on a biofacies map reveals three distinct biofacies. These may be defined as follows:

1. *Bathyrurus* Biofacies

This biofacies is dominated by light grey micritic limestones. Sedimentary structures indicating shallow water and periodic sub-aerial exposure include interference ripples found at AV4B and mudcracks and syneresis cracks observed at AV1. *Bathyrurus teresoma* n. sp. dominates the trilobite fauna, with rare elements of *Borealaspis whittakerensis*, *Sphaerocoryphe* sp., *Harpidella kurrii* and *Ceraurus mackenziensis*.

2. *Tricopelta* - *Ceraurinella* Biofacies

This biofacies is dominated by micritic limestones including both mudstones and wackestones. This trilobite fauna is dominated by *Tricopelta mackenziensis* and *Ceraurinella brevispina*. In addition, *Bumastoides solangeae* n. sp. and *Isotelus dorycephalus* n. sp. appear as important taxa. Rare elements include *Sceptaspis avalanchensis* n. sp., *Hemiarges* n. sp. A, *Cybeloides* sp., *Faileana* sp., *Acanthoparypha palmapyga* n. sp., *Acanthoparypha latipyga* n. sp., *Ceraurus serratus*, and *Ceraurus mackenziensis*. The striking feature of this biofacies is the high diversity of trilobites, up to 19 genera can be found in association with this biofacies. Trace fossils such as burrows also occur within the stratigraphic intervals of this biofacies.

3. *Anataphrus* - *Cryptolithus* Biofacies

This biofacies first appears in the AV4B section after an abrupt lithofacies change from micritic limestones to calcareous shales. The lithology characteristic of this biofacies consists of interbedded argillaceous limestones containing chert and carbonaceous black

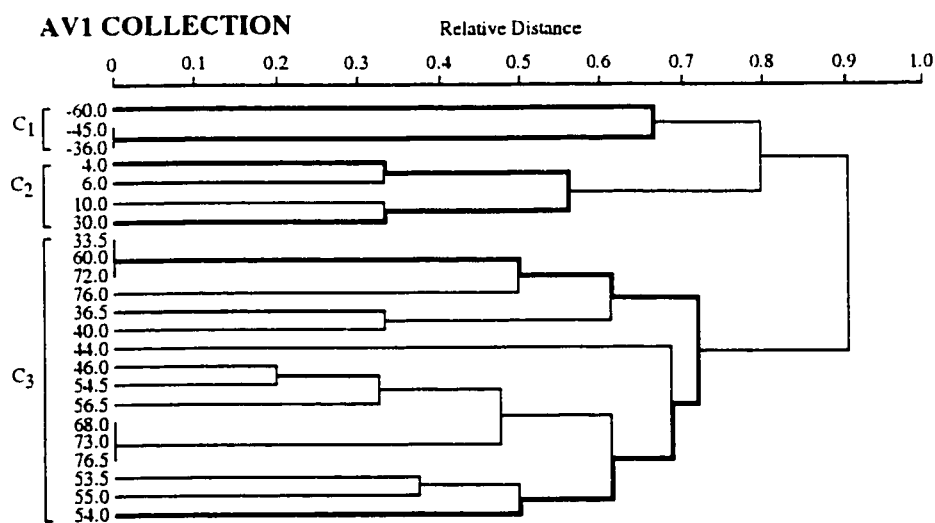
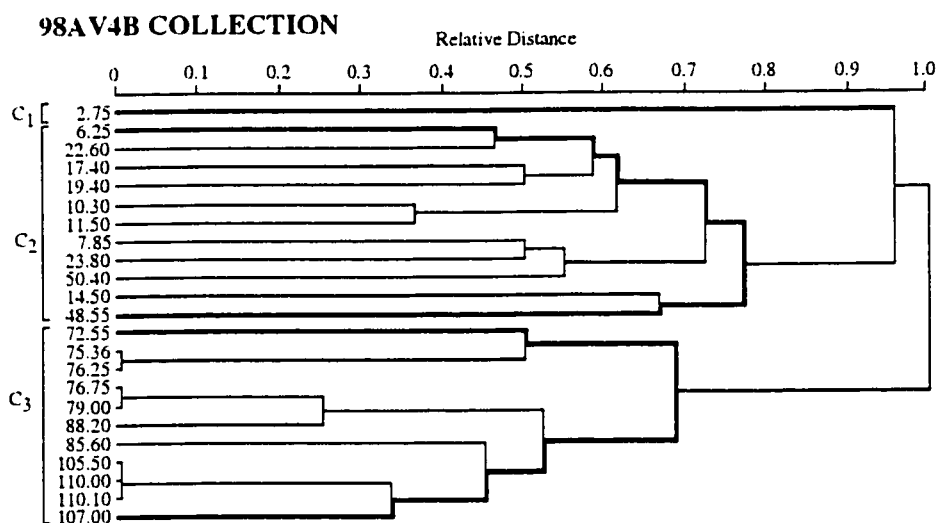
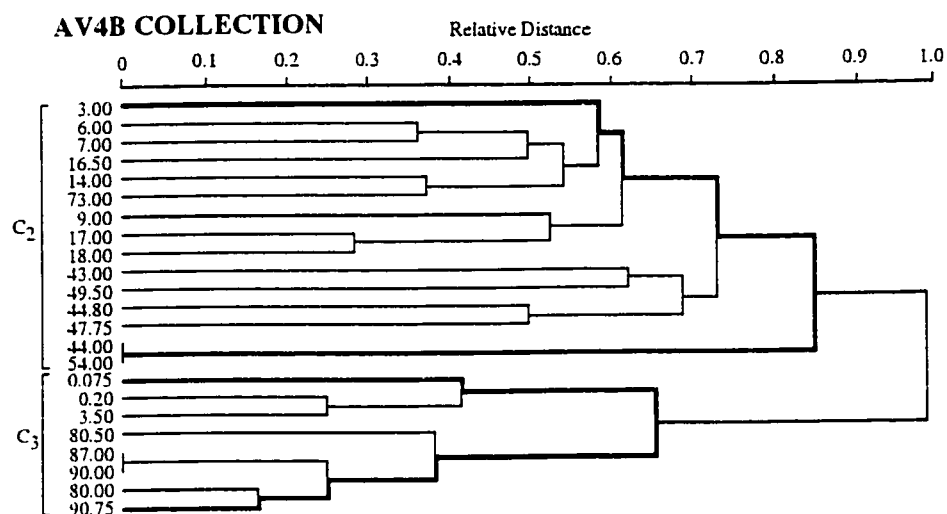


Figure 3.4. Q-mode dendrograms of 24 horizons from the AV4B collection, 23 horizons from the 98AV4B collection, and 24 horizons from the AV1 collection, Whittaker Formation, Avalanche Lake, Mackenzie Mountains, Northwest Territories, Canada.

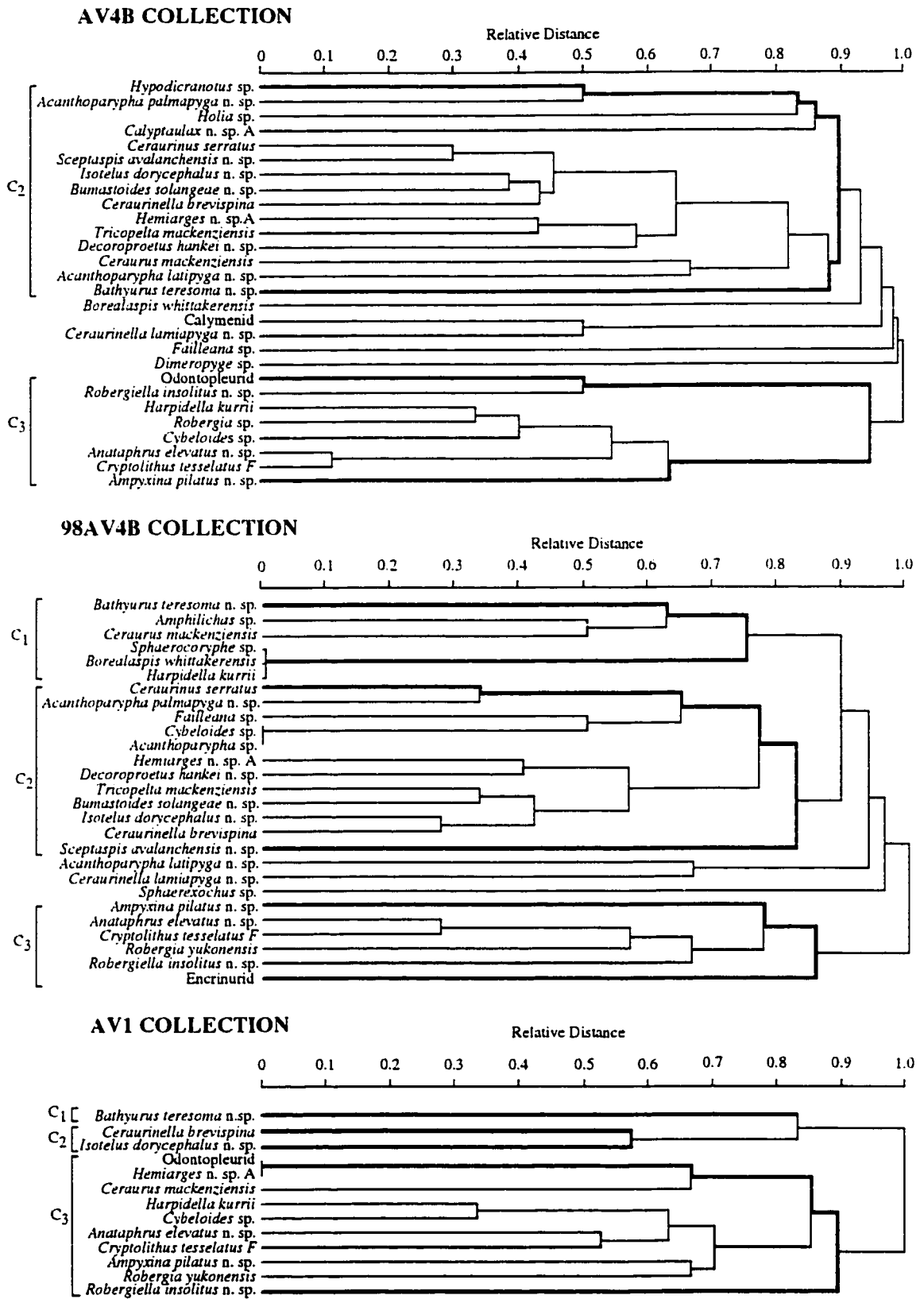


Figure 3.5. R-mode dendrograms of 28 trilobite species occurring in AV4B collections, 27 trilobite species occurring in 98AV4B collections, and 13 trilobite species occurring in AV1 collections, Whittaker Formation, Avalanche Lake, Mackenzie Mountains, Northwest Territories, Canada.

shales. This trilobite fauna is dominated by *Anataphrus elevatus* n. sp. and *Cryptolithus tessellatus*. Other important taxa, although in lower abundances, that are always found in association with this biofacies include *Ampyxina pilatus* n. sp., *Robergiella insolitus* n. sp., and *Robergia yukonensis*. Rare elements include *Cybeloides* sp., and *Harpidella kurrii*. Material within this biofacies frequently consists of articulated remains.

According to the combined R-mode dendrogram (Fig. 3.7), several genera of trilobites are not associated with any of the biofacies. These include *Hypodicranotus* sp., *Ceraurinella lamiapyga* n. sp., *Calyptaulax* n. sp. A, *Sphaerexochus* sp., and *Dimeropyge* sp., and a calymenid. When plotted on the biofacies map (Fig. 3.8), these taxa appear most closely related to the *Tricopelta-Ceraurinella* Biofacies, representing a small portion of the total number of individuals within the biofacies. The small number of individuals of each of these species contributes to their exclusion from any of the biofacies defined by the dendrogram. It is considered that these species belong to the *Tricopelta-Ceraurinella* Biofacies based on their placement within the biofacies map (Fig. 3.8).

Environmental Controls of the Biofacies

The biofacies of Avalanche Lake 4B and Avalanche Lake 1 appear to correspond to a depth gradient, and likely are in part temperature controlled. Other factors associated with bathymetry such as light, oxygen, substrate, and nutrient supply also determined the distribution of the biofacies along the shelf.

The *Bathyrurus* Biofacies as expected is dominated by *Bathyrurus solangeae*, whose morphology is considered to be compatible with a burrowing mode of life (Ludvigsen, 1978). *Bathyrurus* is usually associated with nearshore, shallow warm water environments. Ludvigsen (1978a) noted that in northern Canada *Bathyrurus* is almost totally restricted to Biofacies I (Ludvigsen, 1978) which occurs in micrites and extends into the intertidal zone as evidenced by occasional dessication features. This environment is present in the Avalanche Lake sections. The lithology consists of light, pure micritic limestones and sedimentary structures such as interference ripples, dessication cracks, and syneresis cracks that indicate aerial and subaerial exposure and a shallow water level.

The *Tricopelta-Ceraurinella* Biofacies is a highly diverse assemblage consisting of up to 19 trilobite genera. These trilobites are generally smaller in size, attributed by Ludvigsen (1978) to an adaptation to stay on top of the sediment surface. This biofacies is considered to represent a community comprised of largely epifaunal trilobites living in quiet water and on soft sediment. This association is interpreted to exist on a deeper water shelf environment.

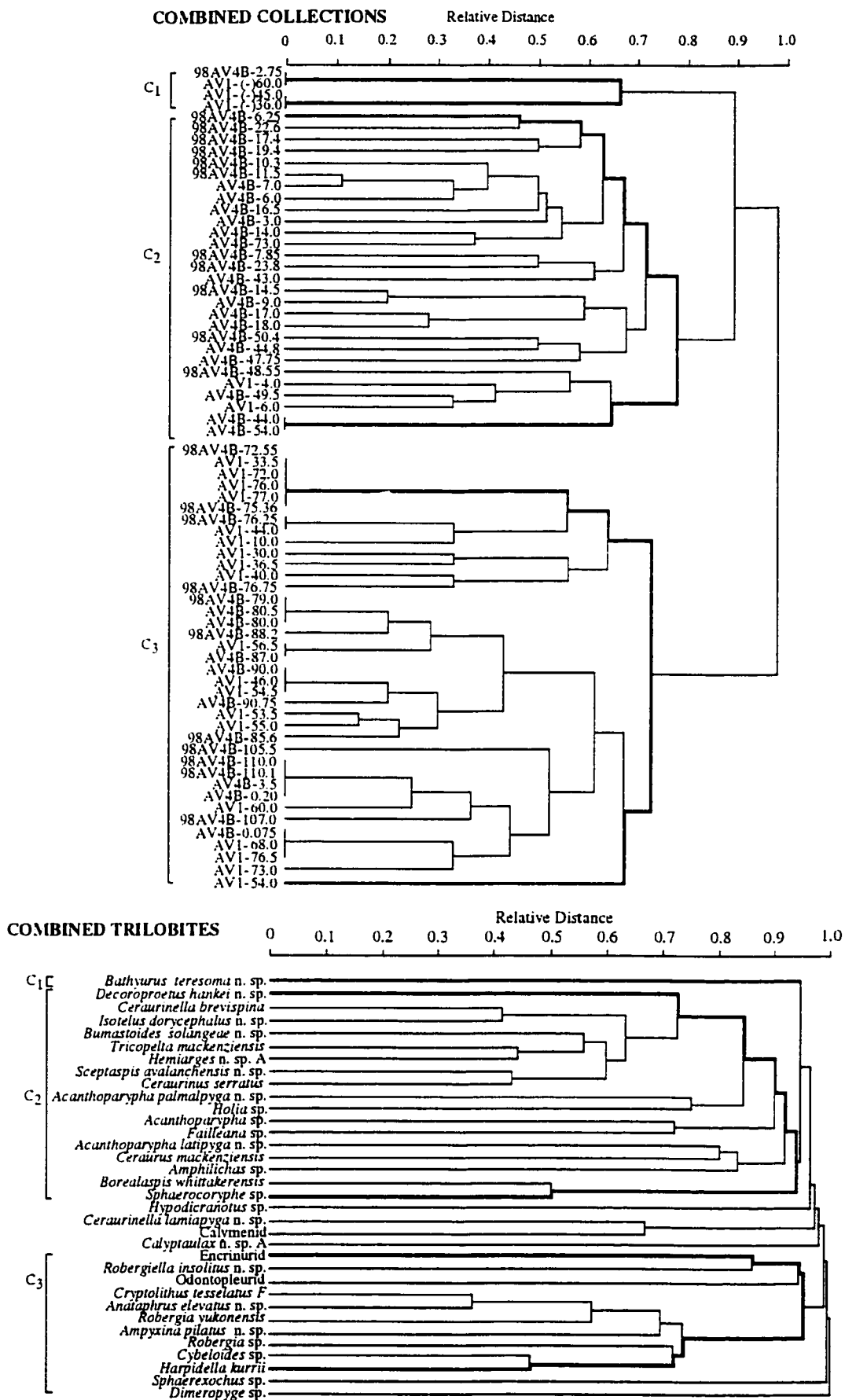


Figure 3.7. Q-mode dendrogram (top figure) of 70 combined Avalanche Lake collections from the Whittaker Formation. R-mode dendrogram (bottom figure) of 34 combined trilobite genera from all Avalanche Lake sections, Whittaker Formation, Mackenzie Mountains, Northwest Territories, Canada.

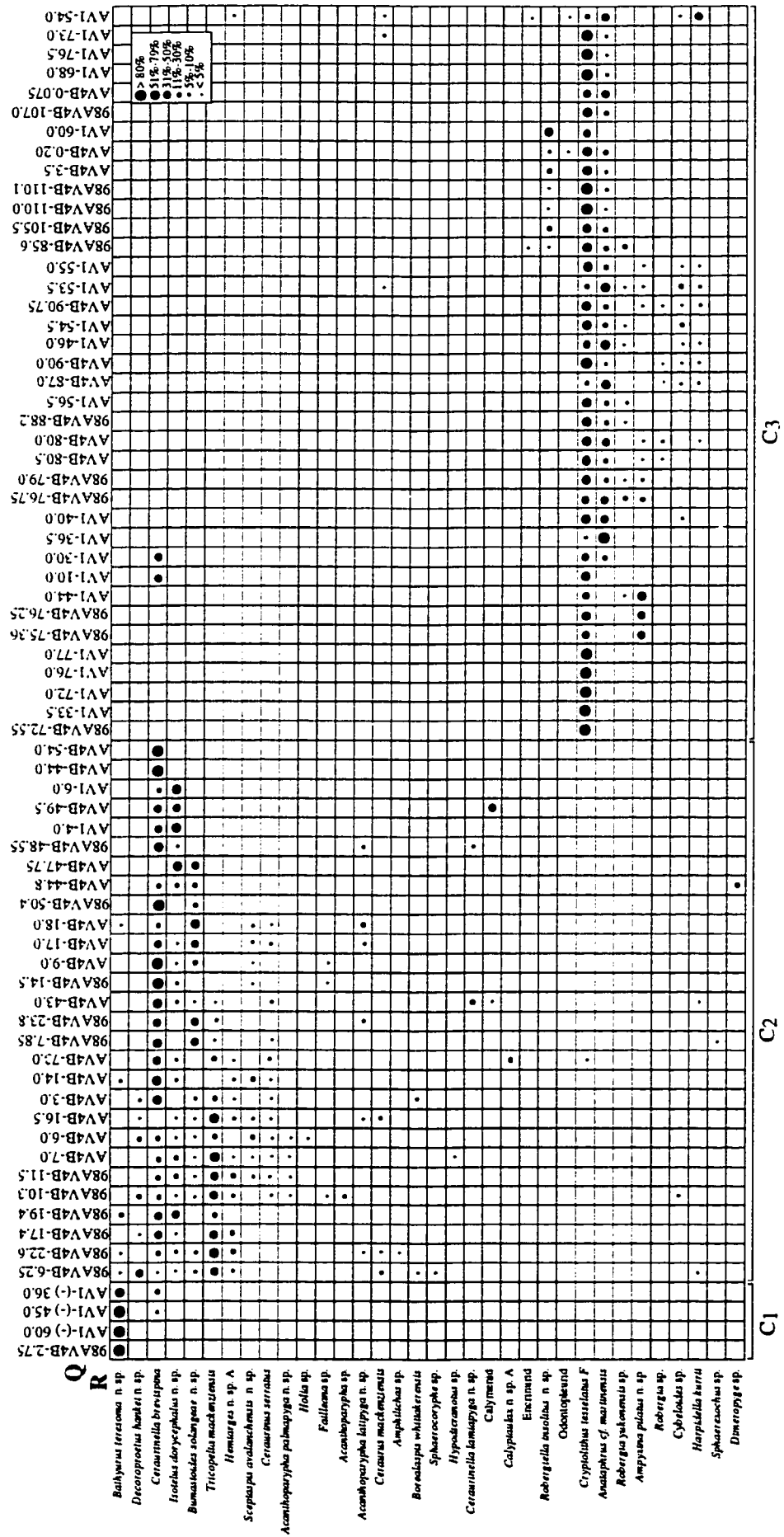


Figure 3.8. Biofacies map of all 3 combined sections and genera within these sections. Collections from Q-mode dendrogram and genera from R-mode dendrogram from Fig. 3.7.

The *Anataphrus-Cryptolithus* Biofacies includes several blind trilobites (*Cryptolithus*, *Ampyxina*) that indicates a deep water association, possibly below the photic zone. This biofacies is well defined by the few genera present. The argillaceous limestones and black shales of this biofacies indicate a deep, cooler water association. This biofacies is interpreted to occur on a slope environment. This biofacies may owe its unique composition and reduced diversity to a combination of isolating parameters such as reduced light and cold-upwelling ocean waters, rather than increased depth (Ludvigsen, 1978).

Diversity within the Avalanche Lake Biofacies

The Diversity Index used by Ludvigsen (1978) presents an interesting problem with diversity analysis. When the Diversity Index (Fig. 3.9B, 3.10B, 3.11B) is compared with the curve generated by the number of species in each horizon (Fig. 3.9A, 3.10A, 3.11A), the curves appear different. The Diversity Index is sensitive to low abundances of trilobites. When species are represented by a few individuals, the diversity index tends to increase, showing a higher diversity relative to the actual number of species present. The Diversity Index curve presents a muted representation of the data compared with diversity curves of the actual number of species present at each horizon.

The *Bathyrurus* Biofacies shows a low diversity relative to the other biofacies. This low diversity is not surprising since the environment appears to have been stressed (variable temperature, salinity, depth, etc.). Stratigraphically above this biofacies, there is a dramatic increase of diversity into the *Tricopelta-Ceraurinella* Biofacies. The significant diversity increase from the *Bathyrurus* Biofacies to the *Tricopelta-Ceraurinella* Biofacies may suggest a parallel in the increase in environmental stability, from a dynamic nearshore environment to a deeper water, calmer shelf environment. Ludvigsen (1978) noted that stability increase in extant faunas is commonly expressed along a depth gradient. This is apparent in the AV4B and 98AV4B collections (Figs. 3.9, 3.10) with an increase in the diversity from the *Bathyrurus* Biofacies to the *Tricopelta-Ceraurinella* Biofacies. Within the *Tricopelta-Ceraurinella* Biofacies, diversity fluctuates, but remains consistently higher than that of the *Bathyrurus* Biofacies.

Within the AV4B collection, diversity increases and fluctuates within the *Tricopelta-Ceraurinella* Biofacies, reaching the lowest diversity at 32 metres. The interval between 20 metres and 50 metres is reflected in the Diversity Index curve as an area of high diversity. This interval contains little material and has a low diversity. Due to the sensitivity of the Diversity Index to rare species, this diversity change represents a lack of silicified material between 20 metres and 40 metres of the section rather than a true high diversity. This phenomenon can also be seen in the 98AV4B collection between the intervals of 25 metres

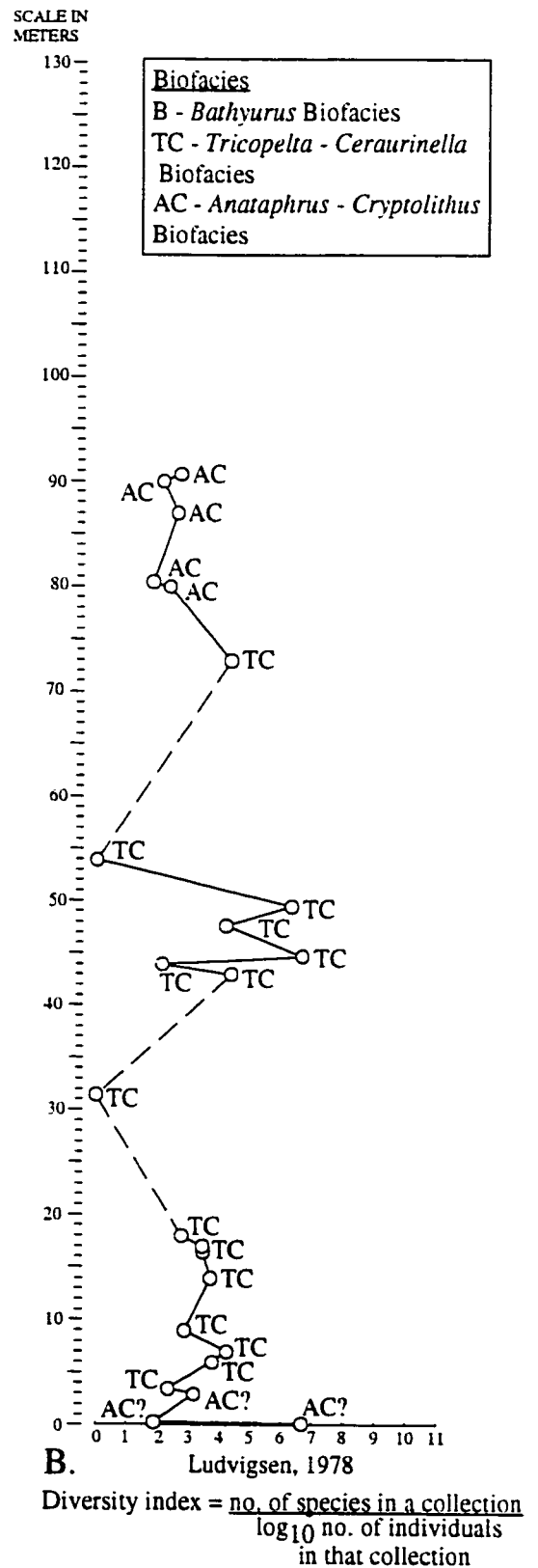
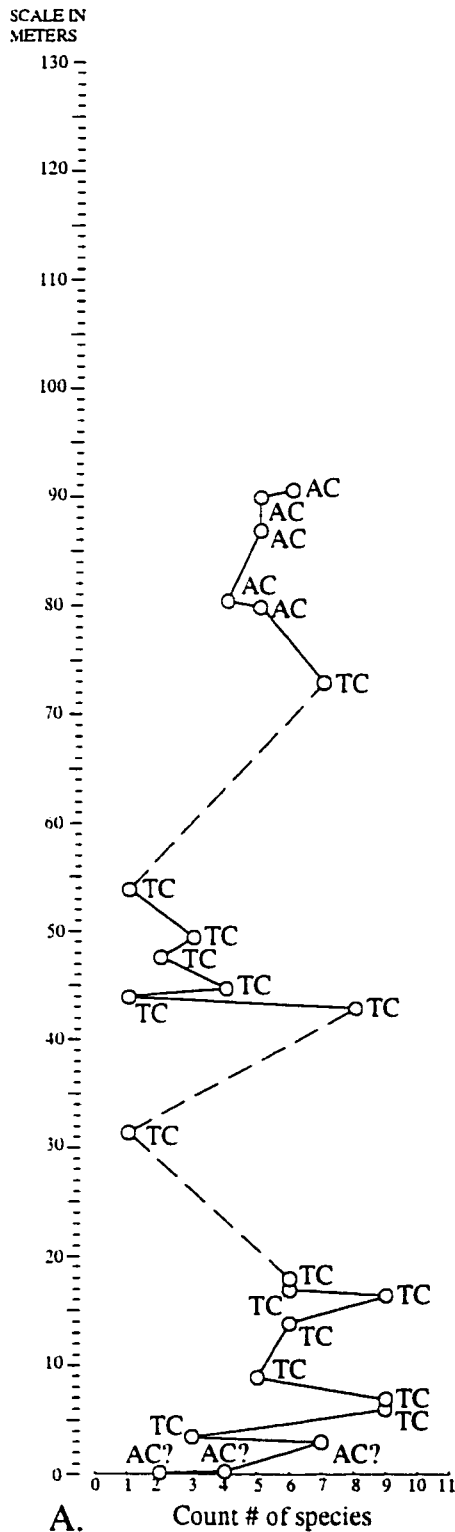


Figure 3.9. Diversity indices of AV4B trilobite collections from the Whittaker Formation. The vertical axis represents the measured section. A. Diversity indices tabulated using species counts at each horizon. B. Diversity indices tabulated using the Diversity Index of Ludvigsen (1978). Dotted lines represent intervals without data.

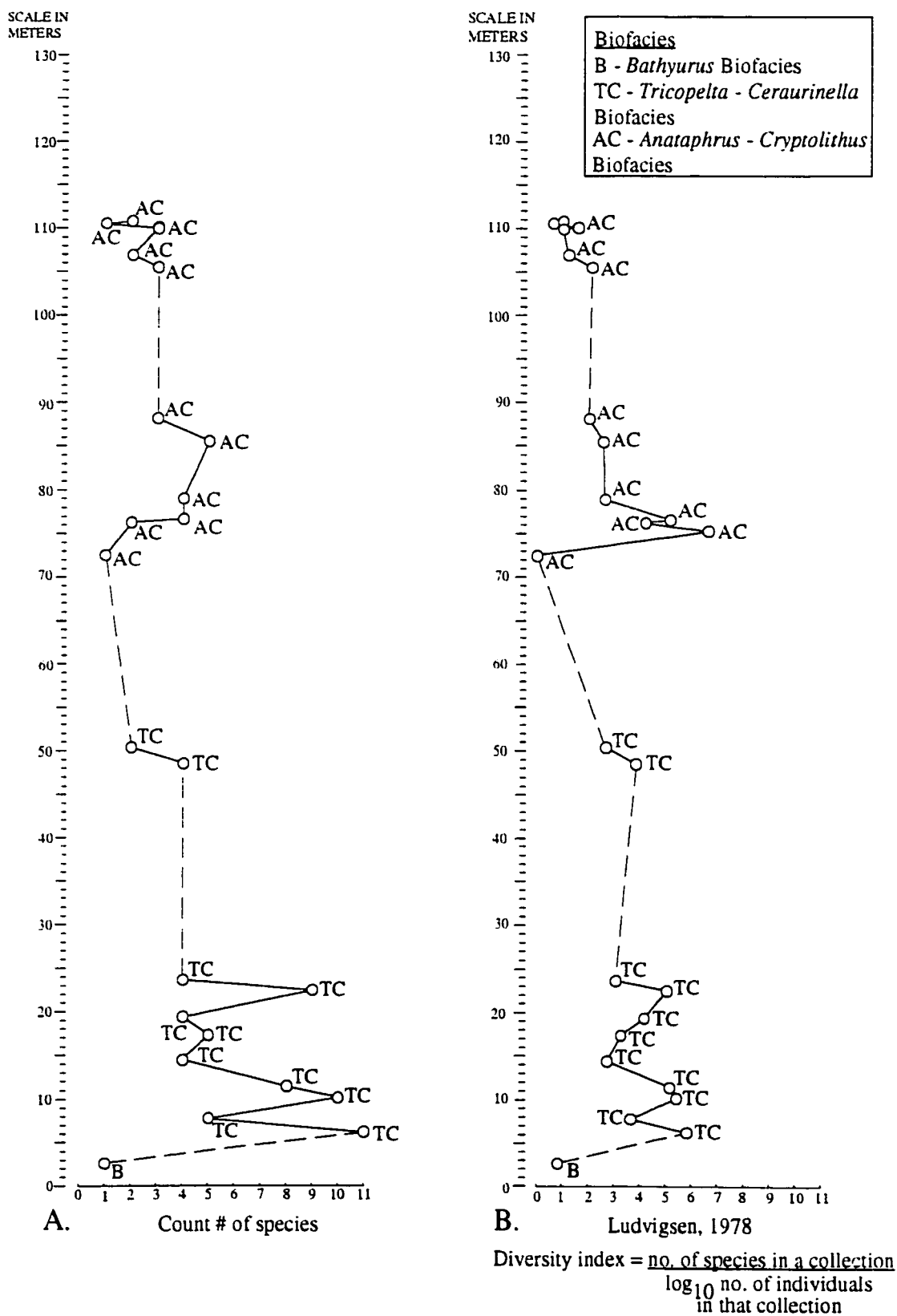


Figure 3.10. Diversity indices of 98AV4B trilobite collections from the Whittaker Formation. The vertical axis represents the measured section. A. Diversity indices tabulated using species counts at each horizon. B. Diversity indices tabulated using the Diversity Index of Ludvigsen (1978). Dotted lines represent intervals without data.

and 72.55 metres. There are few samples within this interval, and material from these horizons is either very poor or not present. This lack of specimens may be attributed to a lack of preservation or sampling error rather than a reflection of the true diversity of trilobites within this interval. Observation of this interval showed no evidence of any silicified fossils within this interval when usually there are other fossil groups associated with the silicified trilobites when present. Absence of any fossils, surface or crack-out, indicates a lack of preservation within this interval.

At 73 m within the 98AV4B and AV4B collections (Figs. 3.9, 3.10), the diversity is low. This low diversity occurs at the same interval as a sharp facies change from micritic limestones to calcareous shales. This interval, as indicated by the material, represents the faunal change from the higher diversity assemblage of the *Tricopelta-Ceraurinella* Biofacies to the lower diversity assemblage of the *Anataphrus-Cryptolithus* Biofacies. The initial low diversity reflects absence of trilobite species within this region after rapid environmental change. A subsequent increase in diversity can be observed above the 73 metre horizon. This may reflect migration of new genera into the region, and the establishment of a new community. It may also reflect the presence of refugia and that the survivors of the extinction event were geographically constrained during the period of cooling. Recovery of diversity shows that it took time to disperse into the new environmental parameters and may reflect on the rate at which these trilobites were able to adapt to new conditions. The eventual stabilization of the community at lower diversity levels than the *Tricopelta-Ceraurinella* Biofacies is observed. The lowest diversity within the *Anataphrus-Cryptolithus* Biofacies is observed near the latest-Ordovician extinction event, at 110.1 metres. At this level the fauna consists primarily of two genera, *Anataphrus* and *Cryptolithus*.

The same general trends in diversity can be observed within the AV1 section (Fig. 3.11). The initial diversity change from the *Tricopelta-Ceraurinella* Biofacies to the *Anataphrus-Cryptolithus* Biofacies is small, and the boundary between these two biofacies is uncertain. The appearance of the *Anataphrus-Cryptolithus* Biofacies at 10 metres is thought to correspond with the 73 metre change at Avalanche Lake 4B. Diversity above this horizon fluctuates to a high at 55 metres and steadily decreases towards the latest-Ordovician extinction event. This pattern mirrors the diversity changes in Avalanche Lake 4B and in addition to the faunal composition and biofacies, may serve to correlate the three sections (Fig. 3.12).

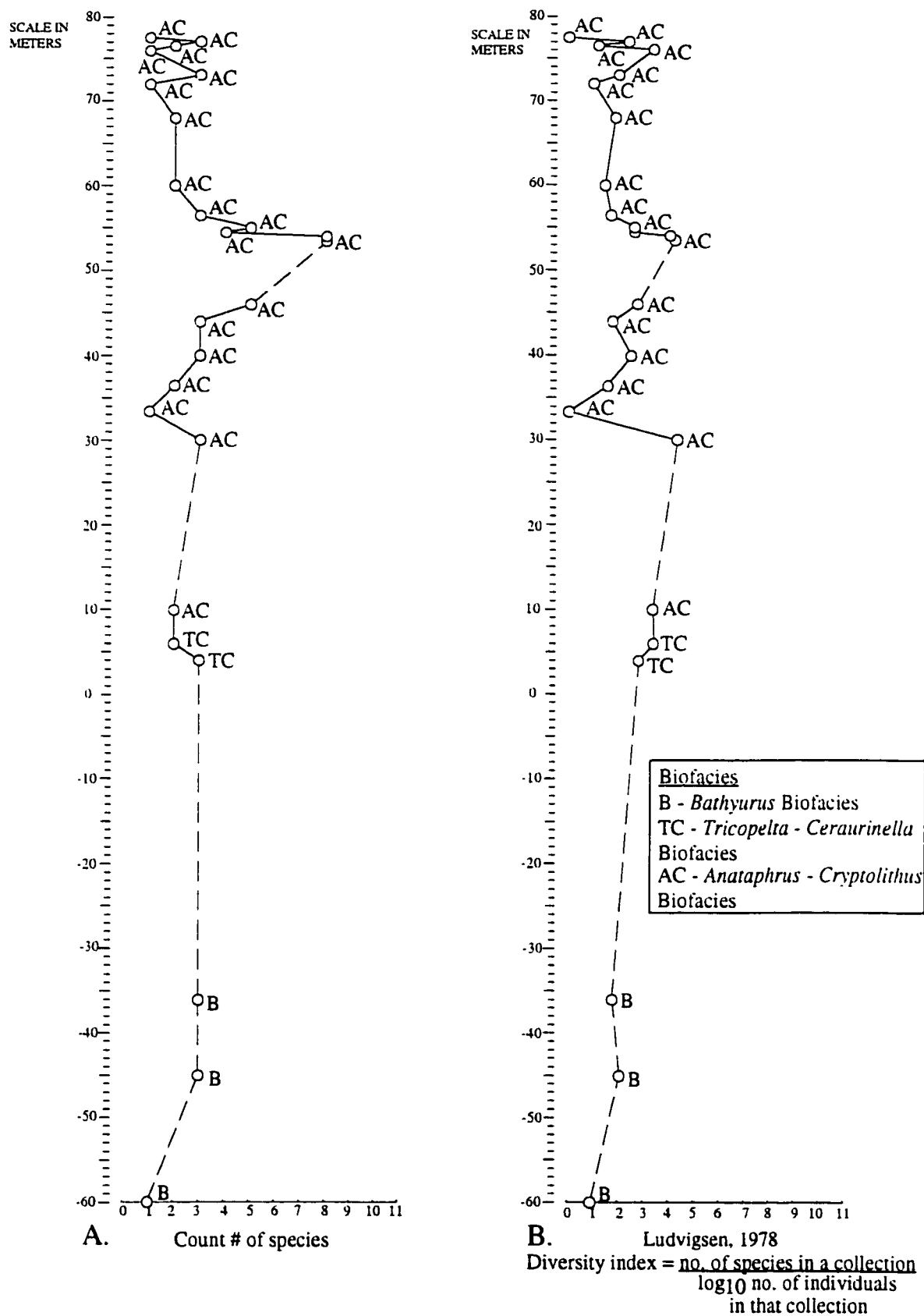


Figure 3.11. Diversity indices of AV1 trilobite collections from the Whittaker Formation. The vertical axis represents the measured section. A. Diversity indices tabulated using species counts at each horizon. B. Diversity indices tabulated using the Diversity Index of Ludvigsen (1978). Dotted lines represent intervals without data.

Interaction within Biofacies

There exists a dynamic association between the Family Pterygometopidae and the Family Cheiruridae within the Avalanche Lake 4B and Avalanche Lake 1 sections (Figs. 3.13, 3.14, 3.15). In most cases, when one family exists in a large abundance (greater than 50% of the total fauna) at a particular horizon, the other family occurs in low numbers (less than 10%). This relationship is interchangeable, with one family dominating at one horizon and the other family dominating at the next sampled horizon. In rare cases, these two families occur in equal abundances. The interchangeable association between the two families may reflect fluctuating environmental conditions, with one family dominating during one set of environmental parameters and the other family dominating during a different set of environmental parameters. At this point, the sedimentology does not reflect fluctuating environmental conditions that are consistent enough within this interval to indicate a similar pattern. Closer analysis of the sedimentology through thin sectioning or isotope analysis may reveal small scale environmental fluctuations within the sediments that can account for the pattern seen here.

Comparison with other Biofacies Work

Lower Ordovician Biofacies

Fortey (1975) and Fortey and Barnes (1977) recognized four communities related to a shallow to deep water profile on the edge of a former continental shelf from the Valhallfonna Formation of the Arenig-Llandvirn of northern Spitsbergen. These communities were defined as follows:

1. Shallow water illaenid-cheirurid community with a diverse fauna including Illaenidae, Cheiruridae, Bathyruridae, and Dimeropygidae. Light colored, coarsely crystalline limestones are typical.
2. Deeper water Nileid community with a diverse fauna of Nileidae, Asaphidae, Raphiophoridae, and Shumardiidae.
3. Relatively deep water "shelf-edge" olenid community. Black, flat-bedded and minutely laminated limestones are characteristic.
4. An association of pelagic trilobites independent of the benthic community.

Fortey and Barnes (1977) did not identify a nearshore community analagous to the *Bathyrurus* Biofacies of AV4B. They noted that an assemblage lying further nearshore can be identified that contains specialized benthic trilobites including pliomerids and asaphids.

The illaenid-cheirurid community of Fortey and Barnes (1977) is similar in composition as the *Tricopelta-Ceraurinella* Biofacies of AV4B. Material is completely

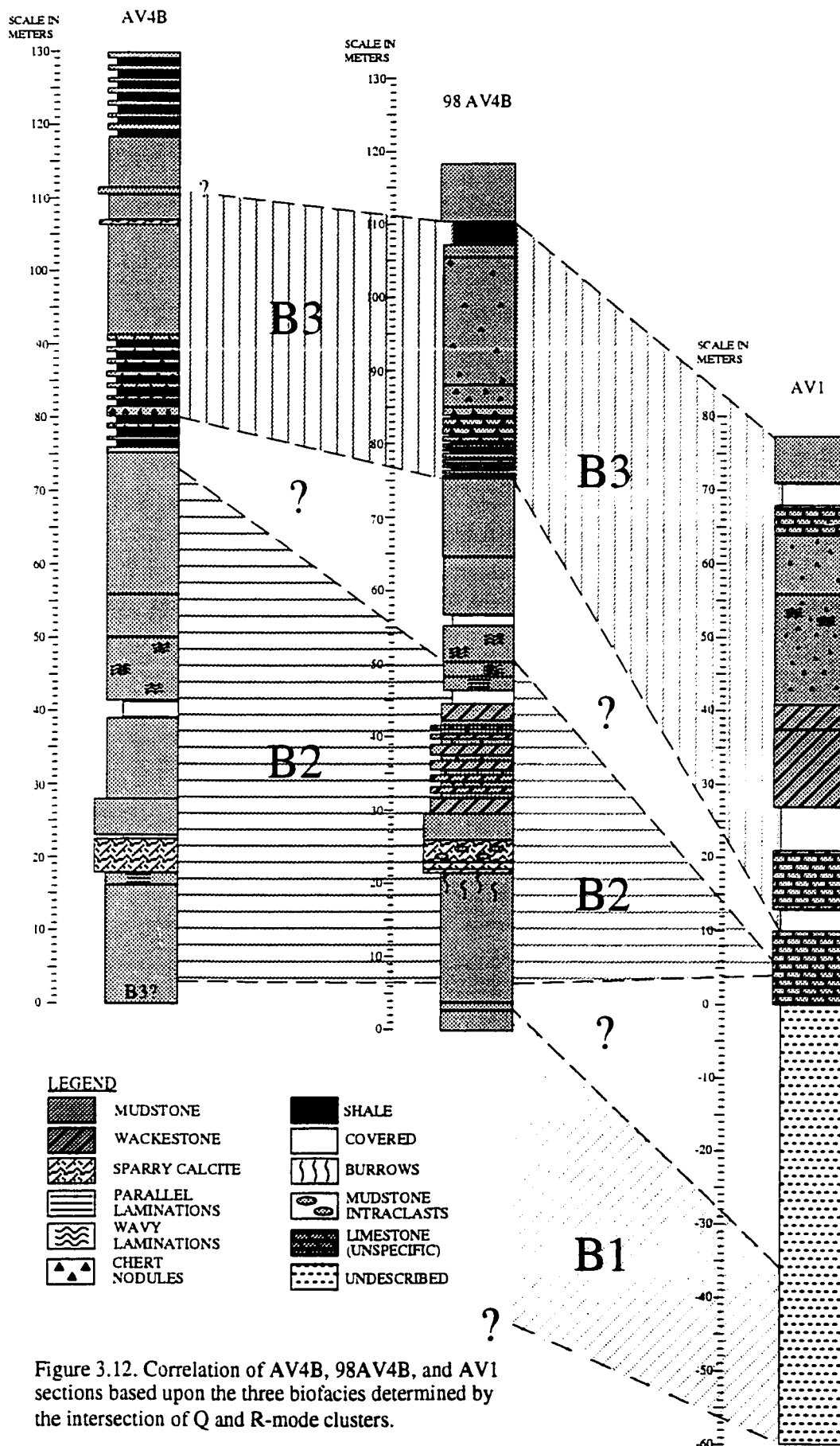


Figure 3.12. Correlation of AV4B, 98AV4B, and AV1 sections based upon the three biofacies determined by the intersection of Q and R-mode clusters.

AV4B Family Distribution by Horizon

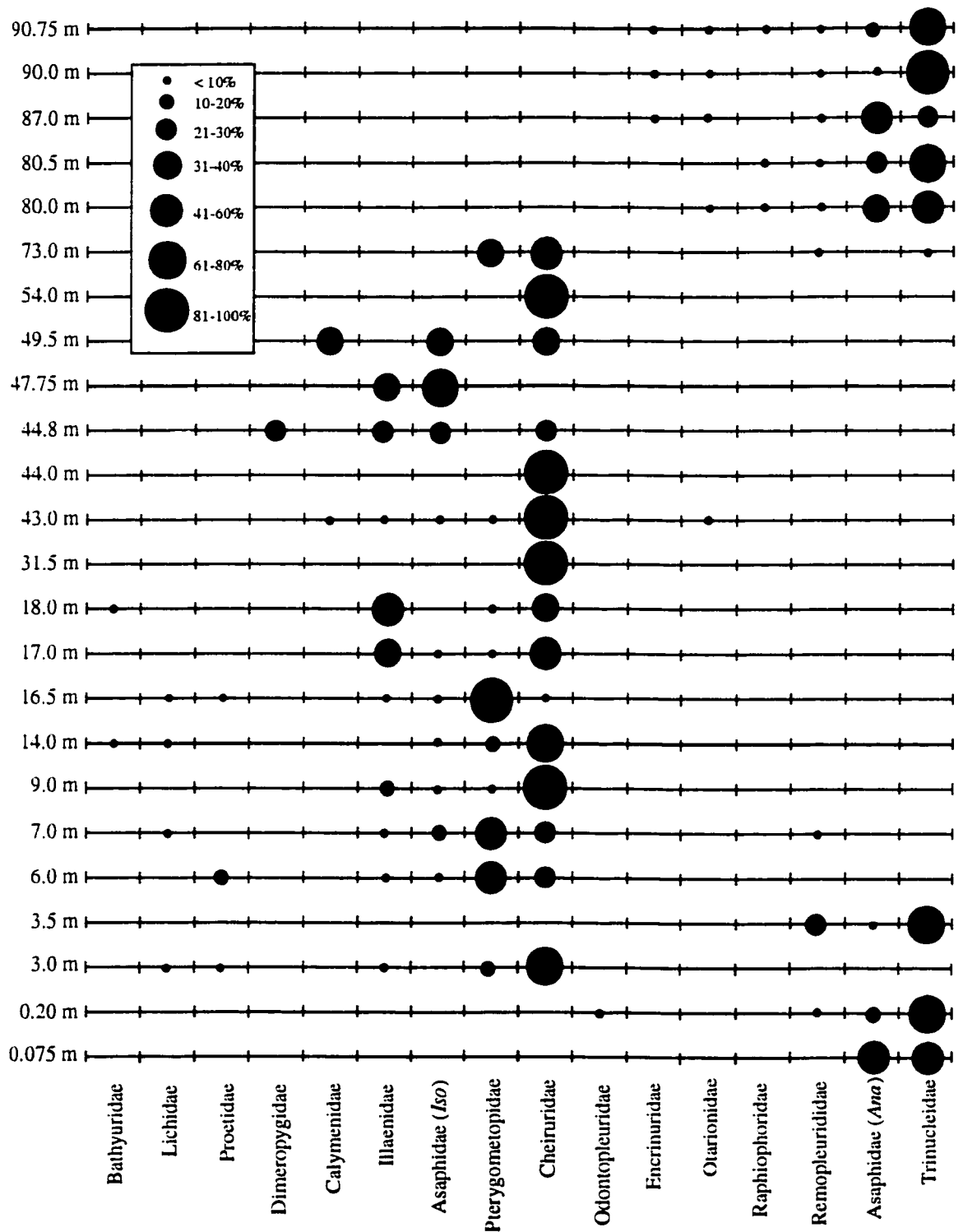


Figure 3.13. Relative abundance of families in trilobite collections from the lower Whittaker Formation at the Avalanche Lake 4B section.

98AV4B Family Distribution by Horizon

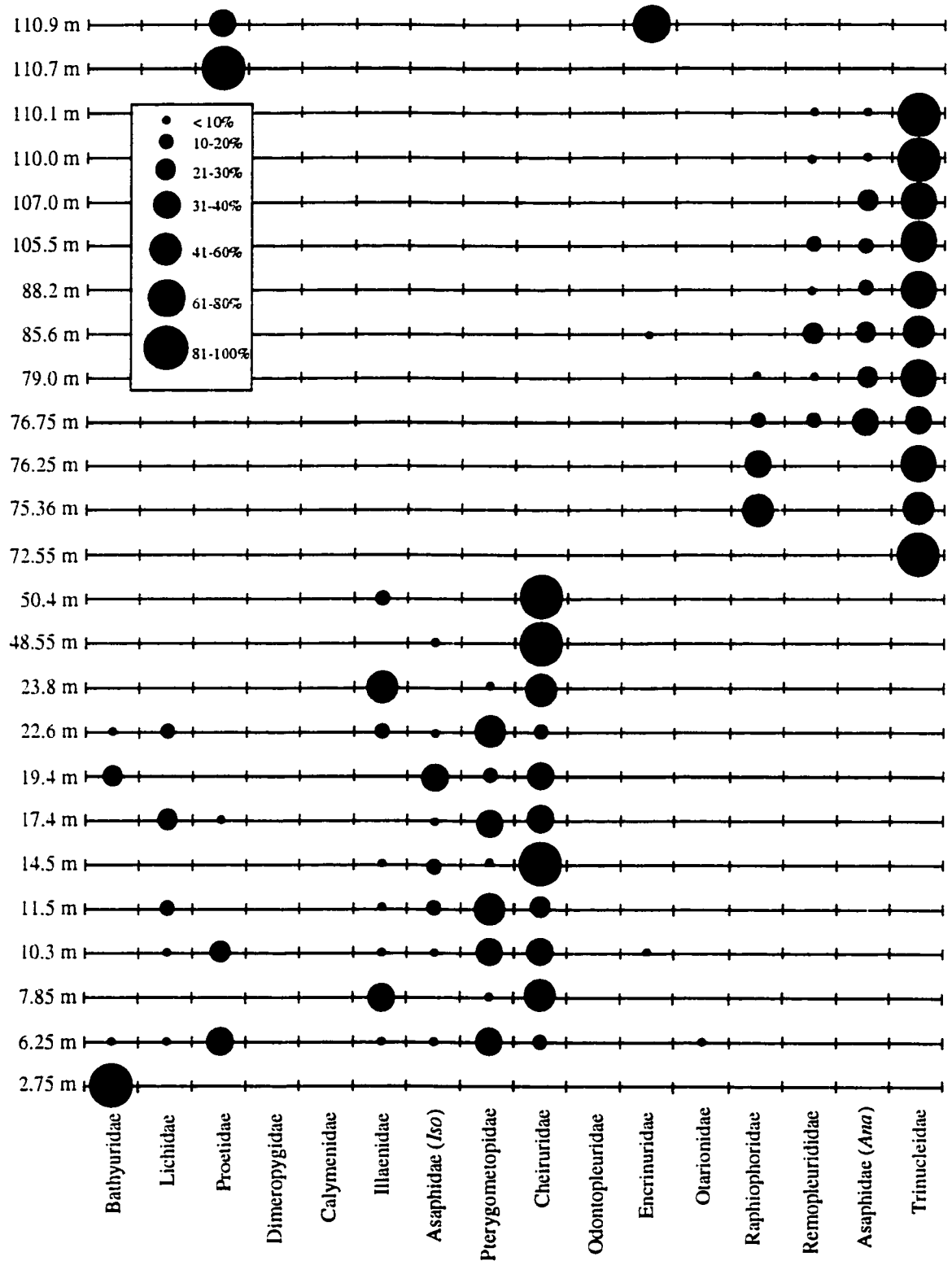


Figure 3.14. Relative abundance of families in trilobite collections from the lower Whittaker Formation at the 98 Avalanche Lake 4B section.

AV1 Family Distribution by Horizon

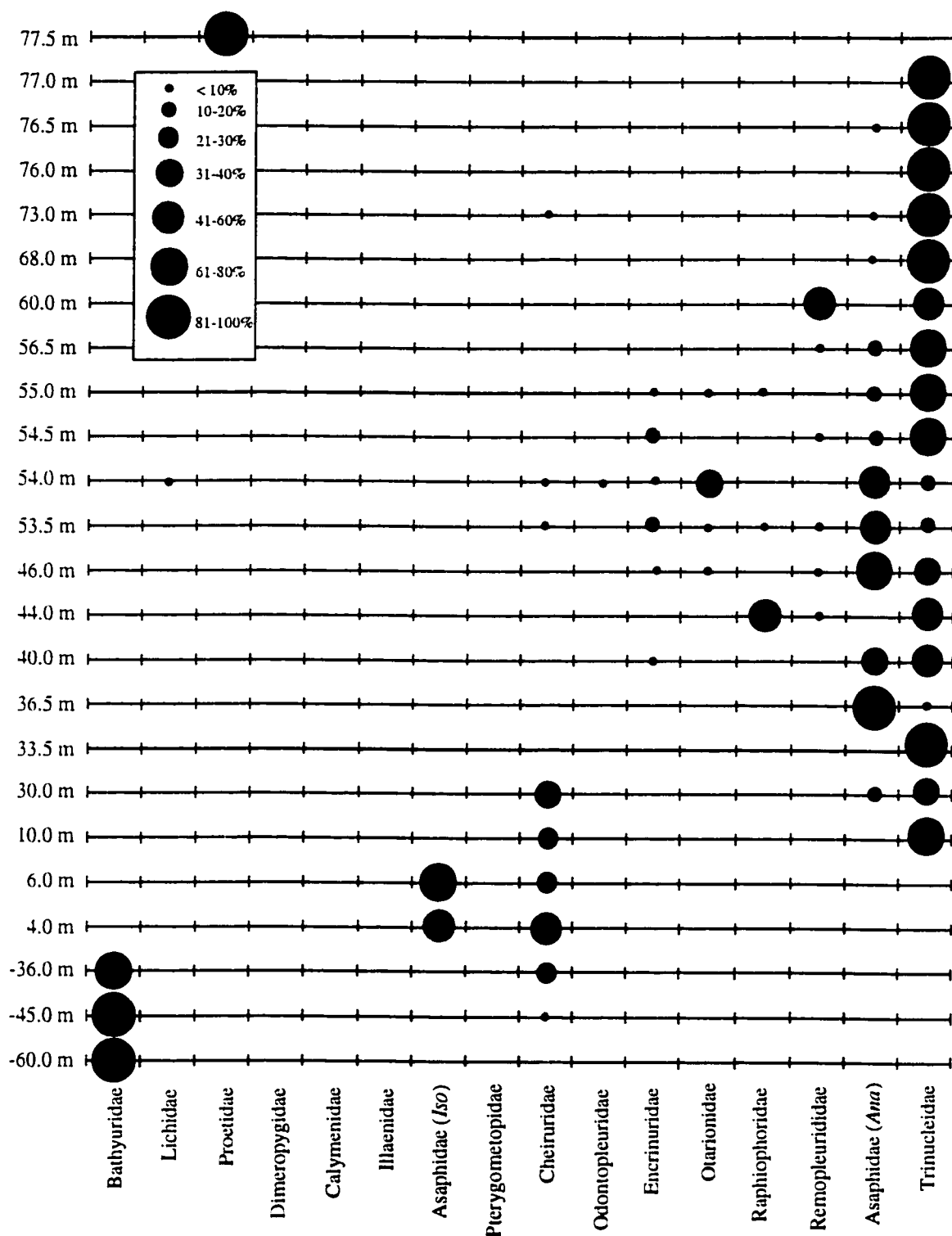


Figure 3.15. Relative abundance of families in trilobite collections from the lower Whittaker Formation at the Avalanche Lake 1 section.

disarticulated and stout exoskeletons are broken. Fortey (1975) suggested that the remains of this community were swept as an allochthon from a shallow water environment into the nileid community by strong currents generated by storms. Transport of the material was sufficiently energetic to break exoskeletons but rapid enough not to result in abrasion of surface sculpture. Clearly, within the shelf environments of the Early and Late Ordovician, cheirurids dominated the community structure.

The nileid community of Fortey and Barnes (1977) has no direct analogue within the Upper Ordovician biofacies. The presence of Raphiophoridae and Asaphidae within this community and the lithology of dark limestones with occasional shales suggests that it may bridge the gap between the shelf community and a deeper water "shelf-edge" community. Occasionally, material from the shelf community was swept into the nileid community. Raphiophoridae and Asaphidae are present in the deeper water biofacies in the Upper Ordovician.

Although the deeper water olenid community contains taxa different from those present in the Upper Ordovician, this community represents the specialized trilobites that lived in this type of environment. This "shelf-edge/slope" biofacies always appears as a distinct low diversity community with a unique fauna that is adapted to living under specialized conditions. The sedimentology, within this biofacies, is consistent within this biofacies through time, consisting of argillaceous limestones, and black, carbonaceous shales interbedded with cherts. Material of delicate olenid remains are preserved without breakage. Similar preservation is found in the *Anataphrus-Cryptolithus* Biofacies of AV4B. Fortey and Barnes (1977) attributed this environment to low dissolved oxygen levels in near quiet bottom waters, conditions to which they state olenids were adapted to since Cambrian times.

Whittington (1963) described a Whiterockian assemblage from a single boulder in the Cow Head Breccia at Lower Head, Newfoundland. Fortey (1975) allied this assemblage with the illaenid-cheirurid assemblage of Spitsbergen, citing the presence of illaenids, cheirurids, bathyurids, and lichids and the absence of olenids and raphiophorids, typical of deeper slope environments from Spitsbergen. This illaenid-cheirurid biofacies is similar in composition at the family level to the *Tricopelta-Ceraurinella* Biofacies of Avalanche Lake. Whittington (1965) also described a trilobite fauna from the lower Whiterockian of the Table Head Formation, Newfoundland, that Fortey (1975) allied with the illaenid-cheirurid association. This fauna is impoverished, but has a similar mode of occurrence within the Valhallfonna Formation. The material is mainly disarticulated, and present in thin fossiliferous bands representing material displaced from the illaenid-

cheirurid assemblage. Based upon preservation, Fortey (1975) stated that the Newfoundland assemblages appear to be similar to those occurring in Spitsbergen.

Middle Ordovician Biofacies

Chatterton and Ludvigsen (1976) noted four distinct biofacies within the Chazyan and early Blackriveran of the Mackenzie Mountains. These consist of:

1. *Bathyurus* Biofacies
2. *Isotelus* Biofacies
3. *Calyptaulax-Ceraurinella* Biofacies
4. *Dimeropyge* Biofacies

The *Bathyurus* Biofacies is similar to the initial biofacies from AV4B in that it is dominated by *Bathyurus* and contains features of sub-aerial exposure such as mudcracks, syneresis cracks (as seen at AV1), and interference ripples, sedimentary structures often associated with shallow water environments.

The *Isotelus* Biofacies does not occur in the Upper Ordovician of AV4B. The taxa that occur in this biofacies of Chatterton and Ludvigsen (1976) occur in association with the third biofacies, the *Calyptaulax-Ceraurinella* Biofacies. These two biofacies occur as one mixed assemblage, the *Tricopelta-Ceraurinella* Biofacies at AV4B. As in Chatterton and Ludvigsen (1976), the second biofacies of AV4B is dominated by cheirurids, with the Upper Ordovician genus *Tricopelta* representing the pterygometopids instead of *Calyptaulax*, the genus of pterygometopid common in the Middle Ordovician. The second and third biofacies of Chatterton and Ludvigsen (1976) are found together at AV4B, and *Isotelus* is present in this joined biofacies but with varying abundance throughout the section. Chatterton and Ludvigsen (1976) noted that *Isotelus* appears as a minor, but integral component to the *Calyptaulax-Ceraurinella* Biofacies. They also note that the *Isotelus* Biofacies may represent a specialized development of the *Calyptaulax-Ceraurinella* Biofacies. AV4B material does not reflect this specialization and groups the two biofacies together. Chatterton and Ludvigsen (1976) admitted that their two biofacies have a close relationship to each other. Samples from AV4B show that the two biofacies of Chatterton and Ludvigsen (1976) are synonymous. These biofacies (*Calyptaulax-Ceraurinella* of Chatterton and Ludvigsen (1976) and *Tricopelta-Ceraurinella* at AV4B) both show a high diversity, containing 20 or more genera of trilobites.

The fourth biofacies of Chatterton and Ludvigsen (1976) is not observed AV4B. Genera present in this last biofacies also occur in the *Tricopelta-Ceraurinella* Biofacies of AV4B. It appears that the shelf platform of the Middle Ordovician of the Mackenzie Mountains consisted of several distinct biofacies, each representing a different community

of trilobites. Shelf communities at this time appear much more diverse and distinct, likely separated by environmental barriers. The shelf community of AV4B appears to be one large trilobite community without much distinction or separation into various components. Chatterton and Ludvigsen (1976) noted that there is generic overlap between the *Calyptaulax-Ceraurinella* Biofacies and the *Dimeropyge* Biofacies, indicating a relationship between the two biofacies. This relationship is not observable at AV4B due to the integration of the shelf community.

The third biofacies of AV4B, *Anataphrus-Cryptolithus* Biofacies, is briefly noted in Chatterton and Ludvigsen (1976). They associate a trinucleid-olenid- graptolite community with platform-edge shales, indicating the presence of a deeper water trilobite association. Although they stated that this biofacies has not been recognized in the Chazy interval, other work indicates that it is sparsely represented (Ludvigsen, 1978). This biofacies is distinct and prevalent at AV4B.

Ludvigsen (1978) described three distinct biofacies in the Chazy, Blackriveran, and Trentonian platform of the South Nahanni River area. These were defined as follows:

1. Biofacies I: *Bathyurus* and *Ceraurus* as core genera.
2. Biofacies II: *Bumastoides*, *Ceraurinella*, *Calyptaulax* and *Isotelus* as core genera.
3. Biofacies III: Core genera numerous (*Cybeloides*, *Dolichoharpes*, *Amphilichas*, *Rempleurides*, *Carrickia*, *Holia*, *Failleana*, *Acanthoparypha*, *Sphaerexochus*) and includes core genera of Biofacies II.

An additional biofacies, Biofacies IV, was not included in the cluster analysis of Ludvigsen (1978). The core genera consist of *Cryptolithus*, *Cryptolithoides*, *Triarthrus*, *Anataphrus*, *Robergiella*, *Ampyxina*, *Ampyx*?, a proetid, and *Robergia*?. Ludvigsen (1978) notes that this biofacies occurs in the Trentonian part of the lower Road River Formation and is sparsely represented in the Chazy.

Ludvigsen's Biofacies I is similar to the *Bathyurus* Biofacies of AV4B. Both are dominated by *Bathyurus* and represent a shallow water environment. Biofacies II and III appear to have a close relationship since Biofacies III incorporates some of the core genera from Biofacies II. The *Tricopelta-Ceraurinella* Biofacies of AV4B includes many of the genera in Ludvigsen's Biofacies II and III, reiterating the differences also found in Chatterton and Ludvigsen (1976). Middle Ordovician shelf biofacies appear much more differentiated and distinctive, while the Upper Ordovician material reflects an amalgamation of these distinct biofacies into one. Biofacies IV of Ludvigsen is similar to the *Anataphrus-Cryptolithus* Biofacies of AV4B. Genera occurring in Biofacies IV, with the exception of *Cryptolithoides* and *Triarthrus*, also occur in the *Anataphrus-Cryptolithus* Biofacies of

AV4B. These trilobites are also found in argillaceous limestones and black shales indicating a deeper water environment.

Hayes (1980) conducted a biofacies analysis of the Chazy and Blackriveran strata of the Sunblood, Esbataottine, and Road River Formations of the southern Mackenzie Mountains, incorporating collections of ostracods, bryozoans, and conodonts to provide a more complete description of the fauna in this region. Using Q and R-mode analysis Hayes (1980) delineated five biofacies: one nearshore, three progressively deeper and one continental slope biofacies.

The first biofacies, the *Bathyrus-Leperditella* Biofacies is similar to Ludvigsen's Biofacies I (Ludvigsen, 1978) and to the *Bathyrus* Biofacies of AV4B. Hayes (1980) interpreted this environment as a shallow, nearshore to intertidal environment dominated by burrowing organisms that were able to protect themselves from rapidly changing environments. This interpretation is consistent with Ludvigsen's Biofacies I and the *Bathyrus* Biofacies of AV4B.

The following three biofacies, the *Eurychilina-Stictopora* Biofacies, the *Ceraurinella-Cybeloides* Biofacies, and the *Faillaena-Krausella* Biofacies, occupy successively deeper positions on the continental shelf, respectively. Hayes (1980) considered these biofacies to be similar to the Biofacies II and III of Ludvigsen (1980). The *Eurychilina-Stictopora* Biofacies and the *Ceraurinella-Cybeloides* Biofacies were considered equivalent to Ludvigsen's Biofacies I and II. *Cybeloides* and *Ceraurinella* are the dominant genera with minor amounts of *Bathyrus* and *Ceraurus* present. These biofacies consist of swimming and burrowing trilobites. The *Faillaena-Krausella* Biofacies includes a diverse assemblage of 56 trilobite genera including *Faillaena*, *Acanthoparypha*, *Holia*, *Calyptaulax*, *Cybeloides*, *Ceraurinella*, *Isotelus*, and *Bumastoides*. The generic composition of this biofacies and the high diversity suggests a close affinity to the *Tricopelta-Ceraurinella* Biofacies of AV4B. Hayes (1980) considered this biofacies to be dominated by epifaunal trilobites and ostracods that occupied a great variety of ecological niches including filter feeding, deposit feeding, scavenging, and grazing. Hayes (1980) considered the great diversity of organisms and life modes to reflect a physically stable environment that allowed for diversification and occupation of a variety of ecological niches.

The final biofacies, the *Ampyx-Triarthrus* Biofacies is very similar to Biofacies IV of Ludvigsen (1978) and the *Anataphrus-Cryptolithus* Biofacies of AV4B. This is the only biofacies with blind trilobites. This biofacies occurs in highly argillaceous limestones and

shales, consistent with the lithology of AV4B. These strata occur seaward of the platform edge and represent quiet, deep water sedimentation on the slope (Ludvigsen, 1978).

Hayes (1980) reiterated the point of Chatterton and Ludvigsen (1976) and Ludvigsen (1978), that many shelf communities existed during the Middle Ordovician. Hayes identified three distinct biofacies on the shelf, whereas the AV4B section contains only one. This may represent stable environmental conditions during the Upper Whiterockian (Chazyan) and Blackriveran which allowed for establishment of complex communities not seen in the Upper Ordovician.

Other Middle Ordovician biofacies analyses show analogues to the Upper Ordovician biofacies of the Mackenzie Mountains. Ludvigsen (1978a) recognized two trilobite biofacies from the Blackriveran of Oklahoma. The first biofacies consists of a shallow water assemblage developed on a platform from the Corbin Ranch Formation and a deeper water biofacies developed within the Pooleville Member. The trilobite fauna from the Corbin Ranch Formation is extremely sparse, consisting of few specimens of two genera (2 *Bathyurus* and 1 *Eomonorachus*). This biofacies is suggestive of Biofacies I (Ludvigsen, 1978) and the *Bathyurus* Biofacies of the Avalanche Lake sections. The Pooleville Member consists of a sequence of interbedded limestones and shales thought to indicate deeper water deposition. The trilobite material from the Pooleville Member is much more diverse and abundant than that of the Corbin Ranch Formation. Ludvigsen (1978a) noted that the Pooleville Member fauna, on the generic level, is very similar to Biofacies III (Ludvigsen, 1978). A similarity between the Pooleville Member biofacies and the *Tricopelta-Ceraurinella* Biofacies of AV4B may be considered.

Fortey and Droser (1996) recently studied the faunas of the Wahwah and Juab Limestone Formations from the Whiterock of western Utah and eastern Nevada. Analysis of the material revealed a predominance of bathyurids (greater than 70%) with pliomerids and dimeropygids present. Illaenids and cheirurids proved to be exceedingly rare. This biofacies is similar in composition to the *Bathyurus* Biofacies of AV4B, with a high percentage of bathyurids present.

Upper Ordovician Biofacies

Few biofacies analyses are available for the Upper Ordovician. Price (1980) studied the faunas of Cautleyan to Rawtheyan in age from the Sholeshook Limestone Formation of South Wales. Based on sedimentological and stratigraphical evidence, the Sholeshook Limestone Formation revealed an environment corresponding to the middle and upper part of the slope between platform edge and basin.

Two associations were found to occupy these environments. The first of these associations occurred in light-colored, pure limestone deposits considered to be part of a reef facies. The trilobite remains within this biofacies were almost entirely intact. The faunas were characterized by a diverse assemblage of illaenids, cheirurids and lichids. This association was thought to represent shelf-edge or near shelf-edge environments. The second association is characterized by mudstone sequences that represent a deeper water, low energy slope environment. The fauna contained completely articulated remains of raphiophorids, pterygometopids, encrinurids, and trinucleids.

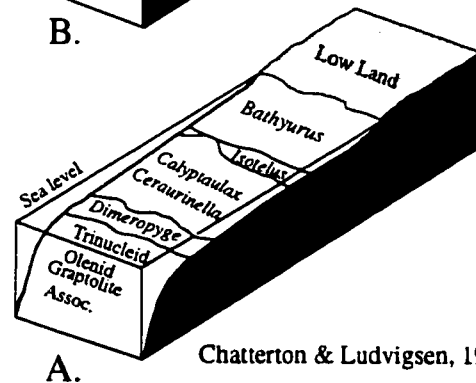
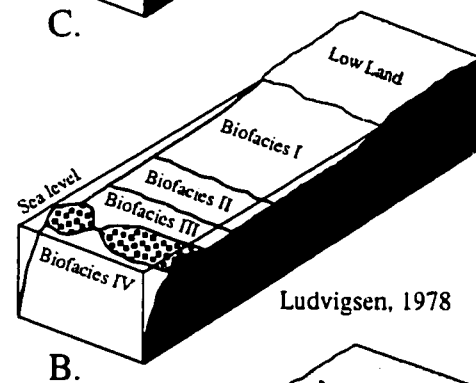
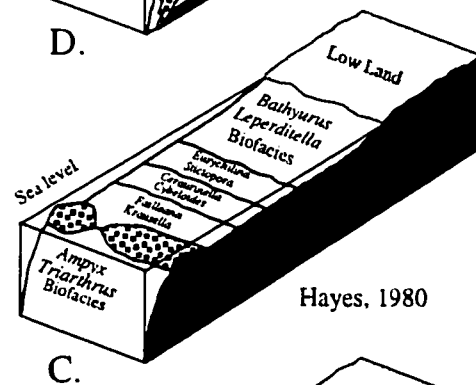
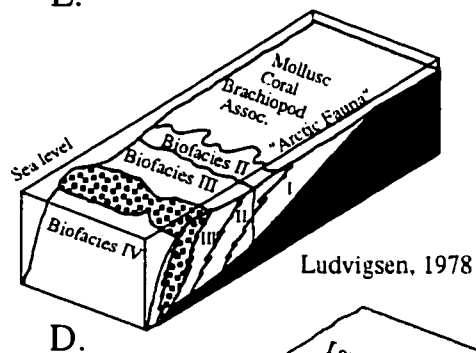
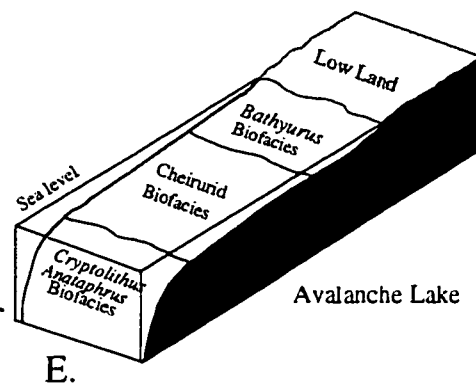
The division of the two associations into shelf-edge and slope by Price (1980) provide a direct comparison with the Ashgill biofacies of the Mackenzie Mountains. The illaenid-cheirurid association of Fortey (1975), Fortey and Barnes (1977), Chatterton and Ludvigsen (1976), Ludvigsen (1978), and Hayes (1980) along with the Avalanche Lake material is very similar to the shelf associations of Price (1980). All of the above faunas are diverse and similar at the familial, possibly generic level. The slope fauna is similar to the deep-water faunas of the Middle Ordovician, with the addition of a larger proportion of pterygometopids. This slope biofacies of Price (1980) is adequately represented in previous studies. The associations of Price (1980) reiterate the stability and dominance of the illaenid-cheirurid and deep-water faunas of the Ordovician.

Biofacies Trends of the Ordovician of the Mackenzie Mountains

Fortey and Droser (1996) noted that Ordovician trilobites, as they occur in Laurentia, are segregated into four major biofacies depending on bathymetry and paleoenvironmental conditions. These biofacies can be recognized by the dominance of characteristic trilobite families. At a finer scale, from the Middle Ordovician to the Upper Ordovician, these biofacies are comparable at the generic level. Addition of the material from Avalanche Lake 4B and Avalanche Lake 1 confirms this observation. The *Bathyrurus* Biofacies and the *Anataphrus-Cryptolithus* Biofacies are stable in their generic composition throughout the Middle and Upper Ordovician (Fig. 3.16). In addition, the illaenid-cheirurid

Figure 3.16. Biofacies trends through the Middle Ordovician to Upper Ordovician in the Mackenzie Mountains, Northwest Territories, Canada. A. Biofacies along a shelf profile for the Upper Whiterockian (Chazy) and Blackriveran of the lower Esbataottine Formation (Chatterton and Ludvigsen, 1976). B. Biofacies along a shelf profile for the Upper Whiterockian (Chazy) and Blackriveran of the upper Sunblood, Esbataottine, and lower Whittaker Formations (Ludvigsen, 1978). C. Biofacies along a shelf profile from the Upper Whiterockian (Chazy) and Blackriveran of the Sunblood and Esbataottine Formations (Hayes, 1980). D. Trentonian biofacies shift of Ludvigsen (1978). E. Biofacies along a shelf profile from the lower Whittaker Formation, Avalanche Lake. The shelf profile was adapted from Ludvigsen (1978).

Ashgill	Hirnantian	Cincinnatian	Gamachian	?
	Rawtheyan		?	
	Cautleyan		?	
	Pusgillian		Richmondian	
Caradoc	Onnian	Cincinnatian	?	?
	Actonian		Maysvillian	
	Marshbrook		Edenian	
	Longvillian			
	Soudleyan	Champlanian	Shermanian	Trentonian
	Harnagian		Kirkfeldian	
	Costanian		Rocklandian	
			Blackriveran	
Llandeilo	Late	Champlanian	Whiterockian	
	Middle			
	Early			
Llandvirm	Late	Champlanian	Whiterockian	
	Early			
Arenig	Late	Champlanian	Whiterockian	

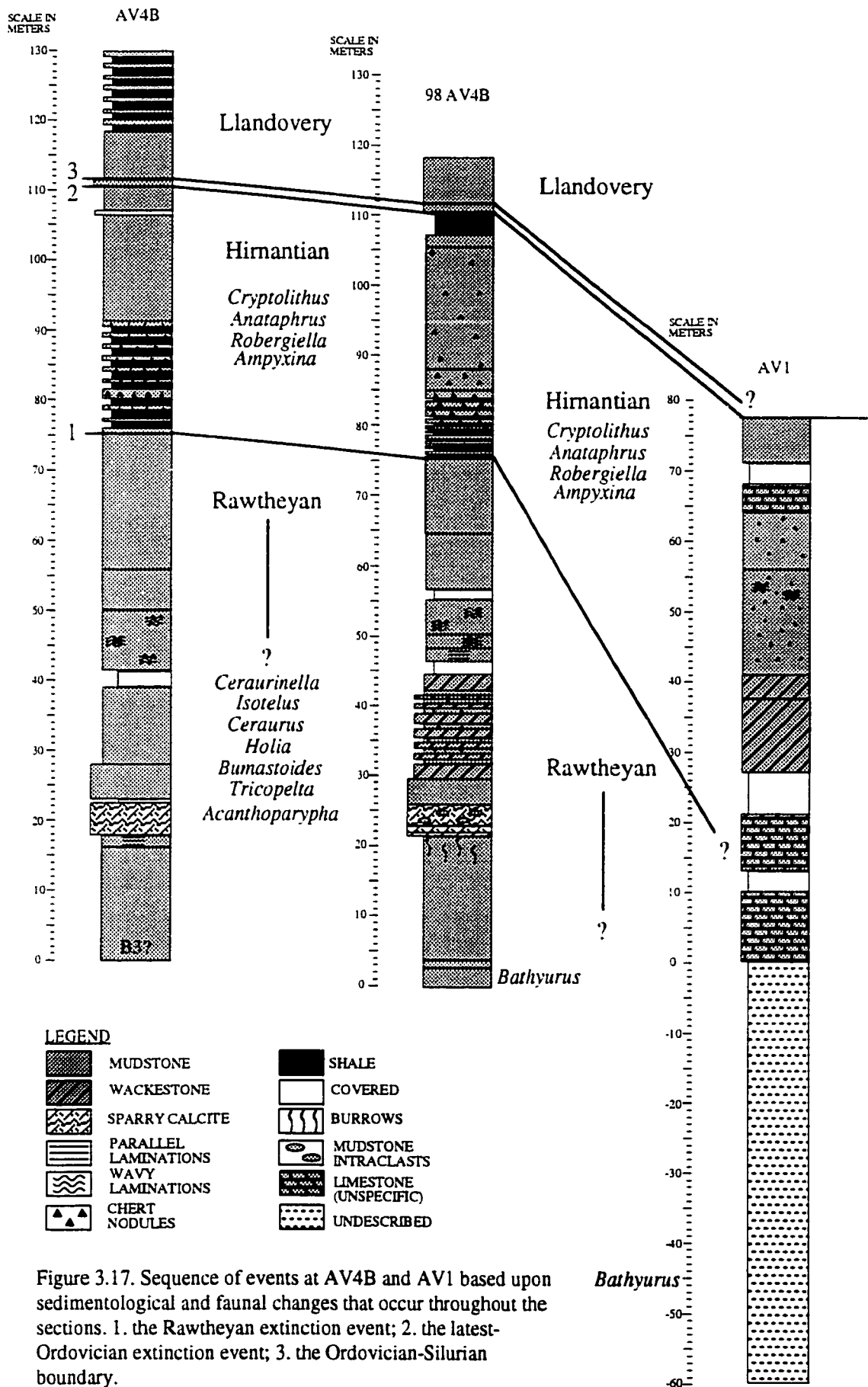


community (known from the Arenig-Llanvirn of Spitsbergen) once established, is persistent in association through to the Upper Ordovician (Ashgill of Mackenzie Mountains). The most apparent changes occur within the shelf environment, with a higher number of biofacies during the Middle Ordovician relative to the Upper Ordovician. As time progressed, shelf biofacies lost their distinctiveness and merged into one biofacies that contains representatives from several individual biofacies of the Middle Ordovician (Fig. 3.16 E). Diversity on the shelf platform fluctuated around a steady level of greater than 20 genera from the Middle Ordovician to the Upper Ordovician, with approximately 23 genera occurring in Chatterton and Ludvigsen (1976), 22 genera from Ludvigsen (1978), 26 genera from Hayes (1980) and 21 genera from Avalanche Lake 4B. It is uncertain why this amalgamation of biofacies occurred. One possibility is that more stable environments allow for diversification of community structure and establishment of many niches. During the Middle Ordovician, stability of the environment provided time for trilobites to diversify and occupy different niches resulting in the diversification of shelf biofacies into discrete communities. Environmental change and instability would favor generalist species able to exploit many environments resulting in fewer recognizable communities. This may have been the cause of the Upper Ordovician biofacies amalgamation, as cooling and eventual glaciation is known to occur during this time.

Discussion - The Late Ordovician Extinctions at AV4B and AV1

Most vertical sequences through rocks of the Rawtheyan and Hirnantian show a change in taxonomic composition and drop in faunal diversity at the base of the Hirnantian, and a further major change at the end of the stage, close to the Ordovician-Silurian boundary (Brenchley, 1984). The Avalanche Lake sections studied here show dramatic shifts in faunal composition and diversity at specific horizons, that correlate with major environmental changes in the Late Ordovician. Figure 3.17 illustrates the major geological events that occur in the AV4B and AV1 sections based upon sedimentological and paleontological data from these sections.

The Avalanche Lake sections span two extinction events of the Ordovician; the Rawtheyan mass extinction event and the latest-Ordovician extinction event. The latest-Ordovician extinction event has been studied at these sections with geochemical analyses, sedimentological changes, and faunal changes above and below the boundary (Copeland, 1989; Wang et al., 1993; Jin and Chatterton, 1997). The Rawtheyan mass extinction event has received little attention in the literature, and has not been studied at AV4B and AV1. The Rawtheyan extinction event is important because it signifies the initiation of the global



changes surrounding the end-Ordovician glaciation and is the precursor to the well-established latest-Ordovician extinction event.

Brenchley and Newall (1984) recognized that the Late Ordovician extinction of trilobites occurred in two phases. The first, at the end of the Rawtheyan, was rapid, resulting in the faunal turnover to a low diversity assemblage. The second, occurring below the Ordovician-Silurian boundary (below the *G. persculptus* Zone), resulted in a faunal turnover to trilobites of Silurian aspect. The low diversity of the Hirnantian fauna testifies to the marked disintegration of the Rawtheyan faunas at the Rawtheyan extinction event (Owen et al., 1991).

Several lines of evidence have been used to establish the existence of the Rawtheyan mass extinction event at AV4B and AV1. Based upon this evidence, the Rawtheyan extinction boundary has been placed at 75.25 m above datum at AV4B. Less precise sampling intervals bracketing the faunal change at AV1 places the event at approximately 10 m above datum.

Faunal Composition and Biofacies Analysis

The faunal composition above and below 75.25 m at AV4B and 10 m at AV1 shows a rapid and drastic change. Below the event horizon, the fauna is dominated by cheirurids and pterygometopids, including such genera as *Ceraurinella*, *Ceraurus*, *Ceraurinus*, *Tricopelta*, *Sceptaspis*, *Isotelus*, *Bumastoides*, *Acanthoparypha*, *Hemiarges*, *Holia*, and *Decoroproetus*. Above this horizon, distinctly different taxa appear, with a complete shift in the families present (Fig. 3.13, 3.14, 3.15). Genera that are abundant above the event horizon include *Cryptolithus*, *Anataphrus*, *Robergiella*, and *Ampyxina*. Biofacies analysis recognizes two distinct biofacies, the *Tricopelta-Ceraurinella* Biofacies below 75.25 m, and the *Anataphrus-Cryptolithus* Biofacies above 75.25 m.

Diversity Changes

A dramatic change in diversity occurs across the extinction event and correlates with the faunal composition shift at 75.25 m. At 75.25 m, there is a decrease in diversity at AV4B. At the AV1 section, this diversity shift is less obvious due to the sampling gap bracketing the appropriate interval. This diversity change represents a faunal shift from the higher diversity assemblage of the *Tricopelta-Ceraurinella* Biofacies to the low diversity assemblage of the *Anataphrus-Cryptolithus* Biofacies.

Sedimentological Evidence

Sedimentology changes across the extinction horizon at AV4B. Below 75.25 m, the dominant lithology consists of dark micritic limestones. Above 75.25 m, the dominant lithology is interbedded shales and argillaceous limestones. The contact between the two lithologies is sharp. The two beds appear conformable.

Two principle hypotheses have been proposed to account for the Rawtheyan extinction. The first hypothesis focuses on exposure of continental shelves following a glacio-eustatic fall in sea level and subsequent habitat reduction. The second hypothesis deals with a lowering of oceanic temperature during the onset of the Gondwana glaciation (Sheehan, 1973; Brenchley, 1984; Brenchley and Newall, 1984). The first signs of falling sea level are recorded at the base of the Hirnantian where shallower water facies are recognizable in many sections, but not until mid-Hirnantian times is there a general development of shallow water sediments and exposure of many areas (Brenchley, 1984). Brenchley and Newall (1984) stated that the fall in sea level at the Rawtheyan-Hirnantian boundary is evidenced by the change from trilobite-dominated faunas in the Rawtheyan to brachiopod-dominated faunas of the Hirnantian.

The first wave of extinction commenced when the sea level started to fall but preceeded the main drop in sea level. Brenchley and Newall (1984) consider the initial sea level drop was insufficient to reduce the area of the continental shelves significantly and cause an extinction. There is no evidence of a significant regression at AV4B. Although a moderate eustatic drop in sea level would not result in a break in the stratigraphic record (Lenz, 1976), sedimentological evidence suggests that a transition occurred at AV4B. The transition from micritic limestones to calcareous shales occurs at 75.25 m within the section, and indicates the occurrence of a transgression, rather than the expected regression thought to occur during the start of the Hirnantian. These shales may reflect local sea level changes resulting from regional tectonism or subsidence. They may also provide evidence for the second hypothesis concerning the Rawtheyan extinction event, the decrease in oceanic temperatures related to the onset of the Gondwana glaciation.

The second hypothesis centers around global cooling as the trigger for the first wave of extinction. There likely was a reduction in ocean temperatures resulting from a deteriorating climatic regime, correlated with a fall in sea level and glaciation (Brenchley, 1984). The spread of cool water may account for the widespread decrease in diversity in Hirnantian times, reflected by the widespread occurrence of the Hirnantian faunas on continental shelves. Brenchley and Newall (1984) noted that the cause of the first wave of extinction remains unclear since substantial temperature changes during the Pleistocene

glaciation did not produce drastic changes to invertebrate faunas of the shelf. They cited the work of Berger and Berger (1981) and Ford (1982) who suggested that invertebrate populations moved with shifting climatic belts and may have acclimated to cooler temperatures. Branchley and Newall (1984) stated that the causal factor may not have been temperature, but a cooling of surface waters spreading outwards from the polar regions and contraction of planktonic belts such that habitable area was severely reduced and extinction resulted.

Sedimentological and paleontological evidence at AV4B and AV1 suggests that decreasing temperatures may have played a significant role in the Rawtheyan extinction event. Faunal turnover at 75.25 m at AV4B and 10 m at AV1 and the development of a cold water assemblage, the *Anataphrus-Cryptolithus* fauna, suggests that oceanic temperatures decreased at the Rawtheyan-Hirnantian boundary allowing migration of a cold water fauna into the region and establishment of a new community prior to the latest-Ordovician extinction event.

The presence of shales at the same interval as the faunal shift also may point to decreased ocean temperatures as a major factor in the Rawtheyan extinction event. Lowering of oceanic temperatures may have altered the position of the calcite compensation depth (CCD), the depth where the rate of calcite supply is balanced by the rate of calcite dissolution (Tucker and Wright, 1990). Dissolution correlates with decreased temperature, increased pressure and increased carbon dioxide concentration associated with deeper water. A decrease in oceanic temperatures may have caused the CCD level to rise, allowing deposition of shales in shallower water. The shales at AV4B may not reflect a change in sea level but rather a change in the position of the CCD in response to decreased water temperatures, and resultant deposition of shales in shallower water. In addition, the decreasing oceanic temperatures may have been responsible for switching off the carbonate factory, due to the greater rate of dissolution of carbonate at lower temperatures.

No single factor can be considered to have caused the Rawtheyan extinction event. Extinctions are caused by a complex combination of circumstances of environmental and ecological changes that are interlinked and inseparable. The hypothesis that the Rawtheyan mass extinction event was triggered by rapid onset of glaciation at the beginning of the Hirnantian, a decrease of marine temperatures and contraction of climatic belts is relatively simple and seems to correlate with available data. Evaluation of the extinction hypotheses and relation to events preserved in the Avalanche Lake sections is beyond the scope of this thesis.

Conclusions

The biofacies at Avalanche Lake 4B and Avalanche Lake 1 occur as well-defined, discrete communities. These biofacies are considered to represent a shelf profile. The *Bathyurus* Biofacies occurs within light grey micritic limestones and is dominated by *Bathyurus teresoma* and represents a nearshore environment. The *Tricopelta-Ceraurinella* Biofacies occurs within micritic limestones and is dominated by *Tricopelta mackenziensis* and *Ceraurinella brevispina*. This biofacies is considered equivalent to the illaenid-cheirurid biofacies of the Middle Ordovician and represents a shelf platform environment. The *Anataphrus-Cryptolithus* Biofacies occurs within interbedded argillaceous limestones and calcareous shales. This trilobite fauna is dominated by *Anataphrus elevatus* and *Cryptolithus tessellatus*, and represents a slope or cooler water environment.

Comparison of Middle Ordovician biofacies of the Mackenzie Mountains shows the stability of nearshore biofacies and slope biofacies through time. The shelf platform biofacies of the Middle Ordovician appear to undergo an amalgamation in the Upper Ordovician, changing from three distinct communities of the Middle Ordovician to one shelf community of the Upper Ordovician. The reason for this merger is unclear but may be related to environmental stresses resulting from global cooling associated with the end-Ordovician glaciation.

Several lines of evidence are used to establish the existence of the Rawtheyan extinction event at AV4B and AV1. Faunal composition and biofacies analysis, diversity changes, and sedimentology has placed the Rawtheyan extinction event at 75.25 m above datum at AV4B and approximately 10 m above datum at AV1. Two principle hypotheses have been proposed to account for the Rawtheyan extinction. The first is exposure of continental shelves during a regression and subsequent habitat reduction. The second is lowering of oceanic temperature related to the onset of the Gondwana glaciation. The Rawtheyan extinction commenced when the first signs of a drop in sea level at the Rawtheyan-Hirnantian boundary, but preceeded the main drop in sea level in the mid-Hirnantian (Brenchley, 1984). Brenchley and Newall (1984) consider the regression an unlikely candidate for the cause of the Rawtheyan extinction event because the fall at the beginning of the Hirnantian was not significant enough to reduce the area of the continental shelves causing an extinction. Contemporaneous with a fall in sea level there was probably a general reduction in oceanic temperatures resulting from a deteriorating climatic regime (Brenchley, 1984). The spread of cool water is supported by the decrease in diversity in Hirnantian times, the widespread occurrence of the Hirnantian fauna, and the introduction of the cold water *Anataphrus-Cryptolithus* fauna at this time in the Avalanche Lake sections. The presence of shales at the same interval as the faunal shift may indicate a shift

in the position of the CCD due to decreased temperatures resulting in deposition of deeper water sediments at a shallower depth.

Literature Cited:

- Berger, E.V., and Berger, W.H. 1981. Planktonic foraminifera and their use in palaeoceanography. In, C. Emiliani (ed.), *The Oceanic Lithosphere, the Sea*, v. 7: 1025-1119. John Wiley, New York.
- Brenchley, P.J. 1984. Late Ordovician extinctions and their relationship to the Gondwana glaciation. In, P.J. Brenchley (ed.), *Fossils and Climate*, p. 291-315. John Wiley and Sons, Ltd.
- Brenchley, P.J., and Newall, G. 1984. Late Ordovician environmental changes and their effect on faunas. In, D.L. Bruton (ed.), *Aspects of the Ordovician System. Palaeontological Contributions from the University of Oslo*, 295: 65-79.
- Brenchley, P.J. 1990. Biofacies. In D.E. Briggs and P.R. Crowther (eds.), *Palaeobiology: a Synthesis*. Blackwell Scientific Publications, Oxford, Boston, pgs. 395-400.
- Bretsky, P.W. 1969. Central Appalachian Late Ordovician communities. *Geological Society of America Bulletin*, 80: 193-212.
- Chatterton, B.D.E. and Ludvigsen, R. 1976. Silicified Middle Ordovician trilobites from the South Nahanni River area, District of Mackenzie, Canada. *Palaeontographica Abt. A*: 154: 1-106.
- Copeland, M.J. 1989. Silicified Upper Ordovician-Lower Silurian ostracodes from the Avalanche Lake area, southwestern District of Mackenzie. *Geological Survey of Canada, Bulletin* 341: 1-100.
- Ford, M.J. 1982. *The Changing Climate*, 190 p. George Allen & Unwin, London.
- Fortey, R.A. 1975. Early Ordovician trilobite communities. *Fossils and Strata* 4: 339-360.
- Fortey, R.A., and Barnes, C.R. 1977. Early Ordovician conodont and trilobite communities of Spitsbergen: influence on biogeography. *Alcheringa*, 1: 297-309.
- Fortey, R.A., and Droser, M.L. 1996. Trilobites at the base of the Middle Ordovician, western United States. *Journal of Paleontology*, 70(1): 73-99.
- Hayes, B.J.R. 1980. A cluster analysis interpretation of Middle Ordovician biofacies, southern Mackenzie Mountains. *Canadian Journal of Earth Sciences*, 17: 1377-1388.
- Hazel, J.E. 1970. Binary coefficients and clustering in biostratigraphy. *Geological Society of America Bulletin*, 81: 3237-3252.
- Jin, J. and Chatterton, B.D.E. 1997. Latest Ordovician-Silurian articulate brachiopods and biostratigraphy of the Avalanche Lake area, southwestern District of Mackenzie, Canada. *Palaeontographica Canadiana*, 13: 1-167.
- Jones, B. 1987. Biostatistics in Paleontology. *Geoscience Canada*, 15(1): 3-22.
- Lenz, A.C. 1976. Late Ordovician - Early Silurian glaciation and the Ordovician-Silurian boundary in the northern Canadian Cordillera. *Geology*, 4: 313-317.

- Ludvigsen, R. 1975. Ordovician formations and faunas, Southern Mackenzie Mountains. *Canadian Journal of Earth Sciences*, 12:663-697.
- Ludvigsen, R. 1978. Middle Ordovician trilobite biofacies, Southern Mackenzie Mountains. In C.R. Stelck and B.D.E. Chatterton (Eds.), *Western and Arctic Canadian Biostratigraphy*. Geological Association of Canada Special Paper 18: 1-37.
- Ludvigsen, R. 1978a. The trilobites *Bathyurus* and *Eomonorachus* from the Middle Ordovician of Oklahoma and their biofacies significance. *Life Sciences Contributions*, Royal Ontario Museum, 114: 1-18.
- Owen, A.W., Harper, D.A.T., and Rong, J. 1991. Hirnatian trilobites and brachiopods in space and time. In, C.R. Barnes and S.H. Williams (eds.), *Ordovician Geology*. Geological Survey of Canada, Paper 90-9: 179-190.
- Pickerill, R.K., and Brenchley, P.J. 1991. Benthic macrofossils as paleoenvironmental indicators in marine siliclastic facies. *Geoscience Canada*, 18(3): 119-138.
- Podani, J. 1993. SYN-TAX-pc Computer Programs for Multivariate Data Analysis, version 5.0. Scientia Publishing, Budapest.
- Price, D. 1980. The Ordovician trilobite fauna of the Sholeshook Limestone Formation, South Wales. *Palaeontology*, 23(4): 839-887.
- Sanders, H.L. 1968. Marine benthic diversity - a comparative study. *American Naturalist*, 106: 414-418.
- Shaw, F.C., and Fortey, R.A. 1977. Middle Ordovician facies and trilobite faunas in N. America. *Geological Magazine*, 114(6): 409-443.
- Sheehan, P.M. 1973. The relation of Late Ordovician glaciation to the Ordovician-Silurian changeover in North American brachiopod faunas. *Lethaia*, 6: 147-154.
- Tucker, M.E., and Wright, V.P. 1990. *Carbonate Sedimentology*. Blackwell Science, Oxford, 482 p.
- Wang, K., Chatterton, B.D.E., Attrep, M., and Orth, C.J. 1993. Late Ordovician mass extinction in the Selwyn Basin, northwestern Canada: geochemical, sedimentological, and paleontological evidence. *Canadian Journal of Earth Sciences*, 30: 1870-1880.
- Whittington, H.B. 1963. Middle Ordovician trilobites from Lower Head, western Newfoundland. *Bulletin of the Museum of Comparative Zoology, Harvard*, 129(1): 1-118.
- Whittington, H.B. 1965. Trilobites of the Ordovician Table Head Formation, western Newfoundland. *Bulletin of the Museum of Comparative Zoology, Harvard*, 132(4): 275-442.

Chapter 4: Conclusions

Collections from exposed sections near Avalanche Lake, N.W.T. provide well preserved Ordovician trilobite assemblages. Collections from Avalanche Lake 4B and Avalanche Lake 1 demonstrate faunal changes through the Upper Ordovician, extending into the Silurian. This is an interval of interest to historical geologists since it includes a major episode of global glaciation, and at least two distinct episodes of mass extinction.

The objectives of this study are to collect and prepare fossils from a sequence of previously unstudied Late Ordovician trilobite assemblages in the lower Whittaker Formation, Mackenzie Mountains. The effects of the end-Ordovician glaciation, including rapid changes in sea level and temperature, on faunal composition, changes in abundances, and diversity will be explored. The finely resolved stratigraphic and faunal data from the Avalanche Lake sections will provide information on the Rawtheyan extinction event.

The age of the trilobites from the upper portion of the sections is determined to be Late Ashgillian in age based upon previous work using brachiopod, ostracod, conodont, and graptolite correlations, as well as trilobite species correlations. The age of material lower within the section could not be determined precisely based upon the trilobites present, but the presence of several species described by Ludvigsen (1979) from the Blackriveran of the Mackenzie Mountains suggests a similar, or slightly younger age assignment for the strata.

The distinctive cosmopolitan cold water Hirnantian fauna is absent at AV4B and AV1. Reconstruction of the continental configuration and Hirnantian faunal distributions for the Late Ashgill indicate a strong relationship between the locations of known Hirnantian faunas and the position of the Gondwana ice sheets. The position of North America during the Late Ordovician places the Avalanche Lake region in an equatorial climatic belt. The low latitudinal position may provide a climate temperature barrier to dispersal of the Hirnantian fauna into the region. In addition, the Selwyn Basin may have been cut off from open ocean circulation during the Late Ordovician and Early Silurian. This restriction may have prevented the Hirnantian fauna from migrating into the region.

A series of sea level changes occurred during the Late Ordovician that coincided with a well established Gondwana glaciation in the Southern Hemisphere, and is believed to have caused the Late Ordovician extinction. This extinction occurred in two main phases. The first phase occurred across the Rawtheyan-Hirnantian boundary and is indicated by a dramatic decrease in animal diversity, and a lithofacies change from marine clastic shelves to shallow marine lithofacies. This change coincided with the start of a substantial glacio-eustatic sea level drop. The second phase of extinction, occurring near the Ordovician-

Silurian boundary, correlated with the melting of the ice cap and a resultant global transgression, indicated by a change from shallow to deep water lithofacies.

Systematics

33 species, representing 15 families, were identified at the Avalanche Lake sections. Thirteen new species were identified, classified and described. *Bumastoides solangeae* n. sp. and *Bathyrurus teresoma* n. sp. are the stratigraphically youngest representatives of their genera in North America. *Decoroproetus hankei* n. sp. is the first Upper Ordovician proetid described from the Mackenzie Mountains.

The addition of two new species of *Acanthoparypha* from the Upper Ordovician of Avalanche Lake 4B to the cladistic analysis of Adrain (1998) will help to clarify relationships within the genus. Parsimony analysis was performed using PAUP version 3.1.1 (Swofford, 1993). An exhaustive search yielded two equally parsimonious trees, each with a branch length of 38, and a consistency index of 0.711. Adrain (1998) presented the relationships between the species as a polytomy and provided no support for the existence of the genus. The addition of 8 new characters and two new taxa to the analysis has helped resolve relationships within *Acanthoparypha*.

Biofacies Analysis

The distribution of organisms in extant and fossil communities depends on a number of environmental parameters, including bathymetry, temperature, salinity, substrate, oxygen supply and nutrient availability. Study of the fossil biota from ancient sediments allows inferences to be made regarding the distribution of fossil communities and the environmental parameters responsible for their distributions. Distinct faunal associations within sediments are studied using biofacies analysis and allow inferences to be made regarding ecological variations that may have caused the observed patterns. The question always remains as to whether the fossil assemblage adequately represents the original population. Large collections are preferable for study rather than making interpretations from small sample sizes. The large collection at the Avalanche Lake sections provides a sufficient number of individuals for biofacies analysis and strengthens interpretations of the data.

The trilobite fauna at AV4B and AV1 is consistently distributed in discrete associations throughout the section. Biofacies analysis using Q-mode (sample to sample) and R-mode (taxon to taxon) was conducted using the Jaccard Coefficient and UPGMA clustering to analyze binary data of 33 taxa of Upper Ordovician trilobites from the

collections of AV4B and AV1. Intersections of Q and R-mode clusters defined three biofacies.

The first biofacies, the *Bathyurus* Biofacies, is defined by the dominant species, *Bathyurus teresoma*. The presence of interference ripples at AV4B and syneresis cracks and mudcracks at AV1 indicate shallow water deposition and periodic subaerial exposure. This biofacies was interpreted to be a nearshore, shallow, warm water environment. The second biofacies, the *Tricopelta-Ceraurinella* Biofacies, is defined by the dominance of *Tricopelta mackenziensis* and *Ceraurinella brevispina* in the fauna. Other abundant taxa include *Bumastoides solangeae* and *Isotelus dorycephalus*. The lithology of this biofacies is dominated by micritic limestones including mudstones and wackestones. The environment of this biofacies is interpreted as a deeper water shelf. The third biofacies, the *Anataphrus-Cryptolithus* Biofacies, is dominated by the trilobite species *Anataphrus elevatus* and *Cryptolithus tessellatus*. This biofacies occurs with interbedded calcareous shales and argillaceous limestones and represents a slope environment.

The *Bathyurus* Biofacies shows low diversity relative to the two other biofacies. This low diversity is thought to be caused by the stressed conditions of a nearshore environment. Stratigraphically above this biofacies, there is a dramatic increase in the diversity in the shift to the *Tricopelta-Ceraurinella* Biofacies. The significant diversity increase from the *Bathyurus* Biofacies to the *Tricopelta-Ceraurinella* Biofacies may suggest a parallel increase in environmental stability. At the same interval as the sharp lithofacies change from micritic limestones to calcareous shales, a drop in diversity occurs. This interval represents the faunal change from the higher diversity assemblage of the *Tricopelta-Ceraurinella* Biofacies to the lower diversity assemblage of the *Anataphrus-Cryptolithus* Biofacies. The initial low diversity reflects absence of trilobite species in the region after rapid environmental change. A subsequent increase and stabilization of diversity prior to the latest-Ordovician extinction boundary reflects migration of new species into the region and establishment of a new community.

Lower Ordovician biofacies from northern Spitsbergen (Fortey, 1975; Fortey and Barnes, 1977) show stability of shallow water illaenid-cheirurid biofacies through the Ordovician and the persistence of the specialized community of the shelf-edge/slope environments. Comparison of Upper Ordovician biofacies with Middle Ordovician biofacies (Chatterton and Ludvigsen, 1976; Ludvigsen, 1978; Hayes, 1980) shows the stability in generic composition of the *Bathyurus* Biofacies and the *Anataphrus-Cryptolithus* Biofacies of the Avalanche Lake sections through time. Apparent changes in biofacies structure in the Ordovician of the Mackenzie Mountains occur within the shelf environment, with more biofacies during the Middle Ordovician relative to the Upper

Ordovician. As time progressed, shelf biofacies lost their distinctiveness and merged into one biofacies containing representatives from several biofacies of the Middle Ordovician. Why this amalgamation occurred is uncertain. Stable environments may allow for diversification of community structure and establishment of many niches, resulting in the development of shelf biofacies into several discrete communities. Environmental change and instability would favor generalist species that would be able to exploit fluctuating environments, resulting in fewer recognizable distinct communities. Environmental instability is considered to have been a possible cause for the Upper Ordovician amalgamation, as cooling and eventual glaciation is known to occur at this time.

The Rawtheyan Extinction Event at AV4B and AV1

Several lines of evidence are used to establish the existence of the Rawtheyan extinction event at AV4B and AV1, placing the Rawtheyan extinction event at 75.25 m above datum at AV4B and 10 m above datum at AV1. The trilobite fauna below 75.25 m at AV4B and 10 m at AV1 is dominated by cheirurids and pterygometopids and defines the *Tricopelta-Ceraurinella* Biofacies. Above this horizon, the fauna is dominated by *Anataphrus* and *Cryptolithus* species. The *Anataphrus-Cryptolithus* Biofacies exists in compliment with the faunal shift at 75.25 m. A drop in diversity occurs in parallel to the faunal shift at 75.25 m, representing the faunal shift from the higher diversity *Tricopelta-Ceraurinella* Biofacies to the lower diversity assemblage of the *Anataphrus-Cryptolithus* Biofacies. Lithofacies across this interval change from a dominant lithology of micritic limestones below 75.25 m, to interbedded calcareous shales and argillaceous limestones.

Two principal hypotheses have been proposed to account for the Rawtheyan extinction. The first is exposure of continental shelves during a regression and subsequent habitat reduction. The second is lowering of oceanic temperature related to the onset of the Gondwana glaciation. The Rawtheyan extinction commenced when the sea level began to drop at the Rawtheyan-Hirnantian boundary, but preceded the main drop in sea level in the mid-Hirnantian (Brenchley, 1984). Brenchley and Newall (1984) consider regression an unlikely cause of the Rawtheyan extinction event since the sea level fall at the beginning of the Hirnantian was not sufficient to reduce the habitable area of the continental shelves. There was a reduction in ocean temperatures contemporaneous with a fall in sea level resulting from a deteriorating climate (Brenchley, 1984). The spread of cool water is suggested by the widespread occurrence of the Hirnantian fauna, and the introduction of the cold water *Anataphrus-Cryptolithus* fauna at the Avalanche Lake sections. The presence of shales at the same interval as the faunal shift may indicate a shift in the position of the CCD, or closing down of the carbonate factory due to decreased temperatures resulting in

deposition of deeper water sediments at a shallow depth. It is difficult to establish a single factor for the cause of the Rawtheyan extinction event. Extinctions are caused by a complex combination of circumstances, both ecological and environmental. The hypothesis that the Rawtheyan extinction was triggered by global cooling and reduction in oceanic temperatures is only one factor that may have caused patterns observed in the Avalanche Lake sections.

Future Work

In addition to sedimentological and paleontological studies, Wang et al. (1993) presented a detailed study of the trace element and stable isotope geochemistry of AV4B and AV1 for the latest-Ordovician extinction event. This work considers sedimentological and paleontological evidence for the existence of the Rawtheyan mass extinction event at AV4B and AV1. Additional work concentrating on geochemical changes within this interval may support the sedimentological and paleontological evidence of a mass extinction and faunal turnover at the Rawtheyan-Hirnantian boundary within the Avalanche Lake sections. Geochemical analysis and thin sectioning of strata within the interval bracketing the Rawtheyan extinction event may provide evidence of isotope changes in response to cooling surface water temperatures and ice cap growth at this time.

Literature Cited

- Adrain, J.M. 1998. Systematics of the Acanthoparyphina (Trilobita), with species from the Silurian of Arctic Canada. *Journal of Paleontology*, 72(4): 698-718.
- Brenchley, P.J. 1984. Late Ordovician extinctions and their relationship to the Gondwana glaciation. In, P.J. Brenchley (ed.), *Fossils and Climate*, p. 291-315. John Wiley and Sons, Ltd.
- Brenchley, P.J., and Newall, G. 1984. Late Ordovician environmental changes and their effect on faunas. In, D.L. Bruton (ed.), *Aspects of the Ordovician System*. Palaeontological Contributions from the University of Oslo, 295: 65-79.
- Chatterton, B.D.E. and Ludvigsen, R. 1976. Silicified Middle Ordovician trilobites from the South Nahanni River area, District of Mackenzie, Canada. *Palaeontographica Abt. A*: 154: 1-106.
- Fortey, R.A. 1975. Early Ordovician trilobite communities. *Fossils and Strata* 4: 339-360.
- Fortey, R.A., and Barnes, C.R. 1977. Early Ordovician conodont and trilobite communities of Spitsbergen: influence on biogeography. *Alcheringa*, 1: 297-309.
- Hayes, B.J.R. 1980. A cluster analysis interpretation of Middle Ordovician biofacies, southern Mackenzie Mountains. *Canadian Journal of Earth Sciences*, 17: 1377-1388.
- Ludvigsen, R. 1978. Middle Ordovician trilobite biofacies, Southern Mackenzie Mountains. In C.R. Stelck and B.D.E. Chatterton (Eds.), *Western and Arctic Canadian Biostratigraphy*. Geological Association of Canada Special Paper 18: 1-37.
- Ludvigsen, R. 1979. A trilobite zonation of Middle Ordovician rocks, southwestern District of Mackenzie. *Geological Survey of Canada, Bulletin* 312: 1-99.
- Swofford, D.L. 1993. PAUP: Phylogenetic Analysis Using Parsimony, Version 3.3.1. Program distributed by the Illinois Natural History Survey, Champaign, Illinois.
- Wang, K, Chatterton, B.D.E., Attrep, M., and Orth, C.J. 1993. Late Ordovician mass extinction in the Selwyn Basin, northwestern Canada: geochemical, sedimentological, and paleontological evidence. *Canadian Journal of Earth Sciences*, 30: 1870-1880.

APPENDIX I: 1998 geological description of Avalanche Lake 4B.

0m - 2.75m

- dark gray micritic limestone
- massive, 85 cm thick bed, changes to 5cm - 15 cm bed thicknesses (medium bedded)
- interference ripples present (seen on talus)
- first massive unit - no observed fossils
- fine-grained mudstones
- top of unit contains *Bathyurus* cranidium
- sample collected at 2.75m

2.75m - 3.75m

- possible base of previous description
- massive with 50 cm beds interbedded with 10 cm beds
- weathers buff color
- no structures or allochems visible
- fine-grained mudstones

3.75m - 21.25m

- 1 gastropod and 1 solitary rugose coral on bedding surface
- rare trilobite fragments
- 5cm - 20cm bed thicknesses
- medium gray micritic limestone
- fine-grained mudstone
- disarticulated cystoid visible
- trace fossils present

21.25m - 21.95m

- medium gray limestone
- weathers in large blocks
- coarse-grained, sparry calcite
- beds both thin and thick
- weathers buff color
- crinoid ossicles visible, not much else visible

21.95m - 22.95m

- dark gray limestone
- beds thin, approximately 5cm - 10cm
- coarse grained, sparry calcite
- similar to previous unit, just thinner beds

22.95m - 25.95m

- medium gray limestone
- weathers buff to orange
- sparry calcite, coarsely crystalline
- massive

- mudstone lumps and flakes within and sparry calcite between

25.95m - 29.45m

- medium gray micritic limestone
- fine-grained mudstones
- mud lumps present, between micrite getting sparry calcite filling spaces
- burrows present

29.45m - 31.65m

- light gray limestone with buff-colored bands
- weathers in massive blocks
- shelly fragments visible
- wackestone

31.65m - 35.65m

- dark grayish-brown limestone
- thinly bedded, approximately 5cm - 10cm
- talus shows good shelly fragments, crinoid ossicles present
- fine to medium grained mudstones with interbedded wackestones approx. 1m thick
- wackestones massive, dark gray, weather out in buff color
- wackestones coarse-grained with sparry calcite

35.65m - 44.65m

- predominately wackestones with interbedded mudstone beds at the bottom of the unit
- top of unit all wackestones
- wackestones and mudstones same as previous unit
- wackestones massive at base of unit, near top wackestone beds become thinner
- thinner beds appear more fine-grained, thicker beds more coarse-grained
- trace fossils/burrows present in fine-grained mudstones

44.65m - 46.15m

- covered interval

46.15m - 48.55m

- equivalent to 43m interval in other description
- evidence of good silicified material
- dark gray limestone, laminated
- interbedded with one bed of buff/light brown laminated limestone
- laminations 1mm thick, dark gray in color
- sample collected at this horizon

48.55m - 50.25m

- light to dark gray limestone
- wavy laminations of dark gray, fine-grained material (micritic)
- good evidence of silicified material
- lenses of coarse material with silicified material in between fine-grained limestone

50.25m - 55.25m

- 50.4m shows brachiopods
- light to dark gray, mottled limestone
- fine laminations throughout, less than 1mm thick
- laminations planar to wavy
- weathers buff to tan
- beds massive, weathers in large blocks
- fine-grained mudstone (micritic)
- no allochems visible

55.25m - 56.75m

- covered interval

56.75m - 64.75m

- dark gray limestone
- wackestone/mudstone
- crinoid ossicles, rare solitary rugose corals, few brachiopods
- massive with irregular fractures
- fine-grained micritic

64.75m - 75.25m

- massive with irregular fractures
- mottled light to medium gray in color
- micritic, fine-grained
- sample taken at 74.5m

75.25m - 79m

- 76.25m sample collected
- *Cryptolithus* present
- light gray limestone interbedded with calcareous shales
- shale bed thicknesses 2-3cm each
- limestone beds 15-20cm thick
- sample taken at 76.75m

79m - 85m

- medium gray limestone with thin beds of calcareous shale at base of unit
- limestone fine-grained, micritic
- interbedded with shales throughout but smaller beds
- trilobites visible on bedding surfaces
- chert nodules present in limestone

85m - 88m

- sample taken at 85.6m
- complete *Anataphrus* at 88.4m
- fine-grained, micritic limestone
- medium to dark gray in color
- beds thin, 10 cm thick

- *Cryptolithus* fragments also present
- chert nodules also present throughout limestone

88m - 105.5m

- sample taken at 88.2m
- contain *Cryptolithus* and *Anataphrus*
- dark gray limestone
- chert nodules approximately 10%
- 20% chert in some beds
- fine-grained, micritic
- thinly bedded
- graptolites present above 101.5m

105.5m - 107m

- dark gray micritic limestone
- wavy bedding present
- beds thicker, approximately 15-20 cm thick
- weathers out in blocks
- *Anataphrus* present
- sample taken at 105.5m

107m - 110.3m

- unit quite shaly, but covered predominately with talus
- shales thinly bedded, dark gray, weathers brown
- 110.6m is the extinction event
- Ordovician/Silurian boundary approximately 1m above this at 111.6 m.

APPENDIX II: List of trilobite taxa present within the horizons of the 1978 collection from the Avalanche Lake 4B section.

- TALUS 0 - *Anataphrus elevatus* n. sp. - 4 cranidia, 4 hypostomes, 6 pygidia, 15 librigenae
Cryptolithus tessellatus - 3 meraspid cranidia, 3 pygidia, 3 articulated thoracic segments
Robergia sp. - 1 cranidium, 1 thoracic segment
- TALUS 1 - *Bathyrurus teresoma* n. sp. - 3 fragmentary cranidia, 7 thoracic segments
- TALUS 2 - *Bathyrurus teresoma* n. sp. - 3 hypostomes, 3 fragmentary cranidia, 8 librigenae
Cryptolithus tessellatus - 2 cranidia, 1 pygidia, 1 thoracic segment
- AV4B 90.75 - *Cryptolithus tessellatus* - 13 partial cranidia, 116 meraspid cranidia, 31 pygidia, 34 meraspid pygidia, 10 thoracic segments, 1 articulated thoracic segments with pygidium
Anataphrus elevatus n. sp. - 35 cranidia, 34 pygidia, 31 hypostomes, 59 librigenae, 51 thoracic segments
Harpidella kurrii - 14 cranidia, 3 pygidia, 1 librigenae
Ampyxina pilatus n. sp. - 4 cranidia, 1 pygidium
Robergia sp. - 3 cranidia, 1 librigenae, 2 thoracic segment tips
Cybeloides sp. - 3 librigenae, 1 hypostome
- AV4B 90 - *Anataphrus elevatus* n. sp. - 18 cranidia, 16 pygidia, 11 hypostomes, 19 librigenae, 7 thoracic segments
Cryptolithus tessellatus - 1 large cranidium, 213 meraspid cranidia, 85 pygidia, 14 thoracic segments
Harpidella kurrii - 3 fragmentary cranidia, 1 complete cranidium, 3 librigenae, 1 pygidium
Cybeloides sp. - 4 hypostomes
Robergia sp. - 1 cranidium
- AV4B 87 - *Harpidella kurrii* - 2 librigenae, 1 pygidium, 8 cranidia
Cybeloides sp. - 5 cranidia, 2 pygidia, 4 librigenae
Anataphrus elevatus n. sp. - 48 cranidia, 37 pygidia, 34 hypostomes, 32 librigenae, 1 pygidium + thorax, 6 thoracic segments
Robergia sp. - 1 cranidium, 1 librigena, 1 partial pygidium
Cryptolithus tessellatus - 19 cranidia, 24 pygidia, 1 thoracic segment
- AV4B 80.5 - *Robergia* sp. - 3 cranidia, 4 librigenae, 1 pygidium, 5 thoracic segments
Cryptolithus tessellatus - 2 cranidia, 4 thoracic segments + pygidia, 73 meraspid cranidia, 16 pygidia, 37 meraspid pygidia, 74 thoracic segments, 54 fragmented cranidia
Ampyxina pilatus n. sp. - 1 whole holaspid
Anataphrus elevatus n. sp. - 49 cranidia, 34 pygidia, 28 hypostomes, 63 librigenae
- AV4B 80 - *Cryptolithus tessellatus* - 23 cranidia, 1 complete holaspid, 53 meraspid cranidia, 41 pygidia, 18 meraspid pygidia, 65 thoracic segments
Anataphrus elevatus n. sp. - 57 cranidia, 49 pygidia, 20 hypostomes, 63 librigenae

- Robergia* sp. - 8 cranidia, 1 partial cranidium, 1 pygidium, 2 librigenae, 3 thoracic segment tips
Ampyxina pilatus n. sp. - 1 cranidium, 1 pygidium
Harpidella kurrii - 2 librigenae
- AV4B 73 - *Ceraurinella brevispina* - 4 cranidia, 11 pygidia, 41 librigenae, 11 hypostomes, 55 thoracic segments
Ceraurinus serratus - 8 thoracic segments, 2 pygidia
Isotelus dorycephalus n. sp. - 3 cranidia, 2 pygidia, 2 hypostomes, 5 librigenae, 8 thoracic segments
Calyptaulax n. sp. A - 6 cranidia
Hemiarges n. sp. A - 1 hypostome, 1 librigenae
Tricopelta mackenziensis - 1 cranidium, 8 pygidia, 3 librigenae, 10 thoracic segments
Cryptolithus tessellatus - 1 cranidium
- AV4B 54 - *Ceraurinella brevispina* - 1 hypostome
- AV4B 49.5 - *Ceraurinella brevispina* - 1 pygidium, 1 hypostome
Isotelus dorycephalus n. sp. A - 1 cranidium, 1 pygidium
Calymenid - hypostome
- AV4B 47.75- *Isotelus dorycephalus* n. sp. - 2 cranidia, 1 hypostome, 1 pygidium
Bumastoides solangeae n. sp. - 1 incomplete cranidium, 1 thoracic segment
- AV4B 44.8 - *Ceraurinella brevispina* - 1 hypostome, 1 librigena, 17 thoracic segments
Isotelus dorycephalus n. sp. - 1 hypostome
Bumastoides solangeae n. sp. - 1 incomplete cranidium
Dimeropyge sp. - 1 pygidium
- AV4B 44 - *Ceraurinella brevispina* - 1 cranidium, 3 hypostomes, 2 librigenae, 1 incomplete pygidium, 149 thoracic segments
- AV4B 43 - *Ceraurinella lamiapyga* n. sp. - 16 pygidia, 21 librigenae
Ceraurinella brevispina - 8 cranidia, 6 pygidia, 15 librigenae, 20 hypostomes, 23 fragmented hypostomes, 25 thoracic segments
Ceraurinus serratus - 1 pygidium, 7 thoracic segments, 3 cranidia
Tricopelta mackenziensis - 1 pygidium
Bumastoides solangeae n.sp. - 1 complete cranidium
Isotelus dorycephalus n. sp. - 4 cranidia, 1 pygidium, 5 librigenae, 5 thoracic segments
Harpidella kurrii - 1 librigenae
Calymenid - 1 rostral plate
- AV4B 31.5 - *Holia* sp. - 1 partial hypostome
- AV4B 18 - *Acanthoparypha latipyga* n.sp. - 30 librigenae, 10 pygidia, 8 hypostomes, 8 thoracic segments, 16 cranidia
Ceraurinella brevispina - 15 cranidia, 26 pygidia, 24 hypostomes, 63 librigenae, 91 thoracic segments
Bumastoides solangeae n.sp. - 32 cranidia, 88 pygidia, 100 librigenae, 37 incomplete thoracic segments
Ceraurinus serratus - 2 pygidia, 3 thoracic segments
Bathyrurus teresoma n. sp. - 1 librigenae, 5 thoracic segments

- Sceptaspis avalanchensis* n. sp. - 14 cranidia, 11 pygidia
- AV4B 17 - *Ceraurinus serratus* - 4 pygidia, 7 thoracic segments
Ceraurinella brevispina - 12 pygidia, 16 cranidia, 23 hypostomes, 17 fragmentary pygidia, 40 librigenae, 54 thoracic segments
Acanthoparypha latipyga n.sp. - 4 cranidia, 4 librigenae, 1 thoracic segment, 2 meraspid pygidia
Bumastoides solangeae n. sp. - 20 cranidia, 17 pygidia, 15 librigenae, 8 thoracic segments
Sceptaspis avalanchensis n. sp. - 3 cranidia, 5 pygidia
Isotelus dorycephalus n. sp. - 1 pygidium, 1 hypostome
- AV4B 16.5 - *Tricopelta mackenziensis* - 148 cranidia, 305 pygidia, 216 hypostomes, 95 partial cranidia, 893 librigenae
Hemiarges n. sp. A - 3 cranidia, 5 partial cranidia, 9 hypostomes, 1 pygidium, 14 librigenae, 19 fragmentary pygidia
Ceraurus mackenziensis - 27 pygidia, 8 hypostomes, 19 cranidia, 15 librigenae
Isotelus dorycephalus n. sp. - 3 cranidia, 2 pygidia, 18 hypostomes, 8 librigenae
Acanthoparypha latipyga n. sp. - 1 pygidium
Ceraurinus serratus - 4 thoracic segments, 1 pygidium
Sceptaspis avalanchensis n. sp. - 39 meraspid cranidia
Decoroproetus hankei n. sp. - 3 cranidia
Bumastoides solangeae n.sp. - 1 hypostome
- AV4B 14 - *Ceraurinella brevispina* - 26 pygidia, 17 cranidia, 18 hypostomes, 44 librigenae
Hemiarges n. sp. A - 2 incomplete cranidium, 3 incomplete pygidia, 1 hypostome
Bathyrurus teresoma n.sp. - 1 cranidium, 3 hypostomes, 3 librigenae, 4 thoracic segments
Sceptaspis avalanchensis n. sp. - 7 cranidia, 1 hypostome, 2 pygidia
Ceraurinus serratus - 3 thoracic segments
Isotelus dorycephalus n. sp. - 2 cranidia, 1 pygidium
- AV4B 9 - *Isotelus dorycephalus* n. sp. - 1 cranidium, 2 hypostomes, 4 librigenae, 4 thoracic segments
Sceptaspis avalanchensis n. sp. - 1 cranidium
Ceraurinella brevispina - 47 fragmentary pygidia, 21 incomplete cranidia, 23 hypostomes, 93 librigenae, 317 thoracic segments
Bumastoides solangeae n.sp.- 6 hypostomes
Faillana sp. - 1 incomplete cranidium
- AV4B 7 - *Acanthoparypha palmipyga* n.sp. - 4 pygidia, 1 cranidium
Isotelus dorycephalus n. sp. - 6 cranidia, 2 pygidia, 16 hypostomes, 6 librigenae, 8 thoracic segments
Tricopelta mackenziensis - 24 cranidia, 74 pygidia, 31 hypostomes, 76 librigenae, 46 thoracic segments
Sceptaspis avalanchensis n. sp. - 2 partial cranidia
Ceraurinella brevispina - 3 cranidia, 26 pygidia, 9 hypostomes, 62 librigenae, 53 thoracic segments
Hypodicranotus sp. - 1 partial hypostome

- Bumastoides solangeae* n.sp. - 3 librigenae, 2 cranidia, 1 incomplete hypostome
Ceraurinus serratus - 3 thoracic segments
Hemiarges n. sp. A - 2 incomplete cranidia
- AV4B 6 - *Tricopelta mackenziensis* - 56 cranidia, 46 pygidia, 6 fragmentary pygidia, 34 hypostomes, 105 librigenae, 58 thoracic segments
Sceptaspis avalanchensis n. sp. - 2 partial cranidia, 66 fragmentary pygidia
Ceraurinella brevispina - 38 incomplete cranidia, 41 pygidia, 43 hypostomes, 118 librigenae, 168 thoracic segments, 21 incomplete pygidia
Acanthoparypha palmapyga n. sp. - 2 thoracic segments, 4 cranidia, 2 pygidia, 1 hypostome, 4 librigenae
Holia sp. - 1 meraspid cranidium, 1 incomplete cranidium
Isotelus dorycephalus n. sp. - 6 hypostomes, 2 thoracic segments, 1 pygidium
Decoroproetus hankei n. sp. - 31 incomplete cranidia, 87 librigenae, 3 hypostomes, 6 pygidia
Ceraurinus serratus - 14 thoracic segments
Bumastoides solangeae n. sp. - 8 hypostomes
- AV4B 3.5 - *Anataphrus elevatus* n. sp. - 1 pygidium, 1 librigenae, 1 hypostome, 12 thoracic segments
Cryptolithus tessellatus - 1 complete enrolled holaspid, 2 pygidia, 10 small cranidia, 19 thoracic segments, 5 articulated thoracic segments
Robergiella insolitus n. sp. - 1 cranidium, 12 librigenae, 1 thoracic segment
- AV4B 3 - *Decoroproetus hankei* n. sp. - 7 fragmentary cranidia, 9 fragmentary pygidia, 5 librigenae
Tricopelta mackenziensis - 22 pygidia, 14 hypostomes, 20 librigenae, 29 thoracic segments
Ceraurinus serratus - 44 thoracic segments
Ceraurinella brevispina - 89 pygidia, 15 cranidia, 61 hypostomes, 230 librigenae, 370 thoracic segments, 17 fragmentary hypostomes
Bumastoides solangeae n. sp. - 10 pygidia, 5 cranidia, 21 librigenae, 9 thoracic segments
Borealaspis whittakerensis - 2 incomplete cranidia, 6 meraspid cranidia
Hemiarges n. sp. A - 1 librigenae
- AV4B 20cm- *Cryptolithus tessellatus* - 2 large cranidia, 100 small cranidia, 96 pygidia, 9 thoracic segments
Anataphrus elevatus n. sp.- 9 cranidia, 17 pygidia, 3 hypostomes, 5 librigenae
Robergiella insolitus n. sp.- 9 cranidia, 1 pygidium, 8 librigenae, 1 hypostome
Odontopleurid - 2 partial pygidia, 1 librigenae
- AV4B 7.5cm *Cryptolithus tessellatus* - 1 partial cranidium, 2 thoracic segments
Anataphrus elevatus n. sp. - 1 librigena

APPENDIX III: List of the trilobite taxa present within the horizons of the 1998 collection from the Avalanche Lake 4B section.

- AV4B 110.9 - Proetid - 3 pygidia, 7 librigenae, 2 cranidia, 13 thoracic segments
Curriella clancyi - 5 pygidia, 5 hypostomes, 4 cranidia, 11 librigenae
- AV4B 110.7 - Proetid - 1 hypostome, 27 cranidia, 33 pygidia, 74 librigenae, 5 thoracic segments
- AV4B 110.1 - *Cryptolithus tessellatus* - 71 cranidia, 15 pygidia
Robergiella insolitus n. sp. - 1 pygidia, 2 cranidia, 6 librigenae
Anataphrus elevatus n. sp. - 3 pygidia, 4 cranidia
- AV4B 110.0 - *Cryptolithus tessellatus* - 1 complete, 167 pygidia, 312 cranidia (large), 432 cranidia (small)
Robergiella insolitus n. sp. - 31 librigenae, 1 pygidium, 3 hypostomes, 33 cranidia
Anataphrus elevatus n. sp. - 11 cranidia, 5 librigenae, 1 hypostome, 35 pygidia
- AV4B 107.0 - *Cryptolithus tessellatus* - 14 cranidia, 27 pygidia
Anataphrus elevatus n. sp. - 7 librigenae, 2 hypostomes, 2 cranidia, 11 pygidia
- AV4B 105.5 - *Cryptolithus tessellatus* - 18 cranidia, 2 pygidia
Robergiella insolitus n. sp. - 4 cranidia, 5 librigenae
Anataphrus elevatus n. sp. - 3 cranidia, 6 librigenae, 4 hypostomes, 2 pygidia
- AV4B 88.2 - *Cryptolithus tessellatus* - 3 pygidia, 22 cranidia
Anataphrus elevatus n. sp. - 1 complete, 2 librigenae, 2 cranidia, 5 pygidia
Robergia yukonensis - 1 pygidium
- AV4B 85.6 - *Anataphrus elevatus* n. sp. - 1 articulated thorax, 1 complete, 23 pygidia, 14 librigenae, 16 cranidia, 3 hypostomes, 33 thoracic segments
Cryptolithus tessellatus - 49 cranidia, 18 pygidia
Robergia yukonensis - 2 hypostomes, 3 librigenae, 20 thoracic segments, 17 pygidia, 9 cranidia
Encrinurid - 1 librigenae
Robergiella insolitus n. sp. - 1 cranidium
- AV4B 79 - *Ampyxina pilatus* n.sp. - 2 cranidia, 1 pygidium
Cryptolithus tessellatus - 18 thoracic segments, 15 pygidia, 23 cranidia
Anataphrus elevatus n. sp. - 2 cranidia, 2 hypostomes, 7 pygidia
Robergia yukonensis - 1 cranidia, 1 pygidia
- AV4B 78T - *Anataphrus elevatus* n. sp. - 3 cranidia, 1 thoracic segment, 1 librigenae, 13 pygidia
Cryptolithus tessellatus - 20 thoracic segments, 10 pygidia, 33 cranidia
Robergia yukonensis - 1 thoracic segment
Cybeloides sp. - 1 hypostome

- AV4B 76.75 - *Cryptolithus tessellatus* - 2 thoracic segments
Ampyxina pilatus n.sp. - 1 cranidium
Robergia yukonensis - 1 cranidium
Anataphrus elevatus n. sp. - 2 pygidia, 1 librigenae
- AV4B 76.25 - *Ampyxina pilatus* n. sp. - 1 pygidium, 1 cranidium, 2 thoracic segments
Cryptolithus tessellatus - 2 cranidia
- AV4B 75.36 - *Ampyxina pilatus* n. sp. - 1 cranidium, 1 pygidium, 1 thoracic segment
Cryptolithus tessellatus - 1 pygidia, 1 thoracic segment
- AV4B 72.55 - *Cryptolithus tessellatus* - 2 cranidial fragments
- AV4B 50.4 - *Ceraurinella brevispina* - 1 pygidium, 5 hypostomes, 4 thoracic segments
Bumastoides solangeae n. sp. - 1 pygidium, 1 cranidium
- AV4B 48.55- *Ceraurinella lamiapyga* n. sp. - 1 pygidium
Ceraurinella brevispina - 8 cranidia, 1 pygidia, 3 hypostomes, 1 librigenae, 7 thoracic segments
Isotelus dorycephalus n. sp. - 1 hypostome, 1 thoracic segment
Acanthoparypha latipyga n. sp. - 1 librigenae
- AV4B 23.8 - *Acanthoparypha latipyga* n. sp. - 1 pygidium, 1 thoracic segment
Bumastoides solangeae n. sp. - 9 pygidia, 9 librigenae, 1 hypostome, 2 cranidia, 4 thoracic segments
Ceraurinella brevispina - 9 pygidia, 20 thoracic segments, 5 cranidia, 5 hypostomes, 12 librigenae
Tricopelta mackenziensis - 1 cranidium
- AV4B 22.6 - *Tricopelta mackenziensis* - 32 cranidia, 32 pygidia, 50 librigenae, 20 hypostomes, 3 thoracic segments
Hemiarges n. sp. A - 6 cranidia, 4 librigenae, 8 pygidia, 8 hypostomes
Ceraurinella brevispina - 7 cranidia, 5 thoracic segments, 4 librigenae, 3 hypostomes, 4 pygidia
Isotelus dorycephalus n. sp. - 3 cranidia, 2 hypostomes, 1 pygidia
Acanthoparypha latipyga n. sp. - 1 cranidium
Bumastoides solangeae n. sp. - 1 cranidium, 6 pygidia
Ceraurus mackenziensis - 1 librigenae, 2 cranidia
Bathyurus teresoma n. sp. - 1 librigena
Amphilichas sp. - 1 hypostome
- AV4B 19.4 - *Ceraurinella brevispina* - 1 cranidium, 3 hypostomes, 5 thoracic segments, 1 librigena
Isotelus dorycephalus n. sp. - 2 pygidia, 3 hypostomes, 2 thoracic segments
Bathyurus teresoma n. sp. - 2 cranidia, 1 hypostome, 1 thoracic segment, 1 rostral plate, 1 pygidium
Tricopelta mackenziensis - 1 hypostome
- AV4B 17.4 - *Isotelus dorycephalus* n. sp. - 1 pygidium, 4 thoracic segments
Ceraurinella brevispina - 10 cranidia, 4 pygidia, 3 hypostomes, 23 thoracic segments, 22 librigenae
Hemiarges n. sp. A - 7 pygidia, 3 librigenae, 1 cranidia

- Tricopelta mackenziensis* - 13 cranidia, 13 librigenae, 1 hypostome, 4 pygidia
Decoroproetus hankei n. sp. - 1 hypostome
- AV4B 14.5 - *Ceraurinella brevispina* - 21 pygidia, 24 cranidia, 24 hypostomes, 27 librigenae, 26 thoracic segments
Isotelus dorycephalus n. sp. - 3 thoracic segments, 1 pygidia, 3 hypostomes
Sceptaspis avalanchensis n. sp. - 1 cranidium
Failleana sp. - 1 cranidium
- AV4B 11.5 - *Ceraurinus serratus* - 1 pygidium, 1 thoracic segment
Isotelus dorycephalus n. sp. - 1 pygidium, 2 hypostomes, 1 cranidium, 5 librigenae, 8 thoracic segments
Tricopelta mackenziensis - 14 cranidia, 11 pygidia, 5 hypostomes, 18 librigenae
Ceraurinella brevispina - 4 pygidia, 9 librigenae, 6 cranidia, 2 hypostomes
Acanthoparypha palmapyga n. sp. - 1 pygidium
Bumastoides solangeae n. sp. - 1 pygidium
Hemiarges n. sp. A - 3 cranidia, 4 pygidia, 2 librigenae, 4 hypostomes
Sceptaspis avalanchensis n. sp. - 3 cranidia
- AV4B 10.3 - *Ceraurinus serratus* - 1 pygidium, 10 thoracic segments
Tricopelta mackenziensis - 38 librigenae, 23 cranidia, 18 pygidia, 14 hypostomes
Hemiarges n. sp. A - 7 librigenae, 4 pygidia, 1 hypostome
Isotelus dorycephalus n. sp. - 1 hypostome, 1 pygidium, 1 thoracic segment
Ceraurinella brevispina - 66 thoracic segment, 26 librigenae, 14 pygidia, 20 cranidia, 16 hypostomes
Bumastoides solangeae n. sp. - 1 pygidium
Decoroproetus hankei n. sp. - 23 librigenae, 16 cranidia, 5 pygidia
Cybeloides sp. - 1 librigenae
Failleana sp. - 1 cranidium
Acanthoparypha palmapyga n. sp. - 2 hypostomes, 2 librigenae, 1 cranidium, 1 thoracic segment, 1 pygidium
Acanthoparypha sp. - 1 cranidium
- AV4B 7.85 - *Ceraurinella brevispina* - 11 pygidia, 16 librigenae, 52 thoracic segments, 12 hypostomes
Tricopelta mackenziensis - 1 librigenae
Bumastoides solangeae n. sp. - 1 pygidium, 2 librigenae, 2 hypostomes, 8 cranidia, 1 thoracic segment
Ceraurinus serratus - 3 thoracic segments
Sphaerexochus sp. - 1 pygidium
- AV4B 6.25 - *Decoroproetus hankei* n. sp. - 48 librigenae, 22 cranidia, 2 hypostomes, 14 pygidia
Bumastoides solangeae n. sp. - 5 pygidia, 2 hypostomes
Tricopelta mackenziensis - 30 cranidia, 28 pygidia, 30 thoracic segments, 39 librigenae, 13 hypostomes
Hemiarges n. sp. A - 4 cranidia, 1 pygidia, 1 hypostome, 1 librigenae
Ceraurinella brevispina - 2 cranidia, 5 thoracic segments

Isotelus dorycephalus n. sp. - 1 cranidium
Bathyurus teresoma n. sp. - 2 cranidia, 2 librigenae
Sphaerocoryphe sp. - 2 cranidia
Harpidella kurrii - 1 cranidium
Ceraurus mackenziensis - 5 hypostomes
Borealaspis whittakerensis - 1 cranidium

AV4B 2.75 - *Bathyurus teresoma* n. sp. - 4 thoracic segments, 7 cranidia, 2 hypostomes,
23 librigenae, 16 pygidia

APPENDIX IV: List of the trilobite taxa present within the horizons of the 1978 and 1979 collections from the Avalanche Lake 1 section.

- AV1 -60: *Bathyurus teresoma* n. sp. - 4 cranidia, 9 pygidia, 2 hypostomes, 1 rostral plate, 25 librigenae, 12 thoracic segments
- AV1 -45: *Bathyurus teresoma* n. sp. - 5 cranidia, 4 hypostomes, 15 pygidia, 2 rostral plates, 50 librigenae, 57 thoracic segments
Ceraurinella brevispina - 1 cranidium, 1 pygidium, 1 librigena, 2 hypostomes, 14 thoracic segments
- AV1 -36: *Bathyurus teresoma* n. sp. - 34 cranidia, 35 pygidia, 8 hypostomes, 1 rostral plate, 71 librigenae, 10 thoracic segments
Ceraurinella brevispina - 7 cranidia, 11 hypostomes, 3 librigenae, 23 thoracic segments
- AV1 4: *Isotelus dorycephalus* n. sp. - 2 cranidia, 12 librigenae, 4 pygidia, 1 hypostome, 18 thoracic segments
Ceraurinella brevispina - 5 cranidia, 2 pygidia, 3 hypostomes, 3 thoracic segments
- AV1 6: *Isotelus dorycephalus* n. sp. - 3 pygidia, 2 hypostomes, 4 librigenae, 14 thoracic segments
Ceraurinella brevispina - 1 cranidium, 1 hypostome
- AV1 10: *Ceraurinella brevispina* - 3 thoracic segments
Cryptolithus tessellatus - 3 cranidia, 3 pygidia
- AV1 30: *Cryptolithus tessellatus* - 2 cranidia
Ceraurinella brevispina - 2 hypostomes, 1 thoracic segments
Anataphrus elevatus n. sp. - 1 cranidium
- AV1 33.5: *Cryptolithus tessellatus* - 3 lamellar fragments
- AV1 36.5: *Cryptolithus tessellatus* - 1 pygidium
Anataphrus elevatus n. sp. - 20 pygidia, 7 thoracic segments
- AV1 40: *Anataphrus elevatus* n. sp. - 6 cranidia, 3 pygidia, 1 hypostome
Cryptolithus tessellatus - 10 cranidial fragments
Cybeloides sp. - 1 cranidium
- AV1 44: *Cryptolithus tessellatus* - 24 cranidia, 6 pygidia, 17 thoracic segments
Ampyxina pilatus n. sp. - 9 complete holaspids, 28 cranidia, 4 pygidia
Robergia yukonensis - 1 thoracic segment
- AV1 46: *Cryptolithus tessellatus* - 24 cranidia, 16 pygidia, 41 thoracic segments
Robergia yukonensis - 1 pygidium
Anataphrus elevatus n. sp. - 12 cranidia, 44 pygidia, 4 hypostomes, 37 librigenae
Cybeloides sp. - 1 librigena
Harpidella kurrii - 1 cranidium

- AV1 53.5: *Cryptolithus tessellatus* - 4 pygidia, 10 cranidia, 1 thoracic segment
Anataphrus elevatus n. sp. - 26 cranidia, 26 pygidia, 43 hypostomes, 37 librigenae
Cybeloides sp. - 11 cranidia, 5 hypostomes, 14 librigenae, 1 pygidium
Harpidella kurrii - 7 cranidia, 4 pygidia, 3 librigenae
Ampyxina pilatus n. sp. - 1 cranidium
Robergia yukonensis - 1 cranidium
Ceraurus mackenziensis - 1 cranidium, 5 hypostomes
- AV1 54: *Cryptolithus tessellatus* - 12 cranidia, 17 pygidia
Anataphrus elevatus n. sp. - 28 cranidia, 43 pygidia, 25 hypostomes, 50 librigenae
Cybeloides sp. - 2 pygidia, 1 cranidium, 4 librigenae, 1 hypostome
Ceraurus mackenziensis - 1 cranidia, 4 hypostomes, 3 pygidia
Harpidella kurrii - 32 cranidia, 10 librigenae
Hemiarges n. sp. A - 1 cranidium, 1 hypostome
Odontopleurid- 1 cranidium
- AV1 54.5: *Cryptolithus tessellatus* - 27 cranidia, 3 pygidia
Anataphrus elevatus n. sp. - 3 cranidia, 4 pygidia, 1 hypostome, 1 librigenae
Robergia yukonensis - 1 pygidia, 1 thoracic segment
Cybeloides sp. - 4 cranidia
- AV1 55: *Anataphrus elevatus* n. sp. - 17 cranidia, 28 thoracic segments, 26 librigenae
Cryptolithus tessellatus - 69 cranidia, 15 pygidia, 14 thoracic segments
Harpidella kurrii - 1 cranidium
Cybeloides sp. - 1 cranidium
Ampyxina pilatus n. sp. - 1 cranidium
- AV1 56.5: *Cryptolithus tessellatus* - 50 cranidia, 13 pygidia, 8 thoracic segments
Anataphrus elevatus n. sp. - 6 cranidia, 14 librigenae, 5 pygidia, 8 hypostomes
Robergia yukonensis - 6 cranidia
- AV1 60: *Cryptolithus tessellatus* - 3 enrolled holaspids, 6 cranidia, 8 pygidia
Robergiella insolitus n. sp. - 16 cranidia, 17 librigenae, 3 hypostomes
- AV1 68: *Cryptolithus tessellatus* - 11 cranidia, 1 pygidia
Anataphrus elevatus n. sp. - 1 pygidium + thorax
- AV1 72: *Cryptolithus tessellatus* - 12 cranidia, 5 pygidia, 10 thoracic segments
- AV1 73: *Cryptolithus tessellatus* - 1 complete holaspid, 27 cranidia, 13 pygidia, 6 thoracic segments
Anataphrus elevatus n. sp. - 2 cranidia, 1 pygidia
Ceraurus mackenziensis - 2 pygidia
- AV1 76: *Cryptolithus tessellatus* - 2 cranidia, 1 pygidia
- AV1 76.5: *Cryptolithus tessellatus* - 56 cranidia, 31 pygidia
Anataphrus elevatus n. sp. - 1 cranidium, 2 pygidia, 2 librigena

- AV1 77: *Cryptolithus tessellatus* - 19 lamellar fragments
- AV1 77.5: Proetid - 1 cranidium, 2 librigenae
- AV1 95.5: Encrinurid - 5 cranidia, 1 pygidia, 1 hypostome

APPENDIX V: Width and length measurements of *Ceraurinella brevispina* holaspid pygidia, width (W) is measured across the anterior margin, length (L) is of first pygidial spines.

Individual	W (mm)	L (mm)	Individual	W (mm)	L (mm)
1	1.37	1.43	47	2.65	2.05
2	3.20	2.50	48	2.35	1.65
3	1.33	1.53	49	2.40	1.90
4	1.93	1.87	50	2.00	1.65
5	3.27	1.70	51	3.20	2.05
6	2.20	2.13	52	2.95	2.30
7	2.10	1.80	53	3.25	2.50
8	1.90	1.87	54	4.45	2.80
9	1.20	1.37	55	3.70	2.60
10	1.30	1.27	56	3.05	2.20
11	0.90	1.30	57	3.75	2.60
12	2.67	2.00	58	3.05	2.20
13	2.27	1.83	59	3.75	2.60
14	3.03	2.00	60	4.40	2.70
15	2.77	1.73	61	3.65	2.05
16	2.87	2.00	62	3.45	2.70
17	2.03	1.90	63	4.20	2.80
18	2.40	1.97	64	3.00	2.15
19	1.60	1.00	65	3.80	2.25
20	1.27	0.70	66	3.25	2.00
21	1.03	0.83	67	3.10	1.80
22	1.27	1.17	68	3.25	2.00
23	1.77	1.50	69	3.25	2.00
24	2.03	1.50	70	3.75	2.65
25	2.30	1.63	71	3.50	2.35
26	1.17	1.10	72	3.05	2.15
27	1.47	1.43	73	4.15	2.80
28	1.83	1.63	74	3.90	2.20
29	1.70	1.33	75	3.90	2.10
30	1.30	1.17	76	4.25	2.80
31	1.50	1.47	77	3.35	2.45
32	1.20	1.17	78	3.15	2.25
33	1.33	1.43	79	3.50	2.05
34	1.67	1.63	80	3.25	2.00
35	1.47	1.50	81	5.10	2.40
36	1.37	1.17	82	5.40	2.60
37	1.23	1.30	83	4.40	2.30
38	2.27	1.87	84	4.40	2.40
39	1.77	1.57	85	4.10	2.50
40	1.90	1.37	86	4.00	2.70
41	2.07	2.27	87	6.40	3.00
42	1.93	1.90	88	4.70	2.30
43	1.50	1.40	89	5.90	3.10
44	2.65	2.10	90	6.00	3.30
45	2.90	2.00	91	4.40	2.50
46	2.20	1.60	92	4.30	2.60

APPENDIX VI: Diversity indices calculated for the AV4B, 98AV4B, and AV1 sections.					
Number of Species (X)	Number of Individuals	(log10)#individuals=Y	X/Y	horizon	section
2	100	2	1	110.9	98AV4B
1	37	1.568201724	0.637673065	110.7	
3	78	1.892094603	1.585544399	110.1	
3	751	2.875639937	1.043246048	110	
2	38	1.579783597	1.265996181	107	
3	26	1.414973348	2.120181277	105.5	
3	28	1.447158031	2.073028609	88.2	
5	91	1.959041392	2.552268686	85.6	
4	33	1.51851394	2.634154284	79	
4	48	1.681241237	2.379194556	78	
4	6	0.77815125	5.140388836	76.75	
2	3	0.477121255	4.191806549	76.25	
2	2	0.301029996	6.64385619	75.36	
1	1	0	0	72.55	
2	6	0.77815125	2.570194418	50.4	
4	11	1.041392685	3.841010271	48.55	
4	20	1.301029996	3.074487147	23.8	
9	61	1.785329835	5.041085307	22.6	
4	9	0.954242509	4.191806549	19.4	
5	33	1.51851394	3.292692855	17.4	
4	29	1.462397998	2.735233504	14.5	
8	35	1.544068044	5.181118817	11.5	
10	70	1.84509804	5.419766204	10.3	
5	23	1.361727836	3.671805678	7.85	
11	77	1.886490725	5.830932457	6.25	
1	16	1.204119983	0.830482024	2.75	

Number of Species (X)	Number of Individuals	(log10)#individuals=Y	X/Y	horizon	section
6	177	2.247973266	2.669070887	90.75	AV4B
5	241	2.382017043	2.099061388	90	
5	86	1.934498451	2.584649265	87	
4	180	2.255272505	1.773621587	80.5	
5	145	2.161368002	2.313349691	80	
7	42	1.62324929	4.312338247	73	
1	1	0	0	54	
3	3	0.477121255	6.287709823	49.5	
2	3	0.477121255	4.191806549	47.75	
4	4	0.60205991	6.64385619	44.8	
1	3	0.477121255	2.095903274	44	
8	70	1.84509804	4.335812963	43	
1	1	0	0	31.5	
6	153	2.184691431	2.746383272	18	
6	57	1.755874856	3.417100017	17	
9	415	2.618048097	3.437675576	16.5	
6	42	1.62324929	3.696289926	14	
5	57	1.755874856	2.847583348	9	
9	133	2.123851641	4.237584126	7	
9	245	2.389166084	3.767004755	6	
3	20	1.301029996	2.305865361	3.5	
7	166	2.220108088	3.152999639	3	
4	130	2.113943352	1.892198292	0.2	
2	2	0.301029996	6.64385619	0.075	
1	12	1.079181246	0.926628408	-60	AV1
3	28	1.447158031	2.073028609	-45	
3	48	1.681241237	1.784395917	-36	

Number of Species (X)	Number of Individuals	(log10)#individuals=Y	X/Y	horizon	section
3	12	1.079181246	2.779885224	4	
2	4	0.602059991	3.321928095	6	
2	4	0.602059991	3.321928095	10	
3	5	0.698970004	4.292029674	30	
1	1	0	0	33.5	
2	21	1.322219295	1.512608391	36.5	
3	17	1.230448921	2.438134528	40	
3	53	1.72427587	1.739860804	44	
5	69	1.838849091	2.719092081	46	
8	81	1.908485019	4.191806549	53.5	
8	100	2	4	54	
4	36	1.556302501	2.570194418	54.5	
5	89	1.949390007	2.56490491	55	
3	64	1.806179974	1.660964047	56.5	
2	27	1.431363764	1.39726885	60	
2	12	1.079181246	1.853256816	68	
1	12	1.079181246	0.926628408	72	
3	32	1.505149978	1.993156857	73	
1	2	0.301029996	3.321928095	76	
2	58	1.763427994	1.134154617	76.5	
3	19	1.278753601	2.346034449	77	
1	1	0	0	77.5	
1	5	0.698970004	1.430676558	95.5	